Gerhard Sauthoff

Intermetallics



ArcelorMittal Ex. 2038
Posco Co. LTD. v. ArcelorMittal
IPR2025-00371
Page 1 of 190

Related Titles from VCH

F. B. Pickering (Ed.)
Constitution and Properties of Steels
ISBN 3-527-26820-0
Volume 7 of the series *Materials Science and Technology*
R. W. Cahn, P. Haasen, E. J. Kramer (Eds.)

K. H. Matucha (Ed.)
Structure and Properties of Nonferrous Alloys
ISBN 3-527-26821-9
Volume 8 of the series *Materials Science and Technology*
R. W. Cahn, P. Haasen, E. J. Kramer (Eds.)

R. W. Cahn (Ed.)
Processing of Metals and Alloys
ISBN 3-527-26828-6
Volume 15 of the series *Materials Science and Technology*
R. W. Cahn, P. Haasen, E. J. Kramer (Eds.)

G. Petzow, G. Effenberg (Eds.)
Ternary Alloys. A Comprehensive Compendium of Evaluated Constitutional Data and Phase Diagrams
Please write for our comprehensive Prospectus

© VCH Verlagsgesellschaft mbH, D-69451 Weinheim (Federal Republic of Germany), 1995

Distribution:
VCH, P.O. Box 101161, D-69451 Weinheim, Federal Republic of Germany
Switzerland: VCH, P.O. Box, CH-4020 Basel, Switzerland
United Kingdom and Ireland: VCH, 8 Wellington Court, Cambridge CB1 1HZ, United Kingdom
USA and Canada: VCH, 220 East 23rd Street, New York, NY 10010-4606, USA
Japan: VCH, Eikow Building, 10-9 Hongo 1-chome, Bunkyo-ku, Tokyo 113, Japan

ISBN 3-527-29320-5

ArcelorMittal Ex. 2038
Page 2 of 190

Gerhard Sauthoff

Intermetallics



Weinheim · New York · Basel · Cambridge · Tokyo

ArcelorMittal Ex. 2038
Page 3 of 190

Gerhard Sauthoff
Max-Planck-Institut für Eisenforschung GmbH
Max-Planck-Straße 1
D-40237 Düsseldorf
Germany

This book was carefully produced. Nevertheless, author and publisher do not warrant the information contained therein to be free of errors. Readers are advised to keep in mind that statements, data, illustrations, procedural details or other items may inadvertently be inaccurate.

Published jointly by
VCH Verlagsgesellschaft, Weinheim (Federal Republic of Germany)
VCH Publishers, New York, NY (USA)

Editorial Directors: Dr. Peter Gregory, Deborah Hollis, Dr. Ute Anton
Production Manager: Dipl. Wirt.-Ing. (FH) Hans-Jochen Schmitt

Cover Illustration: Polarized optical micrograph of an electrolytically polished AlNi20 sample. Magnification 100 ×. Used with the kind permission of Alf Nikolaisen, Elkem Aluminium, Mosjøen, Norway.

Library of Congress Card No. applied for

A catalogue record for this book is available from the British Library

Die Deutsche Bibliothek – CIP-Einheitsaufnahme
Sauthoff, Gerhard:
Intermetallics / Gerhard Sauthoff. – Weinheim ; New York ;
Basel ; Cambridge ; Tokyo : VCH, 1995
ISBN 3-527-29320-5

© VCH Verlagsgesellschaft mbH, D-69451 Weinheim (Federal Republic of Germany), 1995

Printed on acid free and chlorine free paper

All rights reserved (including those of translation into other languages). No part of this book may be reproduced in any form – by photoprinting, microfilm, or any other means – nor transmitted or translated into a machine language without written permission from the publishers. Registered names, trademarks, etc. used in this book, even when not specifically marked as such, are not to be considered unprotected by law.
Composition, Printing and Bookbinding: Konrad Triltsch, Druck- und Verlagsanstalt GmbH, D-97070 Würzburg

Printed in the Federal Republic of Germany

Preface

Intermetallics are a fascinating new group of materials. Due to their unique physical and mechanical properties they occupy an intermediate position between metallic and non-metallic materials. This range of properties has aroused the interest of materials researchers and designers all over the world and has led to various important materials developments as well as to a flood of conferences and publications on intermetallics.

The present monograph was first written as a chapter for Volume 8 of the series "Materials Science and Technology: A Comprehensive Treatment", edited by Robert W. Cahn, Peter Haasen, and Edward J. Kramer (Volume Editor Dr. Karl Heinz Matucha). Its aim is to give an overview of intermetallics, which is both detailed and comprehensive and which includes the fundamentals as well as applications. The result is an extended, critical review of the whole field of intermetallics with an emphasis on those intermetallic phases which have already been applied as functional or structural materials or which are currently the subject of materials developments. A historical introduction and a discussion of the relationship between atomic bonding, crystal structure, phase stability and properties is followed by a discussion of the major classes of intermetallics. The titanium aluminides, nickel aluminides, iron aluminides, copper phases, A15 phases, Laves phases, beryllides, rare earth phases, and silicides are reviewed. In particular, the crystal structures, phase diagrams, and physical properties as well as the mechanical and corrosion behavior are treated. The state of developments as well as prospects and problems are discussed in view of present and future applications. The publisher has decided to publish the review as a separate monograph in order to make it accessible to a wider audience.

The author's research on intermetallics has been supported by the Deutsche Forschungsgemeinschaft (DFG) and the Bundesminister für Forschung und Technologie (BMFT) throughout a decade, and this is gratefully acknowledged. The author is indebted to numerous colleagues whose research is acknowledged in the references, and in particular to his colleagues at the Max-Planck-Institut für Eisenforschung for many valuable and stimulating discussions. The author thanks Mrs. Erika Bartsch for the large number of electron microscopy investigations of various intermetallic alloys and Mr. Gerhard Bialkowski for innumerable mechanical tests on rather brittle materials. I am indebted to the editorial and production staff at VCH for their contribution to the task of assembling this monograph. My particular thanks go to Dr. Peter Gregory, Dr. Ute Anton, and Ms. Deborah Hollis on the editorial side and to Wirt.-Ing. Hans-Jochen Schmitt on the production side.

January 1995

Gerhard Sauthoff

ArcelorMittal Ex. 2038
Page 5 of 190

Biography



Privatdozent Dr. rer. nat. Gerhard Sauthoff is Group Leader at the Max-Planck-Institut für Eisenforschung (Iron Research) GmbH in Düsseldorf, Germany and lectures at the Rheinisch-Westfälische Technische Hochschule in Aachen (Technical University). He received his Ph.D. in 1969 from the University of Göttingen. His dissertation was centered on the kinetics of Ostwald ripening of the intermetallic Ni_3Si phase in Ni–Si alloys. Subsequently, he studied phase transformation kinetics for various metallic and non-metallic systems at the Max-Planck-Institute for Physical Chemistry (then Biophysical Chemistry) in Göttingen. Since 1972 he has been working on the mutual interaction of phase transitions, including ageing processes and mechanical deformation in metallic materials. During the last decade his work has been centered on intermetallics with the emphasis on both fundamental research and materials development. In view of the latter, he has coordinated national research programs on intermetallics and is chairman of the Intermetallics Committee of the German Materials Society. In addition, the author is co-editor of the international scientific journal "Intermetallics".

Contents

List of Symbols and Abbreviations XII

1 **Introduction** 1

1.1 Definition of Intermetallics and Outline of This Report 1

1.2 Historical Remarks 2

2 **General Considerations** 5

2.1 Bonding, Crystal Structure, and Phase Stability 5

2.2 Bonding Strength and Basic Properties 8

2.3 Criteria for Phase Selection 11

3 **Titanium Aluminides and Related Phases** 14

3.1 Ti_3Al 14

3.1.1 Basic Properties and Phase Diagram 14

3.1.2 Microstructure and Mechanical Behavior 16

3.1.3 Environmental Effects 19

3.1.4 Applications 21

3.2 TiAl 22

3.2.1 Basic Properties and Phase Diagram 22

3.2.2 Microstructure and Mechanical Behavior 23

3.2.3 Environmental Effects 27

3.2.4 Applications 29

3.3 Al_3Ti and Other $D0_{22}$ Phases 30

3.3.1 Basic Properties and Phase Diagram 30

3.3.2 Microstructure and Mechanical Behavior 31

3.4 Trialuminides with the $L1_2$ Structure 36

3.4.1 Basic Properties and Phase Diagrams 36

3.4.2 Microstructure and Mechanical Behavior 37

4 **Nickel Aluminides and Related Phases** 38

4.1 Ni_3Al 38

4.1.1 Basic Properties and Phase Diagram 38

4.1.2 Microstructure and Mechanical Behavior 40

4.1.3 Environmental Effects 44

4.1.4 Applications 45

4.2 Other $L1_2$ Phases 47

4.2.1 General Remarks 47

4.2.2 $L1_2$ Phases of Particular Interest 48

4.3 NiAl 51

ArcelorMittal Ex. 2038
Page 7 of 190

4.3.1	Basic Properties	51
4.3.2	Phase Diagram and Martensitic Transformation	53
4.3.3	Microstructure and Mechanical Behavior	55
4.3.4	Creep	58
4.3.5	Environmental Effects	66
4.3.6	Alloy Developments and Applications	67
4.4	Other B2 Phases	77
4.4.1	CoAl	78
4.4.2	NiTi	79
4.4.3	FeTi, CoTi, CoZr, and CoHf	80
4.4.4	FeCo	81
4.5	Heusler-Type Phases	83
4.6	Nickel–Molybdenum Phases	83
5	**Iron Aluminides and Related Phases**	84
5.1	Fe_3Al	84
5.2	Fe_3AlC_x and Related Phases	86
5.3	FeAl	87
6	**Cu-Base Phases**	90
6.1	CuZn	90
6.2	Cu-Zn-Al Shape Memory Alloys	91
6.3	Cu-Al-Ni Shape Memory Alloys	92
6.4	Cu-Au Phases	93
6.5	Cu Amalgams	94
7	**A15 Phases**	94
7.1	Basic Properties	94
7.2	V_3Si	95
7.3	V_3Ga	97
7.4	Nb_3Sn	97
7.5	Nb_3Al	98
7.6	Nb_3Si	100
7.7	Cr_3Si	100
8	**Laves Phases**	100
8.1	Basic Properties	100
8.2	Applications	102
8.2.1	Superconducting Materials	102
8.2.2	Magnetic Materials	103
8.2.3	Hydrogen Storage Materials	103
8.2.4	Structural Alloys	104
9	**Beryllides**	106
10	**Rare-Earth Compounds**	107
10.1	Magnet Materials	108
10.2	Hydrogen Storage Materials	108
11	**Silicides**	109
11.1	M_3Si Phases	110
11.2	M_2Si Phases	111

ArcelorMittal Ex. 2038
Page 8 of 190

11.3 M_5Si_3 Phases 112
11.4 MSi Phases 113
11.5 Disilicides 114
12 **Prospects** 117
Acknowledgements 119
References 120
Index 159

ArcelorMittal Ex. 2038
Page 9 of 190

List of Symbols and Abbreviations

A	dimensionless factor
A_{diff}	dimensionless factor
a, b, c	lattice parameters
$\boldsymbol{B}$	magnetic induction
b	length of Burgers vector
D	effective diffusion coefficient
d	effective diffusion length
G	Gibbs energy; shear modulus
H	enthalpy
$\boldsymbol{H}$	magnetic field strength
H_{form}	formation enthalpy
H_{fus}	enthalpy of fusion
H_{total}	total phase enthalpy
H_{vap}	enthalpy of vaporization
k	Boltzmann's constant
K_{Ic}	fracture toughness
M_{s}	martensite formation temperature
S	entropy
T	absolute temperature
T_{m}	melting temperature
$\dot{\varepsilon}$	secondary strain rate
$\dot{\varepsilon}_{\text{diff}}$	diffusion creep rate
σ	applied stress
σ_{th}	threshold stress
Ω	atomic volume
APB	antiphase boundary
BDTT	brittle-to-ductile transition temperature
EL	tensile elongation
HPSN	hot-pressed silicon nitride
LPS	long-period superlattice
NASP	National Aero-Space Plane
ODS	oxide-dispersion strengthened
PST	polysynthetically twinned
REPM	rare earth permanent magnet
tcp	topologically close-packed
TMP	thermal mechanical processing
UTS	ultimate tensile strength
VEC	valence electron concentration
VLSI	very-large-scale-integrated circuit
YS	yield strength

ArcelorMittal Ex. 2038
Page 10 of 190

Intermetallics
Gerhard Sauthoff
copyright © VCH Verlagsgesellschaft mbH, 1995

„Die Sprödigkeit der metallischen Kristallarten singulärer Zusammensetzung, der Metallverbindungen, kann ihren Grund darin haben, daß ihnen die Fähigkeit, Gleitebenen zu bilden, abgeht, oder daß neben dieser Fähigkeit noch die Eigentümlichkeit der Rißbildung auftritt."

("The reason for the brittleness of metallic crystals with unique compositions, i.e. the metal compounds, may be that they lack the ability to form glide planes, or that in addition to this ability, there exists the characteristic of crack formation.")

Tammann and Dahl (1923)

1 Introduction

1.1 Definition of Intermetallics and Outline of This Report

Intermetallics is the short and summarizing designation for the intermetallic phases and compounds which result from the combination of various metals, and which form a tremendously numerous and manifold class of materials, as will become clear in the following sections. According to a simple definition (Schulze, 1967; Girgis, 1983), intermetallics are compounds of metals whose crystal structures are different from those of the constituent metals, and thus intermetallic phases and ordered alloys are included. During the last ten years intermetallics have been of enormous, and still increasing, interest in materials science and technology with respect to applications at high temperatures, and a new class of structural materials is expected to be developed on the basis of intermetallics. Various materials developments are under way in various parts of the world, in particular in the U.S.A., in Japan, and in Germany. These activities are the main subject of the present report. However, it has to be noted that besides intermetallics with oustanding high-temperature properties there are other intermetallics with outstanding physical properties which have given rise to developments of new functional materials much earlier, and which will also be addressed.

The numerous and manifold activities on intermetallics, as well as the enormous interest, have given rise to many conferences, symposia and workshops on materials research and development of intermetallics during previous years. The results of these activities have been published in the respective proceedings volumes, as well as the publications in scientific journals and research reports, and there are an increasing number of review papers on various aspects of intermetallics in such proceedings and in the scientific journals. Furthermore, particular aspects of intermetallics are treated in various volumes of the Series *Materials Science and Technology* (MST): chapters by Pettifor, and Ferro and Saccone in Volume 1, chapters by Delaey, and Inden and Pitsch in Volume 5, and chapters by Umakoshi and Mukherjee in Volume 6.

It is the aim of the present report to give a summarizing description of the various intermetallics which have already been selected for materials developments, or which have been, and still are, regarded as promising for materials developments. The characteristic properties are shown, the physical mechanisms which control the observed behavior and the problems involved are discussed, and the present state and prospects of the respective materials developments are assessed. This report, however, cannot be exhaustive because of the large and still increasing number of activities, and because many developments have not yet been described in the open literature.

ArcelorMittal Ex. 2038
Page 11 of 190

After an introductory section with a brief account of the history of intermetallics, the fundamentals of intermetallics are discussed by making reference to the respective chapters in various volumes of MST. In particular, the stability of phases, as well as the relation between atomic bonding and basic properties are addressed, and the criteria for grouping the various phases are discussed. Then the various intermetallics and the respective materials developments are described, and finally the prospects, as well as the needs for research and development, are assessed.

1.2 Historical Remarks

The history of intermetallics has been outlined repeatedly in some detail by Westbrook, one of the central people in the research and development of intermetallics in the second half of this century (Westbrook, 1967, 1970, 1977, 1993). Therefore only some important points are noted here.

Intermetallics have been made use of since the beginning of metallurgy, as is exemplified in Table 1 (for nomenclature see the chapter by Ferro and Saccone in Volume 1 of MST). Such intermetallics resulted from the used alloy systems with low melting temperatures, and the applications relied on the outstanding hardness and wear resistance of the intermetallics together with their metallic properties (Westbrook, 1977). Because of the metallic behavior of intermetallics they could be polished, and thus the decorative aspect was also important for many applications. Examples are the bronze coatings in ancient Egypt and the mirrors which were used, not only by the ancient Chinese, but also by Etruscans and Romans (Westbrook, 1977). In this context it has to be mentioned that some intermetallics show beautiful colors, e.g. the violet Cu_2Sb ("Regulus of Venus"), which was also discovered early on (Westbrook, 1977).

Intermetallics became a subject of scientific research during the last century with the development of physical metallurgy, and the first validated instance of intermetallic compound formation was reported by Karsten (1839) in Germany (Westbrook, 1967, 1970). Intensive and broad-scale work on intermetallics was initiated by Tammann in Göttingen, Germany and Kurnakov in St. Petersburg, Russia at the turn of the century, from which a large number of directive papers resulted (e.g. Kurnakov, 1900, 1914; Tammann, 1903, 1906; Kurnakov and Zhemchuzhny, 1908; Tammann and Dahl, 1923). The early work on intermetallics during the first decades of this century included studies of phase stabilities, phase equilibria and phase reactions in order to establish phase diagrams, as well as studies of the various properties, i.e. chemical and electrochemical properties, physical properties including magnetism and superconductivity, and mechanical properties, as are summarized in Tammann (1932). With respect to mechanical behavior it was realized that the outstanding hardness of intermetallics is accompanied by an unusual brittleness, and the reasons for this were also investigated (Tammann and Dahl, 1923).

Intermetallics were used in this century first and primarily for applications as functional materials, as is exemplified in Table 1. Indeed the first industrial applications relied on the special magnetic behavior of certain phases, and respective materials developments led e.g. to Sendust, which shows outstanding magnetic properties and wear resistance and is widely used for magnetic heads in tape recorders (Yamamoto, 1980; Brock, 1986). In the second

ArcelorMittal Ex. 2038
Page 12 of 190

Table 1. Some past and present applications of intermetallics (Sauthoff, 1989).

Since approx.	Material or process	Phase	Application	Reference
2500 B. C.	cementation	Cu_3As	coating of bronze tools, etc. (Egypt, Anatolia, Britain)	Westbrook (1977)
100 B. C.	yellow brass	CuZn	coins, ornamental parts (Rome)	Gmelin-Institut (1955)
0	high tin bronze	$Cu_{31}Sn_8$	mirror (China)	Westbrook (1977)
600	amalgam	$Ag_2Hg_3 + Sn_6Hg$	dental restorative (China)	Westbrook (1977) Waterstrat (1990)
1500	amalgam	Cu_4Hg_3	dental restorative (Germany)	Paufler (1976), Westbrook (1977) Waterstrat (1990)
1505	amalgam	Sn_8Hg	mirror surface (Venice)	Westbrook (1977)
1540	type metal	SbSn	printing	Westbrook (1977)
1910	Acutal	$(Cu, Mn)_3Al$	fruit knife (Germany)	Heusler (1989)
1921	Permalloy	Ni_3Fe	high permeability magnetic alloy	Bozorth (1951)
1926	Permendur	FeCo(–2V)	soft magnetic alloy	Bozorth (1951), Chen (1961)
1931	Alnico	NiAl–Fe–Co	permanent magnet material	De Vos (1969)
1935	Sendust	$Fe_3(Si, Al)$	magnetic head material	Yamamoto (1980)
1938	Cu–Zn–Al Cu–Al–Ni	CuZn–Al $(Cu, Ni)_3Al$	shape memory alloys	Hodgson (1990)
1950	pack aluminide coating	NiAl, CoAl	surface coating for protection from environment	Nicholls and Stephenson (1991)
1956	Kanthal Super, Mosilit	$MoSi_2$	electric heating elements	Fitzer and Rubisch (1958)
1961	A 15 compound	Nb_3Sn	superconductors	Westbrook (1977), Geballe and Hulm (1986)
1962	Nitinol	NiTi	shape memory alloy	Delaey et al. (1974) Hodgson (1990)
1967	Co–Sm magnets	Co_5Sm	permanent magnets	Stadelmaier et al. (1991), Westbrook (1977), Buschow (1986)

half of this century another important application resulted from the development of new superconducting materials based on the A15 compounds which are used for superconducting magnets (B. W. Roberts, 1967; Westbrook, 1977; Dew-Hughes, 1986). A third group of functional materials, the shape memory alloys, makes use of a martensitic phase transformation and has again found manifold applications during the last three decades, e.g. Otsuka and Shimizu (1986).

An important group of functional materials is formed by the III–V compounds, e.g. InSb, InAs, GaAs, which have found applications in electronics and in thermoelectric power generation (C. S. Roberts, 1967; Cadoff, 1967). The constitutive ele-

ArcelorMittal Ex. 2038
Page 13 of 190

ments of these phases represent the transition from metals to semi-metals and nonmetals, and the resulting compounds are semiconductors. Thus these intermetallic semiconductor compounds are outside the field of intermetallics proper, which exhibit metallic behavior.

Intermetallics did not find applications as structural materials in the past because of their brittleness. The only noteworthy exception is the continuing use of amalgams as dental restoratives (Westbrook, 1974, 1977). On the other hand, various intermetallics were successfully used as strengthening second phases in conventional alloys for structural applications (Westbrook, 1970). Thus it was clear that intermetallics are promising for applications as structural materials at high temperatures because of their high hardness and stability, and indeed manifold activities were started at the beginning of the fifties for clarifying the potential of intermetallics for structural applications (Westbrook, 1960a, b). Various promising candidate phases were identified, but the respective materials developments were hampered by the unsolved brittleness problems, and thus the various activities slowly died away during the 1960s (Westbrook, 1965, 1970, 1977; Ryba, 1967; Liu and Stiegler, 1984; Cahn, 1989; Liu et al., 1990).

One offspring of these activities was the development of the electric heating elements based on $MoSi_2$ (see Table 1), which rely on the advantageous chemical behavior of this phase, i.e. its high oxidation resistance at very high temperatures (Fitzer and Rubisch, 1958; Schrewelius and Magnusson, 1966). In this context the surface coatings should be mentioned which have been developed in the course of superalloy developments to protect the coated materials against high temperature corrosion, and which rely primarily on such intermetallics as NiAl and CoAl (Nicholls and Stephenson, 1991).

It should be noted that the mentioned molybdenum disilicide is a borderline case of the intermetallics since silicon is not a metal, but a semiconductor. It is known that the combination of silicon with metals gives rise to compounds with metallic properties, e.g. $MoSi_2$, as well as compounds with semiconductor properties (Nowotny, 1963), i.e., silicides mark the transition from intermetallics to compounds of metals and nonmetals. Nevertheless, silicides are traditionally included in the field of intermetallics because of their many similarities with metals (Wehrmann, 1967).

The first intensive and successful structural materials developments were based on the titanium aluminides Ti_3Al and TiAl, and were started at the beginning of the 1970s with fundamental deformation studies (Shechtman et al., 1974; Fleischer et al., 1989a; Schneibel et al., 1986), whereas the potential of these phases for high-temperature applications had already been recognized during the 1950s (McAndrew and Kessler, 1956). These developments are still continuing with a multitude of activities.

Another similar intensive and successful structural materials development was based on the nickel aluminide Ni_3Al, which is the strengthening second phase in the superalloys, and which was also a candidate phase during the 1950s (Liu and Stiegler, 1984). This development had an enormous impact due to the detection of the "ductilization" effect of small additions of boron (Aoki and Izumi, 1979; Liu and Koch, 1983), since this effect gave rise to large research programs on intermetallics and excited the general and still increasing interest in intermetallics. More

ArcelorMittal Ex. 2038
Page 14 of 190

and more research groups started work on intermetallics, and in most cases during the last decade Ni_3Al was selected as the subject of research. A further related development, which was already started at the beginning of the 1970s, was based on the quaternary phase $(Fe,Co,Ni)_3V$ with the crystal structure of Ni_3Al (Liu and Inouye, 1979). These successful developments have initiated work on other less-common phases recently which aims at low densities and/or high application temperatures (e.g. Sauthoff, 1989). From these various developments over the years the manifold spectrum of present activities has evolved which is the subject of the subsequent sections.

2 General Considerations

2.1 Bonding, Crystal Structure, and Phase Stability

Intermetallics form because the strength of bonding between the respective unlike atoms is larger than that between like atoms. Accordingly, intermetallics form particular crystal structures with ordered atom distributions where atoms are preferentially surrounded by unlike atoms. Simple examples of such crystal structures are shown in Fig. 1. The crystal structures of intermetallics have been discussed in detail by Ferro and Saccone in Volume 1 of MST.

The crystal structure of an intermetallic is determined by the strength and character of bonding in the crystal, which depends on the particular electronic configuration. The relation between structure type and atomic properties of the constituent atoms, however, is not a simple one and thus various criteria have been used for correlating structure type and phase type, i.e., for predicting the crystal structure for a given phase or phase group. Likewise, all the intermetallics cannot be expected to show metallic bonding similar to the constituent metals. This has been discussed in detail repeatedly, and the intermetallics have been grouped traditionally according to various criteria (e.g. Nevitt, 1963; Schulze, 1967; Schubert, 1967; Laves, 1967; Girgis, 1983; Hafner, 1987; Pettifor, 1988; and the chapters by Pettifor and Ferro and Saccone in Volume 1 of MST). It

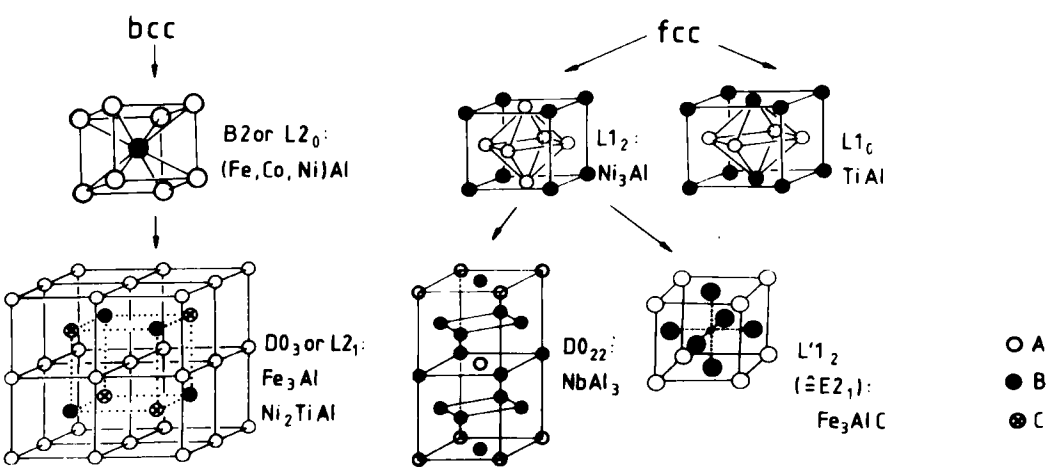


Figure 1. Some simple intermetallic crystal structures which are derived from the b.c.c. and f.c.c. structures, respectively, with typical examples (Sauthoff, 1989).

ArcelorMittal Ex. 2038
Page 15 of 190

copyright © VCH Verlagsgesellschaft mbH, 1995

and more research groups started work on intermetallics, and in most cases during the last decade Ni_3Al was selected as the subject of research. A further related development, which was already started at the beginning of the 1970s, was based on the quaternary phase $(Fe,Co,Ni)_3V$ with the crystal structure of Ni_3Al (Liu and Inouye, 1979). These successful developments have initiated work on other less-common phases recently which aims at low densities and/or high application temperatures (e.g. Sauthoff, 1989). From these various developments over the years the manifold spectrum of present activities has evolved which is the subject of the subsequent sections.

2 General Considerations

2.1 Bonding, Crystal Structure, and Phase Stability

Intermetallics form because the strength of bonding between the respective unlike atoms is larger than that between like atoms. Accordingly, intermetallics form particular crystal structures with ordered atom distributions where atoms are preferentially surrounded by unlike atoms. Simple examples of such crystal structures are shown in Fig. 1. The crystal structures of intermetallics have been discussed in detail by Ferro and Saccone in Volume 1 of MST.

The crystal structure of an intermetallic is determined by the strength and character of bonding in the crystal, which depends on the particular electronic configuration. The relation between structure type and atomic properties of the constituent atoms, however, is not a simple one and thus various criteria have been used for correlating structure type and phase type, i.e., for predicting the crystal structure for a given phase or phase group. Likewise, all the intermetallics cannot be expected to show metallic bonding similar to the constituent metals. This has been discussed in detail repeatedly, and the intermetallics have been grouped traditionally according to various criteria (e.g. Nevitt, 1963; Schulze, 1967; Schubert, 1967; Laves, 1967; Girgis, 1983; Hafner, 1987; Pettifor, 1988; and the chapters by Pettifor and Ferro and Saccone in Volume 1 of MST). It

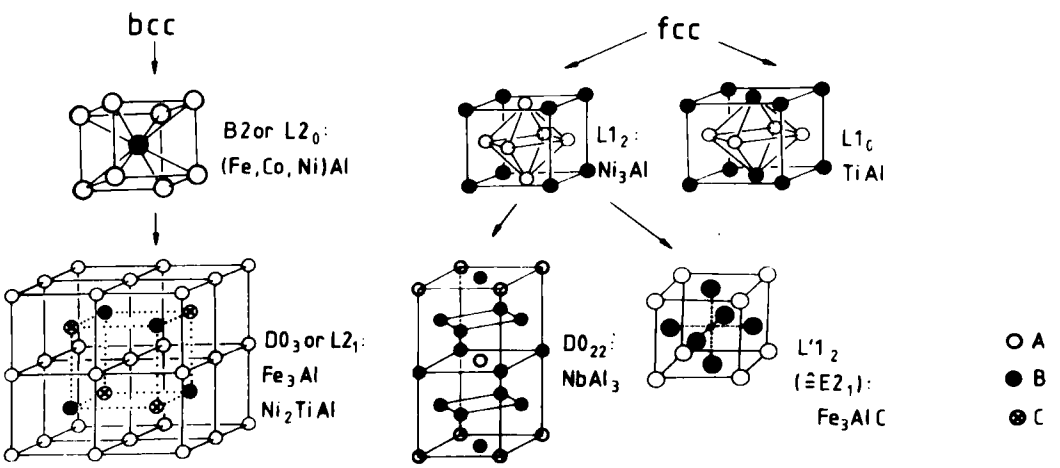


Figure 1. Some simple intermetallic crystal structures which are derived from the b.c.c. and f.c.c. structures, respectively, with typical examples (Sauthoff, 1989).

ArcelorMittal Ex. 2038
Page 16 of 190

should be noted that these groupings are not unambiguous since different authors stress different aspects of the particular intermetallics. In the following, a brief survey on three important and rather different groups of intermetallics is given to illustrate this.

The Zintl phases are formed by metals on the left-hand side and on the right-hand side of the periodic table of elements, and are characterized by completely filled electronic orbitals, normally by a full octet shell (Laves, 1967; Schäfer et al., 1987; Schmidt, 1987). Thus they may be regarded as valence compounds which satisfy the familiar chemical valency rules (Girgis, 1983; Hafner, 1987). The Zintl phases have crystal structures which are characteristic for typical salts, e.g. NaTl with a cubic B32 structure (Strukturbericht designations are used here and in the following for the crystal structures) or Mg_2Si with a cubic C1 structure (Villars and Calvert, 1991), and therefore ionic bonding is expected. However, all types of bonding (ionic, metallic and covalent) and mixtures thereof have been found depending on the particular electronic distribution, i.e. the Zintl phases may also be regarded as electronic compounds for which the electron band-structure energy is a large fraction of the total energy, and crystal structure types are related to particular valence electron concentrations (average number of valence electrons per atom) (Hafner, 1987).

The best-known electron compounds are the Hume-Rothery phases which have the cubic B2 structure, e.g. β-brass at high temperatures and the transition-metal aluminides FeAl, NiAl and CoAl, or the complex cubic A13 structure (β-manganese-type), e.g. Zn_3Co, Cu_5Si, or the close-packed hexagonal A3 structure, e.g. Cu_3Ga, Ag_3Al, for the valence electron concentration VEC = 3/2, the complex cubic $D8_2$ structure (γ-brass type) for VEC = 21/13, e.g. Cu_5Zn_8, Fe_5Zn_2, and again the A3 structure for VEC = 7/4, e.g. $CuZn_3$, Ag_5Al_3 (Girgis, 1983). The bonding in such intermetallics is not purely metallic in spite of the metal-like band structure. For example, the bonding in the above-mentioned NiAl has been found to be essentially covalent with some metallic character and no ionic component (Fox and Tabbernor, 1991), which can be understood in view of the band structures of Ni, Al and NiAl (Engell et al., 1991). It has indeed been shown on the basis of recent ab initio calculations that – strictly speaking – the B2 aluminides are not Hume-Rothery electron compounds (Schultz and Davenport, 1993). This means that the Hume-Rothery rules, which relate crystal structure to valence electron concentration, represent a very simplified picture of the bonding situation. Nevertheless, such rules are useful since they describe reality surprisingly well.

Other intermetallics are best characterized by the size ratios and packing schemes of the constituent atoms, and are therefore called size-factor compounds or topologically close-packed intermetallics or Frank–Kaspar phases (Wernick, 1967; Girgis, 1983; Watson and Bennett, 1985; Hafner, 1987). One important group of these intermetallics are the A15 phases, which were mentioned in the preceding section. The best-known size-factor compounds are the Laves phases, which form the most numerous group of intermetallics and which crystallize in the closely related hexagonal C14, cubic C15 or hexagonal C36 structures with $MgZn_2$, $MgCu_2$, $MgNi_2$, respectively, as typical examples (Wernick, 1967). The valence electron concentration, however, is also an important factor here since it decides between the three crystal structures. These crystal

ArcelorMittal Ex. 2038
Page 17 of 190

structures are characterized by high symmetry, high atom coordination and high density in close analogy to metals, and indeed the Laves phases primarily show metallic bonding according to the limited information available (Schulze, 1967; Hafner, 1987).

There are phases which form by a phase transition with a lowering of the crystal symmetry from the solid solution of the constitutent elements at a transition temperature below the melting temperature, and which are known as Kurnakov phases (Kornilov, 1967). In the simplest case the phase transition results from an ordering reaction in the solid solution lattice from which a superlattice structure is established. Examples of phase formation by atomic ordering are the phases Fe_3Al with a $D0_3$ structure, which forms by two-step ordering from the b.c.c. solid solution (see Sec. 5.1), as well as Ni_3Fe with an $L1_2$ structure (see Sec. 4.2.2), CuAu with an $L1_0$ structure and Cu_3Au with an $L1_2$ structure (see Sec. 6.4), the latter three of which form from f.c.c. solid solutions. This atomic ordering with superlattice formation obviously results from a stronger bonding between unlike atoms compared with bonding to like atoms. The difference in bonding energy between unlike and like atoms is usually known as the interaction energy and corresponds to an ordering energy. Thus a higher crystal stability with a higher ordering temperature is expected for a higher interaction energy. The degree of order, which depends on temperature and composition, as well as the order/disorder temperature can be modeled as a function of the interaction energy for a given phase to various degrees of approximation, e.g. to the first approximation by the simple Bragg–Williams model or to higher approximations by the cluster variation method or the Monte Carlo method (De Fontaine, 1979; see also the chapter by Binder, and Inden and Pitsch in Volume 5 of MST). Apart from the degree of approximation, the predictive power of such models with respect to phase stability and phase diagram calculations relies on the knowledge of the interaction energy, and on whether such interaction energies are sufficient for the characterization of the atomic bonding state. Analyses of various transition metal systems have shown that modeling with the cluster variation method or Monte Carlo method gives good agreement with the experimental observations in most cases, whereas in some cases with b.c.c. structures the simple Bragg–Williams model gave better results than the more sophisticated models (chapter by Inden and Pitsch in Volume 5 of MST).

It follows that single simple atomic parameters like the interaction energy, atomic size or valence electron concentration have only a limited validity and are generally not sufficient for predicting the phase stability as a function of the constituent elements. A better and more general correlation between the atomic properties and the compound crystal structure should be obtained if the particularities of the electronic configurations of the constituent atoms are taken into account, which are reflected by the positions in the periodic table of elements. A better correlation has indeed been found, but the resulting structure maps still have their limitations because the changes in electronic configuration due to compound formation are not considered (Pettifor, 1988; Villars et al., 1989).

It has to be concluded that the bonding character and crystal structure of an intermetallic can be predicted in a significant way only on the basis of a quantum-mechanical, ab initio calculation for the re-

ArcelorMittal Ex. 2038
Page 18 of 190

spective phase (Hafner, 1987, 1989; Majewski and Vogl, 1989). Much progress has been made in this respect (Györffy et al., 1991), and for various important phases with not too complicated structures the crystal energy has been calculated as a function of the lattice structure in order to determine the phase stability (Freeman et al., 1991; Bose et al., 1991; Lin et al., 1991; Pettifor and Aoki, 1991; Gonis et al., 1991; Becker et al., 1991; Vignoul et al., 1991; Sluiter et al., 1990; Huang et al., 1991; De Fontaine et al., 1991; Turchi et al., 1991); see also the chapter by Pettifor in Volume 1 of MST. However, these calculations are very time consuming, even in simple cases, and more progress is necessary in the future in order to give guidance to practical materials developments on the basis of multinary (i.e. ternary, quaternary, etc.) phases with less simple crystal structures.

From the discussion in this section it follows that the intermetallics do not form a homogeneous group of materials at all. Instead the term intermetallics comprises a huge variety of phases which differ drastically with respect to bonding, crystal structure and properties. Thus the properties of intermetallics cannot be discussed generally with respect to all intermetallics; they can only be discussed by referring to specific groups of intermetallics.

It may be supposed that the particular crystal structure of an intermetallic reflects the character and strength of bonding in a sensible way, and thus the crystal structure would be a good criterion for phase classification. However, this does not mean that intermetallics with the same crystal structure are similar with respect to bonding and properties since, e.g. the B2 structure is common to the intermetallic NiAl and to the purely ionic salt CsCl, and in the case of the transition-metal disilicides with a hexagonal C40 structure, $NbSi_2$ is metallic whereas $CrSi_2$ is a semiconductor (Nowotny, 1963). It has indeed been shown recently on the basis of ab initio calculations that atomic coordination and connectivity are more relevant to crystal energy and stability than symmetry (Shah and Pettifor, 1993). In view of the complexity of the classification of intermetallics, intermetallics are often grouped according to more practical criteria which refer to similarities in behavior. In the subsequent sections the intermetallics to be discussed are grouped according to constitution and crystal structure in a somewhat subjective manner.

2.2 Bonding Strength and Basic Properties

A basic property is the melting temperature since it is known that materials' parameters which characterize the deformation behavior are well correlated with the melting temperature (Frost and Ashby, 1982). Examples are the elastic moduli which not only control the elastic deformation, but are also important parameters for describing the plastic deformation, and the diffusion coefficients which control not only the kinetics of phase reactions, but also the kinetics of high-temperature deformation, i.e. creep. Furthermore, the melting temperature is intuitively regarded as a measure of the phase stability since it limits the application temperature range.

However, a phase melts when the Gibbs energy of the solid phase, which is a thermodynamic state function and which controls the phase stability, is higher than that of the liquid phase [see e.g. Denbigh (1971) and chapter by Pelton in Volume 5 of MST]. The Gibbs energy G of a phase is given by

$$G = H - TS \qquad (1)$$

ArcelorMittal Ex. 2038
Page 19 of 190

i.e., it is given by the enthalpy H at a temperature $T = 0$ K, and its temperature dependence is determined by the entropy S. Thus the melting temperature depends on the differences in enthalpy and entropy between the solid and liquid states and is a rather complex function of the bonding strength. Only the enthalpy is directly related to the internal crystal energy which is determined by the bonding strength. Nevertheless, the melting temperature is correlated surprisingly well with the phase formation enthalpy for sufficiently similar phases, as is shown in Fig. 2. For the small number of phases concerned, there is a linear relationship for the phases with a common B2 structure, whereas the phase TiAl with a different crystal structure follows another relationship.

It may be concluded that the phase formation enthalpy may be a better parameter for characterizing bonding strength and phase stability, and for correlating this with the basic properties, e.g. elastic moduli. Formation enthalpies have been determined experimentally (Hultgren, 1963), and they can be calculated by quantum-mechanical calculations (e.g., Hackenbracht and Kübler, 1980), or estimated by more or less empirical approaches (de Boer et al., 1988). Figure 3 shows some data for the Ni–Al system which illustrate the good agreement between theory, estimate and experiment.

However, the enthalpy values in Figs. 2 and 3 refer to compound formation from the constituent elements at room temperature, i.e. from the solid element crystals, and thus these formation enthalpies only characterize the bonding strength changes during compound formation. For complete characterization of the bonding strength the total phase enthalpy is required, which refers to the compound formation from the elements in the gaseous state. The total phase enthalpy H_{total} of a phase C may be estimated by adding up the formation enthalpy H_{form} and the enthalpies of fusion and vaporization H_{fus} and H_{vap} of the constituent elements A and B, according to the reaction cycle given in Fig. 4. As an example, Fig. 5 shows data

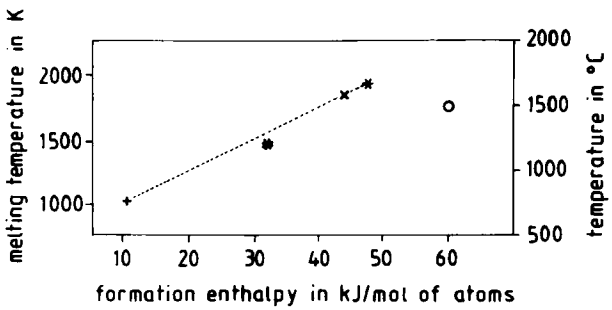


Figure 2. Melting temperature as a function of formation enthalpy (Hultgren, 1963) for the B2 phases CuZn (+), FeAl (#), CoAl (×), NiAl (*) and for the $L1_0$ phase TiAl (o) (Engell et al., 1991).

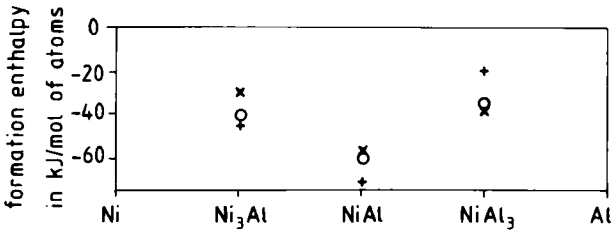


Figure 3. Formation enthalpies from experiments (×) (Hultgren, 1963), quantum-mechanical calculations (+) (Hackenbracht and Kübler, 1980) and estimates (o) according to de Boer et al. (1988), as a function of composition for the Ni–Al system (Engell et al., 1991).

ArcelorMittal Ex. 2038
Page 20 of 190

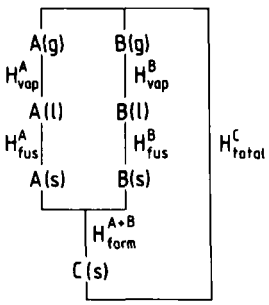


Figure 4. Reaction cycle for the formation of a phase C from the gaseous elements A and B (see text).

for the Ni–Al system, and again the agreement between estimates and experimental data is visible. It is noted that the formation enthalpies are small compared with the total enthalpies, i.e. the enthalpies of the constituent elements are the major contributions to the total enthalpies.

The correlation between the total phase enthalpy and the Young's modulus, which is one of the three elastic moduli, is shown in Fig. 6 for various cubic phases, i.e. for the f.c.c. elements Al and Ni (A1), the f.c.c.-ordered Ni_3Al ($L1_2$), the b.c.c. ordered FeAl, NiAl and CoAl (B2), and the cubic Laves phases $CaAl_2$, YAl_2, $LaAl_2$, $NbCr_2$, $ZrCo_2$ and $HfCo_2$ (C15). The correlation is quite good for the Laves phases, i.e. there seems to be a common scatter band and the data of some other phases are near this scatter band. It has to be noted, however, that the data points may be subject to appreciable experimental uncertainties, as is indicated by the two data points for Ni_3Al. Such uncertainties for the Young's modulus may be due to differences in the microstructure, i.e. texture and artefacts. Apart from this, the data for the B2 phases show that the Young's modulus is not a simple function of the phase enthalpy. This has to be expected because the Young's modulus is a complex function of the potential wells of the atoms, which cannot be characterized by a single parameter. A similar correlation is found for the activation energy of diffusion, as is illustrated in Fig. 7.

It has to be concluded that there are physically justified correlations between parameters which characterize the bonding strength and the phase stability on the one hand, and the macroscopic phase behavior on the other. However, such correlations represent complex functional relationships, and thus they are useful only for order-of-magnitude predictions. More quantitative predictions have to consider the character and strength of bonding in a more detailed way, i.e. they have to rely on quantum-mechanical calculations which are cumbersome and time consuming.

Recently basic properties – in particular the elastic moduli – of various simple phases have been studied by ab initio cal-

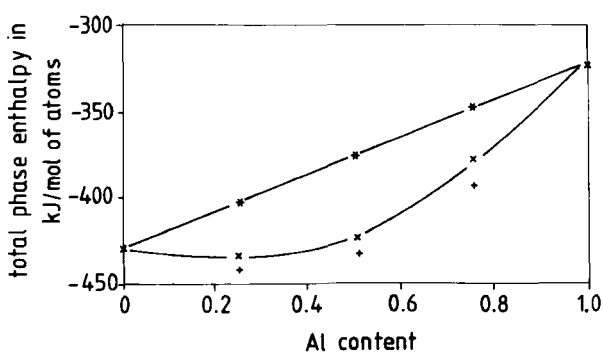


Figure 5. Total phase enthalpy as a function of composition for the Ni–Al system: experimental data (+) (Hultgren, 1963) and estimates (×) according to de Boer et al. (1988) compared with the ideal solid solution (*) with vanishing formation enthalpy (Von Keitz and Sauthoff, 1991).

ArcelorMittal Ex. 2038
Page 21 of 190

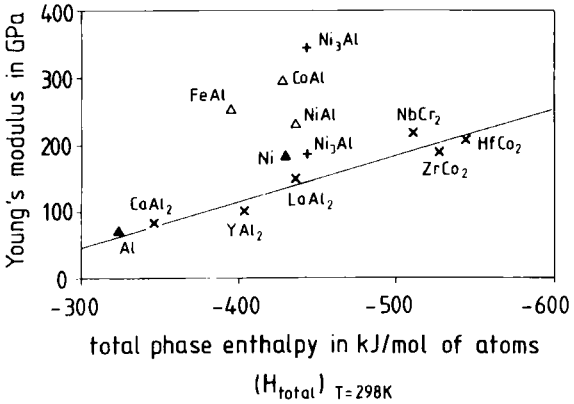


Figure 6. Young's modulus as a function of total phase enthalpy (Hultgren, 1963; Engell et al., 1991; Von Keitz and Sauthoff, 1991) at room temperature for the f.c.c. elements Al and Ni (A1) (▲) (Lide, 1992), the f.c.c.-ordered Ni_3Al with an $L1_2$ structure (+) (Davies and Stoloff, 1965; Munroe and Baker, 1988), the b.c.c. ordered FeAl, NiAl and CoAl with a B2 structure (△) (Harmouche and Wolfenden, 1985), and the cubic Laves phases $CaAl_2$, YAl_2, $LaAl_2$, $NbCr_2$, $ZrCo_2$ and $HfCo_2$ with a C15 structure (×) (Shannette and Smith, 1969; Schiltz and Smith, 1974; Fleischer et. al., 1988).

culations, and a lot of progress has been made in this field (e.g. Fu and Yoo, 1990, 1991; Lee and Yoo, 1990; Guo et al., 1991; Yoo and Fu, 1991, 1993; Yoo, 1991; Fu, 1991). Thus a basic understanding of the bonding character of, e.g. transition-metal aluminides has been reached and it has been shown that the degree of directional d-electron bonding determines the ideal cleavage strength (Fu and Yoo, 1992a). However, it has also been shown for B2 transition-metal aluminides that the ductility or brittleness is too complex a function of the strength and character of bonding to establish simple relations between the electronic distribution parameters and the mechanical properties (Schultz and Davenport, 1992, 1993).

2.3 Criteria for Phase Selection

Candidate phases for materials developments are selected in view of specific applications, i.e. they must show certain properties which make them promising for a particular application. For permanent magnets the "energy product" $|\boldsymbol{B}\cdot\boldsymbol{H}|$ is a figure of merit and should reach high values (e.g. Stadelmaier et al., 1991), whereas for other functional materials other physical parameters are decisive.

Selection criteria with respect to structural applications at high temperatures have already been discussed by Sauthoff (1989). First, such phases must have sufficient strength at the service temperature which also means sufficient creep resistance. The creep resistance scales with the diffusion coefficient and with the shear modulus (e.g. Jung et al., 1987), and both parameters scale with the melting temperature (Frost and Ashby, 1982). Thus the

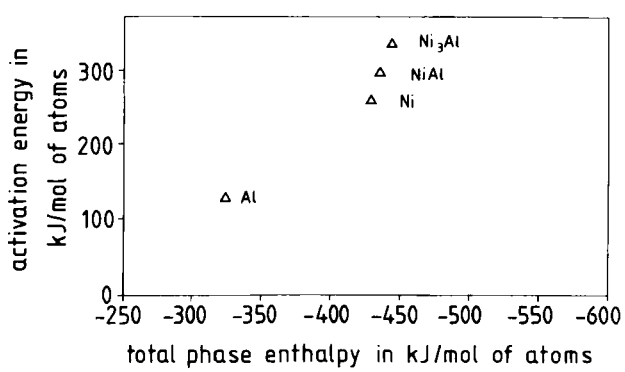


Figure 7. Activation energy of diffusion as a function of total phase enthalpy for Ni, Al, NiAl and Ni_3Al (Frost and Ashby, 1982; Wever et al., 1989; Engell et al., 1991; Von Keitz and Sauthoff, 1991).

ArcelorMittal Ex. 2038
Page 22 of 190

candidate phase should have a sufficiently high melting temperature. The limiting temperature for structural applications of conventional metallic alloys is of the order of 75% of the melting temperature in many cases. The most advanced, high-temperature alloys are the Ni-base superalloys, and they are used in gas turbines with service temperatures of up to about 1100°C (Petrasek et al., 1986). Thus phases with melting temperatures above 1600°C have to be considered if application temperatures above those of superalloys are aimed at. High-melting phases may form low-melting eutectics which may affect the phase stability during processing or service, and therefore such phases with low-melting eutectics should be avoided.

For many functional and structural applications density is a very important and sometimes decisive parameter. Structural intermetallics for moving components must have sufficiently high specific strength, which is the ratio of strength and weight density, and which has the dimension of length. The specific fracture strength, i.e. the rupture length, of advanced superalloys, e.g. the mechanically alloyed, oxide-dispersion strengthened (ODS) superalloy MA 6000, is of the order of 15 km (Inco, 1982), which has to be surpassed by new structural materials. Phases which contain light elements, e.g. Ti, Al, Si, or Mg, may have such a low density that they compare favorably with conventional alloys in spite of lower strength or a restricted temperature range.

The main problem with strong intermetallics is their brittleness, which makes processing and application difficult or impossible. However, the brittleness of intermetallics should be less severe than that of ceramics because the atomic bonding of intermetallics is, at least partially, still metallic, whereas it is primarily covalent or

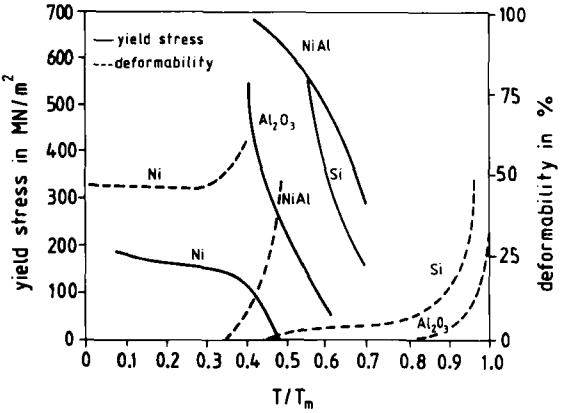


Figure 8. Yield stress and deformability as a function of homologous temperature T/T_m (with T_m = melting temperature) for various materials with different types of atomic bonding (Westbrook, 1965).

ionic in ceramics. This is illustrated in Fig. 8 which compares the temperature dependence of the yield stress and deformability of the intermetallic NiAl with that of nickel, and of silicon and alumina. NiAl, which is a candidate phase for high-temperature applications, softens with rising temperature at about half the melting temperature T_m, which is the range for Si with covalent bonding and which is higher than that of the ceramic Al_2O_3. However, the brittle-to-ductile transition temperature is about 0.4 T_m for NiAl, whereas it is above 0.8 T_m for Si and Al_2O_3, i.e. the deformation behavior of such an intermetallic may be regarded as intermediate between metals and ceramics.

Plastic deformation is more difficult in intermetallics than in metals and conventional metals alloys because of the stronger atomic bonding and the resulting ordered atomic distribution, which gives rise to more complex crystal structures (Paufler, 1985). Experience indeed shows that the brittleness of intermetallics increases with decreasing lattice symmetry and increasing

ArcelorMittal Ex. 2038
Page 23 of 190

unit cell size (Paufler, 1976). Therefore intermetallics with high crystal symmetry – possibly cubic phases – and small unit cells are preferred for developing new structural materials. Figure 1 shows such crystal structures which are cubic (B2, $D0_3$ or $L2_1$, $L1_2$, $L'1_2$) or nearly cubic, i.e. tetragonally distorted ($L1_0$, $D0_{22}$), and some of the examples – FeAl, NiAl, Fe_3Al, Ni_3Al, or TiAl – are candidate phases for developments of structural materials.

However, even for such selected phases brittleness remains a problem and the causes of this are manifold (Liu et al., 1990; Baker and George, 1992). A material fractures in a brittle manner if there is no plastic deformation and stress relaxation at the crack tip, i.e. the yield stress is higher than the stress for cleavage or fracture. The reason for this may be an insufficient number and/or mobility of dislocations, and/or an insufficient number of slip systems. Since these parameters depend not only on crystal symmetry, but also on the specific characteristics of the particular phases, the aim of phase selection and composition variation by alloying must be dislocations with low energies and high mobilities and at least five independent deformation modes, i.e. dislocation slip systems and twinning systems, which are necessary for general homogeneous plastic deformation according to the Von Mises criterion (von Mises, 1928; Kocks, 1958, 1970; Kocks and Canova, 1981; Fleischer, 1988). Crystal anisotropy is an important factor in brittleness and criteria are used which rely on elastic moduli relations (Paxton and Pettifor, 1992). Brittle fracture may be a result of weak grain boundaries and other microstructure heterogeneities leading to localized deformation and stress concentrations. The disproportion of yield stress and fracture stress may also be due to a very low surface energy, which makes cleavage and cracking easy. This may be aggravated by the segregation of impurities which usually decrease the surface energies (Hondros, 1978). Impurities – in particular oxygen – may enter the material from the environment, and thus environmental embrittlement is an important issue for many intermetallics (Liu et al., 1990; Liu, 1991 a). A detailed knowledge of the thermodynamics and kinetics of the particular alloy system is necessary for a reduction in the various embrittling effects.

Intermetallics for any applications must be corrosion resistant in the respective environments. For high-temperature applications this means oxidation resistance in most cases. Oxidation resistance is provided by the presence of elements – in particular Cr, Al, or Si – which can form protective oxide layers (e.g., Aitken, 1967; Hindam and Whittle, 1982; Fitzer and Schlichting, 1983; Meier and Pettit, 1992). However, chromium oxide is volatile above 1000 °C and silicon oxide may form low-melting silicates. Thus aluminides are strongly favored for high-temperature applications. In order to act as protective layers, the scales must have sufficient density and adherence which may be improved by alloying with further elements (macroalloying) and, in particular, by adding minor amounts of "active" elements, e.g., Ti, Zr, or Hf (microalloying) (Rahmel and Schwenk, 1977; Hindam and Whittle, 1982). Furthermore, the scales must exhibit sufficient long-term stability which also means mechanical stability, i.e. they must tolerate strains, e.g. during creep, without being damaged (Riedel, 1982). In the case of insufficient oxidation resistance, protective coatings may be applied (see Pettit and Goward, 1983; Weatherill and Gill, 1988; Patnaik, 1989; Nicholls and Stephenson, 1991). However, the thermal stability of

ArcelorMittal Ex. 2038
Page 24 of 190

such coatings decreases with increasing temperature because of increasing reaction and diffusion rates, and therefore intermetallics for applications above 1100 °C should be inherently oxidation-resistant.

Finally, it must already be possible to prepare an intermetallic of sufficient quality in the laboratory, and from a practical point of view this is the basic requirement for any materials development. The processing of high-strength intermetallics is difficult because of their brittleness, and development of the necessary processing techniques is a very demanding task. It is, however, also a very important task, because a poor quality increases the apparent brittleness and reduces the strength which may then preclude any applications of the tested material.

3 Titanium Aluminides and Related Phases

3.1 Ti_3Al

3.1.1 Basic Properties and Phase Diagram

The titanium aluminide Ti_3Al – often designated α_2 phase – crystallizes with the hexagonal ordered $D0_{19}$ structure (Ni_3Sn-type) which is shown in Fig. 9. The ratio of the lattice parameters c and a is $c/a = 0.8$ (Eckerlin et al., 1971; Villars and Calvert, 1991). The generally accepted value for the density is 4.2 g/cm³ (Fleischer, 1985; Munroe and Baker, 1988; Destefani, 1989), whereas for Ti_3Al-base alloys the range 4.1–4.7 g/cm³ is given (see Table 2). This low density has made the titanium aluminides very attractive for materials developments.

The characteristics of thermal expansion were described by Shashikala et al. (1989).

Table 2. Properties of alloys based on the titanium aluminides Ti_3Al and TiAl compared with conventional titanium alloys and nickel-base superalloys (Morral, 1980; Lipsitt, 1985a; Kim, 1989; Kim and Froes, 1990; Froes et al., 1991).

Property	Ti-base	Ti_3Al-base	TiAl-base	Superalloys
Structure	A3/A2	$D0_{19}$/A2/B2	$L1_0$/$D0_{19}$	A1/$L1_2$
Density (g/cm³)	4.5	4.1–4.7	3.7–3.9	7.9–9.1
Young's modulus at room temperature (GN/m²)	95–115	100–145	160–180	195–220
Yield strength at room temperature (MN/m²)	380–1150	700–990	400–650	250–1310
Tensile strength at room temperature (MN/m²)	480–1200	800–1140	450–800	620–1620
Temperature limit due to creep (°C)	600	760	1000	1090
Temperature limit due to oxidation (°C)	600	650	900	1090
Tensile strain to fracture at room temperature (%)	10–25	2–26	1–4	3–50
Tensile strain to fracture at high temperature (%)	12–50	10–20	10–60	8–125
Fracture toughness K_{Ic} at room temperature (MN/m$^{3/2}$)	high	13–42	10–20	25

ArcelorMittal Ex. 2038
Page 25 of 190

copyright © VCH Verlagsgesellschaft mbH, 1995

such coatings decreases with increasing temperature because of increasing reaction and diffusion rates, and therefore intermetallics for applications above 1100 °C should be inherently oxidation-resistant.

Finally, it must already be possible to prepare an intermetallic of sufficient quality in the laboratory, and from a practical point of view this is the basic requirement for any materials development. The processing of high-strength intermetallics is difficult because of their brittleness, and development of the necessary processing techniques is a very demanding task. It is, however, also a very important task, because a poor quality increases the apparent brittleness and reduces the strength which may then preclude any applications of the tested material.

3 Titanium Aluminides and Related Phases

3.1 Ti_3Al

3.1.1 Basic Properties and Phase Diagram

The titanium aluminide Ti_3Al – often designated α_2 phase – crystallizes with the hexagonal ordered $D0_{19}$ structure (Ni_3Sn-type) which is shown in Fig. 9. The ratio of the lattice parameters c and a is $c/a = 0.8$ (Eckerlin et al., 1971; Villars and Calvert, 1991). The generally accepted value for the density is 4.2 g/cm^3 (Fleischer, 1985; Munroe and Baker, 1988; Destefani, 1989), whereas for Ti_3Al-base alloys the range 4.1–4.7 g/cm^3 is given (see Table 2). This low density has made the titanium aluminides very attractive for materials developments.

The characteristics of thermal expansion were described by Shashikala et al. (1989).

Table 2. Properties of alloys based on the titanium aluminides Ti_3Al and TiAl compared with conventional titanium alloys and nickel-base superalloys (Morral, 1980; Lipsitt, 1985a; Kim, 1989; Kim and Froes, 1990; Froes et al., 1991).

Property	Ti-base	Ti_3Al-base	TiAl-base	Superalloys
Structure	A3/A2	$D0_{19}$/A2/B2	$L1_0$/$D0_{19}$	A1/$L1_2$
Density (g/cm^3)	4.5	4.1–4.7	3.7–3.9	7.9–9.1
Young's modulus at room temperature (GN/m^2)	95–115	100–145	160–180	195–220
Yield strength at room temperature (MN/m^2)	380–1150	700–990	400–650	250–1310
Tensile strength at room temperature (MN/m^2)	480–1200	800–1140	450–800	620–1620
Temperature limit due to creep (°C)	600	760	1000	1090
Temperature limit due to oxidation (°C)	600	650	900	1090
Tensile strain to fracture at room temperature (%)	10–25	2–26	1–4	3–50
Tensile strain to fracture at high temperature (%)	12–50	10–20	10–60	8–125
Fracture toughness K_{Ic} at room temperature (MN/m$^{3/2}$)	high	13–42	10–20	25

ArcelorMittal Ex. 2038
Page 26 of 190

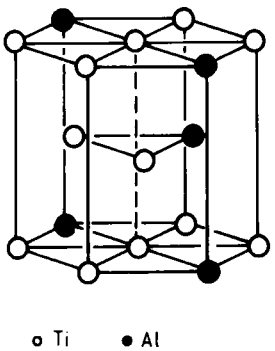
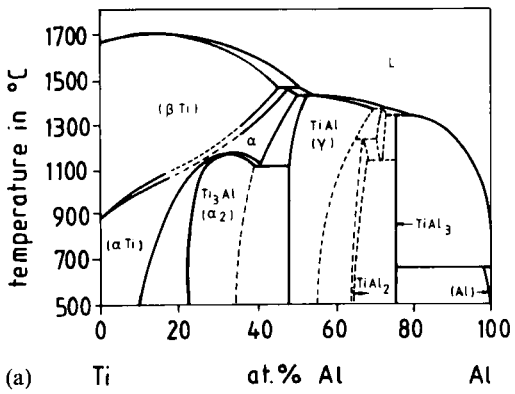


Figure 9. $D0_{19}$ crystal structure of Ti_3Al.



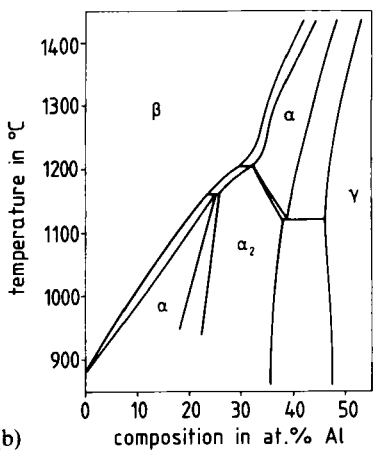


Figure 10. (a) Ti–Al phase diagram according to Huang and Siemers (1989), Froes et al. (1991), Y. A. Chang et al. (1991), and Kim and Dimiduk (1991) and (b) revised version on the basis of new data according to Hellwig et al. (1992) and Kainuma et al. (1994).

The temperature and composition dependence of the elastic constants of polycrystalline Ti_3Al were studied (Schafrik, 1977), and, in particular, Young's modulus = 149 GPa, shear modulus = 58 GPa and Poisson's ratio = 0.29 were found for Ti_3Al with 26 at.% Al at room temperature. Young's moduli for Ti_3Al-base alloys are in the range 100–145 GPa, which compares favorably with 96–110 GPa for conventional Ti-base alloys (Kimura et al., 1990; Froes et al., 1991). It has to be noted that in the case of Ti_3Al (as in other cases) very different values have been measured for the Young's modulus, e.g. 77 MPa (Wolfenden et al., 1989). This emphasizes the fact that the elastic moduli depend sensitively on the alloy composition and microstructure including all artifacts which may be introduced during processing.

Ti_3Al has an extended composition range, as is visible in the commonly used Ti–Al phase diagram (Fig. 10a), which, however, is still in discussion and has recently been revised, as shown in Fig. 10b (Hellwig et al., 1992; Kainuma et al., 1994). It forms stable equilibria with the two disordered Ti phases, α-Ti with a hexagonal close-packed A3 structure and β-Ti with a b.c.c. A2 structure, and with the other important titanium aluminide TiAl, which is the subject of Sec. 3.2. The stabilities of the various phases in the Ti–Al system have been studied theoretically by first-principles calculations (Asta et al., 1993). It is noted that these equilibria, i.e. equilibrium compositions and transition temperatures, depend in a sensitive way on impurity contents, in particular on oxygen (Kahveci and Welsch, 1986; Huang and Siemers, 1989; Froes et al. 1991; Saunders and Chandrasekaran, 1992). Basic knowledge of the Ti–Al–O system is available (Glazova, 1965; Rahmel and Spencer,

ArcelorMittal Ex. 2038
Page 27 of 190

1991; Saunders and Chandrasekaran, 1992; Hoch and Lin, 1993), but the consequences of small oxygen additions on the Ti_3Al equilibria have not yet been worked out in sufficient quantitative detail.

Ti_3Al has been alloyed with various substitutional and interstitial elements in order to control and optimize the mechanical properties and the corrosion behavior (Froes et al., 1991). With respect to the mechanical behavior, alloying with Nb, which substitutes for Ti, is very important (Rowe, 1990). The Ti–Al–Nb system has been analyzed recently (Hellwig, 1990; Kattner and Boettinger, 1992), and Fig. 11 shows a tentative version of the ternary Ti–Al–Nb phase diagram according to Hellwig (1990). It should be noted that the various equilibria in this diagram are not yet completely understood and are still in discussion because of conflicting experimental observations. In particular, additional phases, i.e. the orthorhombic O phase Ti_2AlNb, ω structures, and a T_2 phase have been observed, and used, in the Ti-rich corner besides the B2 phase (Rowe et al., 1991; Rowe, 1990; Koss et al., 1990; Perepezko, 1991a; Muraleedharan et al., 1992a, b; Bendersky et al., 1992; Hsiung and Wadley, 1992). The limited knowledge of the respective phase equilibria has been overviewed (Kim and Froes, 1990; Das et al., 1993a). An improved understanding of these phase equilibria has been achieved by diffusion couple experiments and diffusion path analyses from which diffusion data can be obtained (Ma et al., 1992). The effects of alloying with Mo and V on the phase relationships have been studied recently (Das et al., 1993b; Ma and Dayananda, 1993).

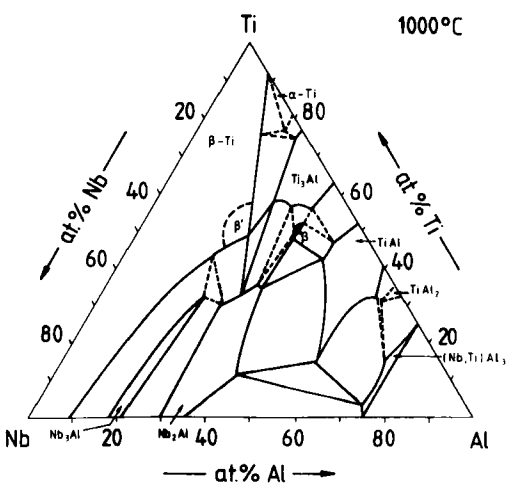


Figure 11. Isothermal Ti–Al–Nb phase diagram section at 1000 °C where the β′ phase with a B2 structure transforms into an ω phase at lower temperatures (Hellwig, 1990).

3.1.2 Microstructure and Mechanical Behavior

Figure 12 shows the temperature dependence of the strength and plastic deformability of single-phase polycrystalline Ti_3Al according to Lipsitt et al. (1980). It can be seen that this phase is brittle with practically no deformability at low temperatures up to 600 °C. Above this temperature plastic deformation was observed which was, however, still paralleled by intergranular cracking. Correspondingly, the fracture strength is nearly 600 MPa up to 600 °C. Above that temperature thermally activated softening occurs, which makes plastic deformation possible, and the resulting yielding leads to yield strengths below the fracture strength.

The micromechanisms of deformation and in particular the dislocation reactions have been analyzed in detail and have been discussed with respect to strength and ductility (Koss et al., 1990; Kim and Froes, 1990; Yamaguchi and Umakoshi, 1990; Froes et al., 1991; Umakoshi et al., 1993a, b). In the $D0_{19}$ structure five independent slip systems are possible (Kim and Froes,

ArcelorMittal Ex. 2038
Page 28 of 190

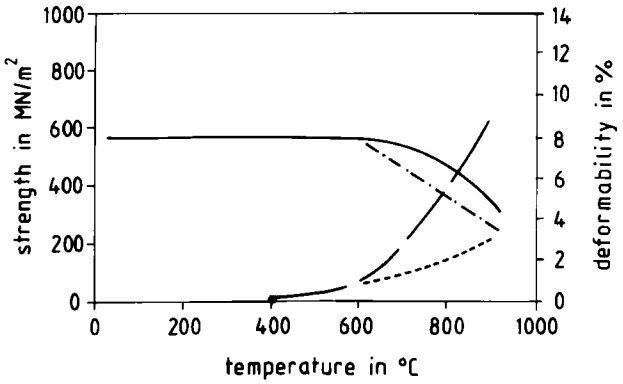


Figure 12. Tensile strength and plastic deformability as a function of temperature for single-phase, polycrystalline, stoichiometric Ti_3Al; ——— = fracture stress (below 600 °C) or ultimate tensile strength, —·— = yield stress, ——— = apparent deformability including microcracking, ---- = estimated deformability without microcracking (Lipsitt et al., 1980).

1990), which would satisfy the Von Mises criterion for uniform deformation (von Mises, 1928). However, single-crystal studies have shown that the yield stresses for the different slip systems are widely different (Minonishi, 1991; Nakano and Umakoshi, 1993), and thus not all five slip systems are activated during the deformation of polycrystalline Ti_3Al. Only a little tensile ductility has been found for basal slip, whereas prism slip results in very large tensile elongations (Inui et al., 1993). Since there is no stress-relieving twinning, as in hexagonal metals, the insufficient number of slip systems, together with the observed planarity of slip, leads to strain incompatibilities and stress concentrations at grain boundaries from which cleavage fracture results (Koss et al., 1990; Kim and Froes, 1990; Froes et al., 1991).

It is noted that one of the possible slip systems in single crystals shows an anomalous temperature dependence for the yield stress (Minonishi, 1991; Umakoshi et al., 1993 b), i.e. the yield stress increases with rising temperature until a maximum is reached. Such an anomalous temperature dependence is characteristic of various intermetallics and has been analyzed in much detail for the well-known case of Ni_3Al, which is discussed in Sec. 4.1.2. The findings for Ni_3Al, however, do not apply in the case of Ti_3Al because of different dislocation configurations (Minonishi, 1991). It has to be emphasized that the effect can only be observed in appropriately oriented, monocrystalline Ti_3Al because the respective slip system is not activated in polycrystalline Ti_3Al.

The aim of the various materials developments based on Ti_3Al is to improve both the strength and ductility by alloying with further elements and by controlling the microstructure (Rowe, 1990; Froes et al., 1991). The most effective element for improving ductility is Nb, as is illustrated in Fig. 13, and indeed Ti_3Al-base alloys of engineering significance, i.e. α_2 alloys and super-α_2 alloys, contain 10–30 at.% Nb (Rowe, 1990; Froes et al., 1991). In spite of the extensive development work and the related numerous studies of microstructure and properties, the mechanism by which Nb improves the ductility of such Ti_3Al-base alloys is not yet clear (Froes et al., 1991). Small amounts of Nb, which substitutes for Ti, lead to the activation of more slip systems which, however, has only a small effect on the ductility. Larger amounts of Nb result in the formation of further phases, i.e. β-Ti in the disordered state with an A2 structure or in the ordered state with a B2 structure and/or the already mentioned orthorhombic O phase,

ArcelorMittal Ex. 2038
Page 29 of 190

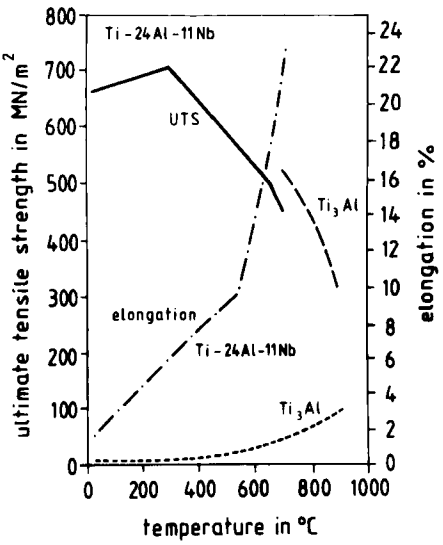


Figure 13. Temperature dependence of strength for Ti_3Al (———) and Ti–24 at.% Al–11 at.% Nb (——), and of tensile elongation for Ti_3Al (-----) and (Ti–24 at.% Al–11 at.% Nb (–·–·–·–) (Rowe, 1990).

which limit the slip length and have a significant, beneficial effect on the ductility. The dislocation configurations in the O phase have recently been studied (Douin et al., 1993).

The alloys with good combinations of strength and ductility are multiphase intermetallic alloys with complex microstructures which may contain primary α_2 grains, fine secondary α_2 Widmanstätten platelets or laths, β grains in the disordered A2 or the ordered B2 state, ω phase grains, and perhaps O phase grains (Koss et al., 1990; Rowe, 1990; Kim and Froes, 1990; J. M. Larsen et al., 1990; Froes et al., 1991). In any case, the mechanical behavior depends in a rather sensitive way on the distributions of the various phases, i.e. on the number, size, shape, composition, crystal structure, interface structure, and neighborhood relationships of the various grains. The phase distribution can be varied appreciably by proper selection of the alloy composition and by thermomechanical treatments (Koss et al., 1990; Rowe, 1990; Kim and Froes, 1990; J. M. Larsen et al., 1990; Froes et al., 1991, 1992). Thus careful control of the processing is necessary for the optimization and reproducible production of α_2 alloys. It was found in particular that the optimum alloy microstructures are different for different mechanical properties, e.g. tensile strength, tensile ductility, creep resistance, fatigue crack growth resistance, and high cycle fatigue resistance (Rowe, 1990). The various toughening mechanisms have been reviewed recently with respect to crack initiation and crack growth in TiAl (Chan, 1993a).

Alloying with Nb improves most of the mechanical properties and the effect increases with increasing Nb. The only notable exception is the creep resistance which is a decisive property for high-temperature applications. Nb was found to reduce the creep resistance although it has also been found that the Nb-containing O phase may be beneficial for the creep resistance (Rowe, 1990; Kim and Froes, 1990; Froes et al., 1991; Nandy et al., 1993). Obviously the creep resistance is also a very sensitive function of the phase distribution, and current research aims at clarifying the conditions for optimum creep resistance (Hayes, 1991; Morris, 1991a; Huang and Kim, 1991; Es-Souni et al. 1991; Lupinc et al., 1991; Onodera et al., 1991; Thompson and Pollock, 1991). The creep mechanisms have been overviewed (Yamaguchi and Umakoshi, 1990; Koss et al., 1990). The observed creep follows the known relationships for conventional disordered alloys, which has also been found for other intermetallics and will be discussed in Sec. 4.3.4 with NiAl alloys as examples. Diffusion data which are needed for analyzing and optimizing the creep behavior are

ArcelorMittal Ex. 2038
Page 30 of 190

available, in particular for the Ti–Al–Nb system (van Loo and Rieck, 1973; Dayananda, 1992).

Other alloying elements for improving the strength are Cr, Ta, and Mo. The latter is also advantageous for the creep resistance (Froes et al., 1991). Minor alloying additions of Fe, C and Si affect the creep behavior significantly, with Fe having the most deleterious effect (Rowe, 1990). Besides the cited elements, V and Sn were used for improving the properties. Alloying with Zr increases both the strength and the ductility, and microalloying with Y and B has been used to control the grain size and improve the ductility and workability (Froes et al., 1991). Very fine and stable grain sizes can be produced by rapid solidification of alloys with fine dispersions of rare earth oxides, e.g. Er_2O_3 (Suryanarayana et al., 1991). In such alloys the small grain size improves the ductility, whereas the dispersoids enhance the strength at the expense of ductility.

Similar effects can be produced by the precipitation of strengthening phases. This has been exemplified by materials developments which rely on the alloying of Ti_3Al with Si to produce Ti_5Si_3 as a strengthening second phase (see Wu et al., 1989; Es-Souni et al., 1991, 1992a). Ti_5Si_3 is a very hard and brittle phase with a complex hexagonal $D8_8$ structure, low density and a melting temperature above 2000 °C (see Sec. 11.3). Further alloying of such two-phase alloys with Nb is beneficial with respect to the mechanical behavior (Wagner et al., 1991; Es-Souni et al., 1991, 1992a).

α_2 alloys of current engineering significance are Ti–24Al–11Nb, Ti–25Al–10Nb–3V–1Mo, Ti–25Al–17Nb–1Mo, and Ti–23.5Al–24Nb (Froes et al., 1991), and the ranges of characteristic properties for these alloys are given in Table 2. The mechanical behavior, i.e. strength, ductility, fatigue, fracture, and creep, has been discussed in detail in various recent reviews, in particular with respect to the various effects of the microstructure (Koss et al., 1990; Rowe, 1990; Kim and Froes, 1990; J. M. Larsen et al., 1990; Yamaguchi and Umakoshi, 1990; Froes et al., 1991; Kumpfert et al., 1992; Stoloff et al., 1993); see also the chapter by Umakoshi in Volume 6 of MST. It is noted that superplastic deformation is also possible, during which dynamic grain growth with a decreasing volume fraction of Ti_3Al occurs (H. S. Yang et al., 1992, 1993).

3.1.3 Environmental Effects

Exposure of Ti_3Al or Ti_3Al-base alloys to oxygen at higher temperatures leads to oxidation on the one hand and to oxygen dissolution in the alloy on the other (Rowe, 1990; Kim and Froes, 1990; Froes et al., 1991). Oxidation resistance would be expected if a protective Al_2O_3, layer could be formed by selective oxidation. However, Al_2O_3 is only slightly more stable than TiO and the activity of Ti is much higher than that of Al in Ti_3Al (Meier and Pettit, 1992). Thus TiO is the stable oxide in contact with Ti_3Al and further oxidation leads to the formation of TiO_2, i.e. rutile. The thermodynamics of the system Ti–Al–O and the equilibrium conditions for the formation of the various oxide phases have been studied in detail (Rahmel and Spencer, 1991; Pajunen and Kivilahti, 1992; Li et al., 1992; Zhang et al., 1992b; Saunders and Chandrasekaran, 1992).

According to these thermodynamic considerations, the observed oxidation behavior is complex leading to a layered oxide scale structure with TiO_2 on the outside and oxides with higher metal contents underneath, including Al_2O_3 (Khobaib and

ArcelorMittal Ex. 2038
Page 31 of 190

Vahldiek, 1988; Shida and Anada, 1993). The kinetics follows a parabolic rate law and the rate constants of Ti_3Al oxidation are only slightly smaller than those of typical TiO_2 formers, i.e. conventional Ti alloys (Choudhury et al., 1976; Perkins et al., 1989; Meier et al., 1989; Welsch and Kahveci, 1989). Nb increases the oxidation resistance to such an extent that the obtained rate constants are intermediate between those of TiO_2 formers and Al_2O_3 formers (Choudhury et al., 1976; Khobaib and Vahldiek, 1988; Wiedeman et al. 1989; Welsch and Kahveci, 1989; Rowe, 1990; Kim and Froes, 1990). The oxidation resistance of Ti_3Al-base alloys may also be improved by alloying with Mo or Ta (Froes et al., 1991; Schaeffer, 1993).

The obtained oxidation resistances are not yet sufficient and limit the application of Ti_3Al-base alloys at high temperatures, as is shown in Table 2. Therefore the coating of these alloys is studied extensively. In particular, pack-cementation techniques are optimized for aluminizing the alloy surface region to Al_3Ti and avoiding surface cracking (Kung, 1990; Smialek et al., 1990 b).

Besides scale formation at the surface, oxygen diffuses into Ti_3Al as a solute since Ti_3Al has a comparatively high solubility for oxygen. This leads to embrittlement, i.e. the strength is increased and the ductility is decreased, and to crack formation at the surface (Balsone, 1989; Rowe, 1990; Kim and Froes, 1990; McKee, 1993). The rate of embrittlement and crack formation is controlled by diffusion processes which can only be slowed down by protective coatings. It is noted that in spite of the inward diffusion of oxygen, internal oxidation with the formation of fine oxide particle dispersions has not been reported. The fact that classical internal oxidation does not occur, even though a protective oxide layer has not formed or has broken down, is a common feature of many intermetallics and results from the particular thermodynamic and kinetic conditions in the respective alloy systems (Meier and Pettit, 1992).

Another important environmental element is hydrogen (Chu and Thompson, 1991; Eliezer et al., 1991). It stabilizes the β phase in the Ti–Al system, i.e. it affects the thermodynamics of the system and thereby the microstructure evolution appreciably. It is indeed used as a temporary alloying element during thermochemical processing of conventional α/β titanium alloys for refining the microstructure. The solubility of H is highest in β-Ti, lower in α-Ti and still lower in Ti_3Al. Nevertheless, Ti_3Al still dissolves significant amounts of H at high temperatures, which is precipitated as hydrides during cooling because of the lower solubility at lower temperatures (Chu and Thompson, 1991; Eliezer et al., 1991). Structure, shape and orientation relationships of the hydrides have been reported (Shih et al., 1989; Gao et al., 1990).

Like other alloys, Ti_3Al-base alloys are embrittled by both dissolved hydrogen and precipitated hydrides which leads to hydrogen-induced cracking (Eliezer et al., 1991; Gao et al., 1990; Chu and Thompson, 1991, 1992; Chu et al., 1992; Thompson, 1992, 1993). However, with special hydrogen loading conditions and heat treatments, i.e. thermochemical treatments, the strength, ductility and toughness can also be improved (Chu and Thompson, 1991). In particular, a hydrogen-tolerant microstructure has been developed for not too high hydrogen contents (Chan, 1992, 1993 b). More work is necessary here in order to understand the microstructural mechanisms and utilize thermochemical processing for the optimization of the mechanical behavior (Eliezer et al., 1991; Thompson, 1992).

ArcelorMittal Ex. 2038
Page 32 of 190

3.1.4 Applications

The developments of Ti_3Al-based α_2 alloys have progressed in such a successful way that the α_2 alloys have been on the brink of commercialization for several years (Lipsitt, 1985a, b, 1993; Fleischer et al., 1989a; Dimiduk et al., 1992; Froes et al., 1992). α_2 alloys are being produced in ingots of up to 4500 kg and are available as cast shapes or wrought forms including billets, bars, plates, and sheet (Peacock, 1989; Wittenauer et al., 1989; Chesnutt, 1990; Bassi et al., 1991). Likewise the powder metallurgy methods which have been developed for conventional titanium alloys are readily adapted, and in addition other powder metallurgy methods – in particular reactive processing – have been applied to Ti_3Al-base alloys (Froes et al., 1991). α_2 alloys can be machined, sheet can be deformed superplastically and diffusion bonded to form complex sheet parts, and the various manufacturing processes can be accomplished on conventional equipment (Lipsitt, 1985a; Wittenauer et al., 1989; Bassi et al., 1991). Joining studies have shown that α_2 alloys can be joined successfully by both diffusion bonding and linear friction welding, whereas with fusion welding problems of microstructure control may be encountered (Threadgill and Baeslack, 1991; Baeslack et al., 1988; Cieslak et al., 1990). Components for applications in flying gas turbines have been produced, they have been engine tested as static structures and they are nearing engine qualification (Lipsitt, 1985a, b; Dimiduk et al., 1992). Examples are combustor swirlers, compressor casing sections, support rings, and afterburner nozzle seals.

In spite of these successes the α_2 alloy components are not yet flying (Froes et al., 1991), i.e. they are not yet implemented because expectations have risen with respect to strength and oxidation resistance, there are problems of ignition in some compressor applications, there is environmental embrittlement, and finally there are economic barriers (Dimiduk et al., 1992). Thus widespread use of α_2 alloys is expected only after further alloy and coating developments.

Nevertheless, the α_2 alloys are being considered for many future aerospace applications (Roland, 1989; Dimiduk et al., 1991; Dauphin et al., 1991; Froes et al., 1991). Major initiatives are programs for developing piloted aerospace vehicles with hypersonic speeds, and examples are the U.S. National Aero-Space Plane (NASP) (Ronald, 1989) and the German Sänger Project (Kuczera et al., 1991; Bunk, 1992). Here specific strength, i.e. strength per unit density or specific gravity, is of primary interest and alloys to be selected have to compete with metallic and nonmetallic high-strength materials. In order to meet the design criteria, α_2 alloys are considered as matrix materials of intermetallic matrix composites, and respective materials developments are in progress (Bassi et al., 1991; Ronald, 1989; Bowman and Noebe, 1989; Destefani, 1989; Stephens, 1990; J. M. Larsen et al., 1990; MacKay et al., 1991; Norman et al., 1990; Feng and Michel, 1991; Jha et al., 1991a, b; Kumar, 1991; Froes et al., 1991; Bryant et al., 1991; Marshall et al., 1992).

Besides the problems of mechanical compatibility of the composite constituents, which are already present in conventional multiphase alloys, there is the problem of chemical stability which may be affected by reactions between the composite constituents (Norman et al., 1990). Thus composite developments aim at the optimization of composition and microstructure with respect to composite sta-

ArcelorMittal Ex. 2038
Page 33 of 190

bility, tensile properties, thermal and mechanical fatigue resistance, creep resistance, and corrosion resistance, as is exemplified by MacKay et al. (1991). Finally, the success of such developments depends on economics, i.e. total life cycle costs.

3.2 TiAl

3.2.1 Basic Properties and Phase Diagram

The titanium aluminide TiAl – often designated as γ phase – crystallizes with the tetragonal $L1_0$ structure (CuAu-type) which is shown in Fig. 1. The $L1_0$ structure results from ordering in the f.c.c. lattice (A1), i.e. it is basically a cubic structure which is tetragonally distorted because of the particular stacking of the atom planes, as is seen in Fig. 1. The ratio of the lattice parameters c and a is $c/a = 1.015$ at the stoichiometric composition and the density is 3.76 g/cm^3 (Kim and Dimiduk, 1991), whereas for TiAl-base alloys the range 3.7–3.9 g/cm^3 is given (see Table 2). This density is still lower than that of Ti_3Al and has made the titanium aluminides most attractive for materials developments.

The temperature dependence of the elastic constants of polycrystalline TiAl was studied (Schafrik, 1977), and Young's modulus = 174 GPa, shear modulus = 70 GPa, and Poisson's ratio = 0.23 were found for stoichiometric TiAl at room temperature, i.e. the elastic constants are larger and Poisson's ratio is smaller than for Ti_3Al. Elastic constants and fault energies of TiAl have been studied theoretically by first-principles total-energy investigations and have been discussed with respect to mechanical behavior (Yoo et al., 1991; Lee and Yoo, 1990; Fu and Yoo, 1990; Yoo, 1991; Woodward et al., 1993; Yoo and Fu, 1991, 1993). Young's moduli for TiAl-base alloys are in the range 160–180 GPa which is only 10–20% lower than that of the superalloys (see Table 2). Recently, it has been found by ab initio calculations that deviations from stoichiometry are due to accommodated antistructure atoms, i.e. constitutional disorder, instead of vacancies in the sublattices, and that the concentration of thermal vacancies is comparatively low because of the high formation energy (Fu and Yoo, 1993). The self-diffusion of Ti in TiAl has been studied (Kroll et al., 1992).

TiAl has an extended composition range and is stable up to the melting point, as is shown in the Ti–Al phase diagram (Fig. 10). The variation in Al content between the solubility limits leads to constitutional disorder with excess Ti or Al atoms on Al or Ti sites, respectively, i.e. antistructure atoms on antisites without constitutional vacancies, and it results in a corresponding variation in the c/a ratio, i.e. the tetragonality, between 1.03 for maximum Al content and 1.01 for minimum Al content (Yamaguchi and Umakoshi, 1990; Kim and Dimiduk, 1991; Shirai and Yamaguchi, 1992). The stability of the various phases in the Ti–Al system has been studied theoretically by first-principles calculations (Asta et al., 1993). It is noted that the Ti–Al phase diagram has been in discussion for many years and presently the version in Fig. 10a is generally used on the basis of various recent studies (Y. A. Chang et al., 1991; Shull and Cline, 1990; Perepezko, 1991a, b; Huang and Siemers, 1989; Kim and Dimiduk, 1991; Rowe und Huang, 1988; Kattner et al., 1992; Jones and Kaufman, 1993; Anderson et al., 1993). Nevertheless, the phase equilibria with TiAl at high temperatures are still not clear, and a new, careful study has resulted in a revised diagram, as shown in Fig. 10b (Hellwig et al., 1992;

ArcelorMittal Ex. 2038
Page 34 of 190

Kainuma et al., 1994). As already noted with respect to Ti_3Al, the phase equilibria, i.e. equilibrium compositions and transition temperatures, depend in a sensitive way on impurity contents, in particular on oxygen (Kahveci and Welsch, 1986; Huang and Siemers, 1989; Froes et al., 1991; Saunders and Chandrasekaran, 1992).

TiAl has been alloyed with various substitutional and interstitial elements in order to control and optimize the mechanical properties and the corrosion behavior (Hashimoto et al., 1986a, b, 1991; Kasahara et al., 1987; Tsujimoto and Hashimoto, 1989; Froes et al., 1991; Kim and Dimiduk, 1991). Alloying elements have different effects on the extension of the TiAl field in the respective ternary phase diagrams, as is shown schematically in Fig. 14. In this crude approximation, V, Mn, and Cr apparently act as Al substituents or as both Ti and Al substituents whereas Nb, Ta, Zr, Mo, and W act as Ti substituents (Kim and Dimiduk, 1991; X. F. Chen et al., 1992). The site preference of such alloying additions in the TiAl lattice and their effect on the tetragonality have been studied recently by ab initio calculations and the results are in partial agreement with the above experimental findings (Erschbaumer et al., 1993). In detail, the effects are complex and also depend on the amount of alloying addition, as is revealed by the available ternary phase diagrams for TiAl with Nb (see Fig. 11), Mn, Zr, V, or Ag (Hashimoto et al., 1986a, b; Kasahara et al., 1987; Tsujimoto and Hashimoto, 1989; Kim, 1989; Ahmed and Flower, 1992). As already mentioned with respect to Ti_3Al (Sec. 3.1.1), the phase equilibria in the Ti–Al-base systems are not yet fully understood and the character of additional phases is the subject of ongoing research (Jackson and Lee, 1992; Jackson, 1993; Nakamura et al., 1993). An improved understanding of these phase equilibria has been achieved by diffusion couple experiments and diffusion path analyses from which diffusion data can be obtained (Ma et al., 1992). The effects of alloying with Mo and V on the phase relationships have recently been studied (Das et al., 1993b; Ma and Dayananda, 1993).

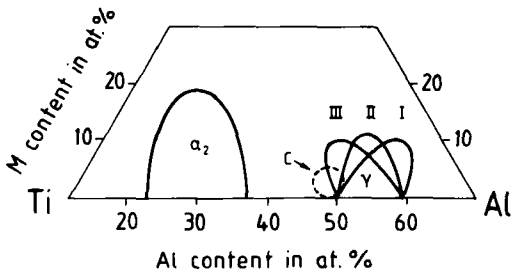


Figure 14. Schematic isothermal section at 900 °C of the ternary phase diagram Ti–Al–M with TiAl lobe I for M = Nb, Ta, Mo, or W and lobe II or III for M = V, Cr, or Mn; area C marks the composition range of commercial interest (Kim and Dimiduk, 1991).

3.2.2 Microstructure and Mechanical Behavior

The variation of strength and ductility with temperature is similar to that of the Ti-rich Ti_3Al in Fig. 12. Figure 15 shows the temperature dependence of the strength and plastic deformability of single-phase polycrystalline TiAl according to Lipsitt et al. (1975). It can be seen that this phase is brittle with practically no deformability at temperatures up to 700 °C, and only above that temperature was plastic deformation observed. Correspondingly, it has a fracture strength of nearly 500 MPa up to about 700 °C. Above that temperature, thermally activated softening occurs making plastic deformation possible, and the resultant yielding leads to yield strengths below the fracture strengths.

ArcelorMittal Ex. 2038
Page 35 of 190

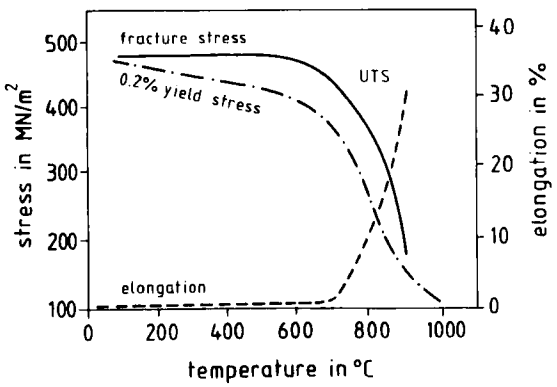


Figure 15. Tensile strength, i.e., fracture stress, ultimate tensile strength (UTS), 0.2% yield stress, and plastic deformability, i.e., tensile elongation, as a function of temperature for single-phase, polycrystalline TiAl with 54 at.% Al (Lipsitt et al., 1975).

The micromechanisms of deformation, and in particular the dislocation reactions, have been analyzed in much detail and have been discussed with respect to strength and ductility (Shechtman et al., 1974; Lipsitt et al., 1975; Yamaguchi and Umakoshi, 1990; Greenberg et al., 1991; Kim and Dimiduk, 1991; Yoo and Fu, 1991; Simmons et al., 1993; Denquin and Naka, 1993; Li and Whang, 1993; Whang and Hahn, 1993); see also the chapter by Umakoshi in Volume 6 of MST. Plastic deformation is achieved by the movement of single dislocations and superdislocations which both exhibit sessile components. In addition, twinning is an important deformation mechanism. Low dislocation mobility is the main cause for the brittle fracture behavior at lower temperatures since it hinders the formation of a plastic zone at the crack tip, which relaxes the stress concentrations (Yoo and Fu, 1991). A recent study has been directed at the effect of grain size on the mechanical behavior, which cannot be described by the Hall–Petch relation (Imayev et al., 1993 a, b).

Single-crystalline TiAl shows an anomalous, positive temperature dependence for the yield stress, i.e. the yield stress increases with rising temperature until a maximum is reached at about 600 °C, and only above this peak temperature is there the normal negative temperature dependence (Kawabata et al., 1985; Huang and Hall, 1991 a; Y. G. Zhang et al., 1991; Veyssière, 1991; Stucke et al., 1993). The anomaly results from thermally activated cross-slip of glissile superdislocations with comparatively high mobility to slip planes where not only the energy of the superdislocation is lower, but also the mobility because of a high Peierls stress, i.e. the superdislocations are immobilized by thermally activated cross-slip pinning (Kawabata et al., 1991 a; Fu and Yoo, 1990; Yoo and Fu, 1991). The energy difference between the dislocation configurations, i.e. the driving force for cross-slip, originates from the orientation dependence of the antiphase boundary (APB) energy and from the torque force between interacting dislocation partials due to the anisotropy of elasticity. These effects, i.e. high and anisotropic APB energies, strong anisotropy of elasticity, and high Peierls stresses opposing dislocation motion, are related to the strong directional bonding between Ti and Al atoms (Fu and Yoo, 1990; Yoo and Fu, 1991).

This anomalous temperature dependence of the yield stress is not always observed in polycrystalline TiAl alloys, as shown in Fig. 15. The reason for this is that there are additional strengthening effects at lower temperatures – in particular grain boundary hardening – which increase the strength to such an extent that the strength peak is no longer discernible (Huang and Hall, 1991 a). A recent study is directed at the effects of grain size, Al content, and impurity content on the flow

ArcelorMittal Ex. 2038
Page 36 of 190

stress anomaly in TiAl (Sriram et al., 1993). Similar anomalies have also been observed for other intermetallics, and the best-known example is Ni_3Al, which is discussed in Sec. 4.1.2. The mechanisms which cause the anomalous temperature dependence in Ni_3Al and in TiAl have similar characteristics, however, the particularities are different because of the different crystal structures and dislocation configurations (Kawabata et al., 1991 a).

The major problem in the use of TiAl is its low ductility at room temperature. The low ductility of single-phase TiAl (with more than 50 at.% Al) is not improved by alloying additions of, e.g. V, Nb, Cr, W, or Mn (J. M. Larsen et al., 1990; Kim and Dimiduk, 1991). A reduction in the Al content improves the ductility. If the Al content is reduced below 50 at.% to form Ti_3Al as a second phase besides the TiAl, the resulting intermetallic two-phase alloys show ductilities of a few percent, which are acceptable for applications (Huang and Hall, 1991 b; Kim and Dimiduk, 1991; Froes et al., 1991; Nonaka et al., 1992). This is illustrated in Fig. 16 which shows the hardness and ductility at room temperature of single-phase and two-phase TiAl alloys. According to these data, 48 at.% Al is the optimum composition for maximum room-temperature ductility of TiAl alloys. The different hardness curves for the as-cast and annealed conditions indicate the strong effect of microstructure variations on the mechanical behavior. The aim of the various materials' developments based on TiAl is to improve both the strength and ductility, first by controlling the microstructure and second by alloying with further elements.

The microstructure, i.e. the distribution of phases, can be varied within wide limits by appropriate heat treatments and thermomechanical processing (Koeppe et al., 1993). During processing, dynamic recrystallization occurs which has been studied systematically (Lee et al., 1993). Depending on the particular heat treatment, coarse equi-axed TiAl grains with stringers of fine TiAl grains pinned by Ti_3Al particles, or a fine duplex microstructure consisting of TiAl grains and lamellar grains, or a nearly lamellar microstructure with coarse lamellar grains and minor amounts of fine TiAl grains, or a fully lamellar microstructure with large lamellar grains can be formed. Lamellar grains in the various microstructures are composed of alternating plates of TiAl and Ti_3Al (Kim and Dimiduk, 1991).

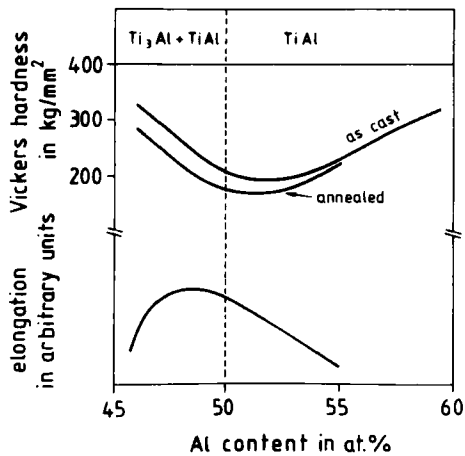


Figure 16. Vickers hardness and tensile elongation at room temperature as a function of Al content for single-phase and two-phase TiAl alloys (Kim, 1989).

The various microstructures result in rather different mechanical properties and offer good possibilities for optimization (Y.-W. Kim, 1992), as is shown in Figs. 17 and 18. It is noted that the small grain size of the duplex alloys is advantageous for short-term strength and ductility, but detrimental to creep resistance, i.e. long-term strength, because of grain boundary sliding. Such thermomechanically processed, fine-grained alloys can be de-

ArcelorMittal Ex. 2038
Page 37 of 190

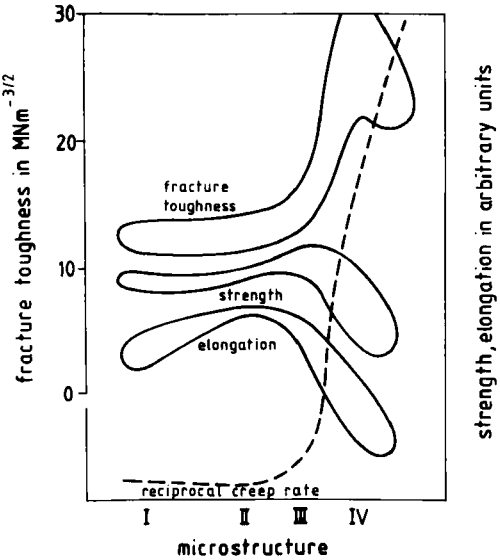


Figure 17. Fracture toughness, tensile strength, and tensile elongation at room temperature, and reciprocal secondary creep rate measuring the creep resistance as a function of microstructure (schematic) for two-phase TiAl alloys (Kim and Dimiduk, 1991).

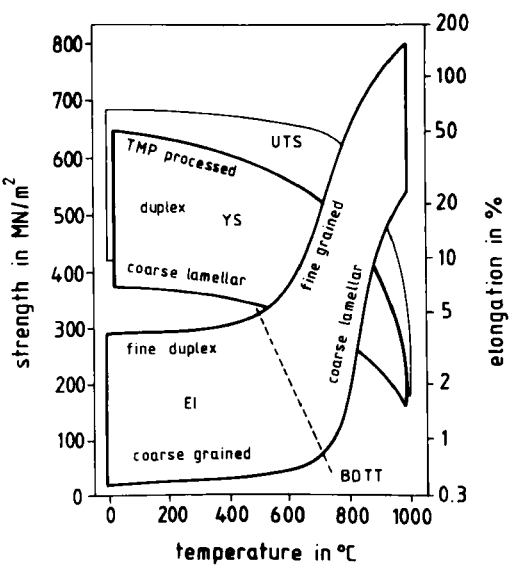


Figure 18. Temperature dependence of ultimate tensile strength (UTS), tensile yield strength (YS), brittle-to-ductile transition temperature (BDTT), and tensile elongation (El) for two-phase TiAl alloys with various microstructures produced under various processing conditions, in particular thermomechanical processing (TMP) (Kim and Dimiduk, 1991).

formed superplastically (Cheng et al., 1992). The character and orientation of the phase boundaries is of particular importance for the deformation behavior, which is controlled by slip and twinning (Wunderlich et al., 1993; Seeger and Mecking, 1993; Appel et al., 1993). The creep behavior of single-phase and two-phase TiAl alloys, which includes twinning, has been studied in detail (Feng et al., 1990b; Huang and Kim, 1991; Oikawa, 1992; Maruyama et al., 1992; Hayes and London, 1992; Jin and Bieler, 1993; Bartels et al., 1993). Analysis of the observed creep with respect to the contributions of the constituent phases has been the subject of Bartholomeusz et al. (1993). Only a few studies have been directed at the fatigue behavior of TiAl alloys (Feng et al.; 1990a; Aswath and Suresh, 1991; Dowling et al., 1991; Froes et al., 1992; Rao et al., 1992; Soboyejo et al., 1993; Stoloff et al., 1993). It has to be noted that particular microstructures may have contrasting effects on the ductility and toughness, as is demonstrated by the properties of the lamellar microstructures in Fig. 17. The various toughening mechanisms have been reviewed recently with respect to crack initiation and crack growth in TiAl (Chan, 1993a).

Two-phase TiAl alloys with a very special microstructure and striking mechanical behavior have been produced by using a special crystal-growth technique (Yamaguchi, 1991; Umakoshi et al., 1992; Inui et al., 1992; Umakoshi and Nakano, 1993; Yamaguchi and Inui, 1993). For example, the alloy with 49.3 at.% Al consists of one or two lamellar grains which are composed of lamellae of the major constituent TiAl and of the secondary phase Ti_3Al, and the TiAl lamellae contain large numbers of thin twins. Accordingly, alloys with this microstructure are called polysynthetically

ArcelorMittal Ex. 2038
Page 38 of 190

twinned (PST) crystals. This special microstructure gives rise to a mechanical behavior which depends sensitively on the orientation of the crystal with respect to the loading direction. There is a hard deformation mode with shearing across the lamella boundaries and an easy mode with shearing parallel to the lamella boundaries. The latter allows tensile elongations of 20 % at room temperature.

Besides carefully controlled heat treatments and thermomechanical processing, small additions of alloying elements – usually 1–3 at.% – are used for the optimization of the mechanical behavior of the two-phase TiAl alloys (Kim, 1989; Tsujimoto and Hashimoto, 1989; Yamaguchi and Umakoshi, 1990; Hashimoto et al., 1991; Froes et al., 1991, 1992; Kawabata et al., 1991 b, 1993; Kim and Dimiduk, 1991; Huang et al., 1991 a; Strangwood et al., 1992; Tsujimoto et al., 1992; Huang, 1993; Hashimoto and Kimura, 1993). V, Hf, Cr, and Mn increase the ductility significantly and produce solid-solution strengthening, with Cr being most effective and Mn being least effective. Nb, Ta, and W also produce solid-solution strengthening, but they decrease the ductility. Interstitial elements such as C and N affect the ductility, depending on the Al content and pre-treatments, and in particular they improve the creep resistance (Kawabata et al., 1991 b; Kim and Dimiduk, 1991). The effects of the various elements have been attributed to changes in the electronic distribution and bonding character leading to changes in the lattice unit cell dimensions, tetragonality and site occupancy. However, these elements also affect the microstructures because of their effects on the thermodynamics of the Ti–Al system, and it is difficult to separate the various effects. Thus a clear understanding of the specific roles of the various alloying elements has not yet been established (Kim and Dimiduk, 1991). A comparatively simple mechanism is precipitate strengthening which has been studied by Nemoto et al. (1992). The various materials developments in progress have led to a spectrum of multinary alloys which differ in Al content, amount of alloying elements, and processing (Tsujimoto and Hashimoto, 1989; Hashimoto et al., 1991; Froes et al., 1991; Kawabata et al., 1991 b; Kim and Dimiduk, 1991; Tsujimoto et al., 1992). The obtained property ranges are illustrated in Table 2.

A special Chinese development relies on alloying TiAl with Nb in order to obtain strong and oxidation-resistant, lightweight alloys (G. Chen et al., 1991, 1992, 1993; W. Zhang et al., 1993). Alloying with Nb leads to atomic ordering in the $L1_0$ structure of TiAl, i.e. a new phase is produced, the crystal structure of which is not yet quite clear.

It has already been emphasized in the preceding section that the phase equilibria of the titanium aluminides are very sensitive to interstitial impurities, in particular oxygen. It was shown recently that an almost single-phase TiAl alloy with 50 at.% Al can be obtained by using high-purity Ti and Al, whereas the conventional Ti–50 at.% Al alloy of low purity is two-phase with a significant amount of Ti_3Al as well as TiAl (Murata et al., 1992, 1993). The high-purity TiAl is ductile with a fracture strain of more than 3 % in contrast to the low-purity TiAl with only about 1 % fracture strain.

3.2.3 Environmental Effects

The oxidation resistance of TiAl is higher than that of Ti_3Al because of its higher Al content, but it is still orders of magnitude lower than that of typical Al_2O_3 formers, e.g. NiAl (Choudhury

ArcelorMittal Ex. 2038
Page 39 of 190

et al., 1976). The oxidation resistance of TiAl relies on the formation of a protective Al_2O_3 layer which is, however, only slightly more stable than TiO, as has already been remarked upon with respect to Ti_3Al in Sec. 3.1.3 (Meier and Pettit, 1992). Because of the high Ti activity in Ti-rich alloys, TiO is the stable oxide in contact with the TiAl alloys with Al contents below 50 at.%, which is the case for alloys with maximum ductility (Kim and Dimiduk, 1991). Further oxidation leads to the formation of TiO_2, i.e. rutile, which is not protective, and thus oxidation is a problem for TiAl alloys which have been optimized with respect to mechanical behavior. The thermodynamics and the equilibrium conditions for the formation of the various oxide phases have been studied in detail (Rahmel and Spencer, 1991; Zhang et al., 1992b). The oxidation behavior of such TiAl alloys is significantly improved by alloying with Nb, which results in the formation of a protective Al_2O_3 layer with an improved resistance to spalling (Becker et al., 1993).

Oxidation of TiAl alloys with sufficiently high Al contents, i.e. single-phase alloys with at least 50 at.% Al, leads to the formation of Al_2O_3 scales with correspondingly low oxidation rates only at temperatures below about 1000 °C, whereas at higher temperatures complex scales develop with an outer rutile layer over a mixed layer of rutile and Al_2O_3, with markedly increased oxidation rates (Meier and Pettit, 1992; Taniguchi et al., 1991a). Oxidation at the surface reduces the Al content of the TiAl to such an extent that a layer of brittle Ti_3Al – usually with cracks – is formed. Below these scales and surface layers internal oxidation is observed, resulting in oxide dispersions in the bulk. The transition from low-temperature oxidation to high-temperature oxidation occurs in a very narrow temperature range, and the reasons for this behavior are not yet understood (Meier and Pettit, 1992). The micromechanisms and kinetics of scale formation have been studied recently (Becker et al., 1992; Shida and Anada, 1993).

The oxidation resistance of TiAl alloys can be improved by special pre-oxidation treatments (Suzuki et al., 1991). Alternatively, it can be improved by alloying with Nb, Ta, and W which, however, reduces the ductility; whereas V, Cr, and Mn, which are used for increasing ductility, reduce the oxidation resistance (Kim, 1989). TiAl-based alloys with high contents of Nb have been studied recently with respect to the conditions for protective scale formation, and indeed protective oxidation has been found at 1400 °C for an Al content of 50 at.% (Brady et al., 1993). In view of the oxidation problems of the titanium aluminides a coating has been proposed for providing sufficient oxidation protection, and various approaches have been studied (Nishiyama et al., 1990; Taniguchi et al., 1991b; Yoshihara et al., 1991; Wu and Lin, 1993).

Besides scale formation, oxygen embrittles TiAl alloys as do other interstitial impurities, i.e. N, C, and B (Kim and Dimiduk, 1991). It is noted that the solubility of oxygen in TiAl is lower than that in Ti_3Al which, however, is present in most TiAl alloys and thus getters the oxygen (Yamaguchi and Umakoshi, 1990; Kim and Dimiduk, 1991). The yield stress is increased at low and high temperatures by both dissolved oxygen and precipitated Al_2O_3 particles (Kawabata et al., 1992). Environmental embrittlement has been found for TiAl as for other intermetallics (Liu and Kim, 1992). This embrittlement is obviously caused by the presence of moisture in the test atmosphere since the ductility of an advanced TiAl alloy (with addi-

ArcelorMittal Ex. 2038
Page 40 of 190

tions of Cr, Mn, and Si) has been found to be lowest in air and highest in pure oxygen. Such embrittlement effects depend sensitively on the temperature, strain rate, microstructure and phase distribution (Chan and Kim, 1993; Kim and Dimiduk, 1993). The environmental embrittlement of polysynthetically twinned TiAl (see the preceding section) is reduced by alloying with Cr, Mo or Mn (Oh et al., 1993a, b).

The solubility of hydrogen in TiAl is still sufficiently high for hydride formation on cooling, which had not been detected in earlier reports (Thompson, 1992). No clear effects of hydrogen on the mechanical behavior have been found for single-phase TiAl, whereas two-phase alloys with Ti_3Al showed embrittlement probably due to the gettering effect of Ti_3Al. More work is necessary for a clear understanding of the embrittling mechanisms (Eliezer et al., 1991; Thompson, 1992).

3.2.4 Applications

The TiAl alloy developments are less advanced than the Ti_3Al-based α_2 alloy developments because of the more severe ductility problems. However, the TiAl alloys are regarded as more promising primarily because of their lower density and the higher application temperatures, and development activities are now concentrated on TiAl in various countries, e.g. in the U.S.A. (Kim and Dimiduk, 1991; Froes et al., 1991, 1992; Dimiduk et al., 1991; Huang et al., 1991 b), in Japan (Nishiyama et al., 1990; Yamaguchi, 1992; Matsuo, 1991; Nakao et al., 1991; Mabuchi et al., 1991; Kusaka, 1991; Yoshihara et al., 1991; Ogishi et al., 1991; Kawabata et al., 1991 b; Fujitsuna et al., 1991; Tokizane et al., 1991; Hashimoto et al., 1991; Masahashi et al., 1991; Matsuo et al., 1991; Nakagawa et al., 1992; Tsujimoto et al., 1992), Great Britain (Peacock, 1989), Russia (Bondarev et al., 1991; Imayev et al., 1993b) and Germany (Sauthoff, 1990a; Dogan et al., 1991; Dahms et al., 1991; Kuczera et al., 1991; Frommeyer et al., 1992). Processing is more difficult than for Ti_3Al alloys because of the higher brittle-to-ductile transition temperature, and in particular because the hot working temperatures are outside the range of conventional titanium processing equipment, which has limited the practical ingot size to about 200 kg (Peacock, 1989; Chesnutt, 1990; Froes et al., 1991; Kusaka, 1991; Matsuo, 1991). Present efforts are directed at improving the alloy quality by improved melting processing and thermomechanical treatments (Sakamoto et al., 1992; Lombard et al., 1992; Szaruga et al., 1992; Mouldckhues and Sahm, 1992; Guan et al., 1994; Austin and Kelly, 1993; London et al., 1993; T. P. Johnson et al., 1993; Takeyama et al., 1993). The problem of upscaling heat treatments for large production billets has been considered (Semiatin et al., 1993). Besides casting and hot working, powder metallurgy has been used for component fabrication, though there are problems with quality, availability, and the cost of powder (Froes et al., 1991; Chesnutt, 1990; Dahms et al., 1991, 1993; Tokizane et al., 1991; Fuchs, 1993; Oehring et al., 1993).

Cast TiAl alloys can be forged isothermally (Fujitsuna et al., 1991; Clemens et al., 1993b), fine grain powder metallurgy material can be formed superplastically (Tokizane et al., 1991; Matsuo, 1991) as well as special cast and thermomechanically treated material (Tsujimoto et al., 1992), sheet of 1–2 mm thickness can be produced by twin-roll casting, special processes have been developed for rolling, and machining is possible as well as joining by diffusion bonding and welding (Matsuo,

ArcelorMittal Ex. 2038
Page 41 of 190

1991; Kim and Dimiduk, 1991; Fujitsuna et al., 1991; Tokizane et al., 1991; Wurzwallner et al., 1993). The diffusion bonding process has been studied in particular detail (Yan and Wallach, 1993). With respect to turbine engine applications, component fabrication techniques have been demonstrated for airfoils and compressor cases (Lipsitt, 1985a; Chesnutt, 1990; Yamaguchi and Umakoshi, 1990; Kim and Dimiduk, 1991; Bondarev et al., 1991). However, much more development work is necessary to overcome the problems of ductility and toughness, corrosion resistance, strength and costs.

Nevertheless, TiAl alloys are being considered for future aerospace applications (Dimiduk et al., 1991; Kim and Dimiduk; 1991; Matsuo, 1991), and in particular for applications in the U.S. National Aero-Space Plane (NASP) (Ronald, 1989) and the German Sänger Project (Kuczera et al., 1991; Bunk, 1992), which were mentioned earlier with respect to Ti_3Al alloys in Sec. 3.1.4. Here specific strength, i.e. strength per unit density or specific gravity, is of primary interest and alloys to be selected have to compete with metallic and nonmetallic high-strength materials. In order to meet the design criteria, TiAl alloys are considered as matrix materials of intermetallic matrix composites, and respective materials developments are in progress (Anton, 1988; Christodoulou et al., 1988; Feng et al., 1990b; Norman et al., 1990; Rösler et al., 1990; Westwood, 1990; Bryant et al., 1991; Froes et al., 1991, 1992; Kumar, 1991; Kumar and Whittenberger, 1991, 1992; Mabuchi et al., 1991; Soboyejo et al., 1993; Sadananda and Feng, 1993). Here the additional problems of chemical and mechanical compatibility have to be solved, as was mentioned earlier with respect to Ti_3Al alloys in Sec. 3.1.4. Deterioration of the tensile strength of a TiAl/SiC composite by interface reactions has recently been studied (Ochiai et al., 1994). The kinetics of the phase reactions is determined by interdiffusion, which has been studied in the case of TiAl–Mo (Zhang et al., 1992a). It has been shown that both the creep resistance and the toughness of a TiAl matrix composite can be improved by using coated fibers with weak fiber/matrix interfaces (Weber et al., 1993).

In any case, ductile reinforcing inclusions in composites offer the valuable possibility of improving the fracture toughness of the composite. The toughening effect of ductile reinforcements in brittle matrices has been studied both experimentally and theoretically for ceramics, e.g. Al_2O_3 reinforced with Al, and metals (Sigl et al., 1988; Flinn et al., 1989; Ashby et al., 1989). Such a toughening effect has also been found for a TiAl/Nb model composite (Cao et al., 1989).

Besides aerospace applications, interest is focused on automotive engine applications, e.g. valves and turbocharger rotors, which may be nearer to realization (Kim and Dimiduk, 1991). A successful development has led to a cast TiAl turbocharger rotor of about 4 cm diameter which compares favorably with both a superalloy Inconel 713C rotor and a ceramic SiN rotor with respect to performance under service conditions, and which is ready for use in high-performance passenger cars (Nishiyama et al., 1990).

3.3 Al_3Ti and Other $D0_{22}$ Phases

3.3.1 Basic Properties and Phase Diagram

The titanium trialuminide Al_3Ti crystallizes with the tetragonal $D0_{22}$ structure which is shown in Fig. 1, and which is common to some other trialuminides, i.e.

ArcelorMittal Ex. 2038
Page 42 of 190

Al_3M with M = V, Nb, Ta, and some other phases, e.g. Ni_3V (Bauer, 1939; Villars and Calvert, 1991). The $D0_{22}$ structure is derived from the close-packed cubic $L1_2$ structure by the stacking of $L1_2$ cubes with periodic antiphase boundaries in between, and thus the $D0_{22}$ structure may be regarded as a tetragonally distorted, long-period ordered, cubic structure (Bauer, 1939; Yamaguchi and Umakoshi, 1990).

The $D0_{22}$ structure is still sufficiently simple for quantum-mechanical, first-principles calculations and indeed such ab initio calculations have been done for Al_3Ti in order to study the bonding type and phase stability, and to obtain theoretical values for the elastic constants, fault energies and cleavage energies (Carlsson, 1991; Lin et al., 1991; Yoo and Fu, 1991). The experimentally determined elastic stiffness values are larger than the theoretical ones, and in particular the resulting experimental value of 216 GPa for the Young's modulus of polycrystalline Al_3Ti at room temperature clearly surpasses those of the other titanium aluminides, and is of the order of that of the superalloys (see Table 2) (Nakamura, 1991; Nakamura and Kimura, 1991).

Because of the high Al content of Al_3Ti its density of 3.3 g/cm^3 is still lower than that of the other titanium aluminides (Yamaguchi and Umakoshi, 1990). Furthermore, its oxidation resistance is significantly higher than that of Ti_3Al and TiAl (Umakoshi et al., 1989; Subrahmanyam and Annapurna, 1986), and thus Al_3Ti is a candidate phase for lightweight structural applications. It is also being considered as a coating material and its oxidation kinetics have been studied in detail (Smialek and Humphrey, 1992).

Al_3Ti melts incongruently at about 1340 °C and is a line compound with a fixed composition according to the available phase diagrams (Glazova, 1965; Murray, 1988; Rowe and Huang, 1988; Huang and Siemers, 1989; Schuster and Ipser, 1990; Shull and Cline, 1990; Y. A. Chang et al., 1991; Perepezko, 1991 a). It should be noted that the high-temperature equilibria are still in discussion. Al_3Ti can be alloyed with the other $D0_{22}$ trialuminides to form ternary $D0_{22}$ phases which are no longer line compounds, but have a range of homogeneity, i.e. the composition can vary between the solubility limits which are given in the respective ternary phase diagrams (Sridharan and Nowotny, 1983; Hashimoto et al., 1986 b; Kumar, 1990; Hellwig, 1990; Paruchuri and Massalski 1991; Weaver et al., 1991; Perepezko, 1991 a).

3.3.2 Microstructure and Mechanical Behavior

Al_3Ti

The deformation behavior of Al_3Ti has been studied and analyzed in detail (Yamaguchi et al., 1987, 1990; Wheeler et al., 1990; Morris and Lerf, 1991; Yamaguchi and Umakoshi, 1990; Shimokawa et al., 1991; and the chapter by Umakoshi in Volume 6 of MST). Figure 19 shows the temperature dependence of the yield stress for polycrystalline material with a grain size of about 1 mm, which was produced by vacuum induction melting and contains a small volume fraction of second phase particles (mostly Al) due to the line compound character of this phase. The strength at room temperature is low compared with the other titanium aluminides (see Table 2) at about 500 °C. The major deformation mode is twinning, which does not affect the $D0_{22}$ symmetry. The reason for the preponderance of twinning is the low mobility of dislocations, according to a theoretical study of the deformation behavior

ArcelorMittal Ex. 2038
Page 43 of 190

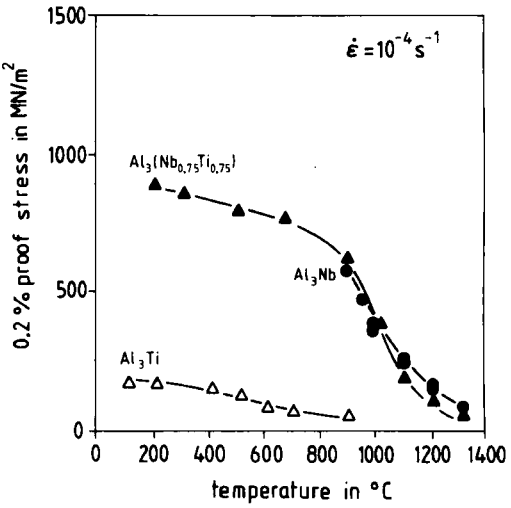


Figure 19. Yield strength of Al_3Ti under vacuum (Yamaguchi et al., 1987) and 0.2% proof stress of Al_3Nb and $Al_3(Nb_{0.75}Ti_{0.25})$ in air (Sauthoff, 1990 b; Reip, 1991; Reip and Sauthoff, 1993) as a function of temperature (coarse-grained, polycrystalline alloys with a $D0_{22}$ structure, tested in compression at a strain rate of $10^{-4} s^{-1}$).

of $D0_{22}$ crystals (Khantha et al., 1992). In spite of the observed microscopic plasticity, there is nearly no ductility at temperatures below 620 °C and cracks are nucleated readily at structure heterogeneities, i.e. inclusions, second phase particles, intersections of twins, and grain boundaries.

The ductility of Al_3Ti is improved by microalloying, i.e. by small additions of Zr and Hf as well as B and Li, and a fracture strain in compression of a few percent is obtained at room temperature (Yamaguchi et al., 1988). The effect of Zr and Hf is supposed to be due to a lowering of the stacking fault energy, since the phases Al_3Zr and Al_3Hf crystallize with a $D0_{23}$ structure which differs from the $D0_{22}$ structure by a longer stacking period of $L1_2$ cubes.

Al_3Ti is being considered for use as an oxidation-resistant coating on Ti alloys and titanium aluminides (Subrahmanyam and Annapurna, 1986; Umakoshi et al., 1989; Smialek and Humphrey, 1992), and as a wear-resistant surface layer (Uenishi et al., 1992). It should be noted that there is another Al-rich titanium aluminide, Al_2Ti, which shows a higher resistance to cracking than identically processed Al_3Ti with a similar hardness (Benci et al., 1993). Recently, Al_3Ti has been applied as thin-film interconnections in microelectronic devices where the Al_3Ti acts as a diffusion barrier (Colgan, 1990; Gupta et al., 1993). Compared with Al metallization, intermetallic aluminides are advantageous because of their lower diffusion coefficients, and the best properties have been shown by Al_3Ti films.

Al_3V

Al_3V is regarded as promising for applications in nuclear reactor technology and has been studied with respect to ductility improvements (Umakoshi et al., 1988). It is isostructural with Al_3Ti and both form a continuous series of mixed crystals. The melting temperature is only slightly higher than that of Al_3Ti and thus a similar deformation behavior is expected. The deformation mechanisms are indeed analogous to those in Al_3Ti. However, the yield stress is higher than that of Al_3Ti by a factor of about 2 and there is no ductility in compression (in vacuum) below about 400 °C.

Microalloying with Al_3Ti improves the ductility in compression – at the expense of the yield stress – to such an extent that $Al_3(V_{0.95}Ti_{0.05})$ shows a fracture strain of about 7%. Further alloying with Al_3Ti leads to a deterioration in the properties, i.e. $Al_3(V_{0.75}Ti_{0.25})$ is significantly stronger than Al_3V, but can only be deformed plastically at 700 °C and above.

It is noted that according to a theoretical study with first-principles calculations, the

ArcelorMittal Ex. 2038
Page 44 of 190

phase Al_3Ru also has the $D0_{22}$ structure and is closely related to Al_3V (Paxton and Pettifor, 1992). The deformation behavior of Al_3Ru is expected to be similar to that of Al_3V but with enhanced ductility.

Al_3Nb

Al_3Nb is a line compound and thus it usually contains second phases – in particular excess Al on the grain boundaries. It deforms by dislocation movements and by twinning, and it is brittle at room temperature (Shechtman and Jacobson, 1975). In spite of its room-temperature brittleness, Al_3Nb is regarded as a candidate phase for high temperature structural service (Rodriguez et al., 1991). The deformation behavior, as well as the physical properties, of Al_3Nb and Al_3Nb-base alloys have been studied in more detail (Reip, 1991; Reip and Sauthoff, 1993); preliminary results have been presented in Sauthoff (1990a, b), and the main findings are briefly reported in the following.

In spite of the high density of Nb, the $D0_{22}$ phase Al_3Nb is still a lightweight material with a density of 4.54 g/cm^3, and the mean thermal expansion coefficient is about $9.6 \times 10^{-6}\,K^{-1}$ between room temperature and 1000 °C which is lower than that for superalloys and steels. It melts congruently, in contrast to Al_3Ti and Al_3V (Massalski et al., 1990), which makes preparation easier. Its melting temperature of 1605 °C is significantly higher than those of the other $D0_{22}$ phases, and thus a much higher strength – in particular at high temperatures – is expected. The Young's modulus, 246 GN/m^2 at room temperature and 224 GN/m^2 at 600 °C with a linear temperature dependence in between, is higher than those of the titanium aluminides and even higher than those of the superalloys (Table 2). Poisson's ratio has been found to be 0.17, and similarly low values have also been found for Al_3Ti and other intermetallics with complex crystal structures (Fleischer et al., 1989b; Nakamura, 1991).

The yield stress, i.e. the 0.2% proof stress of Al_3Nb in air, is shown in Fig. 19 as a function of temperature above 850 °C. Between 600 °C and 800 °C, Al_3Nb fails catastrophically in air tests because of grain boundary oxidation, which is known as a pest phenomenon. Below 500 °C, the fracture strain in compression is smaller than 0.2%, whereas plastic deformation in bending has only been observed above 1050 °C. The plane strain fracture toughness is only about 2 MN/m$^{3/2}$ at room temperature, as was also found by others (Schneibel et al., 1988).

It is noted that the pest phenomenon is most pronounced for Al_3Nb at a critical temperature of about 720 °C and under oxygen partial pressures between 10^{-15} and 10^{-10} bar, whereas no pest is observed in pure oxygen (Steinhorst and Grabke, 1990; Grabke et al., 1991a). The pest-like disintegration of Al_3Nb is proposed to be due to the selective oxidation of Al at the grain boundaries, which leads to Al depletion and the formation of Al_2Nb (Tolpygo and Grabke, 1993). Other intermetallics suffer the pest phenomenon, too, and the mechanism is not well understood (Westbrook and Wood, 1964; Aitken, 1967; Meier and Pettit, 1992).

The observed dislocation slip systems do not differ from those of the other $D0_{22}$ phases, and again twinning, which does not affect the order, is a major deformation mode at low and high temperatures. The number of independent deformation modes is smaller than prescribed by the Von Mises criterion, which contributes to the observed brittleness (see Sec. 2.3). The ductility at high temperatures results from

ArcelorMittal Ex. 2038
Page 45 of 190

thermally activated dislocation motions, i.e. creep.

The creep strength of Al_3Nb is comparatively low – a stress of 10 MN/m^2 produces 1 % strain in only 500 h and fracture in 2300 h – whereas the yield stress compares favorably with the superalloys. This illustrates the fact that the difference between the yield stress and the creep strength is much more pronounced for intermetallics than for conventional alloys. Creep of Al_3Nb is controlled by dislocation climb which is accompanied by subgrain formation. The observed creep behavior corresponds to that of conventional disordered alloys and the creep rates are described by the known constitutive equations. This will be discussed in more detail with respect to NiAl (Sec. 4.3). The secondary creep rate follows the power law, i.e. Dorn equation for dislocation creep

$$\dot{\varepsilon} = A \frac{D G b}{k T} \left(\frac{\sigma}{G}\right)^n \qquad (2)$$

where $\dot{\varepsilon}$ is the secondary strain rate, A a dimensionless factor, D the effective diffusion coefficient, G the shear modulus, b the Burgers vector, k Boltzmann's constant, T the temperature, σ the applied stress, and the exponent n is between 3 and 5. For Al_3Nb a stress exponent of 3.6 and an apparent activation energy of 360 kJ/mol was found, of which 35 kJ/mol are due to the temperature dependence of the shear modulus and the remaining 325 kJ/mol describe the temperature dependence of the other factors in the Dorn equation, in particular the diffusion coefficient. Diffusion data are scarce (Ogurtani, 1972; Slama and Vignes, 1972) and are not sufficient for analysis of the creep data.

As already mentioned in Sec. 3.3.1, Al_3Nb dissolves Ti, i.e. it can be alloyed with Al_3Ti to form a continuous series of mixed crystals with a $D0_{22}$ structure which are no longer line compounds. Figure 19 shows the 0.2 % proof stress of the ternary phase $Al_3(Nb_{0.75}Ti_{0.25})$ as a function of temperature in air, and it can be seen that in contrast to binary Al_3Nb the fracture strain in compression is already greater than 0.2 % at 200 °C, and furthermore there are no indications of the pest phenomenon. However, in bending the brittle-to-ductile transition temperature is only sightly lower than that for Al_3Nb. Small additions of Hf and Li give a further lowering of the brittle-to-ductile transition temperature, as was already found for Al_3Ti (see Sec. 3.3.2). It is noted that, as in the case of Al_3Ti (see Sec. 3.4), attempts to alloy Al_3Nb with a third element have been tried in order to produce the $L1_2$ structure instead of the $D0_{22}$ structure since the $L1_2$ structure is regarded as advantageous for developing ductile intermetallics (Li et al., 1992; Subramanian and Simmons, 1991). However, these efforts have not been successful. The respective ternary phase diagrams, including old literature from Germany and the former Soviet Union, have been reviewed by Kumar (1990).

A more significant improvement in the toughness and the brittle-to-ductile transition temperature is obtained by using Al_3Nb as a constituent in an intermetallic two-phase or multiphase alloy, i.e. by combining Al_3Nb with another, less brittle phase. In particular Al_3Nb forms a stable equilibrium with the B2 phase NiAl, i.e. intermetallic NiAl–Al_3Nb alloys can be formed and are discussed in Sec. 4.3. Other Al_3Nb-base alloys with a complex microstructure are produced by using novel processing methods including rapid solidification and powder metallurgy methods (Bowman and Noebe, 1989; Bowden, 1989; Lu et al., 1990; Alman and Stoloff, 1991; Rodriguez et al., 1991; Ayer and

ArcelorMittal Ex. 2038
Page 46 of 190

Ray, 1991; Ho and Sekhar, 1991). For example, a multiphase Al_3Nb-base alloy which is dispersion-strengthened by TiB_2 was prepared by melt-spinning, pulverization and hot isostatic pressing (Ray and Ayer, 1992). Here much more work is necessary for estimating the potential of Al_3Nb-base alloys for applications as structural, high-temperature materials.

Apart from the mechanical behavior, a sufficient oxidation resistance is a prerequisite for any high-temperature applications. In spite of the fact that Al_3Nb is being considered as an oxidation resistant coating for Nb-based alloys (Bowden, 1989), the oxidation resistance of bulk Al_3Nb by scale formation is only limited (Perkins et al., 1988; Hebsur et al., 1989; Korinko and Duquette, 1990; Steinhorst, 1989; Steinhorst and Grabke, 1989; Grabke et al., 1990, 1991 b). The oxidation resistance is improved by excess Al and by small additions of Hf (Steinhorst, 1989; Grabke et al., 1990, 1991 b). Likewise Al_3Nb that is macroalloyed with Cr and microalloyed with Y exhibits excellent oxidation resistance at 1200 °C, but it still suffers from severe environmental attack during deformation at intermediate temperatures (Raj et al., 1992 a). Such alloys have also been studied with respect to strength and fracture toughness at low and high temperatures. Apart from these improvements by single-phase alloying, the oxidation resistance of Al_3Nb is increased significantly by alloying with the already mentioned NiAl to form intermetallic multiphase alloys (Steinhorst, 1989; Grabke et al., 1990, 1991 b), i.e. the multiphase Al_3Nb–NiAl alloys are advantageous with respect to both their deformation behavior and their oxidation resistance, and they do not show the pest phenomenon.

Al_3Ta

Al_3Ta with a $D0_{22}$ structure is closely related to Al_3Nb (Bauer, 1939). The Al–Ta and Al–Ta–Ti phase diagrams have been studied recently (Subramanian et al., 1990 b; Sridharan and Nowotny, 1983). Al_3Ta has a still higher melting temperature (1627 °C) than Al_3Nb and its deformation behavior seems to be similar (Pak et al., 1990). Fabrication of this phase is difficult because of the widely differing melting points of the constitutive elements. Nevertheless, it is being considered for composite materials developments (Alman and Stoloff, 1991; Anton, 1988; Shah et al., 1990; Kumar, 1991).

Ni_3V

The above presented $D0_{22}$ trialuminides are line compounds and their ordered crystal structure is stable up to the melting point, which may be regarded as an indication of a strong ordering tendency. In contrast to these phases, the $D0_{22}$ phase Ni_3V shows a range of homogeneity and its ordered crystal structure is only stable at lower temperatures, i.e. Ni_3V disorders at 1045 °C to form an f.c.c. Ni–V solid solution (Massalski et al., 1990), which indicates a weak ordering tendency. The deformation mechanisms have been studied and analyzed in detail (Moreen et al., 1971; Vanderschaeve et al., 1979; Faress and Vanderschaeve, 1987; Yamaguchi and Umakoshi, 1990; Khantha et al., 1992). As in the case of the trialuminides, Ni_3V deforms by twinning, which does not affect the order, and its yield stress is comparatively high, e.g. 720 MN/m^2 for polycrystalline Ni_3V with large ordered domains and 1320 MN/m^2 for Ni_3V with small domains. In contrast to the trialuminides, it shows considerable ductility in compression at room temperature. However, the

ArcelorMittal Ex. 2038
Page 47 of 190

ductility in tension is still small, i.e. Ni_3V is also regarded as brittle (Liu and Inouye, 1979).

Alloying Ni_3V with Fe and Co leads to the phases $(Fe,Ni)_3V$ and $(Fe,Co,Ni)_3V$ with an $L1_2$ structure, which is the "parent" structure of the $D0_{22}$ structure. These ternary and quaternary phases are highly ductile with a tensile elongation of 40 % or more at room-temperature, and have been the subject of successful materials developments (Liu, 1984) which are described in Sec. 4.2 together with other $L1_2$ phases in connection with Ni_3Al. This transition from the $D0_{22}$ structure to the $L1_2$ structure by alloying illustrates the fact that these closely related crystal structures (see Sec. 3.3.1) differ little with respect to energy and stability, as has been shown theoretically by ab initio calculations (Stocks et al., 1987; Carlsson, 1991; Freeman et al., 1991).

In this context Ni_3Nb with a $D0_{22}$ structure should be mentioned, which is of practical importance for some Ni-base superalloys. These alloys are strengthened by precipitated metastable Ni_3Nb particles and show excellent weldability (Oblak et al., 1974).

3.4 Trialuminides with the $L1_2$ Structure

3.4.1 Basic Properties and Phase Diagrams

The cubic $L1_2$ structure is more symmetric than the tetragonal $D0_{22}$ structure (see Fig. 1) and has a sufficient number of slip systems according to the Von Mises criterion, and thus it should also be more deformable (George et al., 1991 b). In particular, after the successful "ductilization" of Ni_3Al and Ni_3V (see Secs. 4.1 and 4.2) the $L1_2$ structure is regarded as most advantageous and promising for developing structural intermetallics.

It has long been known that there are Al-rich ternary intermetallics with an ordered f.c.c. $L1_2$ structure (Raman and Schubert, 1965). In the preceding sections (Secs. 3.3.1 and 3.3.2) it was noted that the $L1_2$ and $D0_{22}$ crystal structures are closely related and the enery differences are small. A third, closely related structure is the $D0_{23}$ structure, which is another long-period ordered cubic structure based on the $L1_2$ structure (Bauer, 1939). The binary trialuminides and the Al-rich ternary phases with these closely related crystal structures have recently been reviewed from theoretical and practical points of view with respect to stabilization of the $L1_2$ structure by alloying, and the prospects of materials developments on the basis of such $L1_2$ phases (Kumar, 1990, 1993; Freeman et al., 1991; George et al., 1991 b). The main results are summarized in the following.

The group IIIA element Sc, as well as some rare earths and actinides, forms a stable, binary trialuminide with an $L1_2$ structure, whereas the group IVA and VA elements form trialuminides with the $D0_{22}$ structure, i.e., Al_3Ti and Al_3Hf at high temperature, and Al_3V, Al_3Nb, and Al_3Ta, or with the $D0_{23}$ structure, Al_3Zr and Al_3Hf, at low temperature. Ternary $L1_2$ phases are obtained by alloying Al_3Ti with Cr, Mn, Fe, Co, Ni, Rh, Pt, Pd, Cu, Ag, Au, or Zn, whereas the $L1_2$ structure was not obtained with V, Nb, or Mo (Kumar, 1990; Freeman et al., 1991; George et al., 1991 b; Nakayama and Mabuchi, 1993). Likewise, the $L1_2$ structure has been produced by alloying Al_3Zr with Sc, V, Cr, Mn, Fe, Ni, Cu, or Zn, and by alloying Al_3Hf with Cu, whereas such alloying has not led to $L1_2$ phases in the cases of Al_3V, Al_3Nb, and Al_3Ta. The different alloying

ArcelorMittal Ex. 2038
Page 48 of 190

behavior reflects the different stabilities of the competing structures and can be understood in view of the electron density distributions, as obtained by quantum mechanical ab initio calculations. This has been shown in particular for Al_3Nb–Ni, which is attractive because of its advantageous combination of high melting temperature and low density (Inoue et al., 1991 b). It is noted that metastable binary trialuminides, i.e. powders of Al_3Ti, Al_3Zr, and Al_3Hf, with $L1_2$ structures could be obtained by mechanical alloying, i.e. low-temperature processing (Schwarz et al., 1992). The phase Pd_3Mn, which orders below 530 °C to form the $D0_{23}$ structure in the absence of hydrogen and the $L1_2$ structure in the presence of hydrogen with sufficient partial pressure (Sowers et al., 1992), should be mentioned in this context.

The compositions of the ternary Al-rich $L1_2$ phases can yary within a small range of homogeneity, and are given approximately by various kinds of formulae, e.g. $Al_{66}Ti_{25}M_9$, $Al_{22}Ti_8M_3$ or Al_5Ti_2M with M = Cr, Mn, Fe, etc. – with analogous formulae for the Zr variants – depending on the alloying element. It is not clear in what way the atoms are distributed in the $L1_2$ lattice. Since these compositions are near those of the binary trialuminides in the respective ternary phase diagrams, these ternary $L1_2$ phases are commonly addressed as ternary $L1_2$ trialuminides with a partial substitution of Al by the third M element according to $(Al_{1-x}M_x)_3Ti$, though there are arguments against this view (Durlu et al., 1991; Durlu and Inal, 1992 a). The respective phase diagrams have been discussed (see Kumar, 1990; Mazdiyasni et al., 1989; Mikkola et al., 1991; Nic et al., 1991). In view of the common composition range of the various trialuminides with an $L1_2$ structure, a stability criterion for the existence of the $L1_2$ structure has been deduced which is given by a specific number of valence electrons per atom of the alloy if the effect of atomic interaction on the electronic distribution is considered according to the Engel–Brewer theory (Durlu and Inal, 1992 b).

3.4.2 Microstructure and Mechanical Behavior

Most studies are centered on $Al_{66}Ti_{25}M_9$ and its mechanical behavior is discussed in detail by George et al. (1991 b). Note that the processing of these alloys is crucial since the cast alloys usually contain residual pores and second phase particles. The elimination of these artifacts by post-solidification treatments, i.e., heat treatments, hot working, hot extrusion, or forging, is difficult and alloys of sufficient quality have only recently been obtained. Besides ingot metallurgy, powder metallurgy and rapid solidification have been used.

Elastic moduli have been measured and the Young's modulus has been found to be 200 GN/m^2 for $Al_{67}Ti_{25}Ni_8$ and 192 GN/m^2 for $Al_{67}Ti_{25}Fe_8$ (George et al., 1991 b), i.e., it is between those of Ti_3Al and TiAl on the one hand and Al_3Ti and Al_3Nb on the other, and is of the order of those of the superalloys (Table 2 and Secs. 3.3.1 and 3.3.2).

The compressive yield strength of $Al_{66}Ti_{25}M_9$ with M = Fe, Cr, Mn or mixtures of these transition metals is of the order of 300 MN/m^2 between room temperature and about 800 °C, i.e. there is a strength plateau or a slight positive temperature dependence (Yamaguchi and Umakoshi, 1990; Kumar et al., 1991 b; Kumar and Brown, 1992 b; Wu et al., 1993; Brown et al., 1993). Below room temperature there is a steep yield stress increase with decreasing temperature and

ArcelorMittal Ex. 2038
Page 49 of 190

above 800 °C the material softens in the usual way. Much higher yield stresses can be obtained by variations in the composition and the microstructure (George et al., 1991 b), and in particular by the introduction of dispersoids to produce particulate composites (Kumar et al., 1991 c; Kumar, 1991; Otsuki and Stoloff, 1992). The mechanical behavior has been analyzed as a function of the degree of long-range order (Winnicka and Varin, 1993). The grain size dependence of the yield stress follows a Hall–Petch relationship (Pu et al., 1992). The tensile yield strength corresponds to the compressive yield strength in general, however, there are some complexities which are not yet understood (Kumar et al., 1991 a, b; George et al., 1991 b).

The tensile or flexural elongation is only a fraction of a percent at room temperature and increases slowly with temperature with another ductility minimum at about 500 °C (Z. L. Wu et al., 1990 a, b, 1991; Kumar and Brown, 1992 a, c, 1993). The ductility of the single crystals tested to date is not higher than that of polycrystals and the various variations of composition and microstructure have led to only small ductility improvements (George et al., 1991 b; Brown et al., 1993). Slip systems, dislocation mobilities and reactions, fracture modes, bend ductility and creep strength have been studied in detail (Yamaguchi and Umakoshi, 1990; George et al., 1991 b; Schneibel et al., 1992 a; Morris et al., 1993 b, c; Sizek and Gray, 1993; Miura and Watanabe, 1993; Wu and Pope, 1993). It has to be concluded that the $L1_2$ trialuminides of the $Al_{66}Ti_{25}M_9$ type are brittle and do not fulfill the initial expectations with respect to ductility.

Nevertheless, the $L1_2$ trialuminides are promising because of their low density and there is a potential for aerospace applications though this potential has not been realized to date (Dimiduk et al. 1991). For such applications a sufficient oxidation resistance is a necessity, and indeed a cyclic oxidation resistance has been found which varies from poor for $Al_{67}Ti_{25}Mn_8$ to excellent for $Al_{67}Ti_{25}Cr_8$ (Parfitt et al., 1991). The present work is directed at the optimization of the composition and microstructure of $Al_{66}Ti_{25}M_9$ alloys by careful processing with respect to strength, ductility, toughness, and oxidation resistance.

Besides these studies on Al_3Ti-base trialuminides, similar work has been started on $L1_2$ trialuminide alloys, which are based on the $D0_{23}$ phase Al_3Zr and which again contain Cu, Mn, or Cr (Virk and Varin, 1992; Schwarz et al., 1992; Varin et al., 1993). According to first results the mechanical behavior seems to be similar to that of the Al_3Ti-base alloys, and there is a strong, positive temperature dependence for the yield stress.

4 Nickel Aluminides and Related Phases

4.1 Ni_3Al

4.1.1 Basic Properties and Phase Diagram

Ni_3Al is the most studied and best known intermetallic because it has been used as a strengthening phase in the superalloys for a long time, and because its ductility problems can be overcome, i.e. it can be "ductilized" by microalloying with boron (Aoki and Izumi, 1979; Liu and Koch, 1983; Aoki, 1990). This means that it can be produced and tested without major experimental difficulties, and thus it was selected preferentially in the past for studies on the behavior of intermetallics (see

ArcelorMittal Ex. 2038
Page 50 of 190

Intermetallics
Gerhard Sauthoff
copyright © VCH Verlagsgesellschaft mbH, 1995

above 800 °C the material softens in the usual way. Much higher yield stresses can be obtained by variations in the composition and the microstructure (George et al., 1991 b), and in particular by the introduction of dispersoids to produce particulate composites (Kumar et al., 1991 c; Kumar, 1991; Otsuki and Stoloff, 1992). The mechanical behavior has been analyzed as a function of the degree of long-range order (Winnicka and Varin, 1993). The grain size dependence of the yield stress follows a Hall–Petch relationship (Pu et al., 1992). The tensile yield strength corresponds to the compressive yield strength in general, however, there are some complexities which are not yet understood (Kumar et al., 1991 a, b; George et al., 1991 b).

The tensile or flexural elongation is only a fraction of a percent at room temperature and increases slowly with temperature with another ductility minimum at about 500 °C (Z. L. Wu et al., 1990 a, b, 1991; Kumar and Brown, 1992 a, c, 1993). The ductility of the single crystals tested to date is not higher than that of polycrystals and the various variations of composition and microstructure have led to only small ductility improvements (George et al., 1991 b; Brown et al., 1993). Slip systems, dislocation mobilities and reactions, fracture modes, bend ductility and creep strength have been studied in detail (Yamaguchi and Umakoshi, 1990; George et al., 1991 b; Schneibel et al., 1992 a; Morris et al., 1993 b, c; Sizek and Gray, 1993; Miura and Watanabe, 1993; Wu and Pope, 1993). It has to be concluded that the $L1_2$ trialuminides of the $Al_{66}Ti_{25}M_9$ type are brittle and do not fulfill the initial expectations with respect to ductility.

Nevertheless, the $L1_2$ trialuminides are promising because of their low density and there is a potential for aerospace applications though this potential has not been realized to date (Dimiduk et al. 1991). For such applications a sufficient oxidation resistance is a necessity, and indeed a cyclic oxidation resistance has been found which varies from poor for $Al_{67}Ti_{25}Mn_8$ to excellent for $Al_{67}Ti_{25}Cr_8$ (Parfitt et al., 1991). The present work is directed at the optimization of the composition and microstructure of $Al_{66}Ti_{25}M_9$ alloys by careful processing with respect to strength, ductility, toughness, and oxidation resistance.

Besides these studies on Al_3Ti-base trialuminides, similar work has been started on $L1_2$ trialuminide alloys, which are based on the $D0_{23}$ phase Al_3Zr and which again contain Cu, Mn, or Cr (Virk and Varin, 1992; Schwarz et al., 1992; Varin et al., 1993). According to first results the mechanical behavior seems to be similar to that of the Al_3Ti-base alloys, and there is a strong, positive temperature dependence for the yield stress.

4 Nickel Aluminides and Related Phases

4.1 Ni_3Al

4.1.1 Basic Properties and Phase Diagram

Ni_3Al is the most studied and best known intermetallic because it has been used as a strengthening phase in the superalloys for a long time, and because its ductility problems can be overcome, i.e. it can be "ductilized" by microalloying with boron (Aoki and Izumi, 1979; Liu and Koch, 1983; Aoki, 1990). This means that it can be produced and tested without major experimental difficulties, and thus it was selected preferentially in the past for studies on the behavior of intermetallics (see

Arconic Mittal Ex. 2038
Page 51 of 190

Sec. 1.2). The knowledge obtained on the physical and mechanical metallurgy of Ni_3Al and its alloys has been reviewed in an authoritative way by Stoloff (1989).

The nickel aluminide Ni_3Al – known as the γ' phase – crystallizes with the cubic $L1_2$ structure (Cu_3Au-type) which results from the f.c.c. structure by ordering (see Fig. 1). Deviations from stoichiometry are accommodated primarily by antisite defects (Lin and Sun, 1993). The density of Ni_3Al is 7.50 g/cm^3 (see Liu et al., 1990) and thus is only slightly lower than that of the superalloys (see Table 2) which, however, is still of interest. The elastic constants have been studied experimentally and theoretically by various authors (e.g. Davies and Stoloff, 1965; Dickson et al., 1969; Kayser and Stassis, 1969; Foiles and Daw, 1987; Wallow et al., 1987; Yoo and Fu, 1991, 1993; Yasuda et al., 1991a, 1992). Young's modulus of cast polycrystalline Ni_3Al at room temperature is about the same as that of pure Ni with a weaker temperature dependence (Stoloff, 1989), i.e. it is slightly smaller than that of the superalloys (see Table 2). Data for thermal expansion, thermal conductivity, the Seebeck effect, and electrical resistivity have been presented (Stoloff, 1989). The thermal diffusivity of Ni_3Al has been studied recently (Archambault and Hazotte, 1993).

Figure 20 shows the binary Ni–Al phase diagram which considers some new results. Ni_3Al melts incongruently at about 1383 °C to form liquid Ni–Al and solid, disordered, f.c.c. Ni–Al peritectically (Hilpert et al., 1987; Verhoeven et al., 1991), which is in contrast to the widely accepted phase diagram in Massalski et al. (1990). In addition, there is a eutectic equilibrium at 1380 °C with the B2 phase NiAl and liquid Ni–Al. Ni_3Al is stable, i.e. ordered, up to the melting point according to most investigators (Stoloff, 1989), which may, however, only be true near the stoichiometric composition since there are indications that the critical temperature of ordering may be slightly lower than the

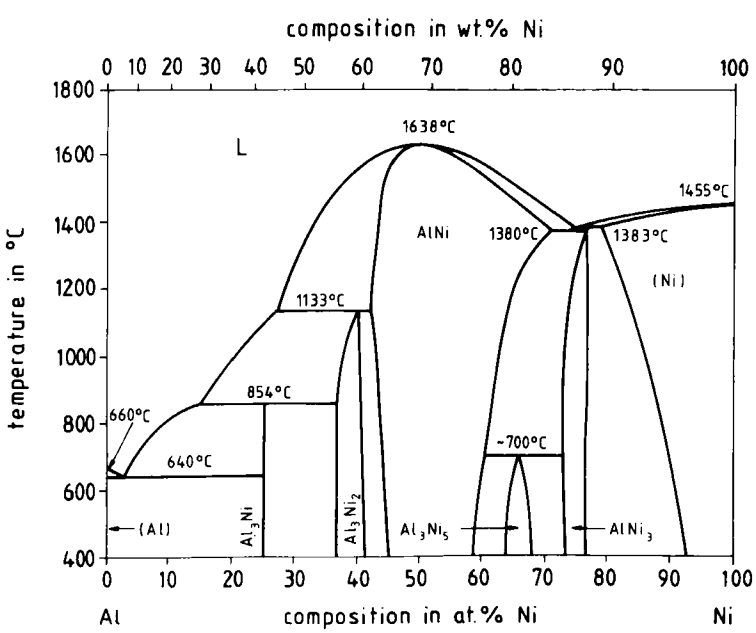


Figure 20. Binary Ni–Al phase diagram which is based on that by Massalski et al. (1990) and considers the new results of Hilpert et al. (1987) and Verhoeven et al. (1991) with respect to the Ni_3Al equilibria.

ArcelorMittal Ex. 2038
Page 52 of 190

melting temperature for Ni_3Al with a high Ni excess (Bremer et al., 1988; Yavari et al., 1991; Ramesh et al., 1992).

Ni_3Al can dissolve further elements, in particular other transition metals, and ternary Ni–Al based phase diagrams have been studied by various investigators (e.g. Guard and Westbrook, 1959; Kornilov, 1960; DasGupta et al., 1984; Chakravorty and West, 1985, 1986; Chakravorty et al., 1985; Nash and Liang, 1985; Vincent et al., 1988; Hong et al., 1989; Enomoto et al., 1991; Lee and Nash, 1991 a). The direction of the Ni_3Al lobes in the isothermal sections of the ternary phase diagrams indicate what sites are occupied by the alloying additions. According to this and the results of specific site occupation studies, Ni sites are occupied by Co, Pd, Pt, Cu, or Sc, and Al sites are occupied by Ti, Zr, Hf, V, Nb, Ta, Mo, W, Zn, Ga, In, Si, Ge, Sn, or Sb, whereas Cr, Mn, or Fe occupy both sites with a slight preference for the Al sites depending on the composition (Ochiai et al., 1984; Miller and Horton, 1987; Shindo et al., 1988; Enomoto and Harada, 1989; Chiba et al., 1991; Hono et al., 1992). The case of Hf demonstrates the difficulties of site determination since there is also further strong experimental evidence of Hf occupying Ni sites instead of Al sites (Bohn et al., 1987 a, b). The chemical activity of Hf in Ni_3Al has recently been determined, according to which, however, Hf substitutes for Al in Ni_3Al (Albers et al., 1992). According to computer modeling, the site occupancy depends on the composition, i.e. different types of deviations from stoichiometry may change the site occupation by a third element (Hosoda et al., 1991).

Deviations from stoichiometry, which are possible on both sides of the stoichiometric composition, lead to constitutional defects which are important for the mechanical behavior at both low and high temperatures since at low temperatures such defects may act as dislocation obstacles and at high temperatures they may promote diffusion. (This will be discussed in some more detail with respect to the deformation behavior of the B2 phases in Sec. 4.3.)

Diffusion in Ni_3Al has been studied by few investigators – in particular Chou and Chou (1985) and Hoshino et al. (1988) – and has been reviewed and discussed with respect to mechanisms and defects (Bakker, 1984; Wever et al., 1989; Stoloff, 1989). The constitutional defects are antistructure atoms on both sides of stoichiometry, i.e. Al on Ni sites and Ni on Al sites, and the concentration of constitutional, i.e. athermal, vacancies is very small. The vacancy content of 6×10^{-4} at the melting temperature and the vacancy formation enthalpy of 1.60 eV correspond to the respective values for Ni, i.e. the vacancy behavior of Ni_3Al is similar to that of pure metals (Schaefer et al., 1992). The diffusion of Ni in Ni_3Al is not very different from that in pure Ni and at high temperatures it is insensitive to deviations from stoichiometry. The diffusion of Al in Ni_3Al is less well studied because a tracer is not readily available. Defects may interact with dissolved third elements which affects diffusion. In particular vacancies interact with B which is needed for "ductilization", and this leads to a complex dependence of the Ni diffusion coefficient on the Al and B content of Ni_3Al (Hoshino et al., 1988). Data for the diffusion of the third elements, Co, Cr, or Ti, in Ni_3Al are available (Minamino et al., 1992).

4.1.2 Microstructure and Mechanical Behavior

The mechanical behavior of Ni_3Al and Ni_3Al-based alloys, including creep, fa-

ArcelorMittal Ex. 2038
Page 53 of 190

tigue and fracture, and in particular the effects of microstructure and alloying with further elements have been reviewed exhaustively (Stoloff, 1989). Only the most important features, i.e. the anomalous temperature dependence of the flow stress and ductilization by the boron effect, are discussed in the following, which also considers more recent studies. Other recent studies concern creep, including inverse creep after the first normal primary creep stage (Hazzledine and Schneibel, 1989; Hayashi et al., 1991 a, b; Hemker et al., 1991; Miura et al., 1991; Schneibel and Hazzledine, 1992; Wolfenstine et al., 1992; Hemker and Nix, 1993; Zhang and Lin, 1993), superplasticity (Valiev et al., 1991; Ochiai et al., 1991; Yang et al., 1992; and the chapter by Mukherjee in Volume 6 of MST), fatigue (Matuszyk et al., 1990; Glatzel and Feller-Kniepmeier, 1991; Gordon and Unni, 1991; Gieseke and Sikka, 1992), and fracture (Kawabata and Takasugi, 1991; Takasugi, 1991 a; Yoo and Fu, 1991). The recrystallization behavior has been studied in more detail only recently (Gottstein et al., 1989, 1991; Cahn, 1991; Inoue and Inakazu, 1991; Ball and Gottstein, 1993; Zhou et al., 1993; Jena et al., 1993).

Anomalous Temperature Dependence of the Flow Stress

The plastic flow of Ni_3Al has been studied in much detail by many authors. The results have been reviewed and discussed intensively and the basic mechanisms are now well understood (Stoloff and Davies, 1966; Paidar et al., 1981; Liu and Stiegler, 1984; Pope and Ezz, 1984; Stoloff, 1984; Liu and White, 1985; Izumi, 1989; Suzuki et al., 1989; Liu et al., 1990; Yamaguchi and Umakoshi, 1990; Liu, 1993 b; Saada and Veyssière, 1993 b; and the chapter by Umakoshi in Volume 6 of MST). The outstanding feature is the positive, i.e. anomalous, temperature dependence of the flow stress which is illustrated in Fig. 21. Between room temperature and about 700 °C the flow stress increases with increasing temperature to reach a maximum and only at higher temperatures does normal softening occur.

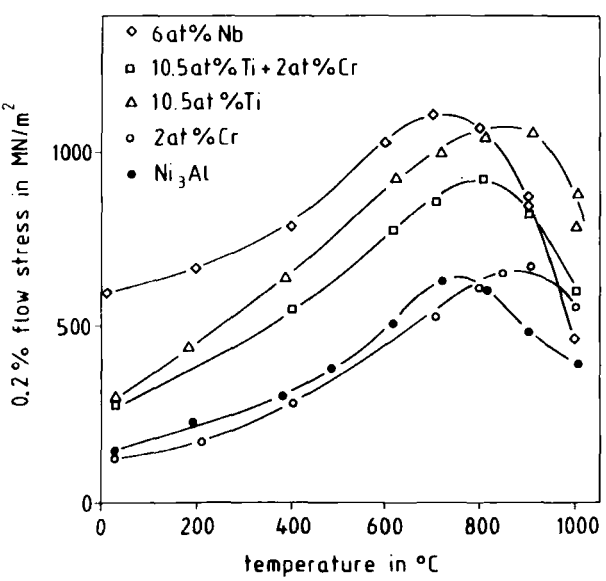


Figure 21. Temperature dependence of the flow stress for cast polycrystalline Ni_3Al and Ni_3Al with various alloying additions (Thornton et al., 1970).

ArcelorMittal Ex. 2038
Page 54 of 190

As already discussed (Sauthoff, 1986), the anomaly results from the anisotropy of the energy and mobility of the superlattice screw dislocations which determine the plastic deformation of Ni_3Al. The screw dislocations can split on {111} planes and on {010} planes. The splitting on {010} is favored energetically because the energy of the antiphase boundaries (APBs) between the partials is lower on {010}. However, a superdislocation on {010} is sessile because the dislocation cores of the partials spread outside the plane of the APB. On the other hand, the superdislocation on {111} with higher energy is glissile because the core spreading is confined to the slip plane.

This glissile state is metastable since the partials must first be coalesced into a single dislocation before cross slip back to {010} can occur. Hence dislocations are generated primarily on {111} planes on loading, and slip is confined to {111} at low temperatures. With rising temperature cross slip to {010} becomes possible by thermal activation, by which the dislocations are immobilized (Kear–Wilsdorf mechanism). The sessile dislocations act as obstacles and give rise to rapid strengthening with increased flow stress. Thus it is clear that the anomalous temperature dependence of the flow stress is observed only with sufficient strain, and indeed the minimum strain for this observable flow stress anomaly was found to be about 10^{-5} (Thornton et al., 1970). At temperatures above the flow stress maximum, the immobilized dislocations are mobilized again by enhanced thermal activation which leads to the familiar softening. The details of these mechanisms and reactions have been and still are the subject of specific studies, and the theoretical description becomes more and more elaborate (Yoo et al., 1988; Suzuki et al., 1989; Pope, 1991; Yoo and Fu, 1991; Webb et al., 1993a; Schoeck, 1993; Dimiduk et al., 1993; Hirsch, 1993; Molenat et al., 1993; Saada and Veyssière, 1993a, b; Khantha et al., 1993a, b).

From this discussion it is celar that the flow stress anomaly of Ni_3Al is a function of the binding forces between the atoms. Indeed the anomaly is exhibited by various $L1_2$ phases to different extents, and the differences are closely correlated with the differences in stability between the $L1_2$ structure and other possible structures, in particular the $D0_{19}$ and $D0_{22}$ structures (Mishima et al., 1985; Suzuki et al., 1989). In Ni_3Si and Ni_3Ge the anomaly is even more pronounced than in Ni_3Al, whereas it is weaker in Co_3Ti, Zr_3Al, Fe_3Ga, and Cu_3Au, and there is a continuous transition from a positive temperature dependence to the familiar negative one in the $L1_2$ ternary phase $(Ni, Fe)_3Ge$ when going from Ni_3Ge to Fe_3Ge. Likewise the flow stress maximum of Ni_3Al can be increased and shifted with respect to temperature by ternary alloying additions, as is exemplified in Fig. 21 (see also Lall et al., 1979). It has to be noted that such flow stress anomalies are also shown by other phases with different crystal structures, e.g. Fe-Co-2V (B2), CuZn (B2), TiAl ($L1_0$), Fe_3Al ($D0_3$), Mg_3Cd ($D0_{19}$), Ni_3V ($D0_{22}$), and Fe_2B (C16), and various mechanisms have been proposed for these phases (Stoloff and Davies, 1964; Westbrook, 1965; Paufler, 1976; Haasen, 1983; Stoloff, 1984; Kawabata et al., 1985).

The positive temperature dependence of the flow stress of Ni_3Al can be obscured by other concurrent strengthening effects. For example, the low-temperature flow stress can be increased by reducing the grain size to such an extent that it becomes higher than the original flow stress maximum at high temperature, i.e. a flow stress maximum is no longer discernible (Schul-

ArcelorMittal Ex. 2038
Page 55 of 190

son, 1985). An analogous effect is produced when C is dissolved in Ni_3Al to gradually increase the low-temperature flow stress (Jung and Sauthoff, 1989b; Wunnike-Sanders, 1993; Wunnike-Sanders and Sauthoff, 1994).

Ductilization

It is well known that only polycrystalline Ni_3Al is brittle and fails by intergranular fracture whereas Ni_3Al single crystals are highly ductile, and thus the brittleness of polycrystals is attributed to grain boundary weakness (Liu and Stiegler, 1984). Correspondingly, directionally solidified, columnar-grained Ni_3Al has been found to be ductile (Hirano and Mawari, 1993). The brittleness of polycrystalline Ni_3Al can be reduced by macroalloying with Co, Cu, or Pt which reduce the ordering tendency of the Ni_3Al (Chiba et al., 1992). Alternatively, the polycrystal brittleness of Ni_3Al can be removed by microalloying Al-deficient Ni_3Al with boron (Aoki and Izumi 1979; Aoki, 1990). The tensile elongation of polycrystalline Ni_3Al with 24 at.% Al, which has been recrystallized for 30 min at 1000 °C, increases with increasing B content from about 0 % for 0 % B to about 44 % for 0.025 wt.% B (Liu et al., 1985). A further increase in the B content produces a maximum tensile elongation of about 54 % for 0.1 wt.% B, after which the ductility gradually decreases with increasing B content.

This ductilization effect of boron depends sensitively on the Al content (Liu et al., 1985; Aoki, 1990). An Al content of 24 at.% corresponds to the Al solubility limit of Ni_3Al and cannot be lowered, i.e. a further reduction only produces the disordered γ-Ni–Al phase (see Fig. 20). With higher Al contents the ductilization effect becomes smaller and above the stoichiometric composition of 25 at.% Al, polycrystalline Ni_3Al with B is as brittle as without B. This stoichiometry effect can be changed significantly by alloying with a third element (Aoki et al., 1993). It should be noted that the ductility increase is accompanied by a significant increase in the ultimate tensile strength, which results from rapid strain hardening during plastic deformation (Liu et al., 1985).

This dramatic ductilization effect of boron has been and still is the subject of elaborate experimental and theoretical studies which, however, have not yet led to an agreement on the physical reasons for the boron effect, i.e. the mechanistic understanding of this ductilization effect is still unclear. This has been the subject of a set of papers recently, and the present state of knowledge and the controversial issues have been overviewed (Liu, 1991b). The important factors are briefly summarized in the following.

It has been found that B strongly segregates to grain boundaries in Al-deficient Ni_3Al in equilibrium, as well as Al, which affects the character and strength of the bonding at the interface. The segregation of both elements depends on the bulk Al content. Boron does not segregate to free surfaces. It has been suggested that this B segregation enhances the cohesive strength at the grain boundary thus preventing cracking along the grain boundary. Theoretical first-principles calculations indeed confirmed the beneficial effect of B on the cohesive strength. A recent study of the microscopic deformation behavior has shown that during deformation grain boundaries with boron emit dislocations to relieve stress concentrations, whereas at grain boundaries without boron such stress concentrations are relieved by the nucleation and propagation of cracks along the grain boundaries (T. C. Lee et al., 1992).

ArcelorMittal Ex. 2038
Page 56 of 190

It has been proposed by others that this B segregation produces disorder at grain boundaries, thus facilitating slip transmission across them. This view is supported by a Hall–Petch type analysis of flow stress data as a function of the grain size. There are observations on disordered grain boundary layers which indicate the formation of the γ-Ni–Al phase at the grain boundaries. This is not improbable since the Al content of Al-deficient Ni_3Al is near the solubility limit, and in the case of the $L1_2$ phase Cu_3Au it has been found (Tichelaar et al., 1992) that the order–disorder transition is preceded by the formation of disordered layers at the interfaces. However, such disordered layers have also been found in Ni_3Al without B, and have not been found in many ductile Ni_3Al alloys with B (see also Lin et al., 1993; Sun and Lin, 1993).

A careful investigation of the order–disorder transformation in Ni_3Al has shown that the order–disorder transition temperature is slightly lower than the solidus temperature for Ni_3Al with less than 23 at.% Al (Cahn et al., 1987). This leads to a more complex ordering process with domain formation which may be beneficial for ductility, whereas in the case of stoichiometric Ni_3Al with an order–disorder transition temperature above the liquidus temperature ordering occurs directly without domain formation.

This B segregation affects the segregation of impurities such as O, S, and P which embrittle conventional alloys. However, such impurities seem to be of little importance for Ni_3Al since Ni_3Al, and other intermetallics of high purity with clean grain boundaries are still brittle.

The experimental evidence for the various proposals is not clear and is even conflicting in some cases (Horton and Liu, 1990; Liu, 1991 b). It has to be concluded that the brittleness of intermetallics is a rather complex function of the crystal structure, composition and microstructure. Obviously this complexity, which seems to be more severe than for conventional alloys, excludes a simple, single-cause explanation. In any case, the ductilization results from changes in the character and strength of the bonding of the atoms involved which may be clarified by adequate quantum-mechanical calculations, and which may be characterized in an approximative way by differences in atomic parameters such as valency, electronegativity, and atomic size.

Furthermore, effects of corroding environments have to be considered, as will be discussed in Sec. 4.1.3. Experimental results have recently been presented which indicate environmental embrittlement as a major cause of the low-temperature brittleness of polycrystalline Ni_3Al, which is suppressed by microalloying with B (George et al., 1992, 1993 a, b; Zhu et al., 1993). However, this environment-induced embrittlement should be diminished by reducing the temperature, but this has not been observed, i.e. this aspect of the ductilization effect is also not yet clear (Lee and White, 1993).

4.1.3 Environmental Effects

The oxidation behavior of Ni_3Al has been studied repeatedly. The Al content of Ni_3Al is sufficient for the formation of a stable, protective, Al_2O_3 scale only at temperatures above about 1200 °C (Pettit, 1967; Meier, 1989). At lower temperatures Al diffusion in Ni_3Al to the surface is too slow to avoid Al depletion at the surface, and thus the first formed Al_2O_3 is overgrown by mixed Ni–Al scales. The initial stages of Ni_3Al oxidation have been studied in detail (Bobeth et al., 1992). The oxi-

ArcelorMittal Ex. 2038
Page 57 of 190

dation reaction is coupled with vacancy production which leads to the formation of voids below the scale and finally to scale spallation. Scale adherence is improved by the addition of Cr (Pan et al., 1991) and by the known oxygen-active elements – in particular Ti, Zr, Hf and the rare earths (Cathcart, 1985; Taniguchi and Shibata, 1989; Krasovec et al., 1992). The oxidation resistance of such Ni_3Al-base alloys has been found to be superior to that of the conventional high-temperature alloys 800 H and 617 (Brill and Klöwer, 1991). A similarly advantageous corrosion behavior has also been shown in carburizing and chloridizing atmospheres, whereas the sulfidation behavior is less advantageous (Natesan, 1988; Brill and Klöwer, 1991).

Apart from corrosion reactions at the surface, exposure to air or oxygen affects the mechanical behavior of Ni_3Al and various effects of environmental embrittlement have been observed. At elevated temperatures of about 800 °C the ductility of ductilized Ni_3Al shows a minimum which is more pronounced in air than in vacuum, and which is significantly alleviated by the addition of Cr (Liu and McKamey, 1990; Liu et al., 1990; Matuszyk et al., 1990; Khan et al., 1990). This embrittlement has been assumed to result from the effect of gaseous oxygen on the crack growth, whereas more recent results indicate that precipitated particles which are formed by internal oxidation may be more relevant to the embrittlement (DeVan and Hippsley, 1989; Chuang and Pan, 1992). The beneficial effect of Cr has been attributed to modifications to the mechanical properties of the scale (Taniguchi and Shibata, 1987; Hippsley et al., 1990), though a complete understanding of the ductility controlling mechanisms has not yet been reached (Liu and McKamey, 1990; Takeyama and Liu, 1992; Chuang and Pan, 1992).

Environmental embrittlement has also been observed at room temperature – in particular in moist air – depending on the Ni_3Al composition and the dopant content, and it was concluded that this embrittlement is caused by hydrogen formation (Masahashi et al., 1988; Liu, 1991 a; Wan et al., 1992 a; George et al., 1993 b, c). Correspondingly, stress corrosion cracking has been observed in aqueous environments, which is also caused by hydrogen (Stoloff, 1989; Ricker et al., 1990). The embrittling effect of hydrogen has been studied directly and has been attributed to a reduction in the cohesive strength of the grain boundaries (Bond et al., 1989; Takasugi, 1991 b; Wan et al., 1992 b). Nevertheless, the physical understanding of the hydrogen embrittlement effect is far from clear (Izumi, 1989; Takasugi, 1991 a; Liu, 1991 a; Li and Chaki, 1993 a).

4.1.4 Applications

Detection of the ductilizing effect of boron on Ni_3Al (see above) was the starting point for successful materials developments based on Ni_3Al which have resulted in a series of closely related Ni_3Al alloys for high-temperature applications (Liu et al., 1990). These alloys – known as nickel aluminides or advanced aluminides – generally contain B at levels below 500 ppm, and Al below the stoichiometric composition, in order to obtain ductility at room temperature, and in addition Hf, Zr, Ta, and Mo at levels of up to 5 at.% to improve the strength at high temperatures and Cr up to 10 at.% to enhance the ductility at intermediate temperatures between 400 °C and 900 °C (Liu et al., 1990; Sikka, 1990; Alexander and Sikka, 1992). The alloys may contain second phases and in particular the Cr-containing alloys generally contain 5 to 15 % of the disordered,

ArcelorMittal Ex. 2038
Page 58 of 190

Ni-rich phase, depending on the Al content (Liu et al., 1990; Khan et al., 1990; Liu and Kumar, 1993).

The Ni_3Al alloys compare favorably with many superalloys with respect to their short-term mechanical behavior, i.e. yield strength, which is higher than that of IN-713C at elevated temperatures, and ductility, which is generally 25 % to 40 % at temperatures up to 700 °C and 15 % to 30 % at up to 1000 °C in air (Liu et al., 1990). The fatigue resistance of Ni_3Al alloys is higher than that of Ni-base superalloys at temperatures below the ductility minimum, i.e. below 500 °C (Stoloff, 1989; Liu et al., 1990; Matuszyk et al., 1990; Gordon and Unni, 1991). The creep resistance of Ni_3Al alloys is comparable to that of many superalloys, but it is not as high as that of some advanced, single-crystal, Ni-base superalloys which are used for jet engine turbine blades (Liu et al., 1990; Khan et al., 1990).

In view of these properties it may be stated that the Ni_3Al alloys are similar to the closely related superalloys and enlarge the superalloy spectrum. However, they cannot compete with the advanced aerospace superalloys which are used in aircraft engines, and thus Ni_3Al alloys are unlikely to displace superalloys in such applications (Liu et al., 1990; Dimiduk et al., 1992). Nevertheless, Ni_3Al alloys are promising for less demanding applications such as gas, water, and steam turbines, aircraft fasteners, automotive components, tooling and permanent molds where good combinations of strength and resistance against fatigue, wear including erosion and cavitation, and oxidation are needed (Liu et al., 1990).

The technologies for fabrication and processing have been developed, i.e. Ni_3Al alloys can be melted by air-induction melting with acceptable quality and by vacuum-induction melting, vacuum-arc remelting, and electroslag remelting for better qualities, ingots up to 1500 kg and components have been cast with low or no porosity depending on the boundary conditions, hot working is possible by conventional hot forging, isothermal forging and hot extrusion, the alloys can be cold worked and property data are available (Sikka, 1988, 1989, 1990; Sanders et al., 1991; Alexander and Sikka, 1992; Haubold et al., 1992). Most of the alloys can be welded with good quality if it is done with care (Bittence, 1987; Chen and Chen, 1988; Stoloff, 1989; Liu et al., 1990; Santella, 1993; Li and Chaki, 1993 b), and cutting is accomplished by high-speed abrasive wheels (Sikka, 1990). Besides ingot metallurgy, powder metallurgy methods have been applied successfully for producing Ni_3Al alloys (Stoloff, 1989; Sampath et al., 1991; Liang and Lavernia, 1991; Withers et al., 1991).

Over recent years the developed technologies have been transferred to various industrial companies for the production of heating element wires, wear parts, diesel engine applications and aircraft fasteners, i.e. Ni_3Al alloys are on their way to commercialization (Sikka, 1990; Liu and Kumar, 1993; Liu, 1993 a). An example is given by the ongoing development of an Ni_3Al turbocharger rotor for heavy duty diesel engines, and it is expected that with further property improvements power cylinder components in high performance, state-of-the-art, diesel engines, i.e. valves, valve seats, piston crowns, piston rings, cylinder liners, and cylinder heads are likely candidates for future applications (Patten, 1990). The only application of Ni_3Al alloys which has been realized up to now is their use in dies for hot pressing permanent magnetic alloys which are already on the market (Baker and George, 1992). Obvi-

ArcelorMittal Ex. 2038
Page 59 of 190

ously, the transfer process from the laboratory to large scale production is handicapped by the limited deformability at elevated temperatures, which makes hot working difficult.

Besides these developments, which are directed at specific applications, Ni_3Al alloys are used for the development of intermetallic matrix composites which contain reinforcing particles or fibers of borides, carbides, oxides or carbon (Fuchs, 1989; Lee et al., 1990; Tortorelli et al., 1990; Alman and Stoloff, 1991; Kumar, 1991; McKamey and Carmichael, 1991; Mukherjee and Khanra, 1991; Brennan et al., 1992). Apart from the mechanical properties and the necessary corrosion resistance, the chemical compatibility of the used phases is of primary importance with respect to the long-term stability. It was found that SiC, B_4C, and TiB_2 react extensively with Ni_3Al alloys, whereas very little reaction has been observed with Al_2O_3 or TiC in Ni_3Al (Fuchs, 1989; Lee et al., 1990; Brennan et al., 1992). It should be noted that Ni_3Al alloys are used not only as the matrix material, but also as a reinforcing phase in, e.g. an Al alloy to form a metal-matrix composite (Metelnick and Varin, 1991).

4.2 Other $L1_2$ Phases

4.2.1 General Remarks

Apart from Ni_3Al, Ni forms other intermetallic phases with an $L1_2$ structure and the composition Ni_3X, where X is either an element near Al in the periodic table, e.g., Ni_3Si, Ni_3Ga, or Ni_3Ge, or another transition metal near Ni, e.g. Ni_3Fe or Ni_3Mn; and there are also analogous examples for other transition metals, e.g. Fe_3Ga, Fe_3Ge, or Co_3Ti (Villars and Calvert, 1991). $L1_2$ phases are among the first and best studied intermetallics because some of them, e.g., Ni_3Fe and Ni_3Mn, as well as the classical example Cu_3Au, transform into disordered solid solutions at temperatures below the melting temperature which allows the effect of atomic ordering on the physical properties and mechanical behavior to be studied (Sachs and Weerts, 1931; Dahl, 1936; Vidoz et al., 1963). Such phases with a critical temperature of ordering below the melting temperature are known as Kurnakov phases.

Lately, the successful ductilization of Ni_3Al and the subsequent materials developments have excited an enormous interest in $L1_2$ phases, which have been studied in great number and much detail in order to understand the physical mechanisms which control the plasticity (see, e.g., Veyssière, 1992). In particular Cu_3Au and Ni_3Fe, which are experimentally easy, are used as model phases for detailed investigations of the microstructural features of deformation (e.g., Korner, 1991; Tichelaar and Schapink, 1991). Jerky flow has been observed in polycrystalline Cu_3Au and Ni_3Fe as well as in the $L1_2$ phases Zr_3Al, Ni_3Mn, and Ni_3Al (Schulson, 1984). Ni_3Ge has been used as a model phase for studying the effects of cyclic deformation in comparison to monotonic deformation in $L1_2$ phases (Pak et al., 1986; Inoue et al., 1991 a).

$L1_2$ phases have been studied systematically in comparison to Ni_3Al in order to clarify the effects of changes in composition on the mechanical behavior. It has been known for a long time that polycrystalline Cu_3Au and Ni_3Fe are ductile at room temperature (Dahl, 1936; Vidoz et al., 1963) whereas polycrystalline Ni_3Al is brittle, as was discussed in the preceding section. This difference in the ductility may be attributed to a difference in the ordering energy, since Cu_3Au and Ni_3Fe as Kurnakov phases disorder below the melting

ArcelorMittal Ex. 2038
Page 60 of 190

temperature and Ni_3Al is ordered up to the melting point. However, there are other $L1_2$ phases that are ordered up to the melting point and which are not brittle, and it can be shown that the ductility of polycrystalline $L1_2$ phases is strongly correlated with the absolute valency difference of the constituent elements, which is reflected by the respective positions and distances in the periodic table; Ni_3Si, Ni_3Ga, Ni_3Ge, Fe_3Ga, and Ni_3Al are brittle whereas Ni_3Fe, Ni_3Mn, Co_3Ti, Cu_3Pd and Cu_3Au are ductile (Takasugi and Izumi, 1985d).

Besides ductility, the temperature dependence of the flow stress may change significantly with changing composition. In particular, some $L1_2$ phases show an anomalous, positive, temperature dependence for the flow stress like Ni_3Al, whereas other $L1_2$ phases show the conventional negative temperature dependence, as was already indicated in Sec. 4.1.2. In Ni_3Si and Ni_3Ge this anomaly is even more pronounced than in Ni_3Al, whereas it is weaker in Co_3Ti, Zr_3Al, Fe_3Ga, and Cu_3Au, and there is a continuous transition from a positive temperature dependence to the familiar negative one in the $L1_2$ ternary phase $(Ni,Fe)_3Ge$ when going from Ni_3Ge to Fe_3Ge. This variation in the temperature dependence of the flow stress has been the subject of systematic studies and it can be shown that the differences are closely correlated with the differences in stability between the $L1_2$ structure and other possible structures, in particular the $D0_{19}$ and $D0_{22}$ structures (Mishima et al., 1985; Suzuki et al., 1989). Furthermore, there is a correlation between the anomalous temperature dependence of the flow stress and the elastic anisotropy which has been revealed by a systematic study of the elastic moduli of various $L1_2$ phases (Yasuda et al., 1991 a, b, 1992), and which supports a theoretical model for the flow stress behavior (Yoo et al., 1988; Yoo and Fu, 1991).

Apart from this scientific interest in $L1_2$ phases, the $L1_2$ structure is regarded as most promising for developing ductile intermetallic materials because of the successful "ductilization" of Ni_3Al. Thus $L1_2$ phases have been the subject of many studies and indeed some $L1_2$ phases are of interest with respect to applications as structural materials. Examples are briefly discussed in the following section. Furthermore, other phases, which do not have an $L1_2$ structure, have been alloyed with further elements in order to produce the $L1_2$ structure. An example of this is given by the so-called trialuminides with an $L1_2$ structure, which result from alloying the binary Al_3Ti phase with a tetragonal $D0_{22}$ structure with the transition metals Cr, Mn, Fe, Ni, and Cu, and which have been discussed in Sec. 3.4. However, it has to be noted that the expected ductilization of these trialuminides has not yet been achieved. Another example of obtaining the $L1_2$ structure by proper alloying is the multinary phase $(Ni,Co,Fe)_3V$, on which a successful materials development has been based and which is also discussed in the following section.

4.2.2 $L1_2$ Phases of Particular Interest

Ni_3Fe

Ni_3Fe is one of the ductile $L1_2$ phases, as mentioned in the preceding section. It shows an order–disorder transition at intermediate temperatures which has been studied in detail with respect to energetics and kinetics (Marty et al., 1990; Cahn, 1992; see also the chapter by Inden and Pitsch in Volume 5 of MST). The mechanical behavior is well known and the characteristics have been discussed with re-

ArcelorMittal Ex. 2038
Page 61 of 190

spect to strength, dislocation behavior and fracture (see, e.g. Vidoz et al., 1963; Davies, 1963b; Takasugi and Izumi, 1985d, 1992; Izumi, 1989; Korner, 1991; D. G. Morris, 1992; Veyssière, 1992). The elastic constants have been measured (Yasuda et al., 1992). As for other $L1_2$ phases, Ni_3Fe is subject to hydrogen embrittlement at room temperature (Liu and Stoloff, 1993).

The importance of Ni_3Fe results from its advantageous physical properties, i.e. it is ferromagnetic with a high permeability (Kouvel, 1967; Dietrich, 1990). Thus Ni_3Fe gave rise to the developments of the magnetically soft, high-nickel alloys which are known as Permalloys. Alloying with further elements improves the magnetic behavior as is demonstrated by the Moly-Permalloys which typically contain 80% Ni and 4 to 5% Mo – the balance being Fe – and the Mu-Metals which typically contain 77% Ni, 5% Cu and 2% Cr, with the balance being Fe (Dietrich, 1990).

Co_3Ti

A promising $L1_2$ phase is Co_3Ti which is deformable over a wide temperature range (including room temperature) and has a high strength at elevated temperatures (Takasugi and Izumi, 1985c; Takasugi et al., 1990b). However, there are indications of environmental embrittlement in air at ambient temperatures due to the embrittling effect of dissolved hydrogen (Takasugi and Izumi, 1986; Liu et al., 1989b; Takasugi et al., 1990b; Liu, 1991a). The deformation behavior of Co_3Ti has been studied in detail with respect to strength and ductility, and in particular an anomalous temperature dependence of the flow stress has been found, as in the case of Ni_3Al (Takasugi and Izumi, 1985b; Takasugi et al., 1987). In view of high temperature deformation, the diffusion coefficient of Co in Co_3Ti has been measured and the constitutional defects have been studied which result from deviations from stoichiometry (Takasugi and Izumi, 1985a; Nakajima et al., 1988, 1991). Co_3Ti can be alloyed with third elements and the site occupation of the various elements has been investigated (Liu et al., 1986; Takasugi et al., 1990a). Such alloying additions can be used for varying the mechanical behavior, i.e. strength, ductility, flow stress anomaly, and sensitivity against hydrogen embrittlement (Liu et al., 1989a; Takasugi et al., 1990b; Hasegawa et al., 1993a).

Ni_3Si

A promising $L1_2$ phase is Ni_3Si, the deformation behavior of which, including the anomalous temperature dependence of the flow stress, is analogous to that of Ni_3Al. It can be alloyed with Ti to form the ternary $L1_2$ phase $Ni_3(Si,Ti)$, which is being considered as a candidate phase for applications which require a high-temperature structural material or a corrosion resistant material since its strength is very high in comparison to other $L1_2$ phases, its ductility is high over a wide temperature range (particularly at lower temperatures when alloyed with B), it has an excellent corrosion resistance in hot sulfuric acid and likewise an excellent oxidation resistance in air at high temperatures, and it can be produced with good properties by various processing methods (Takasugi and Yoshida, 1991b; Baker et al., 1993; Ulvensoen et al., 1993).

Various studies have been directed at the alloying behavior and the effects on the mechanical properties, including fracture (Takasugi et al., 1991b; Takasugi and Yoshida, 1991a; Takasugi, 1991a; Takasugi and Izumi, 1992; Khantha et al., 1991; T. Zhang et al., 1991). The elastic moduli

ArcelorMittal Ex. 2038
Page 62 of 190

have been determined (Yasuda et al., 1992), and the dislocation behavior at low and high temperatures has been studied in detail (Yoshida and Takasugi, 1991 a, 1992; Takasugi and Yoshida, 1992, 1993). The yield stress anomaly, which had already been reported in 1952 (Lowrie, 1952), has been clarified recently on the basis of ab initio calculations of the elastic constants and shear fault energies (Fu et al., 1993 b). $Ni_3(Si,Ti)$ alloys can be deformed superplastically (Nieh and Oliver, 1989; Takasugi et al., 1991 a, c; Stoner et al., 1992) and environmental embrittlement has been observed (Liu and Oliver, 1991; Takasugi et al., 1991 d; Takasugi, 1991 c). Recently, Ni_3Si has been alloyed with Co_3Ti to form two-phase intermetallic alloys with superior creep resistance (Hasegawa et al., 1993 b). Finally, it is noted that at very high temperatures an intermediate, brittle, monoclinic Ni_3Si phase is stable, which may form the matrix of respective Ni–Si alloys with precipitated, ductile, Ni-rich solid solution and $L1_2$ Ni_3Si as the toughening second phases (Baker et al., 1993; Li and Schulson, 1993).

Zr_3Al

The $L1_2$ phase Zr_3Al, which forms peritectically from Zr_2Al and Zr, was studied extensively for use as the cladding material for water-cooled, nuclear power reactors since it has a low cross section for the absorption of thermal neutrons (Schulson, 1984; Liu et al., 1990; Parameswaran et al., 1990). In particular, the mechanical behavior was the subject of detailed studies (Schulson, 1984) according to which the strength is high with an anomalous temperature dependence for the flow stress. The work hardening rate exceeds that for any disordered or ordered f.c.c. alloy. Zr_3Al, with polished surfaces, has a ductility of about 30 % at room temperature with, however, a high notch sensitivity. Fast-neutron irradiation at low doses suppresses the notch sensitivity, whereas irradiation at higher doses produces an embrittling crystalline to amorphous phase transition which is accompanied by significant swelling. These irradiation effects precluded the use of Zr_3Al in nuclear reactors (Parameswaran et al., 1990). Working of Zr_3Al is limited to an area reduction of about 30 % and hot working is best done above the peritectic temperature, i.e. as two-phase $Zr–Zr_2Al$, which is then followed by an annealing treatment below the peritectic temperature to produce the Zr_3Al phase. The material has good oxidation resistance and can easily be fabricated into strip, rod, and tubing.

$(Fe,Co,Ni)_3V$

The brittle phases Ni_3V with a tetragonal $D0_{22}$ structure and Co_3V with a complex hexagonal structure can be alloyed with Fe in such a way that ternary $(Ni,Fe)_3V$ and $(Co,Fe)_3V$ and quaternary $(Fe,Co,Ni)_3V$ phases are formed which have the cubic $L1_2$ structure, and are ductile with tensile ductilities of about 40 % or more (Liu and Inouye, 1979; Liu, 1984; Liu et al., 1990). For these alloys the criterion for the stabilization of the $L1_2$ structure is a valence electron content of less than 7.89 per atom since higher valence electron contents between 7.89 and 8.6 are characteristic of Co_3V and $(Co,Ni)_3V$ with hexagonal structures, whilst tetragonal Ni_3V is characterized by 8.75 valence electrons per atom. The stability of these $L1_2$ alloys has also been studied by means of quantum-mechanical, first-principles calculations (Freeman et al., 1992).

The $L1_2$ alloys $(Ni,Fe)_3V$, $(Co,Fe)_3V$, and $(Fe,Co,Ni)_3V$ disorder at a critical

ArcelorMittal Ex. 2038
Page 63 of 190

temperature between 600 °C and 1000 °C, depending on the Fe content, to form disordered f.c.c. alloys. Recrystallization in the ordered state below the critical temperature is slow compared with the disordered state (Cahn, 1991), whereas diffusion does not seem to be affected much by the order–disorder transition (Mantl et al., 1984). These $L1_2$ alloys can easily be fabricated because of their high ductility, they show an anomalous, positive temperature dependence for the flow stress like Ni_3Al, strength decreases sharply above the critical temperature of disordering, and they have an excellent creep and fatigue resistance [for the latter see Ashok et al. (1983)] (Liu and Inouye, 1979; Liu, 1984; Liu et al., 1990). They can be welded (Bittence, 1987), but they are not sufficiently oxidation resistant above 600 °C because of the absence of Al (Liu, 1984), and they are subject to environmental embrittlement (Liu, 1991a; Nishimura and Liu, 1991, 1992a, b; Liu, 1992; Miura and Liu, 1992). In view of their advantageous mechanical behavior, they are regarded as promising for applications as structural materials in conventional power plants – in particular for steam turbines – as well as for nuclear power plants because irradiation produces relatively little swelling with, however, some lowering of ductility (Liu, 1984; Liu et al., 1990).

4.3 NiAl

4.3.1 Basic Properties

NiAl is the best known example of the intermetallics with a cubic B2 structure (Fig. 1), which form one of the largest groups of intermetallics (Baker and Munroe, 1990). The physical and mechanical properties of NiAl have recently been reviewed in detail (Miracle, 1993). As is illustrated by the phase diagram in Fig. 20, the phase NiAl has an extended range of homogeneity and melts congruently at about 1640 °C for the stoichiometric composition with 50 at.% Al. This melting point is higher than those of the constituent elements which indicates a strong bonding between Ni and Al and a corresponding high phase stability with a strong tendency for atomic ordering. This interpretation has been confirmed by quantum-mechanical, ab initio calculations according to which the strong Ni–Al bonding is of a mixed type, i.e. metallic with contributions of covalent and ionic bonding, which makes the Al atoms slightly electropositive (Fu and Yoo, 1992b; Lu et al., 1992).

Indeed NiAl with a stoichiometric composition is highly ordered up to the melting point according to such ab initio calculations (Stocks et al., 1992). Deviations from stoichiometry result in constitutional disorder, i.e. constitutional point defects are produced which are antistructure atoms, i.e. excess Ni atoms on Al sites on the Ni-rich side of the stoichiometric composition and vacancies in the Ni sublattice on the Al-rich side, as has been shown experimentally and theoretically (Jacobi and Engell, 1971a, b; Nakamura and Takamura, 1982; Koch and Koenig, 1986; Fu and Yoo, 1992a; Kogachi et al., 1992; S. M. Kim, 1992). In this way the number of valence electrons per alloy atom does not exceed a critical value for deviations from stoichiometry, in agreement with the Hume-Rothery rules for electronic compounds (Rusovic and Henig, 1980). These point defects interact with each other from which local ordering results (Georgopoulos and Cohen, 1981). Besides the constitutional point defects, there are the thermal point defects which again are vacancies in the Ni sublattice and Ni antistructure atoms in the Al sublattice since vacancies can only be created in the Ni sublattice,

ArcelorMittal Ex. 2038
Page 64 of 190

and any two such vacancies must be compensated by one Ni antistructure atom for a constant NiAl composition (Rusovic and Henig, 1980; Fu and Yoo, 1992a). The equilibrium configurations of the thermal vacancies have been studied theoretically (Kozubski, 1993).

The density of NiAl is low at 5.9 g/cm^3 for the stoichiometric composition compared with conventional Ni-base alloys, and it increases with decreasing Al content (Rusovic and Warlimont, 1977; Harmouche and Wolfenden, 1987). It is noted that the density change per unit of Al content is larger for Al-rich NiAl than for Ni-rich NiAl because of the difference in the defect structure.

The elastic behavior of NiAl has been studied repeatedly and the elastic moduli have been determined experimentally for polycrystals and single crystals as a function of composition and temperature (Wasilewski, 1966; Rusovic and Warlimont, 1977, 1979; Harmouche and Wolfenden, 1985, 1987). The elastic behavior has also been studied theoretically by quantum-mechanical, ab initio calculations, and the resulting elastic moduli are in close agreement with the experimental values (Yoo et al. 1990; Fu and Yoo, 1992b; Freeman et al., 1992; Yoo and Fu, 1993).

The Young's modulus of polycrystalline NiAl with a stoichiometric composition is about 235 GPa at room temperature (Harmouche and Wolfenden, 1987). The elastic moduli are functions of the composition, and the Young's modulus reaches a maximum of slightly more than 235 GPa, not at the stoichiometric composition as is expected, but at about 48 at.% Al which may be related to the difference in the defect character on both sides of stoichiometry. The effect of excess vacancies, which are produced by quenching from high temperatures, on the elastic behavior was studied by Rusovic and Henig (1980). The elastic anisotropy is larger than that of corresponding disordered metals with an A2 structure, e.g. b.c.c. Fe, and corresponds to that of f.c.c. Cu or Ni (A1 structure) (Wasilewski, 1966). As a consequence of this anisotropy, the elastic constants of polycrystalline NiAl depend sensitively on texture. Ni-rich NiAl shows anomalies in its elastic behavior, and in particular there is an anomalous temperature dependence which indicates lattice softening and is related to the martensitic transformation (Rusovic and Warlimont, 1975, 1977). The martensitic transformation of NiAl is discussed in the following section.

Diffusion in NiAl has been studied repeatedly, from which a reliable data basis has resulted (see, e.g. Hagel, 1967; Hancock and McDonnell, 1971; Shankar and Seigle, 1978; Hao et al., 1985; Wever, 1992). The diffusion coefficient is expected to reach a minimum at the stoichiometric composition since any deviations from stoichiometry reduce the degree of atomic order by introducing constitutional point defects which enhance diffusion. Indeed the diffusion coefficient for Ni in NiAl reaches a minimum at about 49 at.% Al (Hancock and McDonnell, 1971; Shankar and Seigle, 1978), which is slightly below the stoichiometric composition and is related to the effects of point defects, i.e. vacancies and antisite atoms, on diffusion (Wang and Akbar, 1993). The tracer diffusion coefficient of Al in NiAl cannot be measured directly because the necessary Al isotope is not available. The atomic migration processes in NiAl are more complex than in disordered b.c.c. alloys because of the ordered atom distribution and, in spite of detailed analyses of the atom jump processes, a complete understanding and modeling of diffusion in NiAl has not yet been reached (Bakker, 1984; Wever et al., 1989;

ArcelorMittal Ex. 2038
Page 65 of 190

Koiwa, 1992; Bakker et al., 1992). Only recently a model, which is based on a combination of two mechanisms, has been proposed for describing the composition dependence of diffusion in B2 phases (Kao and Chang, 1993). It should be noted that the understanding of the basic diffusion processes for other intermetallics is still less than for NiAl and other B2 phases (Wever, 1992). Diffusion studies of multicomponent systems are rare, and with respect to NiAl base alloys only data for the ternary phase (Ni,Fe)Al are available from a systematic study of the system Ni–Al–Fe (Cheng and Dayananda, 1979; Dayananda, 1992). Recently, the effect of Cr on diffusion in NiAl has been studied (Hopfe et al., 1993).

4.3.2 Phase Diagram and Martensitic Transformation

The equilibria of NiAl with neighboring nickel aluminides at high and low temperatures are shown by the Ni–Al phase diagram in Fig. 20. Al-rich NiAl forms an equilibrium with Al_3Ni_2 only at higher temperatures, whereas at lower temperatures an equilibrium is formed with the phase Al_4Ni_3 which has only recently been identified (Mukherjee et al., 1979; Ellner et al., 1989). Its crystal structure is related to the B2 structure of NiAl and contains ordered vacancies. Ni-rich NiAl is in equilibrium with only Ni_3Al at high temperatures and the mutual solubilities are shown in the phase diagram (according to Nishimura and Liu, 1992b; Bremer et al., 1988; Fang and Schulson, 1992). At low temperatures, Ni-rich NiAl forms an equilibrium with Ni_5Al_3 which has been studied in detail (Robertson and Wayman, 1984; Khadikar and Vedula, 1987; Khadikar et al., 1993). In addition, precipitate particles of a metastable Ni_2Al phase with either a trigonal or a monoclinic crystal structure have been observed in Ni-rich NiAl after quenching and subsequent annealing at intermediate temperatures (Murthy and Goo, 1993; Muto et al., 1993a, b).

Ni-rich supersaturated NiAl, i.e. NiAl with more than 60 at.% Ni, can transform martensitically if decomposition and precipitation of Ni_3Al and/or Ni_5Al_3 can be avoided by annealing at high temperatures with rapid quenching to low temperatures. The martensite formation temperature M_s increases linearly with increasing Ni supersaturation from about $-240\,^{\circ}C$ for 60 at.% Ni to about $1000\,^{\circ}C$ for 70 at.% Ni (Au and Wayman, 1972; Smialek and Hehemann, 1973; Ochiai and Ueno, 1988). The martensitic transformation produces the ordered, face-centered tetragonal $L1_0$ structure with a tetragonality of $c/a = 0.86$, and there is an internally twinned substructure (Chakravorty and Wayman, 1976a, b). In some cases a hexagonal martensite with 2H stacking (a two-layer structure) was also observed (Litvinov et al., 1974; Martynov et al., 1983; Tanner et al., 1990), and furthermore a monoclinic structure with rhombohedral 7R stacking (a seven-layer structure) was found depending on the Al content (Martynov et al., 1983; Tanner et al., 1990; Khachaturyan et al., 1992; Shimizu and Tadaki, 1992). The 7R structure is intermediate in the course of the martensitic transformation of NiAl and is derived from $L1_0$ by introducing periodic stacking faults. It can be shown theoretically that the energy barriers for the martensitic transition from the cubic B2 structure to the tetragonal $L1_0$ structure are lowered by the formation of the intermediate 7R phase (Yegorushkin et al., 1985; Stocks et al., 1992; Khachaturyan et al., 1992; Sluiter et al., 1992). The elastic moduli of the formed martensite have been determined (Robertson, 1990).

ArcelorMittal Ex. 2038
Page 66 of 190

The martensitic transformation of Ni-rich NiAl can be induced by external applied stresses; it is thermoelastic, superelasticity has been observed, and the martensite deforms by twinning and detwinning (Au and Wayman, 1972; Chakravorty and Wayman, 1976b; Enami et al., 1981; Murakami et al., 1992; Kim and Wayman, 1992). Thus all prerequisites for the shape memory effect are fulfilled and indeed the shape memory effect has been produced with NiAl irrespective of the method of alloy preparation – ingot metallurgy or powder metallurgy, i.e. it can be shown that the transformation characteristics do not depend on the processing route (Ochiai et al., 1987; Kim and Wayman, 1990). According to a computer simulation, the stress-induced martensitic transformation is also expected for NiAl which is not supersaturated with Ni, but which is subject to high stress concentrations, e.g. at crack tips (D. Kim et al., 1991).

NiAl can be alloyed with further elements in order to form ternary phases with a B2 structure which is then known as an $L2_0$ structure, too, or to obtain additional phases in equilibrium with NiAl. Fe, as well as Co, can substitute for Ni in NiAl completely without affecting the B2 structure, as is expected in view of the binary B2 phases FeAl and CoAl. Correspondingly, the ternary Ni–Fe–Al phase diagram, which is of importance with respect to conventional high temperature alloys, shows the extended B2 phase field and the respective equilibria with Ni_3Al and Al-rich phases on the one hand and with disordered b.c.c. Fe and f.c.c. Fe on the other (Bradley and Taylor, 1938; Dannöhl, 1942; Bradley, 1951; Hao et al., 1984). The Ni–Al–Co system behaves in an analogous way (Hao et al., 1984; Ishida et al., 1991a, 1993). Other ternary systems have been reviewed (Raman and Schubert, 1965; Kumar, 1990). Another important alloy system is the system Ni–Al–Ti which contains various ternary intermetallics besides NiAl, in particular the Heusler-type phase Ni_2AlTi with an $L2_1$ structure which is derived from the B2 structure (see Sec. 4.5), and the hexagonal Laves phase $Ti_{46}Ni_{27}Al_{27}$ with a C14 structure (see Sect. 8) (Raman and Schubert, 1965; Nash and Liang, 1985; Lee and Nash, 1991b; Yang et al., 1992b). Similar situations are found in the phase diagrams for Ni–Al–Nb (Benjamin et al., 1966; Reip, 1991; Ochiai et al., 1991) and Ni–Al–Ta (Pak et al., 1988).

Ternary alloying is of particular importance with respect to the martensitic transformation of NiAl since it offers the possibility of controlling the martensite formation temperature M_s besides other transformation features. Co reduces the transformation temperature, reduces the transformation strain anisotropy and increases the interfacial mobility (Russell et al., 1989). It is noted that the curves of constant M_s in the ternary Ni–Al–Co diagram remain in the two-phase field, i.e. only the supersaturated (Ni,Co)Al can transform martensitically. The effect of other elements, i.e. Ti, V, Nb, Ta, Cr, Mo, W, Fe, Mn, Cu, Si (Kainuma et al., 1992a) and B (Xie et al., 1993), on M_s has been studied recently and it has been found that alloying with Fe leads to a situation which is similar to the Ni–Al–Co case, whereas alloying with Mn enlarges the B2 field in the ternary Ni–Al–Mn phase diagram to such an extent that the curves of constant M_s are shifted into the B2 field, i.e. it is expected that supersaturation is not necessary for the martensitic transformation of (Ni,Mn)Al (Kainuma et al., 1992b,c).

ArcelorMittal Ex. 2038
Page 67 of 190

4.3.3 Microstructure and Mechanical Behavior

Figure 22 illustrates the variation of the flow stress of polycrystalline NiAl with temperature and composition. The curves show the normal temperature dependence with high strength at low temperatures, a comparatively steep strength decrease at intermediate temperatures around half the melting temperature (about 680 °C for NiAl) and low strength with further softening at high temperatures. It can be seen that variations in the composition lead to variations in the strength, and these effects may be different at low and high temperatures with a transition range around half the melting temperature (Sauthoff, 1990 b).

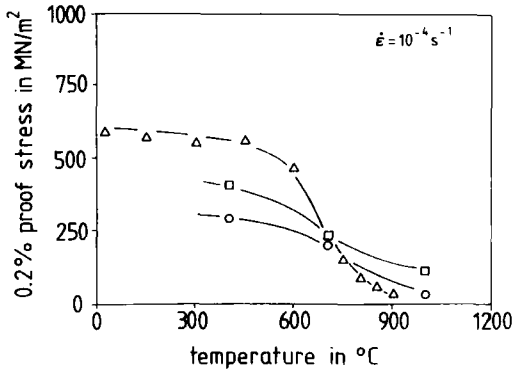


Figure 22. Flow stress (0.2% proof stress in compression at $10^{-4}\,s^{-1}$ strain rate) as a function of temperature for binary and ternary NiAl phases, i.e., stoichiometric NiAl (circles), stoichiometric $(Ni_{0.8}Fe_{0.2})Al$ (squares), and off-stoichiometric $(Ni_{1.0}Fe_{0.2})Al_{0.8}$ (triangles) (Rudy and Sauthoff, 1985; Rudy, 1986).

The softening at high temperatures is related to thermally activated creep processes which are the subject of the next section. Deviations from stoichiometry produce constitutional defects which enhance diffusion and lead to softening at high temperatures, whereas at low temperatures these defects are immobile and act as strengthening deformation obstacles. These different effects of deviations from stoichiometry at low and high temperatures were studied in detail for binary NiAl (Vandervoort et al., 1966).

Alloying of NiAl with a third element, e.g. Fe, leads to solid-solution strengthening in the total temperature range of Fig. 22. These effects depend on both the temperature and the strain rate, as was shown by Rudy and Sauthoff (1985) and Rudy (1986). The effects of various other solutes on the high-temperature strength have been studied (Vedula et al., 1985; Nathal, 1992; Cotton et al., 1993 b). Besides composition, processing was found to be a strength controlling factor which underlines the important role of the microstructure in strengthening. The highest strengths were obtained with alloys with an excess of solute which was precipitated as second phase particles. NiAl alloys with second phases are discussed in Secs. 4.3.4 and 4.3.6.

Plastic deformation of NiAl occurs predominantly by the movement of perfect dislocations in a ⟨100⟩ slip direction which is the shortest lattice translation vector in the B2 structure, and the preferred slip planes are {011}, whereas slip on {001} is also possible (Ball and Smallman, 1966; Strutt and Dodd, 1970; Baker and Munroe, 1990; Darolia et al., 1992 b; Y. Zhang et al., 1993). The details of slip in single crystals have been studied recently as a function of crystal orientation, deformation mode and temperature (Takasugi et al., 1993 b, c). In view of the high ordering energy of NiAl (see Sec. 4.3.1), creation and movement of dislocations is expected to be difficult, i.e. high strength and low ductility are expected. In a more fundamental sense, it is expected that the high strength and low ductility are caused by

ArcelorMittal Ex. 2038
Page 68 of 190

the strength and character of the atomic bonding. However, for NiAl there seems to be no simple correlation between the directionality and ionicity of the bonding and the mechanical behavior, and much more work is necessary (Schultz and Davenport, 1992).

As a consequence of the available slip systems, the strength and ductility are highly anisotropic with a "hard" ⟨100⟩ direction and "soft" ⟨110⟩ and ⟨111⟩ directions (Darolia et al., 1992b; Glatzel et al. 1993b; Takasugi et al., 1993a). NiAl with the "hard" orientation shows practically no ductility – in spite of indications of local plastic deformation (Vehoff, 1992) – below the brittle-to-ductile transition temperature (BDTT) which is of the order of 350 °C – corresponding to 0.33 T_m (T_m = melting temperature) depending on the deformation rate – whereas NiAl with a soft orientation shows ductilities up to 2.5% below the BDTT, which is of the order of 200 °C, corresponding to 0.25 T_m (Lahrman et al., 1991). The low ductility of NiAl at low temperatures is proposed to result from low dislocation mobilities because of extended dislocation cores (Farkas et al., 1991; Mills et al., 1993; Kitano and Pollock, 1993). A recent study has shown the importance of a sufficient density of mobile dislocations since an increased fracture toughness has been obtained by avoiding any annealing treatments (Hack et al., 1992). At the BDTT the ductility increases rather steeply with increasing temperature due to thermal activation which, however, is not yet understood in detail (Darolia et al., 1992b).

Like strength and ductility, the fracture toughness is a sensitive function of the orientation and the temperature, and this has recently been studied in detail (Reuss and Vehoff, 1990, 1992; Vehoff, 1992; K.-M. Chang et al., 1991, 1992; Darolia et al., 1993). Corresponding to the low ductility, the fracture toughness of NiAl at lower temperatures is low. However, it is even lower in the soft ⟨110⟩ direction than in the hard ⟨100⟩ direction which is assumed to be a result of preferred cleavage on {110} planes. However, the details of the fracture processes are more complicated and not yet fully understood, according to recent observations (Schneibel et al., 1993a). The fracture toughness increases substantially above 200 °C, independent of the crystal orientation which is in contrast to the BDTT for the ductility. The crack tip stress and deformation fields in NiAl single crystals have been analyzed in detail (Saeedvafa and Rice, 1992).

Polycrystalline NiAl is usually found to be brittle with practically no ductility (Baker and Munroe, 1990; Reuss and Vehoff, 1992). Crack propagation occurs in an instationary way, and the fracture resistance is not sensitive to the loading rate (Schneibel et al., 1993b). Only with carefully processed, high-purity NiAl with an exact stoichiometric composition can a tensile ductility of 2.5% be obtained at room temperature, whereas similarly processed off-stoichiometric NiAl is brittle (Hahn and Vedula, 1989; Baker et al., 1991). Obviously the constitutional defects in off-stoichiometric NiAl reduce the ductility. In any case, the brittle-to-ductile transition temperature can be reduced significantly by reducing the grain size (Schulson, 1985; Nagpal and Baker, 1990b; Chan, 1990; Cheng, 1992). The limit to the grain size reduction is nanocrystalline NiAl which has been prepared successfully with a grain size of about 10 nm (Haubold et al., 1992). The recrystallization behavior of NiAl was studied by Haff and Schulson (1982). Apart from the grain size effect, the brittleness can be reduced by introducing additional dislocation sources. This effect

ArcelorMittal Ex. 2038
Page 69 of 190

has been observed in the case of NiAl with oxide layers on the surface or with particles in the alloy where dislocations are emitted from the respective phase boundaries (Prakash and Pool, 1981; J. T. Kim et al., 1991; Gibala et al., 1993). As in other cases, a higher ductility and toughness is observed with a superimposed hydrostatic pressure (Margevicius et al., 1993a, b; Pawelski et al., 1994).

One of the reasons for the brittleness of polycrystalline NiAl is the insufficient number of slip systems since there are only three independent slip systems with the ⟨100⟩ slip vector, whereas at least five independent deformation systems are necessary for general homogeneous deformation according to the Von Mises criterion (von Mises, 1928; Baker and Munroe, 1990; Darolia et al., 1992b). Besides ⟨100⟩, other slip vectors, i.e. ⟨110⟩ and ⟨111⟩, have been observed under special circumstances (Field et al., 1991a; Kim and Gibala, 1991; Miracle, 1991; Veyssière and Noebe, 1992; Dollar et al., 1992). The ⟨111⟩ dislocation which corresponds to the common slip direction in b.c.c. alloys is a superlattice dislocation in the B2 structure consisting of two superpartials with an antiphase boundary (APB) in between. The various dislocation types – in particular the dislocation cores – have recently been studied in detail by direct observations and computer simulations, and the consequences of the dislocation mobilities have been discussed (Mills and Miracle, 1993; Parthasarathy et al., 1993; Mei and Cooper, 1993). With these additional slip systems the Von Mises criterion can be fulfilled and an increased ductility is expected.

It has been found experimentally that alloying NiAl with Cr, which reduces the APB energy, may indeed increase the propensity to ⟨111⟩ slip (Field et al., 1991b) and produces a strong solid-solution strengthening effect (Cotton et al., 1993a), though the conditions and mechanisms are still in discussion (Cotton et al., 1993a, c). An improved ductility has been found for NiAl–Cr only in compression (Kowalski and Frommeyer, 1992), whereas the tensile ductility was actually reduced and the brittle-to-ductile transition temperature was increased (Field et al., 1991b; Cotton et al., 1993a). Obviously the Von Mises criterion is not a sufficient criterion and the material fractures in a brittle manner because the fracture strength is lower than the yield strength. Other elements which have been reported to promote ⟨111⟩ slip are Mn, V, Ti, and Zr (George et al., 1991a; Field et al., 1991b). With Fe substituting Ni there is a continuous transition from ⟨100⟩ slip to ⟨111⟩ slip (Patrick et al., 1991). Quantum-mechanical, ab initio calculations have shown that the APB energy is indeed lowered by the addition of Cr, Mn, or V to NiAl (Hong and Freeman, 1989).

Another reason for the brittleness of polycrystalline NiAl may be grain boundary weakness. It was found that alloying with a small amount of B, which is beneficial in the case of Ni_3Al and segregates to the grain boundaries in NiAl, changes the fracture mode from intergranular fracture to transgranular fracture (George et al., 1991a; Xie et al., 1993). However, ductility and fracture toughness are not improved, and a higher amount of B even reduces the ductility which may be related to an increase in the yield strength to levels above the fracture strength and to the precipitation of borides (Wu and Sass, 1993a, b; Jayaram and Miller, 1993; Schneibel et al., 1993b). The hardening effect of B additions is observed for off-stoichiometric, Ni-rich NiAl and is due to the variation in the B solubility (Tan et al.,

ArcelorMittal Ex. 2038
Page 70 of 190

1993). C and Be do not segregate at grain boundaries and do not change the fracture mode. Nevertheless, Be improves the ductility of NiAl slightly and the reasons for this behavior are unclear.

It is known that alloying with, e.g. Fe, can improve the ductility of NiAl (Baker and Munroe, 1990). Indeed substantial increases in the tensile ductility at room temperature of monocrystalline NiAl with a "soft" orientation have been obtained by alloying with small amounts, i.e. about 0.1 at.% of Mo, Ga. or Fe (Darolia et al., 1992a): 0.1 at.% Fe produces 6% ductility in contrast to 1% ductility without Fe whereas 0.5% and more Fe produces only 2% ductility. The physical reasons for this ductilization effect are not yet clear (Noebe and Behbehani, 1992).

4.3.4 Creep

High temperature deformation of metallic and other materials is controlled by various deformation mechanisms depending on the temperature and the deformation rate, as is illustrated by the so-called deformation maps for the respective materials (Frost and Ashby, 1982). The comparison of such maps for various materials with different crystal structures and types of atomic bonding shows that the deformation behavior at temperatures above a third of the melting temperature is controlled by creep processes, not only at low deformation rates of 10^{-7} s^{-1} and lower, which are used during typical creep experiments, but also at higher rates of say 10^{-3} s^{-1} which are used during short-term tests for flow stress determinations, and this may also be assumed to be the case for intermetallic phases (Sauthoff, 1990b). Thus any discussion of high temperature deformation behavior has to be centered on the strength-controlling creep mechanisms.

The creep behavior of NiAl has been studied and discussed repeatedly in the past (Stoloff and Davies, 1966; Vandervoort et al., 1966; Strutt and Dodd, 1970; Strutt and Kear, 1985; Yaney and Nix, 1988). In addition, the creep behavior of NiAl and NiAl-based alloys has been investigated systematically and the findings have been the subject of various summarizing reports (Jung et al., 1987; Sauthoff, 1990b, 1991a, b, 1992). Further creep studies have been directed at NiAl single crystals (Forbes et al., 1993; Glatzel et al., 1993b; Forbes and Nix, 1993). In the following sections the main characteristics of the creep behavior of NiAl are reviewed, the effects of structure and composition changes are outlined and both single-phase materials and alloys which contain other intermetallic phases besides the B2 phases are considered. The creep behavior of NiAl is discussed here in further detail since the obtained understanding of the rate-controlling mechanisms is also valid for other intermetallics, and thus the NiAl case may serve as a characteristic example for other intermetallic alloy systems.

Creep Resistance of Single-Phase B2 Alloys

The creep behavior of the ternary B2 phase (Ni,Fe)Al was studied in detail as a function of stress, temperature, composition, and grain size (Rudy and Sauthoff, 1985; Rudy, 1986; Jung et al., 1987). At high temperatures, e.g. 60% of the melting temperature or higher, the secondary creep at rates between about 10^{-8} s^{-1} and 10^{-6} s^{-1} exhibits power law behavior, i.e. the observed secondary creep rates are described by the familiar Dorn equation for dislocation creep [Eq. (2)] (Mukherjee et al., 1969).

Dislocation creep of conventional disordered alloys is produced by gliding and

ArcelorMittal Ex. 2038
Page 71 of 190

climbing dislocations. If climb is the slower step, as in pure metals, the creep rate is controlled by dislocation climb, which gives rise to a well defined subgrain structure, and the stress exponent is 4 or 5. This is characteristic of class II alloys. Otherwise, viscous dislocation glide is rate controlling, which leads to dislocation tangles without subgrain formation and a stress exponent of 3, with behavior characteristic of class I alloys (Sherby and Burke, 1967; Nix and Ilschner, 1979).

The secondary creep behavior of (Ni,Fe)Al shows analogous characteristics. In the Ni rich phases and in the binary NiAl a well-defined substructure is found after creep. The subgrain size is of the order of 10 μm, and the dislocation density within the subgrains is about 10^{11} m^{-2}. In agreement with this, stress exponents between 4 and 4.5 have been found for the Ni-rich phases, i.e., these phases behave like class II alloys with dislocation climb controlling the creep.

In the Fe-rich phases and in FeAl, however, no subgrain formation has been observed even after long creep times. The dislocation density remains high at about 10^{14} m^{-2}, and the stress exponent varies between 3 and 3.6. This indicates class I behavior, i.e. here the creep is controlled by the viscous glide of dislocations. In both cases only undissociated ⟨100⟩ dislocations have been observed. Obviously the driving force and the atom mobility which are necessary for subgrain formation are sufficient only in the Ni-rich phases. The line energies, line tensions and derivatives of dislocations have been calculated theoretically for NiAl, and good agreement with observed dislocation configurations after creep has been found (Glatzel et al., 1993a).

These findings show that the dislocation creep of such intermetallic alloys and of conventional disordered Ni-base or Fe-base alloys is controlled by the same mechanisms. Even the observed dislocation densities correspond to those in conventional disordered alloys (Rudy, 1986; Sauthoff, 1991a). This close similarity is surprising since the elementary atomic diffusion processes and the types and numbers of the dislocation slip systems are quite different because of the different crystal symmetries.

Besides dislocation creep, grain boundary sliding was observed in (Ni,Fe)Al. The process is, of course, not an independent deformation mechanism since the resulting grain shifts lead to stress concentrations at grain boundary junctions and must be accommodated by deformation processes within the grains, i.e. by dislocation creep of the grains in the stress–temperature range concerned. For such coupled deformation processes, the total creep rate is controlled by the slower process, which is dislocation creep for not too small grain sizes. With decreasing grain size the contribution of grain boundary sliding increases, from which a decrease in the total creep resistance results, as is well known for disordered alloys (Frost and Ashby, 1982) and has also been observed for (Ni,Fe)Al (Rudy, 1986; Sauthoff, 1990b). The contribution of grain boundary sliding to creep in binary NiAl has recently been studied in more detail (Raj and Farmer, 1993).

At lower stresses, which produce secondary creep rates below 10^{-8} s^{-1}, the observed stress–strain rate relationship deviates from power law behavior, i.e. the apparent stress exponent is smaller than 3 and decreases with decreasing stress. This deviation indicates the contribution of diffusion creep, which is a linear function of stress

$$\dot{\varepsilon}_{\text{diff}} = A_{\text{diff}} \frac{\Omega D}{k T d^2} \sigma \qquad (3)$$

ArcelorMittal Ex. 2038
Page 72 of 190

where A_{diff} is a dimensionless factor (usually $A_{diff} = 14$), Ω is the atomic volume, D is the effective diffusion coefficient which considers diffusion both through the grain (Nabarro–Herring creep) and along the grain boundaries (Coble creep), and d is the effective diffusion length which is usually approximated by the grain size (Frost and Ashby, 1982). Dislocation creep and diffusion creep are independent creep processes that act in parallel in the grains, and the total creep rate is given by the sum of the partial rates. Because of the stronger stress dependence of dislocation creep [Eq. (2)], the contribution of diffusion creep becomes more dominant with decreasing stress.

In view of the observed creep behavior of (Ni,Fe)Al and other phases (Polvani et al., 1976; Nicholls and Rawlings, 1977; Ashby et al., 1978; Hirsch, 1985; Schneibel et al., 1986; Kampe et al., 1991; Hayes, 1991; Hayashi et al., 1991a; Miura et al., 1991; Rowe et al., 1991; Takahashi and Oikawa, 1991; Nathal, 1992; Nabarro and de Villiers-Filmer, 1993), it is concluded that the creep of intermetallic phases is controlled by the same creep mechanisms and is described by the same constitutive equations as the creep of the familiar disordered alloys, though the crystal structures of the intermetallics are much less symmetric than the simple structures of the disordered alloys. The lower crystal symmetry leads to particular dislocation types and higher dislocation energies, including special superlattice dislocations, and to a reduced number of slip systems. However, dislocation creep is controlled by nonconservative dislocation motions, i.e. dislocation motions are coupled with local diffusion fluxes, and the latter are rate controlling. Thus the particular dislocation mechanisms are not of primary importance for the total macroscopic creep rate which explains the similar behavior of metallic and intermetallic alloys.

Figure 23 shows the effect of composition variations, i.e. deviations from stoichiometry and variations in the Ni:Fe ratio, on the creep resistance of (Ni,Fe)Al. It can be seen that the creep resistance decreases with decreasing Al content, i.e. increasing deviation from stoichiometry. As already noted in the preceding section, deviations from stoichiometry introduce constitutional disorder, i.e. point defects which increase the diffusion coefficient

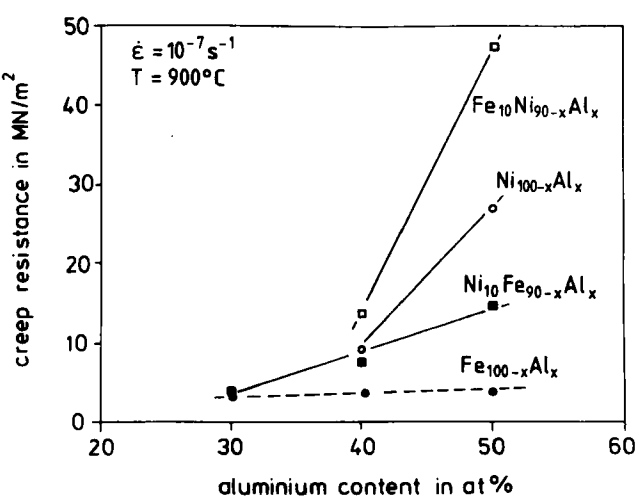


Figure 23. Creep resistance of binary and ternary B2 aluminides at 900 °C (in compression with $10^{-7}s^{-1}$ strain rate) as a function of Al content (Rudy, 1986; Rudy and Sauthoff, 1986).

ArcelorMittal Ex. 2038
Page 73 of 190

and thereby the creep rate. However, at lower temperatures these point defects become immobile and act as obstacles to dislocation movements, i.e. they increase the low-temperature strength. At intermediate temperatures the two effects balance each other and deviations from stoichiometry do not affect the creep resistance, as was found for NiAl (Vandervoort et al., 1966). In Fig. 23 the Ni-rich phases show a strong stoichiometry effect with decreasing Al content, whereas the effect is significantly smaller for the Fe-rich phases, i.e. the test temperature of 900 °C leads to high-temperature behavior by the Ni-rich phases and to intermediate-temperature behavior by the Fe-rich phases. This behavior is surprising since it is commonly supposed that such thermally activated effects scale with the melting temperature, which is higher for NiAl than for FeAl. The reasons for the observed behavior of (Ni,Fe)Al at intermediate temperatures are still to be clarified.

Apart from the effect of deviations from stoichiometry, Fig. 23 shows a marked dependence of the creep resistance for the ternary B2 phases (Ni,Fe)Al on the Ni:Fe ratio. It can be shown for (Ni,Fe)Al that this composition dependence results from the composition dependence of the diffusion coefficient, which can be estimated by using data from Cheng and Dayananda (1979) and Moyer and Dayananda (1976) (see Rudy, 1986; Rudy and Sauthoff, 1986). The maximum in the creep resistance of (Ni,Fe)Al is directly related to the minimum in the diffusion coefficient. It has to be noted that the analysis of creep data with respect to diffusion coefficients poses problems because, apart from the scarcity of data, the diffusion coefficients in Eqs. (2) and (3) are effective ones depending on the particular creep process which determines the coupling of partial diffusion fluxes, i.e. the needed effective diffusion coefficients are not those which are measured in diffusion experiments. For binary solid solutions, expressions for the effective diffusion coefficients are available for various creep mechanisms (Chin et al., 1977; Fuentes-Samaniego and Nix, 1981; Dominguez-Rodriguez and Castaing, 1993), whereas for multinary phases an expression for the effective diffusion coefficient is known only for the case of diffusion creep (Herring, 1950). Here more theoretical and experimental work is necessary.

Figure 24 shows the correlation between the observed creep resistance of various binary and ternary B2 phases and the respective diffusion coefficients, as found in the literature or estimated on the basis of literature data (Rudy, 1986; Rudy and Sauthoff, 1986; Sauthoff, 1991 a). It can be seen that the correlation is surprisingly good and corresponds to Eq. (2), in spite

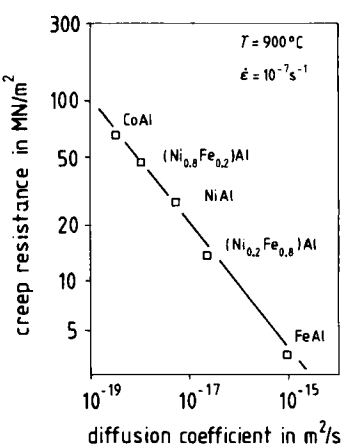


Figure 24. Creep resistance of binary and ternary stoichiometric B2 aluminides at 900 °C (in compression with $10^{-7}\,s^{-1}$ strain rate) as a function of the diffusion coefficient, as found in the literature or estimated from available data (Rudy, 1986; Jung et al., 1987; Sauthoff, 1991 a; Shankar and Seigle, 1978; Akuezue and Whittle, 1983; Cheng and Dayananda, 1979; Moyer and Dayananda, 1976).

ArcelorMittal Ex. 2038
Page 74 of 190

of the problems with the appropriate determination of the effective diffusion coefficients. The question now is why the diffusion coefficient depends in this way on the composition of the B2 phases. As for other properties, the diffusion coefficient depends on the crystal properties, i.e. on the character and strength of the atomic bonding, and indeed the activation energy of diffusion increases with increasing total enthalpy of phase formation, as is illustrated by Fig. 7. The question is whether such a correlation can be established – at least for a group of closely related phases – in such a way that it can be used for predicting the effects of alloying additions on the diffusion coefficients. For this the correlation of the diffusion coefficients with the character and strength of bonding must be studied in more detail. Here again much more theoretical and experimental work is necessary.

In view of the discussed composition dependence of the creep resistance, it is concluded that the effective diffusion coefficient is of primary importance for controlling the creep resistance (Sauthoff, 1993b). This of course does not mean that the other parameters in Eq. (2) can be neglected. This is demonstrated by the temperature dependence of the creep of B2 (Ni,Fe)Al, as was discussed earlier (Sauthoff, 1991a). In view of Eqs. (2) and (3), the apparent activation energy for creep is expected to correspond to that for diffusion since the other parameters depend less sensitively on temperature, and indeed this has been confirmed repeatedly in the case of conventional disordered alloys. However, in the case of B2 (Ni,Fe)Al, the apparent activation energy for creep only corresponds to that for diffusion at temperatures up to 900 °C, whereas at higher temperatures the apparent activation energy for creep is much higher. Activation energies for creep that are higher than those for diffusion have also been reported for other cases (Vandervoort et al., 1966; Stoloff, 1984; Whittenberger, 1986). This means that in contrast to conventional disordered alloys, the microstructure-dependent parameter A in Eq. (2) may also exhibit a strong temperature dependence, since the shear modulus G still depends only weakly on the temperature (Harmouche and Wolfenden, 1987).

The material parameter of secondary importance for creep is the shear modulus in Eq. (2). Elastic moduli can be calculated by quantum-mechanical, ab initio calculations (see, e.g. Fu and Yoo, 1992a), and thus there is a physical understanding of the relation between the strength and character of bonding and the elastic behavior. However, experimental and/or theoretical data are scarce and there is little knowledge on the effects of changes in composition and structure on the elastic moduli. Figure 6 shows some Young's modulus data, e.g. for some B2 phases in comparison to some C15 Laves phases, which are discussed in Sec. 8. Obviously there is only a correlation between the Young's modulus and the total enthalpy of formation for the Laves phases. This correlation is less apparent for the B2 phases, which may be due to experimental errors and to the complexities of the elastic behavior of the B2 phases. The question is again whether such correlations can be established – at least for a group of closely related phases – and whether these correlations can then be used for predicting the effects of alloying additions on the elastic behavior.

In summary, it is concluded that the creep behavior of intermetallic phases can be described as that of the conventional disordered alloys given by the familiar phenomenological constitutive equations,

ArcelorMittal Ex. 2038
Page 75 of 190

and indeed deformation maps have been calculated as a function of available data (Jung et al., 1987). However, the physical mechanisms which control the creep behavior are only partially understood and much more work is necessary.

With respect to applications as structural materials at high temperatures, the creep resistance of candidate phases should be as high as possible for increasing the service temperatures as much as possible. In view of Eqs. (2) and (3), the decisive materials' parameters for increasing the creep resistance are the diffusion coefficient D and the shear modulus G. Both parameters are determined by the atomic bonding energy to which the macroscopic enthalpy of phase formation is related (Engell et al., 1991). The latter is related to the melting temperature, and indeed there is a correlation between the parameters D and G and the melting temperature (Frost and Ashby, 1982). This means that in principle alloys with increased melting temperatures should be used for obtaining increased high temperature strengths. However, a strict validity of this rule cannot be expected since the above correlations are complex ones which depend on many parameters. An example is given by the phases NiAl and CoAl which have the same crystal structure and nearly the same melting temperature, but different creep resistances (Fig. 24).

Diffusion depends sensitively on the crystal structure (Wever et al., 1989), and it may be supposed intuitively that a lower diffusion coefficient and thereby a higher creep resistance may be obtained by lowering the crystal symmetry. Atomic ordering in the B2 lattice results in the $L2_1$ structure with four sublattices, which is the case for the Heusler-type phases Ni_2TiAl and Co_2TiAl. Indeed Co_2TiAl shows a much higher flow stress than $(Co_{0.8}Fe_{0.2})Al$ according to data in Sauthoff (1989), and Ni_2TiAl is more creep resistant than NiAl (Strutt and Polvani, 1973). Besides crystal symmetry, atomic packing should also be considered, and it is well known that, e.g. the self-diffusion coefficient of Fe in the close-placked f.c.c. lattice is lower by two orders of magnitude than that in the more open b.c.c. structure (Fridberg et al., 1969). The B2 structure results from ordering in the b.c.c. lattice, whereas ordering in the f.c.c. lattice leads, e.g. to the $L1_2$ structure of Ni_3Al or with carbon to the $L'1_2$ structure of Fe_3AlC (Jung and Sauthoff, 1989 b) and, furthermore, ordering in the $L1_2$ lattice leads to the $D0_{22}$ structure of Al_3Nb, as is shown in Fig. 1.

Figure 25 combines creep data for all these structures, and it can be seen that the differences in crystal structure with respect

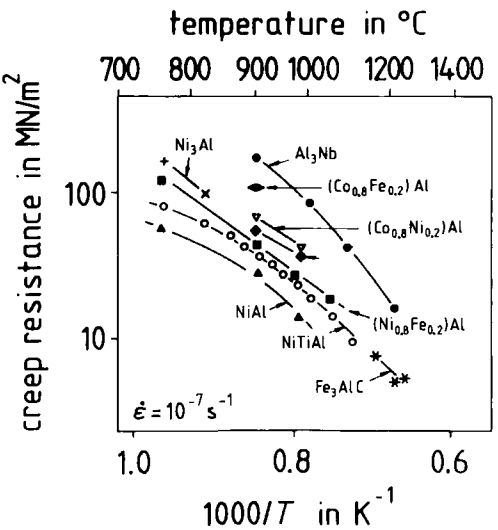


Figure 25. Temperature dependence of creep resistance (in compression with 10^{-7} s^{-1} secondary strain rate) for various single-phase intermetallic alloys: NiAl, CoAl and related alloys with a B2 structure (Jung et al., 1987; Sauthoff, 1989), Ni_2TiAl with an $L2_1$ structure (Strutt and Polvani, 1973), two Ni_3Al variants with $L1_2$ structures, i.e., an advanced aluminide (+) (Schneibel et al., 1986) and Ni_3Al–Fe (×) (Nicholls and Rawlings, 1977), Fe_3AlC with an $L'1_2$ structure (Jung and Sauthoff, 1989 b), and Al_3Nb with a $D0_{22}$ structure (Sauthoff, 1990 a, b; Reip, 1991).

ArcelorMittal Ex. 2038
Page 76 of 190

to symmetry and atomic packing indeed result in correspondingly significant differences in the creep resistance. However, it can also be seen that the variation in the creep resistance with varying sublattice occupation in the B2 structure is as large as the variation with varying lattice structure, i.e. both effects have to be considered for increasing the high temperature strength.

Creep Resistance of Multiphase NiAl-Base Intermetallic Alloys

Precipitated particles are usually used in conventional alloys for increasing the creep resistance. The strengthening effect of precipitated particles was studied in NiAl–Fe alloys with a B2 NiAl matrix and α-Fe particles (Jung and Sauthoff, 1989a). It was found that the effect of the α-Fe particles was quite analogous to that of B2 NiAl particles in Fe–NiAl alloys with an α-Fe matrix, which were studied by Jung and Sauthoff (1987) and Jung (1986). In both cases the particles act as dislocation obstacles because of the dislocation–particle interaction, and indeed adhering dislocations were observed at particles before detachment in the NiAl–Fe case. Such obstacles are surmounted by climb which gives rise to a threshold stress σ_{th} and increases the creep resistance according to

$$\dot{\varepsilon} = A \frac{D G b}{k T} \left(\frac{\sigma - \sigma_{th}}{G} \right)^n \qquad (4)$$

This threshold stress is proportional to the Orowan stress, as was shown theoretically for various climb processes (Arzt and Rösler, 1988), and thus is proportional to the reciprocal particle distance, in agreement with the experiments (Jung and Sauthoff, 1987, 1989a). The observed, secondary dislocation creep can be described by Eq. (4) and deformation maps can be calculated on the basis of the experimental data (Jung and Sauthoff, 1989a).

In particulate alloys one phase, i.e. the matrix, is distributed continuously, whereas the second phase is distributed discontinuously. In nonparticulate alloys all phases are distributed continuously, as is the case in lamellar or fibrous composites. The effect of phase distribution on the creep behavior of NiAl–Fe alloys with lamellar microstructures was studied in detail (Klöwer, 1989; Klöwer and Sauthoff, 1991, 1992). For this an Ni–40 at.% Fe–18 at.% Al alloy was chosen which was produced by directional solidification to give a lamellar microstructure of the phases B2 NiAl and disordered f.c.c. γ-Fe–Ni with equal volume fractions. It was found that the creep resistance of such a lamellar alloy is related to the creep resistance of the constituent phases according to a rule of mixtures as long as the lamellae spacing is larger than a critical spacing, which is of the order of the free dislocation path. If the lamellae spacings are smaller than this critical value, then the lamellae interfaces give rise to an additional strengthening effect. This strengthening effect can be described, as in Eq. (4), by a threshold stress which again is proportional to the reciprocal lamellar spacing.

Similar effects have been observed in other intermetallic NiAl-base alloys with less regular distributions of hexagonal C14 Laves phases (Machon, 1992; Sauthoff, 1993a), and have been discussed by Sauthoff (1991b). In those alloys with coarse phase distributions the observed secondary creep rates follow a rule of mixtures at a first approximation, and additional strengthening effects are only observed for alloys with fine phase distributions. From this it is concluded that particulate and nonparticulate intermetallic alloys creep in similar ways and can be described by the same constitutive equations as conventional multiphase alloys.

ArcelorMittal Ex. 2038
Page 77 of 190

However, the above discussion has only referred to secondary creep. The situation is less clear for the transient primary creep stage which precedes secondary creep. As already discussed (Sauthoff, 1991 b), the primary creep strain is reduced significantly by the presence of second phases and it decreases with increasing stress and with decreasing interface spacing, at least in some NiAl-base alloys (Reip, 1991; Klöwer, 1989). Such a behavior is also known for conventional alloys, but there are other alloys which show an opposite behavior, i.e. an increasing primary strain with increasing stress (see Sauthoff, 1991 b). Such effects are not yet understood even for disordered alloys. It is further noted that not only the normal primary creep with a decelerating creep rate is observed, but also inverse primary creep with an accelerating creep rate, e.g. in the case of ternary Laves phases (Sauthoff, 1990a, 1991a; Machon, 1992). Such inverse primary creep has also been reported for Ni_3Al, where it is due to the activation of various slip systems (Hazzledine and Schneibel, 1989; Schneibel and Hazzledine, 1992). Inverse creep results from an insufficient number of mobile dislocations, and a classic example for such a deformation behavior is silicon, where the deformation behavior has been analyzed in detail (Alexander and Haasen, 1968; Alexander, 1986).

In any case, the creep resistance of NiAl can be increased significantly by alloying with other stronger intermetallics to form multiphase intermetallic alloys which may be regarded as intermetallic in situ composites. This is exemplified by Fig. 26 with creep resistance data for various Ni–Al–Nb alloys which contain the tetragonal $D0_{22}$ phase Al_3Nb and the hexagonal Laves phase NbNiAl with a C14 structure, as well as NiAl. It can be seen that the

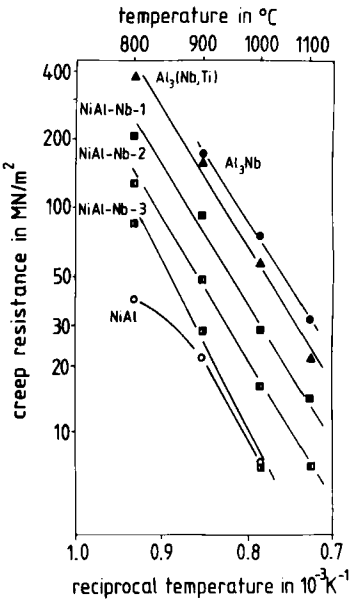


Figure 26. Creep resistance (in compression with $10^{-7}s^{-1}$ secondary strain rate) as a function of temperature for various NiAl–Al_3Nb alloys, i.e. for the three-phase alloys NiAl–Nb-1, -2, and -3 with 22 vol.%, 46 vol.%, and 78 vol.% NiAl, and 4 vol.%, 15 vol.%, and 15 vol.% NbNiAl, respectively, compared with single-phase NiAl (Rudy and Sauthoff, 1985; Rudy, 1986), and Al_3Nb and $Al_3(Nb_{0.75}Ti_{0.25})$ – both with a $D0_{22}$ structure (Reip, 1991).

creep resistance of these intermetallic alloys increases continuously with increasing volume fractions of stronger phases from that of the comparatively soft NiAl to that of the hard phases Al_3Nb and $Al_3(Nb,Ti)$, which have been discussed in Sec. 3.3.2 [the $Al_3(Nb,Ti)$ data have been introduced into this figure because only this ternary trialuminide could also be tested at lower temperatures].

Another example is given in Fig. 27, which illustrates the strengthening of NiAl by ternary C14 Laves phases. The data points for TaNiAl–NiAl seem to follow a rule of mixtures, but the data for NbNiAl–NiAl clearly indicate a significant deviation from a lineal superposition for the creep resistances. Furthermore, the extrap-

ArcelorMittal Ex. 2038
Page 78 of 190

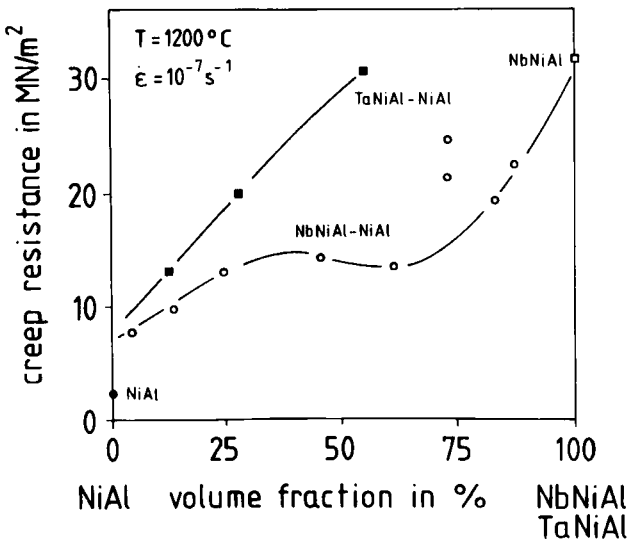


Figure 27. Creep resistance (compressive stress for $10^{-7} s^{-1}$ secondary creep rate) at 1200 °C as a function of the volume fraction of the second phase for the intermetallic NiAl-base alloys NiAl–NbNiAl and NiAl–TaNiAl with the C14 Laves phases NbNiAl and TaNiAl, respectively (Sauthoff, 1990a; Machon, 1992).

olated creep resistance for 0 % strengthening phase is appreciably higher in this case than the measured value for binary NiAl. This additional strengthening effect is due to precipitated, fine particles of the Heusler-type phase Nb_2NiAl with an $L2_1$ structure, which give rise to a threshold stress (Sauthoff, 1991 b; Machon, 1992).

Further examples are given by Nathal (1992), where a wealth of data from various alloy systems based on the B2 phases are analyzed.

4.3.5 Environmental Effects

Unlike most other aluminides which are considered for high temperature applications, NiAl with a B2 structure exhibits excellent oxidation resistance since a protective Al_2O_3 scale is readily formed during oxidation (Doychak et al., 1989; Nesbitt and Lowell, 1993). According to present knowledge, NiAl seems to be the only really oxidation resistant intermetallic, apart from some silicides (Meier et al., 1993). The physical reason for this high oxidation resistance is that the Al content is sufficiently high and the Al diffusion is sufficiently fast in NiAl at all temperatures to form stable Al_2O_3 scales at the surface and avoid internal oxidation in the bulk (Pettit, 1967). The details of scale growth have been described by Doychak et al., (1989).

During oxidation voids are formed at or near the $NiAl/Al_2O_3$ interface because of unbalanced diffusion fluxes, corresponding to the Kirkendall effect (Cathcart, 1985; Meier et al., 1993). This void formation, which has also been observed for other Al-rich alloys, leads to spalling of the Al_2O_3 scale and affects the oxidation resistance. Void formation is enhanced by the segregation of sulfur to the free NiAl surface of the voids, thus giving rise of the deleterious "sulfur effect" (Grabke et al., 1990, 1991 b). Scale adherence is also affected by the presence of TiB_2 dispersoids, as has been shown for an $NiAl–TiB_2$ composite (Pregger et al., 1992).

As in many other cases, scale adherence and oxidation resistance are improved by microalloying with "oxygen active" elements, e.g. Y, Zr, Hf, Ce, or La (Mrowec

ArcelorMittal Ex. 2038
Page 79 of 190

and Jedlinski, 1989; Grabke et al., 1991 b). In particular, Zr has been used to increase the resistance of NiAl to cyclic oxidation (Doychak et al., 1989; Nesbitt et al., 1992). The physical understanding of the beneficial effect of such "oxygen active" elements is still insufficient, as is also the case for conventional disordered alloys. The effect of alloying with Cr and Si, which are used in other alloys for providing oxidation resistance, has been reviewed (Meier, 1989). It is noted that the sulfidation resistance of NiAl is reduced by Cr (Mrowec et al., 1989).

Apart from oxidation with external scale formation, NiAl, as well as various other intermetallics, is subject to a special oxidation phenomenon which is known as pesting (Aitken, 1967; Meier and Pettit, 1992). Pesting occurs in a critical temperature range – usually at about 800 °C – and may lead to complete disintegration of the material. NiAl is less susceptible to pesting than other intermetallics, and it shows pesting only at very low oxygen pressures when oxygen penetrates the thin surface scale and diffuses inwards along the grain boundaries (Grabke et al., 1991 a, b; Meier et al., 1993).

Environmental embrittlement, which affects the mechanical behavior of various other intermetallics, e.g. the other B2 aluminide, FeAl, has not been found for NiAl (Liu, 1992; Lahrman et al., 1993 b).

4.3.6 Alloy Developments and Applications

Magnetic Alloys

The advantageous magnetic properties of Fe–Ni–Al alloys with a suitable composition were first discovered by Mishima in 1931, which initiated the development of the Alnico alloys for applications as permanent magnet materials (see, e.g. Jellinghaus, 1936, 1943; De Vos, 1969). The basic alloy contains about 50 at.% Fe, 25 at.% Ni, and 25 at.% Al to which various other elements – Co or Cu as macroalloying elements and Nb or Ti as microalloying elements – are added for property optimization (McCurrie, 1986). The alloys are single-phase at high temperatures and decompose spinodally after cooling at a critical rate to form a two-phase microstructure with an interlocking phase distribution. The constituent phases of these alloys are an NiAl-base phase with a B2 structure and a disordered b.c.c. Fe-rich phase, according to the Ni–Al–Fe phase diagram (Bradley and Taylor, 1938; Dannöhl, 1942; Bradley, 1951; Hao et al., 1984).

The B2 phase in the Alnicos is only weakly ferromagnetic whereas the Fe-rich phase is strongly ferromagnetic, and thus the interlocking phase distribution and the strong shape anisotropy of the Fe-rich phase results in a high coercivity (De Vos, 1969; McCurrie, 1986). The magnetic behavior is a sensitive function of the pretreatment, not only with respect to the phase distribution, but also with respect to the concentration and distribution of the defects, e.g., vacancies and antistructure atoms (Kilner and Harris, 1981). The effect of the additional alloying elements – Co, Mn, Ti, or Cu which dissolve preferentially in the B2 phase and Cr, Mo, V, Nb, or Si which dissolve preferentially in the disordered Fe-rich phase – on the decomposition process of the Alnico alloys was studied by Hao et al. (1985).

Alnico alloys are brittle and hard, they can only be machined by grinding, spark erosion, and electrochemical milling, and they resist atmospheric corrosion well up to 500 °C (Fiepke, 1990). The mechanical behavior, in particular creep, of Alnico-type, Fe–Ni–Al alloys has been studied in detail, and both Fe-rich alloys with precip-

ArcelorMittal Ex. 2038
Page 80 of 190

itated NiAl particles and NiAl-rich alloys with precipitated Fe particles have been considered (Jung and Sauthoff, 1987, 1989a). The magnetic properties are summarized and compared to those of other alternative alloys by Fiepke (1990) and McCurrie (1986). Alnico alloys are superior to other permanent magnet materials at resisting temperature effects on magnetic properties.

It is noted that presently NiAl is also considered an attractive candidate phase for other functional applications, e.g. contacts in electronic thin film devices or high voltage electrodes in electron-optical instruments (Miracle, 1993).

Shape Memory Alloys

It is well known that the martensitic transformation of Al-deficient NiAl (see Sec. 4.3.2) is thermoelastic and produces the shape memory effect. Consequently materials developments have been started which aim at applications as shape memory alloys (Furukawa et al., 1988; Kainuma et al., 1992b, c). The martensitic transformation temperature can be varied within a broad temperature range up to 900 °C, and thus the shape memory effect can be produced at high temperatures which allows the development of high-temperature shape memory alloys. The problem of low room temperature ductility of NiAl has been overcome by alloying with a third element – in particular Fe – to produce a ductile second phase with an f.c.c. structure.

Coating Alloys

Many high-temperature alloy components with insufficient resistance to corrosion in hot gases, e.g. in gas turbines, are coated with a corrosion resistant surface layer for providing the necessary protection from the particular corrosion (see, e.g. Grünling et al., 1983; Pettit and Goward, 1983; Nicholls and Stephenson, 1991). In view of the exceptionally high oxidation resistance of the B2 phase NiAl (see Sec. 4.3.5) it has long since been used as a coating material. Indeed, one of the oldest processes for producing coatings is pack aluminizing, by which Al diffuses from the Al-rich pack into the alloy to be coated and forms an aluminide surface layer, which consists of NiAl in the case of Ni base alloys (Patnaik, 1989). Such diffusion coatings are still extensively used for protecting turbine blades under various turbine conditions. The coating performance is improved by adding alloying additions, i.e Cr, Si, Ta, rare earths, or precious metals, which is achieved by modifying the pack aluminizing process (Nicholls and Stephenson, 1991).

Besides such diffusion coatings, overlay coatings are used which are produced by depositing a specifically designed corrosion resistant alloy onto the component surface (Nicholls and Stephenson, 1991). These coating alloys, which are described by the general composition formula MCrAlY with M = Fe, Ni, and/or Co again rely on the presence of MAl phases with a B2 structure (see, e.g. Gudmundsson and Jacobson, 1988). The advantage of these coatings is the negligibly small chemical interaction between the coating and the substrate during deposition, the choice of the corrosion resistant alloy composition and the ability to deposit thicker coatings for extended service lives. It is noted that during service interdiffusion occurs between the coating and the substrate from which an Al depletion of the coating may result. Al deficient NiAl may transform martensitically because of cooling cycles, which promotes spalling,

ArcelorMittal Ex. 2038
Page 81 of 190

i.e., it contributes to the degradation of the coating (Smialek and Hehemann, 1973).

Structural Alloys

For a long time NiAl has been considered as a basis for developing structural materials for high temperature applications (Fitzer and Gerasimoff, 1959; Imai and Kumazawa, 1959; Grala, 1960; Jellinghaus, 1961, 1967). NiAl is advantageous because of its low density, good thermal conductivity, high melting point, and excellent oxidation resistance, whereas its little deformability at room temperature and its low strength and creep resistance at high temperatures above 1000 °C is always a disadvantage compared to the superalloys (Vedula and Stephens, 1987a; Darolia, 1991). The low strength at high temperatures is related to the excellent oxidation resistance, since both effects result from easy diffusion at high temperatures which is due to the open B2 structure of NiAl (see Secs. 4.3.4 and 4.3.5). In view of applications as high-pressure turbine blade material in flying gas turbines, NiAl is regarded as highly promising for developing alloys which are competition for superalloys because the strength deficit is compensated for by the advantage in density and thermal conductivity, and respective materials developments are under way (Darolia et al., 1992b; Liu and Kumar, 1993; Walston and Darolia, 1993; Locci et al., 1993; Field et al., 1993; Goldman, 1993; Igarashi and Senba, 1993; Oti and Yu, 1993; Darolia, 1993). Microalloying additions of Mo, Fe, Nb, Ta, Zr, Hf, B, and C as well as special processing routes, e.g. hot extrusion after melting and casting, are used, and the aim is always improved room temperature ductility and increased high temperature strength (Walston et al., 1993; Field et al., 1993; Lahrman et al., 1993a; Locci et al., 1993; Hack et al., 1993). The mechanical behavior of NiAl under complex conditions has not yet been studied systematically, as is exemplified by the only work on fatigue to date (Noebe and Lerch, 1992, 1993; Smith et al., 1992; Stoloff, 1992; Cullers et al., 1993; Edwards and Gibala, 1993).

As in the case of conventional disordered alloys, NiAl alloys can be strengthened appreciably by second phases. Apart from the effects on strength, second phases may also be beneficial for ductility and toughness, as has been discussed with respect to NiAl-based intermetallic alloys (Noebe et al., 1991; Clemens and Bildstein, 1992). In any case, the effects of second phases depend on the properties of the respective phases and on the phase distribution. This is illustrated in the following sections by regarding various NiAl alloy systems which have been studied in some more detail. The creep behavior of NiAl alloys with strengthening second phases is addressed in Sec. 4.3.4.

NiAl–Fe Alloys:

The ternary Ni–Fe–Al phase diagram in Fig. 28 shows various two-phase and three-phase fields neighboring the (Ni,Fe) Al field, i.e. there are various possibilities for producing NiAl alloys with second phases. For example, fine b.c.c. Fe-rich particles can be precipitated from the NiAl–Fe matrix by careful adjustment of the Fe and Al contents and by adequate heat treatment (Jung and Sauthoff, 1989a). The strengthening effect of these disordered particles in the ordered intermetallic matrix is quite analogous to that of ordered NiAl precipitate particles in a disordered Fe-base alloy (Jung and Sauthoff, 1987), and thus corresponds to particle strengthening in conventional alloys. The

ArcelorMittal Ex. 2038
Page 82 of 190

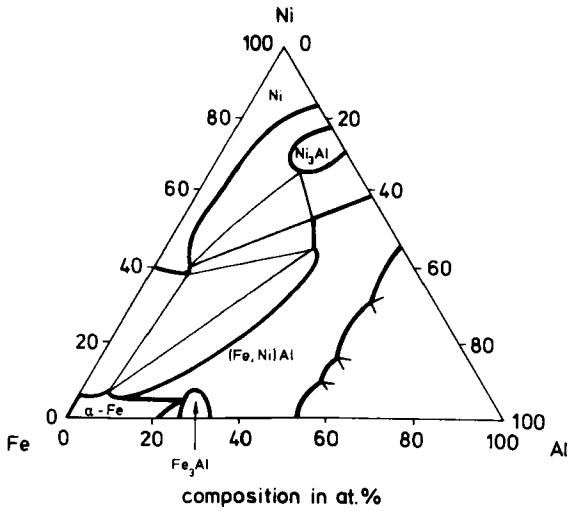


Figure 28. Isothermal section of the Ni–Fe–Al phase diagram at 400 °C with the f.c.c. Ni solid solution (A1), the b.c.c. α-Fe solid solution (A2) and the intermetallic phases Ni_3Al ($L1_2$), Fe_3Al ($D0_3$) and (Ni,Fe)Al (B2 or $L2_0$) [schematic diagram from Sauthoff (1986) according to Bradley and Taylor (1938), Dannöhl (1942), Bradley (1951), and Hao et al. (1984)].

two-phase equilibrium between NiAl and disordered f.c.c. γ-Fe–Ni has been used to produce lamellar two-phase alloys, i.e. in situ composites, by directional solidification (Klöwer and Sauthoff, 1991). The strength is described by a rule of mixtures as long as the lamellar spacing is large, i.e. for coarse microstructures, whereas an additional strength increase is obtained for fine microstructures with small lamellar spacings (see Sec. 4.3.4).

Besides strengthening, second phases may also be useful for improving the ductility and the toughness – in particular if they are soft, as is the case for the abovementioned, disordered phases (Noebe et al., 1991). Even the two-phase eqilibrium between NiAl and the other nickel aluminide Ni_3Al can be used to produce a two-phase NiAl–Ni_3Al alloy with improved strength and toughness (Baker and Munroe, 1990). Consequently, the composition range of the Ni–Fe–Al system, which includes the phase equilibria between NiAl, α-Fe, γ-Fe and Ni_3Al, has been studied intensively in order to identify NiAl-base alloys with good combinations of strength and ductility, and promising materials developments have been started (Guha et al., 1989, 1992; Baker and George, 1992; M. Larsen et al., 1990; Noebe et al., 1991; Raj et al., 1991, 1992b; Raj, 1992; J. H. Lee et al., 1992; Tsau et al., 1992; Golberg and Shevakin, 1991; Misra et al., 1993; Kostrubanic et al., 1993). In particular, alloys with 20 at.% Al and 30 at.% Fe, as well as with 30 at.% Al and 20 at.% Fe, are subjects of materials developments. The fatigue behavior has been studied by Stoloff (1992). It has to be emphasized that both composition and processing have to be controlled carefully, since the balance of strength and ductility depends sensitively on the distribution of the phases. It is noted that similar Ni–Co–Al alloys have been prepared which also offer good possibilities for optimizing the strength and ductility (Kimura et al., 1993).

The NiAl phase in NiAl alloys with second Fe-rich and/or Ni-rich phases is off-stoichiometric with an Al deficiency. Thus NiAl in these alloys may transform martensitically, as has been discussed in Sec. 4.3.2, which offers a further possibility for improving the strength and ductility. Indeed such alloys with martensitically transformable NiAl exhibit some room temperature tensile ductility (Khadikar et al., 1987; Furukawa et al., 1988; Ishida et al., 1991a; Kainuma et al., 1992b). It is noted that these alloys show a shape memory effect and are of interest in view of respective applications.

ArcelorMittal Ex. 2038
Page 83 of 190

NiAl–Cr Alloys:

As has been already discussed (Sauthoff, 1990a), NiAl forms eutectics with the refractory metals Cr, Mo, and W which may be used to produce composite materials by directional solidification (Cline et al., 1971), and indeed the NiAl–Cr composite shows promising high-temperature strength (Walter and Cline, 1970). Such alloys – in particular NiAl–Cr and NiAl–Mo – are now studied intensively in order to develop high-temperature, high-strength alloys (Kowalski and Frommeyer, 1992; Subramanian et al., 1990a; D. R. Johnson et al., 1992, 1993; Bowman, 1992; Chang, 1992; Heredia and Valencia, 1992; Goldman, 1993). For the preparation of alloys, both powder metallurgy and ingot metallurgy – in particular directional solidification – are used.

Compressive and tensile strength and toughness have been studied and preliminary data have been presented in Sauthoff (1990a). Strength increases significantly with increasing Cr content, i.e. increasing volume fraction of the disordered b.c.c. α-Cr phase in these two-phase alloys. Furthermore, strength – in particular at high temperatures – increases with increasing grain size, whereas ductility decreases. In any case ductility and toughness are sensitive functions of the microstructure and can be improved by appropriate thermomechanical processing. This means on the one hand that the processing of such alloys must be controlled carefully for a good and reproducible materials' quality, and on the other hand there are good chances of increasing the low toughness by optimizing the alloy with respect to composition, phase distribution and microstructure. The fracture resistance of directionally solidified NiAl–Cr and NiAl–Mo alloys has recently been studied (Heredia et al., 1993). It has been found that the crack-initiation toughness is appreciably higher than that of NiAl, which has been rationalized by available models.

The excellent oxidation resistance of pure NiAl decreases with increasing Cr content and increases with increasing temperature (Brumm and Grabke, 1992; Grabke et al., 1992). In any case the oxidation resistance of NiAl–Cr alloys is still acceptable for not too high volume fractions of the α-Cr phase.

NiAl–Ti Alloys:

Alloying of NiAl with Ti produces the hard and brittle Heusler-type phase Ni_2AlTi with an $L2_1$ structure (Villars and Calvert, 1991). It is very stable and strongly bonded which makes deformation difficult, and the strength increases with deviations from stoichiometry (Umakoshi et al., 1985). Ni_2AlTi forms a stable two-phase equilibrium with NiAl (Raman and Schubert, 1965; Nash and Liang, 1985; Mazdiyasni et al., 1989; Kumar, 1990; Lee and Nash, 1991b) and accordingly two-phase alloys can be produced with either Ni_2AlTi precipitate particles in an NiAl matrix or NiAl precipitate particles in an Ni_2AlTi matrix. Such alloys were studied intensively with respect to creep (Strutt and Polvani, 1973; Polvani et al., 1976). In particular it was found that the creep resistance of alloys with an Ni_2AlTi matrix and small NiAl particles reaches that of the Ni-base superalloy MARM-200.

The microstructure of the Ni_2AlTi–NiAl alloys is quite analogous to that of superalloys with semicoherent phase boundaries and analogous particle shapes and orientation relationships. This semicoherency and the orientation relationship result from the fact that the B2 structure and the $L2_1$ structure are closely related

ArcelorMittal Ex. 2038
Page 84 of 190

(see Fig. 1), and the lattice misfit between the two phases is small (Takeyama et al., 1991). However, the lattice misfit is not negligible since it gives rise to an elastic energy contribution which controls the microstructure evolution (Bendersky et al., 1988). The oxidation rate of Ni_2AlTi is of the same order of magnitude as that of dilute γ-Ni–Al alloys (Lee and Shen, 1989). Presently, a materials development on the basis of NiAl with strengthening Ni_2AlTi is under way which aims at applications such as turbine blades in aero-engines (Darolia, 1991; 1993) (see Sec. 4.3.6.).

The problem with such alloys is their brittleness. Recently it has been found that the brittleness can be relieved by making use of the three-phase equilibrium between NiAl, Ni_2AlTi, and Ni_3Al (Yang et al., 1992a, b). The resulting three-phase alloys are plastically deformable in compression at room temperature and compare favorably to superalloys with respect to strength. The slip transfer from the NiAl phase to the Ni_3Al phase in such alloys has been studied in detail (R. Yang et al., 1993). In view of these properties and the comparatively low density in the range 6.6–6.9 g/cm^3, the three-phase NiAl–Ni_2AlTi–Ni_3Al alloys are regarded as promising for applications in aero-engines (Yang et al., 1992a).

NiAl–Nb and NiAl–Ta Alloys:

In view of the ternary Ni–Al–Nb phase diagram (see Fig. 29) there are various possible ways to form two-phase or three-phase alloys on the basis of NiAl by alloying with Nb. For the strengthening of NiAl, second phases with not too low Al contents are preferred with respect to de sity and oxidation resistance. Al_3Nb witl tetragonal $D0_{22}$ structure, which has be discussed in Sec. 3.3.2, and the Lav phase NbNiAl with a hexagonal C

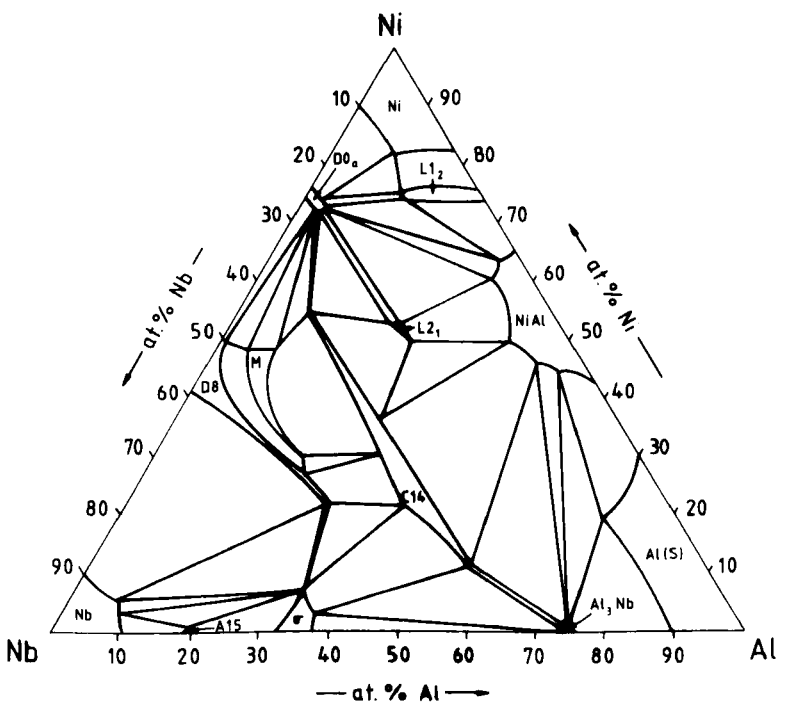


Figure 29. Isothermal section of the Ni–Al–Nb phase diagram at 1140 °C (Benjamin et al., 1966).

ArcelorMittal Ex. 2038
Page 85 of 190

structure, which will be discussed in Sec. 8, are such phases, and both phases are significantly stronger and more brittle than NiAl.

Figure 30a shows flow stress data as a function of temperature for these phases and for three three-phase alloys which are composed of NiAl, Al_3Nb and NbNiAl and are either NiAl-rich or Al_3Nb-rich. It can be seen that NiAl is indeed strengthened significantly by the hard phases Al_3Nb and NbNiAl. At high temperatures the flow stress increases with increasing volume fraction of the hard phases according to a rule of mixtures at a first approximation. At low temperatures an inverse behavior is observed. This may be related to the fact that the phases – in particular NiAl – which are in mutual equilibrium have off-stoichiometric compositions, and the resulting constitutional defects which are immobile at low temperatures give rise to additional strengthening. It is noted that the flow stress curves for Al_3Nb and NbNiAl do not extend to low temperatures because at low temperatures the fracture strain is smaller than the 0.2% proof strain. The three-phase alloys can be tested at much lower temperatures because microcracks in the hard phases are stopped at the phase boundaries of NiAl at intermediate temperatures. Indeed the apparent brittle-to-ductile transition temperature of these alloys is between that of NiAl at about 400 °C, and that of Al_3Nb and NbNiAl at about 1100 °C, as is shown in Fig. 30b. The oxidation resistance of these alloys with Al_3Nb has also been studied in some detail, and it was found that the good oxidation resistance of binary NiAl can nearly be reached by proper adjustment of the volume fractions of the respective phases (Steinhorst, 1989; Steinhorst and Grabke, 1989; Grabke et al., 1990, 1991b, 1992).

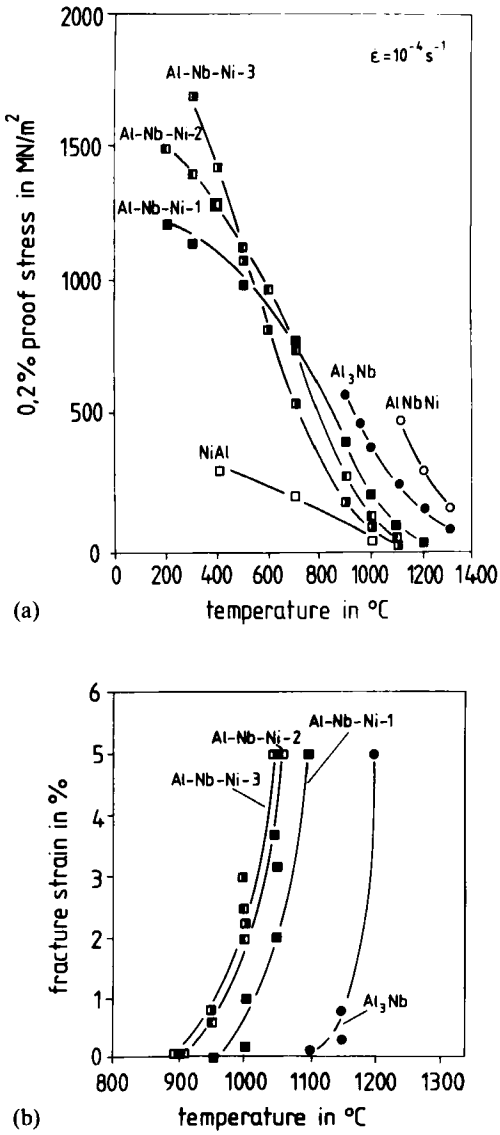


Figure 30. (a) 0.2% proof stress (in compression with $10^{-7}\,s^{-1}$ secondary strain rate) and (b) fracture strain (in bending with $10^{-4}\,s^{-1}$ strain rate – always referred to the specimen edge) as a function of temperature for various NiAl–Al_3Nb alloys, i.e. for the three-phase alloys NiAl–Nb-1, -2, and -3 with 22 vol.%, 46 vol.%, and 78 vol.% NiAl (B2), and 4 vol.%, 15 vol.%, and 15 vol.% NbNiAl (C14), respectively – balance Al_3Nb ($D0_{22}$) – compared with single-phase NiAl, Al_3Nb and NbNiAl (Rudy and Sauthoff, 1985; Rudy, 1986; Sauthoff, 1990a, b; Reip, 1991; Machon, 1992; Reip and Sauthoff, 1993).

ArcelorMittal Ex. 2038
Page 86 of 190

In spite of the obtained strength increases with Al_3Nb, the strength of the NiAl alloys with Al_3Nb – in particular the creep resistance – is not yet sufficient to enter the temperature range above that of the superalloys. Thus one has to rely on the Laves phase NbNiAl, which can be precipitated from NiAl, to obtain particle-strengthened NiAl alloys (Sherman and Vedula, 1986; Vedula and Stephens, 1987b). NbNiAl is significantly stronger than Al_3Nb, but also more brittle, and crack-free NbNiAl specimens can be produced only by powder metallurgy. However, the Laves phase forms a stable equilibrium with the B2 phase NiAl (Fig. 29), and the resulting NbNiAl–NiAl alloys, which have been studied in some detail (Sauthoff, 1990a, b, 1993a; Machon, 1992), can be produced without defects by vacuum induction melting. The brittleness of these two-phase alloys is reduced to such an extent that the alloys can be hit by a hammer at room temperature without cracking, i.e. they can be handled safely.

Figure 31 shows yield strength data of two-phase NiAl–NbNiAl alloys as a function of temperature for increasing volume fractions of the strengthening Laves phase. It is noted that the Laves phase precipitates on the grain boundaries and forms a continuous skeleton in all alloys so that the Laves phase plays the role of the matrix even in the NbNiAl-poor alloys. The compressive strength again follows a rule of mixtures to a first approximation. The bending strength does not increase with the NbNiAl volume fraction at higher volume fractions of NbNiAl. This is supposed to be due to alloy defects, i.e. pores and microcracks, and thus further work has to concentrate on improving the materials' quality.

Up to now the fracture toughness at room temperature is 2–4 $MNm^{-3/2}$ (see data in Sauthoff, 1990a, b) for these alloys, and the brittle-to-ductile transition temperature is between about 500 °C and 700 °C depending on composition and preparation method. Analysis of the microstructures of the deformed alloys has shown that in the brittle-to-ductile transition range cracks in the Laves phase are stopped at the Laves phase–NiAl interface by producing a plastic zone in the NiAl phase ahead of the crack (Machon, 1992; Wunderlich et al., 1992).

Recently similar alloys have been prepared by mechanical alloying (Arzt et al., 1993; Clemens et al., 1993a). Fully dense and completely aligned, lamellar, in situ composite NiAl–NbNiAl alloys have been

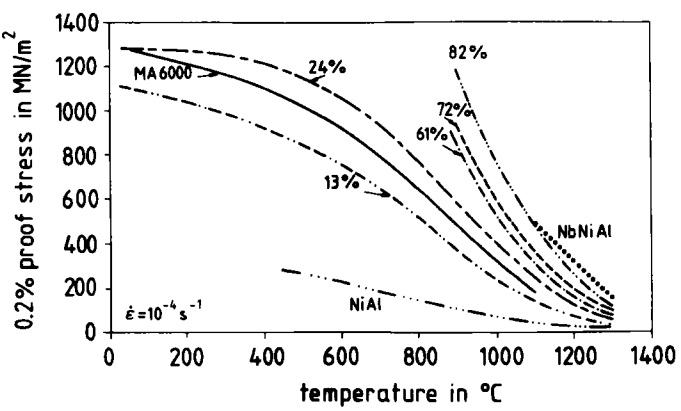


Figure 31. 0.2% proof stress in compression ($10^{-4}s^{-1}$ deformation rate) as a function of temperature for NiAl (B2), the Laves phase NbNiAl (C14) and various two-phase alloys with these two phases (the percentages at the curves are the respective amounts of NbNiAl) (Sauthoff, 1989, 1990a, 1991a; Machon, 1992) compared with data for the ODS superalloy MA 6000 (in tension) (Inco, 1982).

ArcelorMittal Ex. 2038
Page 87 of 190

produced successfully by directional solidification (Reviere et al., 1992; Whittenberger et al., 1992a). This special microstructure leads to a further increase in the strength, but has no beneficial impact on the low-temperature ductility and fracture strength.

Other ternary Laves phases with Al are NbFeAl, TaFeAl, and TaNiAl (see Sec. 8.1), and the latter in particular has been considered for strengthening NiAl (Pathare et al., 1987; Vedula and Stephens, 1987b). These phases are still harder than NbNiAl, they also form stable equilibria with the respective B2 aluminides FeAl and NiAl, and preliminary data for the respective one-phase and two-phase alloys have been presented in Sauthoff (1990a, b, 1993a). Figure 32 shows yield strength data for two-phase NiAl–TaNiAl alloys. It can be seen that the obtained flow stresses are significantly higher than those of the NiAl–NbNiAl alloys, and thus it should be possible to enter the strength–temperature range above that of superalloys by making use of such alloys. The Arrhenius plot of the data shows that a rule of mixtures may be supposed not only for the yield strength, but also for the apparent activation energy. It has to be noted, however, that these alloys compare less favorably with superalloys with respect to long-term behavior, i.e. creep strength, which has been addressed in Sec. 4.3.4.

Since the transition metal elements in these ternary Laves phases can substitute for each other freely, and since the distribution of Laves phase can be controlled by thermomechanical treatments there are possibilities for optimizing such NiAl alloys with Laves phases with respect to creep resistance and the brittle-to-ductile transition temperature (BDTT) by controlling the composition and phase distribution, and this is being studied presently

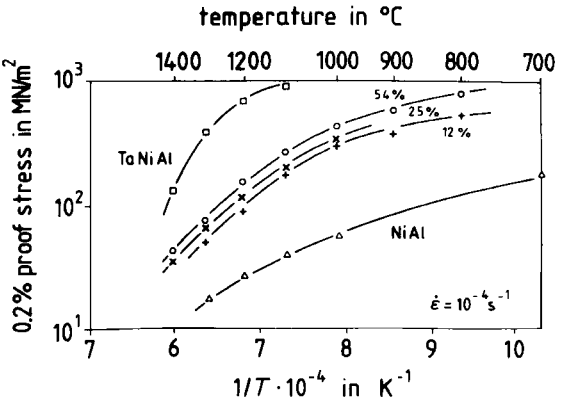


Figure 32. 0.2% proof stress in compression ($10^{-4}\,s^{-1}$ deformation rate) as a function of temperature for NiAl (B2), the Laves phase TaNiAl (C14) and various two-phase alloys with these two phases (the percentages at the curves are the respective amounts of TaNiAl) (Sauthoff, 1989, 1990a, 1991a; Machon, 1992).

(Zeumer et al., 1991; Sauthoff, 1993a). Variation of the BDTT with changing alloy composition is illustrated in Fig. 33.

Finally, it is noted that besides the Laves phases the Heusler-type phases Ni_2AlNb and Ni_2AlTa with an $L2_1$ structure may

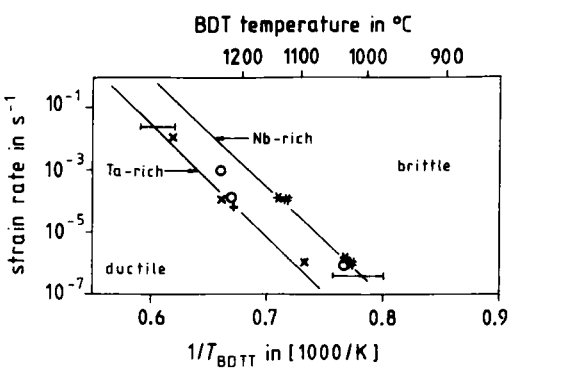


Figure 33. Brittle-to-ductile transition temperature BDTT as a function of strain rate in bending (referred to the specimen edge) for various two-phase NiAl–(Ta,Nb)NiAl alloys with 23.5 vol.% Laves phase: Ta10Ni45Al45 (×), Ta9Nb1Ni45Al45 (+), Ta7.5Nb2.5Ni45Al45 (o), Ta1Nb9Ni45Al45 (#), and Nb10Ni45Al45 (*) (Sauthoff, 1991a; Zeumer et al., 1991; Zeumer and Sauthoff, 1992).

ArcelorMittal Ex. 2038
Page 88 of 190

form in the ternary systems Ni–Al–Nb and Ni–Al–Ta, respectively, in close analogy to the Ni–Al–Ti system, as is shown in the respective phase diagrams [see Fig. 29 and Pak et al. (1988) and Darolia (1991)]. Indeed two-phase NiAl alloys with these strengthening precipitates have been studied with respect to mechanical behavior and are regarded as promising for materials developments (Pak et al., 1988; Yasuda et al., 1992), as well as three-phase NiAl alloys with a coarse distribution of the NbNiAl Laves phase and a fine particle distribution of Ni_2AlNb (Machon, 1992; Machon and Sauthoff, 1994). In summary, it is concluded that there are good prospects for developing materials on the basis of NiAl with strengthening Laves phases and/or Heusler-type phases which have sufficient creep strength at temperatures above the application temperatures of superalloys and tolerable brittleness.

ODS NiAl Alloys and Composites:

In view of the advantageous properties of NiAl for high-temperature applications, i.e. excellent oxidation resistance, moderate density, high stability, and good thermal conductivity, and the disadvantageous poor strength at high temperatures, NiAl has been considered as a matrix material for intermetallic matrix composites, and respective materials developments are under way (see reviews by Bowman and Noebe, 1989; Rigney et al., 1989; Kumar, 1991; Vedula, 1991; Kumar and Whittenberger, 1992; Kumar et al., 1992b; Shah and Anton, 1993). Such composite materials have been produced primarily by powder metallurgy methods, and a variety of phases have been used for strengthening the NiAl matrix, i.e. Al_2O_3 and other oxides (Jellinghaus, 1961; Noebe et al., 1990; Alman and Stoloff, 1991; Dimiduk et al., 1991; Kostrubanic et al., 1991; Kumar, 1991; Nourbakhsh et al., 1991; Baker and George, 1992; Dymek et al., 1992; Bowman, 1992; Anton and Shah, 1992b; Arzt et al., 1993; Hebsur et al., 1993; Dymek et al., 1993; Bieler et al., 1993), the nitrides SiN and AlN (Shah et al., 1990; Whittenberger et al., 1990b, 1992a; Moser et al., 1990; Kumar, 1991; Bieler et al., 1992; Arzt et al., 1993; Hebsur et al., 1993), SiC, B_4C and other carbides (Whittenberger et al., 1990a; Moser et al., 1990; Nardone et al., 1990; Shah et al., 1990; Chou and Nieh, 1991; Dimiduk et al., 1991; Dunmead et al., 1991; Kumar, 1991), the boride TiB_2 (Rigney et al., 1989; Sagib et al., 1990; Moser et al., 1990; Whittenberger et al., 1990b; Alman et al., 1991; Cheng and Cantor, 1992; Kumar et al., 1992a, b; Pregger et al. 1992; Viswanadham et al., 1988; Korinko et al., 1992), and the beryllide $TiBe_{12}$ (Carbone et al., 1988).

At service temperature chemical reactions may occur between the constituent phases of a composite and thus chemical compatibility of the phases to be combined is of primary importance. Microstructural long-term stability is guaranteed only if the constituent phases form stable equilibria with each other. Even then the phase distributions coarsen slowly by ageing processes, i.e. Ostwald ripening occurs which is slower the smaller the interface energies, the mutual solubilities and the diffusivities are (Pitsch and Sauthoff, 1992). Studies of the compatibility of the various strengthening phases with NiAl have shown that Al_2O_3 and TiB_2 are sufficiently stable in NiAl (Sagib et al., 1990; Moser et al., 1990; Shah et al., 1990; Chou and Nieh, 1991; Trumble and Rühle, 1990; Wang and Arsenault, 1991; Korinko and Duquette, 1994). Apart from chemical compatibility, dispersoids may affect the environmental be-

ArcelorMittal Ex. 2038
Page 89 of 190

havior, e.g. the oxidation resistance, as has been shown recently with respect to an NiAl/AlN composite (Lowell et al., 1990).

Besides powder metallurgy methods, directional solidification of eutectic NiAl alloys is used for producing in situ composites. Examples are NiAl–Cr (Walter and Cline, 1970; Kowalski and Frommeyer, 1992). NiAl–Mo (Sauthoff, 1990a; Subramanian et al., 1990a), NiAl–W (Sauthoff, 1990a; Saigal and Kupperman, 1991), and NiAl–Re (Mason et al., 1990). In these composites the second continuous phase is disordered, which is expected to improve the ductility of NiAl. However, the obtained ductilities of these composites are still low. Other intermetallic phases are also used for reinforcing an NiAl matrix composite, and an example is given by NiAl containing the Heusler-type phase Ni_2AlTi (Whittenberger et al., 1989; Kumar and Whittenberger, 1992) (see also Sec. 4.3.6.). A special type of composite is being developed (Nardone et al., 1990; Nardone and Strife, 1991; Nardone, 1992) which combines a continuous ductile phase and a particulate hard and brittle phase with NiAl. In such alloys cracking occurs in the NiAl matrix during deformation at about 0.2% strain, whereas the final fracture strain of the composite is 30–35%.

The various NiAl matrix composites usually exhibit an increased strength and brittleness compared to single-phase NiAl. However, there are exceptions to this rule, i.e. a decreased high-temperature strength has been observed for an NiAl–Ni_2AlTi composite and furthermore, increased toughness has been obtained for an NiAl–Al_2O_3 composite (Kumar, 1991). Such toughening by dispersed particles is a well-established process for improving the toughness of metals and ceramics (Wiederhorn, 1984; Sigl et al., 1988; Ashby et al., 1989). Another toughening mechanism in ceramics relies on the transformation of dispersed zirconia particles which transform during deformation (Wiederhorn, 1984; Evans and Cannon, 1986; Rühle and Evans, 1989). This transformation toughening with zirconia has been used not only for ceramics, but also for metals and in particular for the intermetallic NiAl, i.e. the fracture toughness of sintered NiAl has been increased from about 14 $MN/m^{3/2}$ to 22 $MN/m^{3/2}$ by the addition of 20 vol.% ZrO_2 which contained 2 mol% Y_2O_3 (Barinov et al., 1992; Barinov and Evdokimov, 1993). Present efforts of various NiAl developments are directed at improving the processing for optimizing the mechanical behavior. The physical understanding of the deformation controlling mechanisms is only limited and necessitates much further work.

4.4 Other B2 Phases

Intermetallic phases with a B2 structure form one of the largest groups of intermetallics, and there is a broad variation of chemical, physical and mechanical properties within this group (Dwight, 1967). Other B2 aluminides are FeAl and CoAl. They are closely related to NiAl since Ni, Fe, and Co can substitute for each other completely in the B2 structure – this was made use of for improving the high temperature strength and creep resistance (Jung et al., 1987; Sauthoff, 1991a) – and they are also considered for high temperature applications (Vedula and Stephens, 1987a; Liu et al., 1990; Kumar and Whittenberger, 1992). Besides these aluminides, the B2 structure is adopted by compounds of group VIII metals and group IVA metals, e.g. NiTi, CoTi, and FeCo. These B2 phases, which are oft interest with respect to applications, are briefly overviewed in

ArcelorMittal Ex. 2038
Page 90 of 190

the following sections with the exception of FeAl which is the subject of Sec. 5.3. The classical B2 phase CuZn (β-brass) is addressed in Sec. 6.

Intermetallics with precious metals have recently been studied with respect to strength, ductility and oxidation resistance (Fleischer, 1992b; Fleischer and McKee, 1993). Outstanding properties have been found for the B2 phases AlRu and RuSc with melting temperatures of 2060 °C and 2200 °C, respectively. AlRu shows very high strength with high work hardening and extensive compressive ductility at room temperature. The effects of constitutional defects and ternary solutes on the hardening behavior of AlRu have been studied in detail (Fleischer, 1993a, b, d, f). The fracture behavior of AlRu has been studied theoretically by a molecular dynamics simulation (Becquart et al., 1993). The oxidation resistance of AlRu allows the use of uncoated AlRu up to about 1250 °C. Of course the high costs of such intermetallics will not allow the application of these phases as structural materials in the near future (Fleischer, 1992b). PdIn is noteworthy because of its gold color which makes it promising for dental prosthetics and jewellery (Baker and George, 1992). PdIn has been studied with respect to deformation behavior (Munroe et al., 1991) and diffusion (Koiwa, 1992; Wever, 1992).

4.4.1 CoAl

The B2 aluminide CoAl is very similar to NiAl with respect to density, thermal expansion behavior, melting temperature and phase diagram (Westbrook, 1956; Whittenberger, 1985; Stephens, 1985; Massalski et al., 1990; Harmouche and Wolfenden, 1987). The thermodynamic properties and point defects have been studied experimentally and theoretically (Bakker and Ommen, 1978; Chen and Dodd, 1986; Koch and Koenig, 1986; chapter by Inden and Pitsch in Volume 5 of MST). Young's modulus, which is higher than that of NiAl, has been determined as a function of temperature for polycrystalline CoAl with the stoichiometric composition and with various deviations from stoichiometry (Harmouche and Wolfenden, 1985, 1986). Diffusion in CoAl is slower with a higher activation energy than in NiAl, and deviations from stoichiometry enhance diffusion as in the case of NiAl (Hagel, 1967).

The hardness of CoAl is higher than that of NiAl with a minimum for the stoichiometric composition at temperatures below 800 °C (Westbrook, 1956), i.e. deviations from stoichiometry produce constitutional defects with restricted mobility at lower temperatures which strengthen the CoAl, as in the case of NiAl. The characteristics of slip correspond to those of NiAl (Baker and Munroe, 1990). The hardening of CoAl by constitutional defects and ternary solutes, i.e. Mn, Re, and Ti, has been studied in detail (Fleischer, 1993c, d, e).

At high temperatures above 1000 °C the flow stress and creep resistance are again higher than those of NiAl and reach a maximum at the stoichiometric composition (Hocking et al., 1971; Whittenberger, 1985; Yaney and Nix, 1988) because the constitutional defects, which are produced by deviations from stoichiometry, are mobile at high temperatures and enhance diffusion and thereby creep, as in the case of NiAl. The enhanced creep resistance of CoAl is attributed to lattice friction effects limiting the dislocation mobility in CoAl (Yaney and Nix, 1988). The creep resistance of CoAl is increased significantly by partial substitution of Co by Ni, and still more by Fe (Jung et al., 1987; Whitten-

ArcelorMittal Ex. 2038
Page 91 of 190

berger, 1987; Sauthoff, 1991a). Further strengthening is achieved by reinforcing CoAl with particulate TiB_2 (Mannan et al., 1990).

The high strength of CoAl is correlated with low ductility and toughness, and indeed the fracture toughness is lower than the already low toughness of NiAl (K.-M. Chang et al., 1992). The fracture characteristics, however, are quite analogous to those of NiAl, i.e. the preferred cleavage plane is {110} and the fracture toughness is lowest for directions in the cleavage plane. The differences in strength and brittleness between CoAl and NiAl cannot yet be correlated with differences in the strength and the character of bonding, which have been studied by quantum-mechanical ab initio calculations (Schultz and Davenport, 1992).

Because of its high brittleness and because Co is a strategic material, CoAl has not been selected for materials development in the past in spite of its attractive high-temperature strength (Vedula and Stephens, 1987a). Recent work on CoAl–TiB_2 composites has led to the conclusion that the more damage-tolerant NiAl matrix composites are a better choice for creep applications (Mannan et al., 1990).

4.4.2 NiTi

The B2 phase NiTi has been used for 30 years as a shape memory alloy for couplings, fasteners, connectors, and actuators in automotive and aerospace industries, electronics, mechanical engineering and medical applications (Schmidt-Mende and Block, 1989; Stöckel, 1989; Thier, 1989; Hodgson, 1990; Stoeckel, 1990). NiTi melts congruently at 1310 °C and has an extended homogeneity range (Massalski et al., 1990).

NiTi transforms martensitically from the parent B2 phase to a monoclinic martensite phase with an intermediate orthorhombic R phase from which a reversible shape memory effect – with the best shape memory behavior of all shape memory alloys – and pseudoelasticity results (Hwang et al., 1983; Hwang and Wayman, 1983; Nishida and Honma, 1984; Van Humbeek and Delaey, 1989). The characteristics of such shape memory alloys have been discussed in detail with respect to crystallography, microstructure, thermodynamics, kinetics and macroscopic mechanical behavior, and applications have been described (Delaey et al., 1974; Krishnan et al., 1974; Warlimont et al., 1974; Ahlers, 1986; Van Humbeek and Delaey, 1989; Hornbogen, 1991). The crystallography of the martensitic transformation has been analyzed in detail (Shimizu and Tadaki, 1992).

The shape memory behavior of NiTi is improved by prior thermomechanical treatments which produce advantageous microstructures and textures (Van Humbeek and Delaey, 1989; Lin and Wu, 1992; Mulder et al., 1993). The transformation temperature is about 110 °C for stoichiometric NiTi and is decreased by excess Ni (Hodgson, 1990). Likewise, the transformation temperature is lowered by alloying with Fe and Cr whereas Cu decreases the transformation temperature hysteresis. A widened transformation temperature hysteresis was found recently for NiTi–Nb alloys, which is attractive with respect to coupling and sealing applications (Piao et al., 1992a, b). The tranformation temperature is increased up to 500 °C by the partial substitution of Ni with Pd which, however, affects the ductility (Yang and Mikkola, 1993).

The elastic and plastic deformation behavior, including mechanical twinning, of

ArcelorMittal Ex. 2038
Page 92 of 190

NiTi alloys has been studied intensively (see, e.g. Saburi et al., 1984; Matsumoto and Ishiguro, 1989; Goo et al., 1985). Noteworthy is the high ductility of NiTi which allows deformations up to 70% (Van Humbeek and Delaey, 1989). Furthermore, the yield strength of NiTi depends on the temperature in an anomalous way, i.e. it increases with rising temperature to reach a maximum, and only above this peak temperature does normal softening occur (Takasugi et al., 1991a). This strength anomaly is also shown by other, closely related B2 phases, i.e. CoTi, CoZr, and CoHf (see next section), but not by FeTi and not by the aluminides NiAl, CoAl and FeAl, i.e. the transition from normal behavior to anomalous behavior is obviously related to a critical number of valence electrons per atom (Takasugi et al., 1991e). The general characteristics of the mechanical behavior of such shape memory alloys and the mutual interaction of deformation and phase transformation have been discussed in detail, and the thermodynamics and kinetics of the involved processes have been addressed (Delaey et al., 1974; Krishnan et al., 1974; Warlimont et al., 1974; Hornbogen 1991).

Processing of NiTi alloys is difficult and has to be done with care to obtain advantageous properties (Van Humbeek and Delaey, 1989; Hodgson, 1990). Melting must be done in a vacuum or in inert atmospheres because of the reactivity of Ti, and thus vacuum-induction melting, plasma-arc melting, and electron-beam melting are all used commercially. Hot working is possible without problems. Processing at low temperatures is difficult because of extremely high work hardening, and thus intermediate annealing treatments are required for cold rolling, machining, etc. The ductility problem of the (Ni,Pd)Ti alloys with a high transition temperature is relieved by alloying with B (Yang and Mikkola, 1993). Joining by welding, brazing or soldering is generally difficult. The excellent shape memory behavior of the NiTi alloys is accompanied by excellent corrosion resistance – comparable to stainless steels – which make these alloys the only shape memory alloys suitable for implantation in human bodies (Van Humbeek and Delaey, 1989). Recently NiTi has been used as a strengthening phase in Al matrix composites which experience an additional strengthening effect from the shape memory effect in NiTi (Furuya et al., 1993; Yamada et al., 1993).

4.4.3 FeTi, CoTi, CoZr, and CoHf

FeTi with a B2 structure is one of the most promising intermetallic phases for use as a hydrogen storage material and related applications (Reilly, 1979; Nathrath, 1986; Lynch, 1991). Dissolved hydrogen orders to form a substructure in which the B2 structure becomes rhombic, i.e. a stable hydride is formed in a reversible way (Somenkov and Shilstein, 1979; Reilly, 1979). FeTi with excess Ti is more easily hydrogenized then stoichiometric FeTi since Ti activates the absorption and desorption of hydrogen catalytically (Sicking and Jungblut, 1983; Amano et al., 1984). Second phases, including oxides, shorten the incubation time for hydrogenization (Nagai et al., 1987; Amano et al., 1983), whereas oxygen may poison the FeTi surface at room temperature (Schlapbach et al., 1979). The electronic structure has been studied theoretically (Bose et al., 1991). CoTi is also of interest for use as a hydrogen storage material (Izumi, 1989), as well as the ternaries (Fe,-Co)Ti (Boulghallat and Gerard, 1991) and (Fe,Ni)Ti (Bershadsky et al., 1991) which show more advantageous storage properties than the binaries.

ArcelorMittal Ex. 2038
Page 93 of 190

The plastic deformation behavior of CoTi has been studied in detail since the B2 phases CoTi, CoZr, and CoHf exhibit an anomalous temperature dependence of the yield strength, which is also shown by NiTi, but not by FeTi and the aluminides NiAl, CoAl, and FeAl (Nakamura and Sakka, 1988; Takasugi and Izumi, 1988; Takasugi et al., 1990c, 1991a, e; Yoo et al., 1990; Yoshida and Takasugi, 1991b). Slip occurs by ⟨100⟩ dislocations at low and intermediate temperatures as in the case of NiAl, whereas at higher temperatures above the peak strength temperature the activation of ⟨111⟩ dislocations has also been observed (Takasugi et al., 1992b). The elastic moduli have been measured (Yasuda et al., 1991b). The transition from the anomalous temperature dependence of the yield strength in NiTi, CoTi, CoZr, and ZrHf to the normal one in FeTi and the aluminides NiAl, CoAl, and FeAl is related to the change in the number of valence electrons per atom, i.e. to changes in the atomic bonding, but a clear and complete understanding has not yet been reached (Yoo et al., 1990; Takasugi et al., 1991e, 1992b). It is noted that alloying CoTi with CoSi results in the formation of the Heusler-type compound Co_2TiSi with an $L2_1$ structure, which is strongly ferromagnetic with a Curie temperature far in excess of room temperature though both CoTi and CoSi are nonmagnetic (see also Sec. 4.5).

4.4.4 FeCo

FeCo – in particular with a 2% V addition – has found widespread use as a magnetically soft material with a high saturation induction, e.g. as electromagnet pole tips, and the respective alloys are known as Permendur alloys (Chen, 1961; Kouvel, 1967; Dietrich, 1990). These alloys also exhibit a high, positive magnetostrictive coefficient, which has made them useful in sonar transducers and in extremely accurate positioning devices.

The B2 phase FeCo is stable only at temperatures below 730 °C and has a broad range of homogeneity (Massalski et al., 1990). At 730 °C there is an order–disorder transition with a 0.2% change in volume from B2 to A2 (b.c.c.), and a further structure change from A2 to A1 (f.c.c.) occurs at about 985 °C (Buckley, 1975). The ordering reaction proceeds heterogeneously or homogeneously depending on the temperature (Cahn, 1993). The ordering process has been studied in detail and the thermodynamics of the binary Fe–Co phase diagram, as well as the ternary Fe–Co–Al phase diagram, have been analyzed by model calculations (Rajkovic and Buckley, 1981; chapter by Inden and Pitsch in Volume 5 of MST). The ordering kinetics are affected by alloying additions and in particular alloying with 2 at.% V reduces the ordering rate significantly, which allows freezing of the high-temperature, disordered structure by quenching to low temperatures. It is noted that the addition of more than 2% V leads to alloy decomposition, as is indicated by the Fe–Co–V phase diagram (Mahajan et al., 1974; Raynor and Rivlin, 1983). A still larger effect on the ordering kinetics is produced by alloying with Cr (Alekseyev et al., 1977). Below the critical temperature of ordering, the degree of long-range order in equilibrium increases continuously from 0 at 730 °C to 0.9 at 500 °C to reach 1 – corresponding to perfect order – asymptotically at low temperatures (Stoloff and Davies, 1964).

The mechanical behavior of FeCo has been studied intensively since the order–disorder transition allows a direct study of the effects of ordering on the mechanical properties including creep, fatigue and

ArcelorMittal Ex. 2038
Page 94 of 190

fracture (Stoloff and Davies, 1964; Boettner et al., 1966; Jordan and Stoloff, 1969; Marcinkowski, 1974b; Pitt and Rawlings, 1983; Kawahara, 1983a, c; Delobelle and Oytana, 1983; Müller, 1986; Stoloff et al., 1992; Zhao et al., 1993). At room temperature FeCo is ductile – with 15% uniform elongation and subsequent necking – in the disordered state, i.e. after quenching from above the ordering temperature, whereas in the ordered state, i.e. after annealing below the ordering temperature, it shows only a little ductility with 5% uniform elongation and no necking (Stoloff and Davies, 1964). Thus cold rolling is difficult in the ordered state (see Müller, 1986). Furthermore, FeCo is subject to hydrogen embrittlement at room temperature (Liu and Stoloff, 1993).

Plastic deformation at room temperature occurs by the movement of $\langle 111 \rangle$ superlattice dislocations which are pairs of superpartials (Baker and Munroe, 1990; Yamaguchi and Umakoshi, 1990). The flow stress increases with decreasing degree of order, i.e. with rising temperature, to reach a maximum at about 700 °C, just below the ordering temperature where FeCo is only partially ordered (Stoloff and Davies, 1964). This behavior results from a decoupling of the superpartials of the superlattice dislocations since the coupling force decreases with increasing disorder. Above the flow stress peak temperature normal softening is observed which is due to thermal activation. In other words, FeCo, like other intermetallics, exhibits an anomalous positive temperature dependence of the flow stress, which, however, is not related to special dislocation mechanisms as in the case of Ni_3Al, but is related to incomplete atomic order, i.e. to structure changes.

Ordered FeCo–2V exhibits a more homogeneous deformation and a higher strain hardening rate than disordered FeCo–2V at all temperatures (Jordan and Stoloff, 1969). The grain size dependence of the yield stress and the fracture stress is described by the usual Hall–Petch relationship. The fatigue resistance is improved by ordering with only a small effect of the environment (Boettner et al., 1966; Stoloff et al., 1992). The low ductility can be increased by adding Ni as a fourth element, which changes the microstructure, and still more by thermomechanical treatments which lead to a Hall–Petch-type dependence of ductility on grain size or subgrain size (Pinnel et al. 1976; Pitt and Rawlings, 1983). Even cold rolling can reduce the brittleness (Kawahara, 1983c). The brittle-to-ductile transition temperature in the ordered state can be reduced significantly by deviations from stoichiometry which decrease the critical temperature of ordering and introduce configurational disorder (Konoplev and Sarrak, 1982). Positive effects on cold workability have been produced – apart from alloying with V or Cr which both slow down the ordering kinetics – by alloying with Nb, Ta, Mo, W, and C whereas Be, Ti, Zr, Mn, Cu, Ag, Au, B, Al, and Si are ineffective (Kawahara, 1983a, b). The physical understanding of such effects is still to be clarified.

Finally, it may be noted that alloying Fe and Co with precious metals leads to the phases FePt, CoPt, and FePd with an $L1_0$ structure, which is an ordered f.c.c. structure with tetragonal distortion (see Fig. 1). These phases have been of importance for applications as permanent magnetic materials, and in particular CoPt, which is used in the only partially ordered state, excels because of isotropy, ductility, easy machinability and resistance to corrosion and high temperatures (Jellinghaus, 1936; Kouvel, 1967; Chin and Wernick,

ArcelorMittal Ex. 2038
Page 95 of 190

1986; Fiepke, 1990; Leroux et al., 1991; Watanabe, 1991). However, CoPt alloy magnets are seldom used now since these alloys have been replaced by the rare earth magnets with superior magnetic properties.

4.5 Heusler-Type Phases

The classic Heusler-type alloys are Cu_2AlMn and Cu_2SnMn (Dwight, 1967; Kouvel, 1967) which will be addressed in Sec. 6. Their unique feature is their ferromagnetism, since the constituent elements are not ferromagnetic. These phases crystallize with the $L2_1$ structure which is derived from the B2 structure (see Fig. 1), and which is also adopted by a series of other ternary phases (Dwight, 1967).

Outstanding examples are Ni_2AlX and Co_2AlX phases with X = Ti, Zr, Hf, Nb, or Ta which are of interest for high-temperature applications, and some of them have been studied with respect to high-temperature deformation (Strutt et al., 1976; Umakoshi et al., 1985, 1986; Sauthoff, 1989; Takeyama et al., 1991). In particular, Ni_2AlTi has been used for reinforcing NiAl (see Sec. 4.3.6 under the heading Structural Alloys) and a two-phase Ni_2AlTi–NiAl showed a creep resistance which was higher than that of single-phase NiAl and even Ni_2AlTi, and reached that of a high-strength Ni-base superalloy (Polvani et al., 1976). The high strength is correlated with brittleness which has handicapped respective materials developments until now. Only recently Ni_2AlTa–NiAl has been identified as a more promising system because of the improved ductility (Pak et al., 1988).

4.6 Nickel – Molybdenum Phases

Various intermetallic phases are formed in the binary Ni–Mo system (Brooks et al., 1984). The most Ni-rich phase Ni_4Mo has the body-centered tetragonal crystal structure $D1_a$ and is stable only up to about 880 °C with peritectic decomposition. The ordered atom distribution can be established in various ways in this structure which gives rise to a domain structure with various types of domain interfaces. Ni_3Mo is orthorhombic and is stable up to about 910 °C. This phase, however, can also be formed with the metastable, tetragonal $D0_{22}$ structure, which is common to the trialuminide Al_3Ti and related phases (see Sec. 3.3). NiMo is another orthorhombic phase and decomposes peritectically at 1362 °C. Finally, there is the metastable, orthorhombic Ni_2Mo phase which is formed as an intermediate phase during ordering.

These phases are of general interest with respect to alloying Ni-base alloys since Mo is an important alloying element for superalloys. Corresponding multinary phase diagrams have been studied experimentally and theoretically (see, e.g., Brooks et al., 1984; Chakravorty and West, 1986; Kodentzov et al., 1988; Enomoto et al., 1991), in particular with respect to equilibria with the aluminide Ni_3Al which forms the basis of the advanced aluminides (see Sec. 4.1).

Special interest is directed at Ni_4Mo since Ni–Mo alloys with about this composition (20 at.% Mo) and additions of further elements – in particular Fe, Cr, and C – have been of industrial significance since the early 1930s because of their excellent corrosion resistance in nonoxidizing environments and their high strength at high temperatures, as is exemplified by the Hastelloy B alloys (Brooks et al., 1984). In these alloys ordered Ni_4Mo may form on slow cooling from temperatures above 900 °C, where the f.c.c. solid solution is stable, or on ageing at 500–850 °C.

ArcelorMittal Ex. 2038
Page 96 of 190

Ni_4Mo formation in Ni–Mo alloys leads to both hardening and embrittlement (in tension) with fracture occurring along grain boundaries. In compression such embrittled alloys can still be deformed plastically and furthermore, monocrystalline ordered Ni_4Mo shows significant ductility even in tension (Brooks et al., 1984; Kao et al., 1989). The physical properties of ordered Ni_4Mo have been determined and the deformation behavior has been studied in detail (Brooks et al., 1984). The mechanical properties are a sensitive function of the microstructure. The microstructure development is controlled by the kinetics of the decomposition and ordering reactions during cooling and ageing of these Ni–Mo alloys (see, e.g. Brooks and Cao, 1992; Cahn, 1992). The low ductility of hypostoichiometric ordered Ni_4Mo can be improved significantly by microalloying with B, whereas there is only a small effect of B on the stoichiometric phase (Tawancy, 1991).

5 Iron Aluminides and Related Phases

An overview of the Fe–Al phases is given by the binary Fe–Al phase diagram (Massalski et al., 1990). The Al-rich phases with melting temperatures of about 1150 °C are of interest for Al alloys and are not addressed here. The remaining phases Fe_3Al and FeAl, and related phases, have been selected for materials developments because of their outstanding physical, mechanical, and chemical properties and are the subjects of the following sections.

5.1 Fe_3Al

Fe_3Al is formed on cooling by ordering reactions in the solid state that transform the b.c.c. disordered solid solution, which is stable above about 800 °C, first into the FeAl phase with a B2 structure, which is stable between about 800 °C and 550 °C and which is the subject of Sec. 5.3, and then into Fe_3Al with the $D0_3$ structure (see Fig. 1). The critical temperature of ordering is much lower than the melting temperature (Massalski et al., 1990) which indicates less strong bonding between unlike atoms compared with, e.g. the nickel aluminides. The ordering process and its kinetics have been studied in detail both experimentally and theoretically for the determination of the field of existence and the equilibria of Fe_3Al in the Fe–Al phase diagram (see, e.g. Köster and Gödecke, 1980; Gödecke and Köster, 1985; Wachtel and Bahle, 1987; Inden and Pepperhoff, 1990; Vennégues et al., 1990; Maziasz et al., 1993; chapter by Inden and Pitsch in Volume 5 of MST). Recently a transient B32 phase has been observed during ordering (Gao and Fultz, 1993). On the Fe-rich side there is a two-phase equilibrium between Fe_3Al and b.c.c. Fe–Al solid solution which shows short-range order. On the Al-rich side there is a second order transition from Fe_3Al with a $D0_3$ structure to FeAl with a B2 structure without a two-phase equilibrium. The generally accepted phase diagram with the $D0_3$/B2 transition has been questioned recently on the basis of neutron scattering results (Hilfrich et al., 1991) which, however, are not unambiguous (Inden, 1993). The critical temperature of ordering, which is about 550 °C in the binary case (Massalski et al., 1990), can be shifted to higher temperatures by as much as 250 °C by alloying with a third element, in particular Cr, Mo, Mn, Ti, or Si (Mendiratta and Lipsitt, 1985; Fortnum and Mikkola, 1987; Longworth and Mikkola, 1987; Prakash et al., 1993).

Thermal vacancies are formed readily because of a low formation enthalpy,

ArcelorMittal Ex. 2038
Page 97 of 190

Intermetallics
Gerhard Sauthoff
copyright © VCH Verlagsgesellschaft mbH, 1995

Ni_4Mo formation in Ni–Mo alloys leads to both hardening and embrittlement (in tension) with fracture occurring along grain boundaries. In compression such embrittled alloys can still be deformed plastically and furthermore, monocrystalline ordered Ni_4Mo shows significant ductility even in tension (Brooks et al., 1984; Kao et al., 1989). The physical properties of ordered Ni_4Mo have been determined and the deformation behavior has been studied in detail (Brooks et al., 1984). The mechanical properties are a sensitive function of the microstructure. The microstructure development is controlled by the kinetics of the decomposition and ordering reactions during cooling and ageing of these Ni–Mo alloys (see, e.g. Brooks and Cao, 1992; Cahn, 1992). The low ductility of hypostoichiometric ordered Ni_4Mo can be improved significantly by microalloying with B, whereas there is only a small effect of B on the stoichiometric phase (Tawancy, 1991).

5 Iron Aluminides and Related Phases

An overview of the Fe–Al phases is given by the binary Fe–Al phase diagram (Massalski et al., 1990). The Al-rich phases with melting temperatures of about 1150 °C are of interest for Al alloys and are not addressed here. The remaining phases Fe_3Al and FeAl, and related phases, have been selected for materials developments because of their outstanding physical, mechanical, and chemical properties and are the subjects of the following sections.

5.1 Fe_3Al

Fe_3Al is formed on cooling by ordering reactions in the solid state that transform the b.c.c. disordered solid solution, which is stable above about 800 °C, first into the FeAl phase with a B2 structure, which is stable between about 800 °C and 550 °C and which is the subject of Sec. 5.3, and then into Fe_3Al with the $D0_3$ structure (see Fig. 1). The critical temperature of ordering is much lower than the melting temperature (Massalski et al., 1990) which indicates less strong bonding between unlike atoms compared with, e.g. the nickel aluminides. The ordering process and its kinetics have been studied in detail both experimentally and theoretically for the determination of the field of existence and the equilibria of Fe_3Al in the Fe–Al phase diagram (see, e.g. Köster and Gödecke, 1980; Gödecke and Köster, 1985; Wachtel and Bahle, 1987; Inden and Pepperhoff, 1990; Vennégues et al., 1990; Maziasz et al., 1993; chapter by Inden and Pitsch in Volume 5 of MST). Recently a transient B32 phase has been observed during ordering (Gao and Fultz, 1993). On the Fe-rich side there is a two-phase equilibrium between Fe_3Al and b.c.c. Fe–Al solid solution which shows short-range order. On the Al-rich side there is a second order transition from Fe_3Al with a $D0_3$ structure to FeAl with a B2 structure without a two-phase equilibrium. The generally accepted phase diagram with the $D0_3$/B2 transition has been questioned recently on the basis of neutron scattering results (Hilfrich et al., 1991) which, however, are not unambiguous (Inden, 1993). The critical temperature of ordering, which is about 550 °C in the binary case (Massalski et al., 1990), can be shifted to higher temperatures by as much as 250 °C by alloying with a third element, in particular Cr, Mo, Mn, Ti, or Si (Mendiratta and Lipsitt, 1985; Fortnum and Mikkola, 1987; Longworth and Mikkola, 1987; Prakash et al., 1993).

Thermal vacancies are formed readily because of a low formation entropy,

ArcelorMittal Ex. 2038
Page 98 of 190

which is even lower than the migration enthalpy, and consequently there is a high thermal-equilibrium vacancy concentration in contrast to e.g. Ni_3Al and pure metals (Schaefer et al., 1990, 1992). The resulting activation energy of diffusion, which has been determined by studying the ordering kinetics, varies strongly with the Al content (Vennégues et al., 1990). The diffusion coefficients for B, Ni, V, and Ti in Fe_3Al with a $D0_3$ or a B2 structure have been determined recently (Hasaka et al., 1993a, b).

Fe_3Al exhibits an outstanding, high magnetic permeability which makes it useful as a magnetic material (Nachman and Buehler, 1954). The magnetic behavior can still be improved by partial substitution of Al by Si, which does not change the crystal structure. This gave rise to the development of the Sendust alloys which are based on $Fe_3(Al,Si)$ and which have found widespread use as magnetic head materials in recorders (Yamamoto and Utsushikawa, 1977; Yamamoto, 1980; Watanabe et al., 1984; Brock, 1986).

Besides this application as a functional material, Fe_3Al is now also being considered for structural applications since it not only shows a higher strength than comparable iron alloys, but also a high corrosion resistance in oxidizing and sulfidizing environments (McKamey et al., 1991). Problems for application are the low ductility at ambient temperatures and the strength drop above the ordering temperature.

The plastic deformation, including twinning, of Fe_3Al and the effect of atomic order on strength and ductility has been studied in detail (Marcinkowski and Brown, 1961; Stoloff and Davies, 1964, 1966; Morgand et al., 1968; Leamy and Kayser, 1969; Marcinkowski, 1974a; Hanada et al., 1981a, b; Park et al., 1991; Ehlers and Mendiratta, 1984; Schröer et al., 1991; Shindo et al., 1991). Ductility depends sensitively on prior processing (McKamey and Pierce, 1993), and plastic deformation may reduce the degree of long-range order (Dadras and Morris, 1993). A special feature is the anomalous temperature dependence of the flow stress, which reaches a maximum slightly below the ordering temperature because of partial disorder. This behavior is thought to be due to the decrease in order, as in the case of FeCo which has been discussed in Sec. 4.4.4. However, new results have shown that the yield stress anomaly is a result of the complex temperature dependence of the dislocation mobilities (Schröer et al., 1993). Dislocation line energies and line tensions as well as elastic moduli have been determined for both Fe_3Al and $Fe_3(Al,Si)$ (Kötter et al., 1989). Plastic deformation of Fe_3Al under special experimental conditions gives rise to pseudoelasticity and a shape memory effect (Kubin et al., 1982; Nosova et al., 1986).

Fe_3Al has been alloyed successfully with Ni and Cr to improve the ductility (Horton et al., 1984; Morris et al., 1993a). Good combinations of strength and ductility have been obtained by thermomechanical treatments which resulted in large amounts of B2 phase (Sun et al., 1993). If the alloying additions surpass the solubility limits, precipitation of second phases, e.g. a Heusler-type phase with a cubic $L2_1$ structure or a Laves phase with a hexagonal C14 structure, occur which may be used for improving the strength of Fe_3Al (Dimiduk et al., 1988; Ranganath et al., 1991; Maziasz and McKamey, 1992). The respective Fe–Al–Ni alloys are closely related to the NiAl-based Ni–Fe–Al alloys which have been addressed in Sec. 4.3.6 (under the heading Structural Alloys) and which have given rise to corresponding materials developments.

ArcelorMittal Ex. 2038
Page 99 of 190

In view of structural applications, Fe_3Al has been studied with respect to creep (Lawley et al., 1960; Davies, 1963a; Prakash et al., 1991b), fatigue (Fuchs and Stoloff, 1988; Prakash et al., 1991b; Castagna and Stoloff, 1992; Stoloff et al., 1993), fracture (Sainfort et al., 1963; Horton et al., 1984; Mendiratta et al., 1987a; Shan and Lin, 1992), and oxidation resistance, including Fe_3Al-based alloys and composites (Cathcart, 1985; DeVan, 1989; Tortorelli and DeVan, 1992; Nourbakhsh et al., 1993). The ductility of Fe_3Al is a very sensitive function of the environment, i.e. Fe_3Al is subject to environmental embrittlement which is due to the presence of moisture in the surrounding atmosphere (McKamey and Liu, 1990; Kasul and Heldt, 1991; McKamey et al., 1991; Sanders et al., 1991; Liu, 1992; Hippsley and Strangwood, 1992; Shan and Lin, 1992; Vyas et al., 1992; Lin et al., 1992; Castagna et al., 1993; Stoloff and Duquette, 1993). Even very low partial pressures of water vapor are sufficient for embrittlement (McKamey and Lee, 1993). These embrittling effects are absent only for such low Al contents that $D0_3$ long-range ordering no longer occurs (Sikka et al., 1993b). In spite of the mentioned shortcomings of Fe_3Al, this iron aluminide is of great industrial interest, and various alloy developments have been initiated which rely on composition optimization and thermomechanical treatments for improving the mechanical behavior (Liu et al., 1990; Esslinger and Smarsly, 1991; Baker and George, 1992; Liu and Kumar, 1993; Viswanathan et al., 1993; Sikka et al., 1993a). Recently an Fe_3Al matrix composite with reinforcing Al_2O_3 dispersoids has been produced with good strength and oxidation resistance, and with sufficient ductility (Suganuma, 1993).

As to processing, both powder metallurgy and ingot metallurgy – including arc melting, vaccum-arc remelting, induction melting in air and vacuum, and electroslag remelting – have been studied (Sanders et al., 1991; Sikka et al., 1991, 1993a; Sikka, 1991; Gieseke et al., 1993). These developments aim at applications as automotive exhaust systems and resistance heating elements, which are close to commercialization. Other potential applications are steam turbine discs and superheater tubes in power plants, hot gas filters in coal gasification plants, and chemical processing equipment. Recently combustion synthesis of Fe_3Al, which has been used to join SiC composites, has been proposed for coating structural steels in view of the corrosion and wear resistance of Fe_3Al (Wright et al., 1993).

5.2 Fe_3AlC_x and Related Phases

The dissolution of carbon in Fe_3Al produces the so-called K phase which is usually given as Fe_3AlC_x with $x \approx 0.66$ for simplicity (Huetter and Stadelmaier, 1958; Goldschmidt, 1967a, 1969; Nowotny, 1972b) though it shows an extended range of homogeneity corresponding to $Fe_{3-y}Al_{1+y}C_x$ with $-0.2 < y < +0.2$ and $0.42 < x < 0.71$ (Andryushchenko et al., 1985; Palm, 1990). Its crystal structure $L'1_2$ is related to the $L1_2$ structure of Ni_3Al since the Fe and Al atoms occupy the sites of an $L1_2$ sublattice in this phase, whereas the C atoms occupy the centers of the $L1_2$ unit cells (see Fig. 1). Thus it may be regarded as an intermetallic $L1_2$ phase which is stabilized by the interstitial C. On the other hand, it is an interstitial compound and is usually regarded as a complex carbide with a crystal structure corresponding to the perovskite-type structure $E2_1$ (with $x=1$). Fe_3AlC_x is hard and brit-

ArcelorMittal Ex. 2038
Page 100 of 190

tle, it has an appreciable range of homogeneity, tranformations are not known, and – in contrast to Morral (1934), and Huetter and Stadelmaier (1958) – it is not ferromagnetic (Löhberg and Schmidt, 1938; Parker et al., 1988).

The Fe-rich corner of the Fe–Al–C phase diagram has been studied recently in order to clarify the phase equilibria of Fe_3AlC_x with the Fe solid solution on the one hand and with the graphite on the other (Palm, 1990). It was found that Fe_3AlC_x melts at about 1400 °C depending on its composition, and its field of existence in the ternary phase diagram is shifted to higher C contents with decreasing temperature which makes the preparation of monophase Fe_3AlC_x difficult.

Other recent work has been directed at the mechanical behavior of Fe_3AlC_x (Jung and Sauthoff, 1989b; Wunnike-Sanders, 1993). It can be shown that the deformation behavior of Fe_3AlC_x corresponds to that of Ni_3Al with dissolved C, which is expected because of the structural similarity. The variation of the C content of Fe_3AlC_x leads to the precipitation of either α-Fe or graphite, which both affect the deformation behavior, i.e. flow stress, causing the creep resistance and the brittle-to-ductile transition temperature to increase in the sequence $Fe_3AlC_x + \alpha$-Fe, Fe_3AlC_x, Fe_3AlC_x + graphite. Thus there are some prospects for alloy development by optimizing composition and phase distribution. The fracture toughness increases with increasing deformation rate, which indicates the presence of environmental embrittlement (Vehoff, 1993).

Finally, it is noted that such perovskite-type phases are also formed in other alloy systems by alloying with carbon as well as with oxygen, and that such phases are considered for strengthening intermetallic alloys (Goldschmidt, 1967a; Nowotny, 1972b; Kassem and Koch, 1991; Ellner et al., 1992; Nemoto et al., 1992). Recently multiphase Co–Co_3AlC alloys have been prepared with good combinations of strength and ductility (Hosoda et al., 1993).

5.3 FeAl

FeAl is closely related to NiAl (Sec. 4.3) since both phases show the B2 structure and complete mutual miscibility (Bradley and Taylor, 1938; Bradley, 1951; Baker and Munroe, 1990). However, FeAl melts incongruently in contrast to NiAl, and its melting temperature is lower, which indicates lower stability and atomic bonding strength. The binary Fe–Al phase diagram and the phase equilibrium with Fe_3Al have already been addressed in Sec. 5.1. It has to be noted that a subdivision of the field of existence for the B2 phase in the binary Fe–Al phase diagram was proposed according to observed changes in the physical properties (Köster and Gödecke, 1980; Gödecke and Köster, 1985, 1986). However, these changes are not related to changes in crystal symmetry or atomic order, and thus the understanding of this subdivision of the B2 phase field is still unclear.

FeAl has been studied in detail with respect to density (Baker and George, 1992), elastic behavior – both experimentally and theoretically by quantum-mechanical, ab initio calculations (Marcinkowski, 1974a; Harmouche and Wolfenden, 1985, 1986; Gödecke and Köster, 1986; Fu and Yoo, 1991, 1992a; Yoo and Fu, 1991), point defects (Paris et al., 1975; Ho and Dodd, 1978; Koch and Koenig, 1986) and diffusion (Hagel, 1967; Cheng and Dayananda, 1979; Akuezue and Whittle, 1983; Bakker, 1984; Vogl and Sepiol, 1994). Most work on FeAl has been directed at the mechanical behavior and in particular, at the

ArcelorMittal Ex. 2038
Page 101 of 190

strength and ductility (Sainfort et al., 1963; Morgand et al., 1968; Marcinkowski, 1974a; Crimp et al., 1987; Baker and Munroe, 1990; Baker et al., 1991; Lefort et al., 1991; Nagpal and Baker, 1991; Prakash et al., 1991b; Tassa et al., 1991; Baker and Nagpal, 1993), and special attention has been paid to the analysis of dislocation behavior (Strutt and Dodd, 1970; Marcinkowski, 1974a; Umakoshi and Yamaguchi, 1980; Mendiratta et al., 1984; Rudy and Sauthoff, 1986; Mendiratta and Law, 1987; Feng and Sadananda, 1990; Munroe and Baker, 1991; Takahashi and Umakoshi, 1991). In particular, ⟨100⟩ slip, which is characteristic for NiAl, has been reported only at high temperatures, whereas ⟨111⟩ slip has been observed at lower temperatures with a transition temperature that increases with decreasing Al content (Yamagata and Yoshida, 1973; Umakoshi and Yamaguchi, 1980, 1981; Mendiratta et al., 1984). The ⟨100⟩ dislocations are perfect single dislocations, whereas the ⟨111⟩ dislocations are superlattice dislocations consisting of two partial dislocations with an antiphase boundary (APB) in between. The APB energy, which contributes to the superlattice dislocation energy, decreases with decreasing Al content according to quantum-mechanical, ab initio calculations (Freeman et al., 1991). The transition from ⟨111⟩ slip to ⟨100⟩ is correlated with a yield strength peak and a ductility drop at about 450 °C for off-stoichiometric FeAl (Xiao and Baker, 1993; Guo et al., 1993; Yoshimi and Hanada, 1993).

It is noted that strength and hardness at low temperatures do not reach a minimum at the stoichiometric composition, which is in contrast to the behavior of the isomorphous phases NiAl and CoAl (see Sec. 4.3.3), and which is not yet understood (Westbrook, 1956; Crimp and Vedula, 1991). Recently it has been found that the room temperature hardness increases with increasing vacancy concentration, and the latter increases with increasing Al content through the stoichiometric composition (Chang et al., 1993). The vacancy formation energy is low with a strong tendency for vacancy clustering according to theoretical ab initio calculations (Fu et al., 1993a).

Single-crystalline FeAl shows some ductility in compression at low temperatures whereas the tensile ductility is not known (Yamagata and Yoshida, 1973; Baker and Munroe, 1990). The tensile ductility at low temperatures, as well as the compressive ductility, of polycrystalline FeAl is practically nil at the stoichiometric composition – which again is in contrast to NiAl – and it increases with decreasing Al content, i.e. increasing deviation from stoichiometry (Baker and Gaydosh, 1987; Mendiratta et al., 1987b; Schmidt et al., 1989). It has to be emphasized that the reported ductilities of off-stoichiometric FeAl are obtained only with well-annealed specimens, i.e. if the low-temperature deformation is preceded by anneals with very low cooling rates (Schmidt et al., 1989; Nagpal and Baker, 1990a). This behavior is supposed to be due to retained excess vacancies which increase the hardness and yield strength and decrease the ductility, and which are not equilibrated after high-temperature anneals with normal cooling rates (Schmidt et al., 1989; Nagpal and Baker, 1990a; Crimp and Vedula, 1991; Kong and Munroe, 1993; Baker and Nagpal, 1993). Vacancy equilibration seems to be a very slow process and thus anneals of several hundred hours at about 400 °C are recommended for producing ductility in off-stoichiometric FeAl (Nagpal and Baker, 1990a).

ArcelorMittal Ex. 2038
Page 102 of 190

In view of the similarities and differences between FeAl and NiAl, the question again arises in what way the strength and character of atomic bonding changes with composition, and in what way such changes are correlated with the observed changes in the mechanical behavior. However, in spite of the much improved knowledge and understanding of the electronic distribution in these B2 aluminides simple correlations between strength and character of bonding and mechanical behavior are not visible (Schultz and Davenport, 1992), which means that there may be no such simple correlations.

FeAl has been alloyed with various elements to improve the mechanical behavior (see e.g., Munroe and Baker, 1990; Lefort et al., 1991; Prakash et al., 1991 a, b; D. Li et al., 1993). Alloying with Ni has initiated promising alloy developments which have been discussed in Sec. 4.3.6. It is noted that the above-mentioned transition from ⟨111⟩ slip to ⟨100⟩ slip at elevated temperatures is also effected by alloying with Ni (Patrick et al., 1991). Microalloying with B increases the strength and toughness of FeAl significantly, whereas the brittle-to-ductile transition temperature is reduced only slightly (Crimp and Vedula, 1986; Webb et al., 1993 b; Schneibel et al., 1993 b; Baker, 1993).

FeAl is subject to environmental embrittlement, i.e. its ductility depends sensitively on the test environment (Liu and George, 1991; Liu et al., 1991; Lynch et al., 1991; Shea et al., 1991; Klein and Baker, 1992; Schneibel and Jenkins, 1993; Nagpal and Baker, 1991; Klein et al., 1993). This embrittling effect is due to the dissolution of hydrogen in FeAl at the crack tip and is reduced by increasing the deformation rate sufficiently (Nagpal and Baker, 1991; Liu and George, 1991; Liu et al., 1991; Lynch et al., 1991; Shea et al., 1991; Klein and Baker, 1992; Schneibel and Jenkins, 1993; Schneibel et al., 1993 b). Dispersoids have been used successfully for strengthening FeAl and respective developments of particulate composites have been initiated (see, e.g. Mendiratta et al., 1987 b; Moser et al., 1990; Decamps et al., 1991; Kumar, 1991; Prakash et al., 1991 b; Baker and George, 1992; Schneibel et al., 1992 b; Xu et al., 1993).

Apart from strength and ductility, FeAl has been studied with respect to creep, which has been discussed together with NiAl in Sec. 4.3.4, fracture – both experimentally and theoretically by quantum-mechanical, ab initio calculations – (Baker and Gaydosh, 1987; Baker et al., 1991; K. M. Chang et al., 1992; Prakash et al., 1992; Yoo and Fu, 1992; Schneibel and Jenkins, 1993), fatigue (Prakash et al., 1991 b; Stoloff, 1992), and corrosion which is oxidation in most cases (Cathcart, 1985; Schmidt et al., 1989; Smialek et al., 1989, 1990 a; Nesbitt and Lowell, 1993). In view of the reported advantageous properties and the comparatively low density, FeAl is regarded as potential structural material for high temperature applications and respective processing developments are making use of both ingot metallurgy and powder metallurgy (Stephens, 1985; Vedula et al., 1985; Vedula and Stephens, 1987 a, b; Vedula, 1989, 1991; Liu and Kumar, 1993). The published results are quite promising and FeAl alloy compositions have been identified, e.g. for good weldability (Maziasz et al., 1992) and for high corrosion and wear resistance in aggressive gasification environments (Magnee et al., 1991).

ArcelorMittal Ex. 2038
Page 103 of 190

Intermetallics
Gerhard Sauthoff
copyright © VCH Verlagsgesellschaft mbH, 1995

6 Cu-Base Phases

Various intermetallic Cu-base phases have been and are major constituents of many Cu-base alloys – in particular bronzes, i.e. Cu–Sn alloys, and brasses, i.e. Cu–Zn alloys – which have been in use since the beginning of metallurgy (Gmelin-Institut, 1955; Westbrook, 1977; Flinn, 1986), and examples are given in Table 1. Various Cu–Sn and Cu–Zn phases have been reviewed with respect to their basic properties (Schubert, 1967; Dwight, 1967; Guillet and Le Roux, 1967; Hagel, 1967). Alloying with a third element results in a still larger multitude of phases. An outstanding example is given by the Heusler-type phases Cu_2MnAl and Cu_2MnSn with an $L2_1$ structure (see Fig. 1), which are ferromagnetic though the constituent metals are not ferromagnetic (Dwight, 1967; Kouvel, 1967). It is noted that Cu_2MnAl-base alloys were used for applications as fruit knives at the beginning of this century (Heusler, 1989) – see Table 1. Another similar Cu phase is Ni_2CuSn with an $L2_1$ or a $D0_3$ structure which is considered for structural applications (Kratochvil, 1990; Kratochvil et al., 1992).

Some of these binary and ternary phases have been studied to a larger extent because of special physical and/or mechanical properties. Of particular interest are the Cu phases CuZn, $Cu_{\approx 1+1.3x}Zn_{\approx 1-2.3x}Al_x$, and $(Cu,Ni)_3Al$, on which the Cu–Zn–Al and Cu–Al–Ni shape memory alloys are based and which are the subject of the following sections. In addition, the Cu–Au phases Cu_3Au and CuAu and the Cu–Sn phases Cu_3Sn and Cu_6Sn_5 will be addressed, which are important constituents of Cu–Au alloys and amalgams for dental restorative applications.

6.1 CuZn

The major or exclusive constituent of yellow brass is β brass which is the intermetallic CuZn phase. It exhibits an A2 structure at high temperatures and a B2 structure at low temperatures, i.e. there is an order–disorder transition at about 460 °C (Flinn, 1986; Massalski et al., 1990). Its range of homogeneity – between about 40 and 50 at.% Zn at higher temperatures – depends sensitively on temperature and does not include the stoichiometric 50 at.% composition at intermediate temperatures. This order–disorder transition has been used to study the effect of ordering, e.g. on elastic behavior (Westbrook, 1960a; Guillet and Le Roux, 1967), diffusion (Girifalco, 1964; Hagel, 1967; Wever et al., 1989; Wever, 1992), recrystallization (Cahn, 1991), and hardness (Westbrook, 1960a).

The deformation behavior of B2 CuZn has been analyzed in detail with respect to the operating slip mechanism (Rachinger and Cottrell, 1956; Fleischer, 1988; Baker and Munroe, 1990), and the dislocation energies and the antiphase boundary energies which control the slip characteristics have been determined (Marcinkowski, 1974a; Beauchamp et al., 1992; Beauchamp and Dirras, 1993). A special feature of the deformation behavior is the anomalous positive temperature dependence of the yield stress which is also known for other intermetallics. It has to be noted that the case of CuZn was the first to be observed and analyzed which led to the understanding of the variation of yield stress with degree of long-range order (Brown, 1959; Saka et al., 1985; Dirras et al., 1992; Matsumoto and Saka, 1993). With increasing temperature the degree of order decreases continuously until the critical temperature of disordering is reached and

ArcelorMittal Ex. 2038
Page 104 of 190

the second-order transition from B2 order to A2 disorder occurs. Correspondingly, the yield stress reaches a maximum below the critical temperature of disordering. Apart from yielding, creep has been studied in detail (Westbrook, 1960a; Stoloff and Davies, 1966; Strutt and Dodd, 1970; Delobelle and Oytana, 1983; Hong and Weertman, 1986), as well as hot deformation processing (Padmavardhani and Prasad, 1991), and cyclic deformation (Kawazoe et al., 1989).

Besides the order–disorder transition, CuZn in the B2 state can transform martensitically after sufficiently rapid cooling (Ahlers, 1986). Various types of martensite, which differ by the stacking sequence of the close-packed lattice planes, can be formed depending on composition, i.e. electron concentration. It is noted that this martensitic transformation is related to an exceptionally low value of the elastic shear constant which additionally shows an anomalous, positive temperature dependence (Verlinden and Delaey, 1988a). The martensitic transformation of B2 ordered CuZn can be induced by external elastic stress which gives rise to a shape memory effect for not too small grain sizes (Schroeder et al., 1976). The characteristics of such shape memory alloys have been discussed in detail with respect to crystallography, microstructure, thermodynamics, kinetics and macroscopic mechanical behavior, and applications have been described (Delaey et al., 1974; Krishnan et al., 1974; Warlimont et al., 1974; Ahlers, 1986; Van Humbeek and Delaey, 1989; Hornbogen, 1991).

6.2 Cu-Zn-Al Shape Memory Alloys

The Cu-Zn-Al shape memory alloys are derived from the B2 CuZn phase by alloying with Al, and the composition of the resulting ternary phases is approximately described by $Cu_{1+1.3x}Zn_{1-2.3x}Al_x$ (Van Humbeek and Delaey, 1989; Hodgson, 1990). The complete ternary Cu-Zn-Al phase diagram was given in Guertler et al. (1969). The crystal structure of this Cu-Zn-Al phase is the disordered A2 structure at high temperatures which transforms to the B2 structure by nearest neighbors ordering on cooling and to the $L2_1$ structure by next-nearst neighbors ordering on further cooling (Ahlers, 1986; Wu and Wayman, 1991). It has to be emphasized that these structures are stable only at elevated temperatures whereas at room temperature they are only metastable, i.e. these alloys decompose if annealed at too low temperatures.

The $L2_1$ phase can be transformed martensitically to form various types of martensite which differ by the stacking sequence of the close-packed crystallographic planes (Ahlers, 1986). The crystallography and thermodynamic stability of the martensite variants have been analyzed in detail (Bidaux and Ahlers, 1992; Ahlers and Pelegrina, 1992; Pelegrina and Ahlers, 1992a, b; Saule et al., 1992). The martensite stability is correlated with elastic anomalies, as in the case of CuZn (Verlinden and Delaey, 1988b). It can be shown that different types of martensite can coexist at certain compositions (Segui et al., 1991). In any case, the martensite formation temperature is a very sensitive function of the composition (Van Humbeek and Delaey, 1989; Hodgson, 1990), and can be varied by prior thermal cycling (Tadaki et al., 1987). In particular, alloying with Mn is used to depress the martensite formation temperature.

As already mentioned for CuZn, the characteristics of such shape memory alloys have been discussed in detail with respect to crystallography, microstructure,

ArcelorMittal Ex. 2038
Page 105 of 190

thermodynamics, kinetics, and macroscopic mechanical behavior (Delaey et al., 1974; Krishnan et al., 1974; Warlimont et al., 1974; Ahlers, 1986; Van Humbeek and Delaey, 1989; Hornbogen, 1991). A special feature of the Cu-Zn-Al alloys is the so-called two-way memory effect which produces a reversible shape change on cooling and heating (Stalmans et al., 1992a, b, c). This effect results from martensite transformation and retransformation after specific thermomechanical treatments which are designated as "training".

The processing of Cu-Zn-Al alloys poses few problems (Hodgson, 1990). The alloys are usually produced by induction melting. Various dopants are in use for grain refinement to improve formability (Lee and Wayman, 1986). Apart from this, powder metallurgy is used for obtaining fine-grained materials. The alloys are readily hot worked in air and the cold workability decreases with increasing Al content. Applications have been described (e.g. by Hodgson, 1990; Hornbogen, 1991).

6.3 Cu-Al-Ni Shape Memory Alloys

The Cu-Al-Ni shape memory alloys are based on the intermetallic phase Cu_3Al with a disordered A2 structure, which is usually known as the β phase, and which is stable only at high temperatures between 567 and 1049 °C with compositions between 71 and 82 at.% Cu (Murray, 1985). At 567 °C this phase decomposes by a eutectoid reaction at such a sluggish rate that it can be retained with the then metastable A2 structure by cooling below this temperature. At about 500 °C the β phase undergoes an ordering reaction to form the metastable β_1 phase with a DO_3 structure. Both phases can be transformed martensitically by quenching to form various types of martensite depending on the Al content and the quench rate (Murray, 1985).

Cu_3Al can be alloyed with Ni without changing the transformation characteristics of this phase (see Guertler et al., 1969 for the ternary Cu-Al-Ni phase diagram). Both binary Cu_3Al and ternary $(Cu,Ni)_3Al$ show the shape memory effect due to thermoelastic martensite formation (Otsuka and Shimizu, 1970; Nagasawa and Kawachi, 1971; Delaey et al., 1974). This ternary phase has given rise to the development of the Cu-Al-Ni shape memory alloys with about 11–15 wt.% Al and 3–5 wt.% Ni (Van Humbeek and Delaey, 1989; Hodgson, 1990). The crystallography of martensite formation has been discussed recently in detail for Cu-Al-Ni alloys (Shimizu and Tadaki, 1992), and likewise the thermodynamics and kinetics have been studied (Warlimont et al., 1974; Zhou and Hsu, 1991; Ortin et al., 1992). The deformation modes of the martensites include various twinning modes and stress-induced transformations (Ichinose et al., 1991). The shape memory effect is a two-way effect, i.e. it is completely reversible (Sakamoto et al., 1991). The martensite start temperature has an upper limit of about 180 °C and can be lowered to a large degree by increasing the Al content, and to a smaller degree by increasing the Ni content (Van Humbeek and Delaey, 1989; Hodgson, 1990).

The Cu-Al-Ni alloys are advantageous because of their higher stability at higher temperatures compared with the Cu-Zn-Al alloys. However, second-phase precipitation cannot be suppressed and embrittles the Cu-Al-Ni alloys and precludes cold working, i.e. such alloys can only be hot finished (Van Humbeek and Delaey, 1989; Hodgson, 1990). Thermomechanical treatments and microalloying additions – in particular Mn, Ti, and Zr – are used for

ArcelorMittal Ex. 2038
Page 106 of 190

improving the mechanical behavior. An important effect is grain refinement, which increases both the fracture strength and the fracture strain according to a Hall–Petch relationship (Roh et al., 1991). Indeed precipitated particles have been found to reduce the as-cast grain size and hinder later grain growth during annealing (Ratchev et al., 1993). The alloying additions affect the transformation and decomposition behavior which is to be considered for establishing the optimum conditions for the induction of the two-way effect (Eucken et al., 1991; Hornbogen and Kobus, 1992). Recently the ductilizing effect of small boron additions has been found, which has been studied in detail with respect to transformation behavior and microstructure (M. A. Morris, 1991 b, 1992). Finally it is noted that there are other similar Cu-base alloys which also show the shape memory effect (Delaey et al., 1974). A well-studied example is given by the Cu-Al-Mn shape memory alloys which order by a two-step reaction on rapid cooling, i.e. the initial, disordered A2 structure is transformed first to the intermediate B2 structure and then to the final $L2_1$ structure (Guilemany and Peregrin, 1992; Prado et al., 1993).

6.4 Cu-Au Phases

The Cu-Au system is the classic textbook example for discussing ordering reactions in solid solutions and the effects of atomic order on properties (see, e.g., Schulze, 1967; Honeycombe, 1968). At higher temperatures above 410 °C the Cu-Au alloys form the disordered A1 structure with complete mutual solid-solubility of Cu and Au, whereas at lower temperatures ordering reactions occur which produce various intermetallic phases, depending on temperature and composition, with broad ranges of homogeneity (Okamoto et al., 1987). On the Cu-rich side there is the well-known phase Cu_3Al with an $L1_2$ structure, which is the prototype phase for this crystal structure and which is designated Cu_3Au I. The phase Cu_3Au II forms at intermediate temperatures with off-stoichiometric compositions and is described as either tetragonal or orthorhombic. In any case, the Cu_3Au II structure results from the $L1_2$ structure by the introduction of equally spaced antiphase boundaries (APBs). Such a structure is usually known as a long-period superlattice (LPS). At the equiatomic composition the tetragonal $L1_0$ phase CuAu I forms, and again an orthorhombic LPS is observed at intermediate temperatures, which is known as CuAu II. The Au-rich phase Au_3Cu shows the $L1_2$ structure as Cu_3Au. All phases are separated from each other by two-phase equilibria.

The elastic behavior is known (Guillet and Le Roux, 1967) as well as the diffusion behavior (Wever et al., 1989; Wever, 1992) and vacancy formation (Schaefer et al., 1992). The deformation behavior of Cu_3Au was studied in detail to clarify the effects of atomic order, and it was found in particular that order decreases the yield stress and increases the work hardening rate, with still high ductility (Sachs and Weerts, 1931; Vidoz et al., 1963; Stoloff and Davies, 1966). Inversely, strong cold deformation destroys the order, as was observed for various phases with ordering reactions (Dahl, 1936). The ordering reaction produces antiphase domains which give rise to an additional strengthening effect in this and similar phases, with strength increasing with decreasing domain size (Marcinkowski, 1974a). The domain size can be varied by prior processing, and it increases during ageing in analogy to Ostwald ripening (Sauthoff, 1973a, b).

ArcelorMittal Ex. 2038
Page 107 of 190

The Portevin–Le Chatelier effect with serrated yielding was observed for both the ordered and disordered state (Mohamed et al., 1974). Recovery and recrystallization have been analyzed in detail (Vidoz et al., 1963; Cahn, 1990, 1991). Experimental and theoretical studies have been directed at dislocations and antiphase domain boundaries (see, e.g. Tichelaar and Schapink, 1991; D. G. Morris, 1992; Veyssière, 1992), grain boundaries (Yan et al., 1992), and the electronic structure (Bose et al., 1991). It is noted that disordered layers are formed in ordered Cu_3Au on antiphase boundaries and twin boundaries just below the order–disorder transition temperature (Tichelaar et al., 1992). This may be expected in other phases, too, and may improve the ductility of less ductile phases, as is discussed for Ni_3Al (see Sec. 4.1.2).

Au-Cu-Ag alloys based on the intermetallic phases CuAu and Cu_3Au have found applications in dentistry because of their extremely high corrosion resistance, their advantageous mechanical properties such as high strength and ductility, and their decorative gold color (Yasuda, 1991). These alloys age-harden as a result of complex ordering and decomposition reactions by which the phases Cu_3Au I, CuAu I, CuAu II, and an Ag-rich α_2 phase are formed, depending on the composition.

6.5 Cu Amalgams

Dental amalgams have been in use for more than a thousand years (Waterstrat, 1990). Amalgams are still a very important class of material for dental restoration, in spite of corrosion problems with mercury release because the amalgams offer an advantageous combination of properties with respect to processing and use (Watts, 1992; Waterstrat and Okabe, 1994). These amalgams are formed by alloying Ag-Sn-Cu alloys based on the phases Ag_3Sn and Cu_3Sn, with mercury. The amalgamation reaction results in the formation of a complex multiphase alloy structure which contains the phases Ag_2Hg_3, Sn_8Hg, Ag_3Sn, and Cu_6Sn_5, depending on the composition.

The processing with mixing and compaction of powders is comparatively simple and is analogous to mechanical alloying. The amalgams must show sufficient compressive strength and creep resistance since the oral temperature is only about 10% below the melting temperature. The dental amalgams are very brittle, which leads to failure with tensile or bending stresses in unsupported regions. The fracture processes are correlated with corrosion processes which primarily attack the phases Sn_8Hg and Cu_6Sn_5 and lead to the release of mercury and SnO, respectively. Attempts to substitute for mercury in these amalgams have not yet been successful.

7 A15 Phases

7.1 Basic Properties

The A15 crystal structure is a complex, cubic structure derived from the b.c.c. lattice (A2) with 8 atoms per unit cell (Pearson, 1958). It is a typical example of the topologically close-packed (tcp) structures which result from the stacking of polyhedra of various shapes to accommodate atoms of different sizes (Sinha, 1973; Watson and Bennet, 1984; Gladyshevskii and Bodak, 1994). These tcp structures allow a closer packing of atoms of different sizes than the geometrically close-packed f.c.c. (A1) and h.c.p. (A3) structures. The A15 structure may be regarded as the basis of the family of tcp structures since the other

ArcelorMittal Ex. 2038
Page 108 of 190

Intermetallics
Gerhard Sauthoff
copyright © VCH Verlagsgesellschaft mbH, 1995

The Portevin–Le Chatelier effect with serrated yielding was observed for both the ordered and disordered state (Mohamed et al., 1974). Recovery and recrystallization have been analyzed in detail (Vidoz et al., 1963; Cahn, 1990, 1991). Experimental and theoretical studies have been directed at dislocations and antiphase domain boundaries (see, e.g. Tichelaar and Schapink, 1991; D. G. Morris, 1992; Veyssière, 1992), grain boundaries (Yan et al., 1992), and the electronic structure (Bose et al., 1991). It is noted that disordered layers are formed in ordered Cu_3Au on antiphase boundaries and twin boundaries just below the order–disorder transition temperature (Tichelaar et al., 1992). This may be expected in other phases, too, and may improve the ductility of less ductile phases, as is discussed for Ni_3Al (see Sec. 4.1.2).

Au-Cu-Ag alloys based on the intermetallic phases CuAu and Cu_3Au have found applications in dentistry because of their extremely high corrosion resistance, their advantageous mechanical properties such as high strength and ductility, and their decorative gold color (Yasuda, 1991). These alloys age-harden as a result of complex ordering and decomposition reactions by which the phases Cu_3Au I, CuAu I, CuAu II, and an Ag-rich α_2 phase are formed, depending on the composition.

6.5 Cu Amalgams

Dental amalgams have been in use for more than a thousand years (Waterstrat, 1990). Amalgams are still a very important class of material for dental restoration, in spite of corrosion problems with mercury release because the amalgams offer an advantageous combination of properties with respect to processing and use (Watts, 1992; Waterstrat and Okabe, 1994). These amalgams are formed by alloying Ag-Sn-Cu alloys based on the phases Ag_3Sn and Cu_3Sn, with mercury. The amalgamation reaction results in the formation of a complex multiphase alloy structure which contains the phases Ag_2Hg_3, Sn_8Hg, Ag_3Sn, and Cu_6Sn_5, depending on the composition.

The processing with mixing and compaction of powders is comparatively simple and is analogous to mechanical alloying. The amalgams must show sufficient compressive strength and creep resistance since the oral temperature is only about 10% below the melting temperature. The dental amalgams are very brittle, which leads to failure with tensile or bending stresses in unsupported regions. The fracture processes are correlated with corrosion processes which primarily attack the phases Sn_8Hg and Cu_6Sn_5 and lead to the release of mercury and SnO, respectively. Attempts to substitute for mercury in these amalgams have not yet been successful.

7 A15 Phases

7.1 Basic Properties

The A15 crystal structure is a complex, cubic structure derived from the b.c.c. lattice (A2) with 8 atoms per unit cell (Pearson, 1958). It is a typical example of the topologically close-packed (tcp) structures which result from the stacking of polyhedra of various shapes to accommodate atoms of different sizes (Sinha, 1973; Watson and Bennet, 1984; Gladyshevskii and Bodak, 1994). These tcp structures allow a closer packing of atoms of different sizes than the geometrically close-packed f.c.c. (A1) and h.c.p. (A3) structures. The A15 structure may be regarded as the basis of the family of tcp structures (Arcelor Mittal Ex. 2038

known tcp structures – in particular the Laves phase structures C14, C15, and C36 (see Sec. 8) – can be derived from the A15 structure by various crystallographic operations (Ye et al., 1985). The intermetallic phases with tcp structures are known as Frank–Kaspar phases.

The phases with A15 structures form a large and comparatively homogeneous group of intermetallic phases (Nevitt, 1967) which have been the subject of fundamental studies, e.g. with respect to electronic structure and phase stability (Turchi and Finel, 1991) or the micromechanisms of diffusion (Bakker and Westerveld, 1988; Bakker et al., 1985, 1992; Wever et al., 1989; Koiwa, 1992; Wever, 1992), twinning (Khantha et al., 1989), and plastic deformation (chapter by Umakoshi in Volume 6 of MST). The A15 phases are of enormous practical importance since many of them are superconductors (B. W. Roberts, 1967; Geballe and Hulm, 1975; Furuto, 1984; Dew-Hughes, 1986; Muller, 1986; Stekly and Gregory, 1994). Some of them, i.e. V_3Ga, V_3Si, Nb_3Al, Nb_3Ga, Nb_3Ge, and Nb_3Sn, exhibit critical temperatures between 15 K and 23 K which are only surpassed by those of the ceramic superconductors based on the perovskite-type oxides (Bednorz and Müller, 1988; Dew-Hughes, 1988; Sharp, 1991); see also the chapter by Clarke and Daumling in Volume 11 of this Series. However, the latter are inferior with respect to critical current density, i.e. the best combination of critical temperatures, critical current density and critical magnetic field strength is found in the A15 superconductors compared with all other superconducting materials.

Recently A15 phases – in particular Nb_3Al and Cr_3Si – have also been considered for applications as structural materials at high temperatures (Shah et al., 1990; Shah and Anton, 1992a; Kamata et al., 1992a, 1993; Suyama et al., 1993). The application of A15 phases as structural or functional materials is handicapped by the brittleness of the A15 phases, which makes processing difficult. In the following, a brief overview is given of those A15 phases which have already been applied, or have been considered for application, and which have been studied in some detail.

7.2 V_3Si

V_3Si was the first A15 phase discovered to be superconducting, with a critical temperature of 17K (Smathers, 1990). Stoichiometric V_3Si melts congruently at 1925 °C and is stable at high and low temperatures (Massalski et al., 1990). A deviation from stoichiometry is possible on the Si-poor side which, however, reduces the critical temperature due to the resulting constitutional disorder. The critical temperature is also reduced by dissolved hydrogen (Stepanov and Skripov, 1982). Likewise the critical current density and the critical field strength are reduced by elastic tensile or compressive straining (Smathers, 1990). Slightly above the critical temperature V_3Si transforms martensitically to a weakly tetragonal, still superconducting phase with twin-related thin lamellae, which is due to lattice softening with vanishing shear modulus (Batterman and Barrett, 1964, 1966; Kondratyev and Pushin, 1985; Mendelson, 1986; Onozuka et al., 1988). Prior plastic deformation with large strains at high temperatures stabilizes the tetragonal martensite even at temperatures above the martensite formation temperature (Ullrich et al., 1978). The martensitic transformation gives rise to superelasticity and a shape memory effect (Zakrevskiy et al., 1986).

V_3Si is hard and brittle, as are all the A15 phases, which makes processing very

ArcelorMittal Ex. 2038
Page 110 of 190

difficult (Fleischer, 1989; Fleischer and Zabala, 1990c). The reason for this is the electronic structure of V_3Si which leads to strong covalent bonding between the nearest neighbor V atoms (Medvedev et al., 1984; Muller, 1986). V_3Si has a high Young's modulus of 213 GPa (Fleischer et al., 1989b) and an apparent brittle-to-ductile transition temperature (BDTT) of the order of 1200 °C (Mahajan et al., 1978; Nghiep et al., 1980). The plastic deformation behavior above the BDTT has been studied in detail and the dislocation slip systems have been analyzed (Levinstein et al., 1966; Bertram and Paufler, 1983; Krämer, 1983; Wright and Bok, 1988; Smith et al., 1993). The creep behavior is characterized by subgrain formation, dislocation climb controlling the creep rate and a comparatively high activation energy in the range of 2–11 eV/atom depending on the stress and the composition (Nghiep et al., 1980). Creep can be enhanced by superimposed electric currents, i.e. there is the so-called electroplastic effect, and thermal gradients, which is proposed to be due to the favorable effect of the electrotransport and thermotransport of point defects on the dislocation mobility (San Martin et al., 1980, 1983).

The transition from superconduction to normal conduction in A15 superconductors occurs by the penetration of small fluxoids, i.e. quantized magnetic flux vortices, which is characteristic for the type II, high-field superconductors (Geballe and Hulm, 1986). These fluxoids can be pinned by microstructural inhomogeneities – in particular grain boundaries and precipitated particles – which is beneficial with respect to critical current density and field strength (Muller, 1986; Smathers, 1990). Consequently, microstructural changes by prior plastic straining with or without recrystallization affect the superconducting properties, depending on the deformation conditions and the composition (Quyen et al., 1979). The thin lamellae, which are produced by the already-mentioned martensitic transformation, are less effective with respect to flux pinning than grain boundaries, i.e. their effect on the superconducting properties becomes relevant only in single crystals (Brand and Webb, 1969).

V_3Si is of interest for applications because of its favorable superconducting properties and its high stability (Smathers, 1990). Apart from hot extrusion, V_3Si can be deformed plastically at room temperature in spite of its brittleness by superimposing a high hydrostatic pressure which makes the production of multifilament, superconducting wires feasible for applications in solenoid magnets (Wright, 1977). Laminar V_3Si can be prepared by solid-state, thin film reactions between V and SiO_2 on Si substrates (Hayashi et al., 1991). However, Nb_3Sn has been found to be more favorable with respect to superconducting properties, mechanical behavior, and processing, which has precluded the use of V_3Si as a magnet material (Smathers, 1990).

Recently V_3Si has become of interest with respect to structural, high-temperature applications (Shah and Anton, 1992a). Combination with a ductile phase, e.g. V-rich solid-solution, offers the possibility of overcoming the brittleness problem, and indeed a directionally-solidified, eutectic V_3Si–V alloy has been successfully prepared (Goldman, 1993). The fracture toughness of V_3Si–V composites with discontinuous V_3Si has been found to increase monotonically with increasing fraction of V and decreasing impurity content (Strum and Henshall, 1993).

ArcelorMittal Ex. 2038
Page 111 of 190

7.3 V_3Ga

V_3Ga with an A15 structure is stable only up to 1300 °C where it transforms congruently to a V–Ga disordered, b.c.c. solid-solution (Massalski et al., 1990). There are indications of a martensitic transformation at very low temperatures, in close analogy to V_3Si, though the conditions for martensite formation are not yet clear for V_3Ga (Nembach et al., 1970; Snead, Jr. and Bussière, 1985). It has a broad range of homogeneity centered on the stoichiometric composition, i.e. it is very stable with respect to deviations from stoichiometry. Because of this stability, which is advantageous for fabrication, and the still high, critical temperature of about 16 K, V_3Ga is of interest for applications (Smathers, 1990).

The superconducting properties and the deformation behavior of V_3Ga are similar to those of V_3Si. The superconducting transition can be affected by prior plastic deformation (Wright and Ho, 1986). V_3Ga is ductile in compression above 1000 °C and the creep behavior has been studied in detail (Soscia and Wright, 1986; Shah and Anton, 1992a). As in the case of V_3Si, V_3Ga can be deformed plastically by hot extrusion and at room temperature by superimposing a high hydrostatic pressure, which makes the production of multifilament, superconducting wires feasible for applications in solenoid magnets (Wright, 1977). Hybrid high-field magnets with V_3Ga tape coils have been produced successfully (Noto et al., 1986). However, Nb_3Sn has been found to be more favorable with respect to superconducting properties, mechanical behavior, and processing which has precluded the commercialization of V_3Ga up to now (Smathers, 1990).

7.4 Nb_3Sn

Nb_3Sn with an A15 structure forms peritectically at 2130 °C from the liquid solution and solid Nb, and is stable only above 775 °C where it decomposes eutectically (Massalski et al., 1990). The decomposition reaction can be suppressed by not too slow cooling, i.e. Nb_3Sn with an A15 structure is maintained at lower temperatures in a metastable condition. Nb_3Sn transforms to a twinned, tetragonal martensite at 43 K (Mailfert et al., 1969; Mendelson, 1986), and the transition to superconductivity occurs at about 18 K (Muller, 1986; Smathers, 1990). This critical temperature is reduced by deviations from stoichiometry, which affect the atomic order, and by elastic strains. Small increases in the critical temperature are possible using ternary alloying additions. The transition temperature does not depend sensitively on prior plastic deformation (Wright and Ho, 1986).

As for the other A15 phases, Nb_3Sn can be deformed readily at high temperatures, e.g. by hot extrusion, whereas deformation at low temperatures is possible only by superimposing a high hydrostatic pressure (Wright, 1977; Eisenstatt and Wright, 1980; Clark and Wright, 1983). The high temperature deformation and creep behavior have been studied in detail and a beneficial effect of grain size reduction on the brittle-to-ductile transition temperature (BDTT) has been found (Clark et al., 1983; Shah and Anton, 1992a).

Nb_3Sn superconductors with multifilamentary geometry, which is needed for electromagnet applications, are easily fabricated by the so-called bronze process, which has led to the wide-spread commercial application of Nb_3Sn (Smathers, 1990). In the bronze process Nb rods are inserted in a bronze rod or tube which is

ArcelorMittal Ex. 2038
Page 112 of 190

then processed to obtain a multifilament wire. At the end of the wire processing, Nb_3Sn shells are formed around the Nb cores by reaction heat treatments. The final multifilament, composite superconductor consists of Nb_3Sn fibers with Nb cores which are embedded in a bronze matrix; the latter is surrounded by a coating of Nb, which serves as a diffusion barrier, and an outer Cu tube, which serves as a stabilizer and carries the current in case of transition to normal conduction. Various specific processing routes, including powder metallurgy routes, have been developed for optimized superconductor production and hybrid superconductor coils are commercially available (Hillman et al., 1980; McDonald, 1984; Gregory, 1984; Noto et al., 1986; Hecker et al., 1988; Smathers, 1990).

The superconducting properties of the composite superconductor, as well as the mechanical properties, depend on the particular microstructure which is a function of the various prior processing steps. Much work has been directed towards the details of the various processes, e.g. the effects of alloying additions (Zwicker et al., 1979), the Sn diffusion during Nb_3Sn formation (Glowacki and Evetts, 1988; Cheng and Verhoeven, 1988), the grain size dependence of the flux pinning force and the tensile strength and fracture at room temperature (Ochiai et al., 1986a, b, 1988; Watari et al., 1986), or the effects of the hardnesses of the constituent phases on the composite workability (Dew-Hughes et al., 1987). Recent new developments rely on the beneficial effects of additions of Ti, Hf, Ta, and/or Ge on the superconducting properties (Kohno et al., 1992; Kamata et al., 1992b; Tachikawa et al., 1992; Murase et al., 1992; Noto et al., 1992).

7.5 Nb_3Al

Nb_3Al with an A15 structure forms peritectically at 2060 °C and is stable below this temperature in the whole temperature range only with Al-deficient, off-stoichiometric compositions (Jorda et al., 1980; Massalski et al., 1990). The stoichiometric composition corresponds to the maximum solubility of Al in Nb_3Al, and is reached only at 1940 °C in eutectic equilibrium with the liquid Nb–Al and the σ phase Nb_2Al. The phase stability is a function of the electronic band structure which has been studied as a function of temperature (Kuzmichev et al., 1983). The formation enthalpy of Nb_3Al is significantly smaller than that of the Al-rich phase Al_3Nb, which has been discussed in Sec. 3.3 (Meschel and Kleppa, 1993). The transition to superconduction occurs at 19 K and there is no martensitic transformation (Smathers, 1990). The transition temperature of Nb_3Al is affected by deviations from stoichiometry and perfect order, as are those of the other A15 phases, but in a less sensitive way. It is noted that the A15 phase with the highest transition temperature is Nb_3Ge, which can be alloyed with Nb_3Al to form the ternary A15 phase $Nb_3(Al_{0.7}Ge_{0.3})$ with the highest critical field strength (Muller, 1986).

Nb_3Al has long been considered for electromagnet applications because of its advantageous superconducting properties (Smathers, 1990). However, the processing of Nb_3Al is very difficult because of the brittleness of Nb_3Al. Powder metallurgy methods have been used successfully for preparing Nb_3Al by reaction synthesis and producing, e.g. an Nb_3Al–Ag composite superconductor (Bowden, 1989; Tsuchida et al., 1989; Schulze et al., 1990). Nb_3Al tapes have been prepared by rapid solidification (Togano et al., 1992). A novel pro-

ArcelorMittal Ex. 2038
Page 113 of 190

cess with thin Nb–Al sandwiches as the starting material has allowed the fabrication of Nb_3Al superconducting wires with good workability (Saito et al., 1990, 1993; Ikeda et al., 1992). Furthermore, various other processes have been used successfully for producing Nb_3Al wires (Noto et al., 1992).

Presently Nb_3Al is also being considered for structural applications at high temperatures in spite of its low-temperature brittleness because of its high stability and strength at high temperatures, and various developments have been initiated (Dimiduk et al., 1991; Anton and Shah, 1991a; Yamaguchi, 1992; Bunk, 1992; Kamata et al., 1993; Suyama et al., 1993). The mechanical properties at low and high temperatures have been determined and the brittle-to-ductile transition has been observed at about 1000 °C (Barth et al., 1992; Shah and Anton, 1992a). At lower temperatures Nb_3Al is inherently brittle according to theoretical ab initio calculations (Kim et al., 1993). The dislocation configurations and slip systems have been analyzed (Aindow et al., 1991; Murayama et al., 1993a–c). The yield stress can be varied by varying the Al content and by alloying with a third element (Fujiwara et al., 1991; Kamata et al., 1992a). The solubilities of third metals in Nb_3Al differ enormously depending on the particular metal, which offers manifold possibilities of alloying (Shah and Anton, 1992a). The diffusion behavior has been studied (Slama and Vignes, 1972), and the oxidation resistance is only poor because of nonprotective scale formation (Shah and Anton 1992a; Tomizuka, 1992; Fujiwara et al., 1993).

A reduction in the Al content below the solubility limit leads to two-phase Nb_3Al–Nb alloys which offer the possibility of relieving the brittleness of Nb_3Al (Anton and Shah, 1990; Marieb et al., 1991; Kumagai et al., 1991; Davidson and Anton, 1993). The brittle-to-ductile transition temperature (BDTT) decreases with increasing volume fraction of the Nb-rich phase, and a brittle-to-ductile transition at room temperature has been obtained for an Nb–16 at.% Al alloy (Suyama and Hashimoto, 1992). The Nb phase toughens the alloy by crack bridging, plastic stretching, and interfacial bonding (Murugesh et al., 1992). However, the fracture toughness controlling, microstructural details are not yet clear (Davidson and Anton, 1993). It is noted that the Nb-rich phase, which usually crystallizes with the b.c.c. A2 structure, may be ordered with a B2 structure due to the presence of interstitial impurities (Marieb et al., 1991). The transformation and precipitation reactions have been studied in detail (Yang and Vasudevan, 1993).

Powder metallurgy methods and infiltration techniques with reaction synthesis result in such two-phase alloys with even higher Al contents because of incomplete reactions (Kumagai et al., 1991; Murayama et al., 1991). Nb–Al alloys with still higher Al contents in the range 25–33 at.% contain the σ phase Nb_2Al, which is also regarded as attractive for high-temperature applications (Bhattacharya et al., 1992). Apart from the above Nb_3Al–Nb alloys, which may be regarded as discontinuously reinforced, in situ composites, Nb_3Al has been considered for use in intermetallic matrix composites which are reinforced by continuous ceramic fibers (Anton, 1988; Shah et al., 1990). Laminated composites have been prepared in situ by high rate sputtering (Rowe and Skelly, 1992). Alloying of Nb_3Al with Ti leads to a ternary phase with a B2 structure (Shyue et al., 1993) which is related to the Ti_3Al-base, super-α_2 alloys of Sec. 3.1.2.

ArcelorMittal Ex. 2038
Page 114 of 190

7.6 Nb_3Si

Nb_3Si is a high-temperature line compound which forms with a tetragonal crystal structure by a peritectic reaction at 1980 °C and is stable only above 1770 °C (Massalski et al., 1990). Rapid solidification of the liquid produces amorphous Nb_3Si (Bertero et al., 1991 a). The A15 structure is unstable and is obtained only by special rapid solidification techniques and by crystallization of amorphous Nb_3Si. Nb_3Si with an A15 structure is of interest because a high transition temperature for superconduction is expected, and indeed a transition temperature of 19 K was reported for near-stoichiometric Nb_3Si with an A15 structure, which was prepared by crystallization of amorphous Nb_3Si under high pressure (Wang et al., 1988). Other crystal structures are obtained for Nb_3Si doped with impurities, i.e. the $L1_2$ structure with oxygen and a hexagonal structure with carbon (Kassem and Koch, 1991). The present interest is directed at Nb–Si in situ composite alloys which contain the Nb_3Si phase and are considered for high-temperature applications (Bertero et al., 1991 a, b; Cockeram et al., 1991, 1992 a, b; Bewlay et al., 1992; Goldman, 1993).

7.7 Cr_3Si

Cr_3Si crystallizes congruently with an A15 structure from the melt and is stable down to very low temperatures with a range of homogeneity which includes the stoichiometric composition (Massalski et al., 1990). Cr_3Si does not exhibit superconduction (Smathers, 1990). However, Cr_3Si has been regarded for a long time as promising for high-temperature applications because of its high creep strength and oxidation resistance (Arbiter, 1953 a, b; Silverman, 1956; Anton and Shah, 1991 b; Dimiduk et al., 1991). The elastic moduli have been determined as well as the temperature dependence of the hardness (Fleischer et al., 1989 b, 1991; Fleischer and Zabala, 1990 c). Compressive ductility has been observed only above 1200 °C and its extent is expected to be limited because of an insufficient number of slip systems (Chang and Pope, 1991). Creep data are available (Shah and Anton, 1991). At lower temperatures Cr_3Si is brittle with a low fracture toughness (Fleischer, 1990; Fleischer et al., 1991). Sufficient oxidation resistance has been observed only below 1200 °C, i.e. below the apparent brittle-to-ductile transition temperature (McKee and Fleischer, 1991). An improved toughness may be obtained with two-phase Cr_3Si–Cr alloys, i.e. by combining the brittle Cr_3Si phase with the Cr-rich solid solution (Mazdiyasni and Miracle, 1990; Newkirk and Sago, 1990; Bewlay et al., 1992). An improved mechanical behavior is also expected for Cr_3Si-based, intermetallic matrix composites, e.g. Cr_3Si–TiC, Cr_3Si–TiB_2, or Cr_3Si–Y_2O_3, for which good bonding and chemical compatibility of matrix and reinforcements have been found (Yang et al., 1990).

8 Laves Phases

8.1 Basic Properties

The Laves phases – sometimes designated as Friauf–Laves phases – with an AB_2 composition in the binary case form a very large group of intermetallics which crystallize with the hexagonal C14 structure, the cubic C15 structure, or the dihexagonal C36 structure (Laves, 1967; Wernick, 1967; Livingston, 1992). These structures are topologically close-packed (tcp) structures (Wernick, 1967; Schulze et al., 1973; Watson and Bennet, 1984), i.e. the Laves

ArcelorMittal Ex. 2038
Page 115 of 190

Intermetallics
Gerhard Sauthoff
copyright © VCH Verlagsgesellschaft mbH, 1995

The Portevin–Le Chatelier effect with serrated yielding was observed for both the ordered and disordered state (Mohamed et al., 1974). Recovery and recrystallization have been analyzed in detail (Vidoz et al., 1963; Cahn, 1990, 1991). Experimental and theoretical studies have been directed at dislocations and antiphase domain boundaries (see, e.g. Tichelaar and Schapink, 1991; D. G. Morris, 1992; Veyssière, 1992), grain boundaries (Yan et al., 1992), and the electronic structure (Bose et al., 1991). It is noted that disordered layers are formed in ordered Cu_3Au on antiphase boundaries and twin boundaries just below the order–disorder transition temperature (Tichelaar et al., 1992). This may be expected in other phases, too, and may improve the ductility of less ductile phases, as is discussed for Ni_3Al (see Sec. 4.1.2).

Au-Cu-Ag alloys based on the intermetallic phases CuAu and Cu_3Au have found applications in dentistry because of their extremely high corrosion resistance, their advantageous mechanical properties such as high strength and ductility, and their decorative gold color (Yasuda, 1991). These alloys age-harden as a result of complex ordering and decomposition reactions by which the phases Cu_3Au I, CuAu I, CuAu II, and an Ag-rich α_2 phase are formed, depending on the composition.

6.5 Cu Amalgams

Dental amalgams have been in use for more than a thousand years (Waterstrat, 1990). Amalgams are still a very important class of material for dental restoration, in spite of corrosion problems with mercury release because the amalgams offer an advantageous combination of properties with respect to processing and use (Watts, 1992; Waterstrat and Okabe, 1994). These amalgams are formed by alloying Ag-Sn-Cu alloys based on the phases Ag_3Sn and Cu_3Sn, with mercury. The amalgamation reaction results in the formation of a complex multiphase alloy structure which contains the phases Ag_2Hg_3, Sn_8Hg, Ag_3Sn, and Cu_6Sn_5, depending on the composition.

The processing with mixing and compaction of powders is comparatively simple and is analogous to mechanical alloying. The amalgams must show sufficient compressive strength and creep resistance since the oral temperature is only about 10% below the melting temperature. The dental amalgams are very brittle, which leads to failure with tensile or bending stresses in unsupported regions. The fracture processes are correlated with corrosion processes which primarily attack the phases Sn_8Hg and Cu_6Sn_5 and lead to the release of mercury and SnO, respectively. Attempts to substitute for mercury in these amalgams have not yet been successful.

7 A15 Phases

7.1 Basic Properties

The A15 crystal structure is a complex, cubic structure derived from the b.c.c. lattice (A2) with 8 atoms per unit cell (Pearson, 1958). It is a typical example of the topologically close-packed (tcp) structures which result from the stacking of polyhedra of various shapes to accommodate atoms of different sizes (Sinha, 1973; Watson and Bennet, 1984; Gladyshevskii and Bodak, 1994). These tcp structures allow a closer packing of atoms of different sizes than the geometrically close-packed f.c.c. (A1) and h.c.p. (A3) structures. The A15 structure may be regarded as the basis of the family of tcp structures (Arcelor Mittal Ex. 2038

known tcp structures – in particular the Laves phase structures C14, C15, and C36 (see Sec. 8) – can be derived from the A15 structure by various crystallographic operations (Ye et al., 1985). The intermetallic phases with tcp structures are known as Frank–Kaspar phases.

The phases with A15 structures form a large and comparatively homogeneous group of intermetallic phases (Nevitt, 1967) which have been the subject of fundamental studies, e.g. with respect to electronic structure and phase stability (Turchi and Finel, 1991) or the micromechanisms of diffusion (Bakker and Westerveld, 1988; Bakker et al., 1985, 1992; Wever et al., 1989; Koiwa, 1992; Wever, 1992), twinning (Khantha et al., 1989), and plastic deformation (chapter by Umakoshi in Volume 6 of MST). The A15 phases are of enormous practical importance since many of them are superconductors (B. W. Roberts, 1967; Geballe and Hulm, 1975; Furuto, 1984; Dew-Hughes, 1986; Muller, 1986; Stekly and Gregory, 1994). Some of them, i.e. V_3Ga, V_3Si, Nb_3Al, Nb_3Ga, Nb_3Ge, and Nb_3Sn, exhibit critical temperatures between 15 K and 23 K which are only surpassed by those of the ceramic superconductors based on the perovskite-type oxides (Bednorz and Müller, 1988; Dew-Hughes, 1988; Sharp, 1991); see also the chapter by Clarke and Daumling in Volume 11 of this Series. However, the latter are inferior with respect to critical current density, i.e. the best combination of critical temperatures, critical current density and critical magnetic field strength is found in the A15 superconductors compared with all other superconducting materials.

Recently A15 phases – in particular Nb_3Al and Cr_3Si – have also been considered for applications as structural materials at high temperatures (Shah et al., 1990; Shah and Anton, 1992a; Kamata et al., 1992a, 1993; Suyama et al., 1993). The application of A15 phases as structural or functional materials is handicapped by the brittleness of the A15 phases, which makes processing difficult. In the following, a brief overview is given of those A15 phases which have already been applied, or have been considered for application, and which have been studied in some detail.

7.2 V_3Si

V_3Si was the first A15 phase discovered to be superconducting, with a critical temperature of 17K (Smathers, 1990). Stoichiometric V_3Si melts congruently at 1925 °C and is stable at high and low temperatures (Massalski et al., 1990). A deviation from stoichiometry is possible on the Si-poor side which, however, reduces the critical temperature due to the resulting constitutional disorder. The critical temperature is also reduced by dissolved hydrogen (Stepanov and Skripov, 1982). Likewise the critical current density and the critical field strength are reduced by elastic tensile or compressive straining (Smathers, 1990). Slightly above the critical temperature V_3Si transforms martensitically to a weakly tetragonal, still superconducting phase with twin-related thin lamellae, which is due to lattice softening with vanishing shear modulus (Batterman and Barrett, 1964, 1966; Kondratyev and Pushin, 1985; Mendelson, 1986; Onozuka et al., 1988). Prior plastic deformation with large strains at high temperatures stabilizes the tetragonal martensite even at temperatures above the martensite formation temperature (Ullrich et al., 1978). The martensitic transformation gives rise to superelasticity and a shape memory effect (Zakrevskiy et al., 1986).

V_3Si is hard and brittle, as are all the A15 phases, which makes processing very

ArcelorMittal Ex. 2038
Page 117 of 190

difficult (Fleischer, 1989; Fleischer and Zabala, 1990c). The reason for this is the electronic structure of V_3Si which leads to strong covalent bonding between the nearest neighbor V atoms (Medvedev et al., 1984; Muller, 1986). V_3Si has a high Young's modulus of 213 GPa (Fleischer et al., 1989b) and an apparent brittle-to-ductile transition temperature (BDTT) of the order of 1200 °C (Mahajan et al., 1978; Nghiep et al., 1980). The plastic deformation behavior above the BDTT has been studied in detail and the dislocation slip systems have been analyzed (Levinstein et al., 1966; Bertram and Paufler, 1983; Krämer, 1983; Wright and Bok, 1988; Smith et al., 1993). The creep behavior is characterized by subgrain formation, dislocation climb controlling the creep rate and a comparatively high activation energy in the range of 2–11 eV/atom depending on the stress and the composition (Nghiep et al., 1980). Creep can be enhanced by superimposed electric currents, i.e. there is the so-called electroplastic effect, and thermal gradients, which is proposed to be due to the favorable effect of the electrotransport and thermotransport of point defects on the dislocation mobility (San Martin et al., 1980, 1983).

The transition from superconduction to normal conduction in A15 superconductors occurs by the penetration of small fluxoids, i.e. quantized magnetic flux vortices, which is characteristic for the type II, high-field superconductors (Geballe and Hulm, 1986). These fluxoids can be pinned by microstructural inhomogeneities – in particular grain boundaries and precipitated particles – which is beneficial with respect to critical current density and field strength (Muller, 1986; Smathers, 1990). Consequently, microstructural changes by prior plastic straining with or without recrystallization affect the superconducting properties, depending on the deformation conditions and the composition (Quyen et al., 1979). The thin lamellae, which are produced by the already-mentioned martensitic transformation, are less effective with respect to flux pinning than grain boundaries, i.e. their effect on the superconducting properties becomes relevant only in single crystals (Brand and Webb, 1969).

V_3Si is of interest for applications because of its favorable superconducting properties and its high stability (Smathers, 1990). Apart from hot extrusion, V_3Si can be deformed plastically at room temperature in spite of its brittleness by superimposing a high hydrostatic pressure which makes the production of multifilament, superconducting wires feasible for applications in solenoid magnets (Wright, 1977). Laminar V_3Si can be prepared by solid-state, thin film reactions between V and SiO_2 on Si substrates (Hayashi et al., 1991). However, Nb_3Sn has been found to be more favorable with respect to superconducting properties, mechanical behavior, and processing, which has precluded the use of V_3Si as a magnet material (Smathers, 1990).

Recently V_3Si has become of interest with respect to structural, high-temperature applications (Shah and Anton, 1992a). Combination with a ductile phase, e.g. V-rich solid-solution, offers the possibility of overcoming the brittleness problem, and indeed a directionally-solidified, eutectic V_3Si–V alloy has been successfully prepared (Goldman, 1993). The fracture toughness of V_3Si–V composites with discontinuous V_3Si has been found to increase monotonically with increasing fraction of V and decreasing impurity content (Strum and Henshall, 1993).

ArcelorMittal Ex. 2038
Page 118 of 190

7.3 V_3Ga

V_3Ga with an A15 structure is stable only up to 1300 °C where it transforms congruently to a V–Ga disordered, b.c.c. solid-solution (Massalski et al., 1990). There are indications of a martensitic transformation at very low temperatures, in close analogy to V_3Si, though the conditions for martensite formation are not yet clear for V_3Ga (Nembach et al., 1970; Snead, Jr. and Bussière, 1985). It has a broad range of homogeneity centered on the stoichiometric composition, i.e. it is very stable with respect to deviations from stoichiometry. Because of this stability, which is advantageous for fabrication, and the still high, critical temperature of about 16 K, V_3Ga is of interest for applications (Smathers, 1990).

The superconducting properties and the deformation behavior of V_3Ga are similar to those of V_3Si. The superconducting transition can be affected by prior plastic deformation (Wright and Ho, 1986). V_3Ga is ductile in compression above 1000 °C and the creep behavior has been studied in detail (Soscia and Wright, 1986; Shah and Anton, 1992a). As in the case of V_3Si, V_3Ga can be deformed plastically by hot extrusion and at room temperature by superimposing a high hydrostatic pressure, which makes the production of multifilament, superconducting wires feasible for applications in solenoid magnets (Wright, 1977). Hybrid high-field magnets with V_3Ga tape coils have been produced successfully (Noto et al., 1986). However, Nb_3Sn has been found to be more favorable with respect to superconducting properties, mechanical behavior, and processing which has precluded the commercialization of V_3Ga up to now (Smathers, 1990).

7.4 Nb_3Sn

Nb_3Sn with an A15 structure forms peritectically at 2130 °C from the liquid solution and solid Nb, and is stable only above 775 °C where it decomposes eutectically (Massalski et al., 1990). The decomposition reaction can be suppressed by not too slow cooling, i.e. Nb_3Sn with an A15 structure is maintained at lower temperatures in a metastable condition. Nb_3Sn transforms to a twinned, tetragonal martensite at 43 K (Mailfert et al., 1969; Mendelson, 1986), and the transition to superconductivity occurs at about 18 K (Muller, 1986; Smathers, 1990). This critical temperature is reduced by deviations from stoichiometry, which affect the atomic order, and by elastic strains. Small increases in the critical temperature are possible using ternary alloying additions. The transition temperature does not depend sensitively on prior plastic deformation (Wright and Ho, 1986).

As for the other A15 phases, Nb_3Sn can be deformed readily at high temperatures, e.g. by hot extrusion, whereas deformation at low temperatures is possible only by superimposing a high hydrostatic pressure (Wright, 1977; Eisenstatt and Wright, 1980; Clark and Wright, 1983). The high temperature deformation and creep behavior have been studied in detail and a beneficial effect of grain size reduction on the brittle-to-ductile transition temperature (BDTT) has been found (Clark et al., 1983; Shah and Anton, 1992a).

Nb_3Sn superconductors with multifilamentary geometry, which is needed for electromagnet applications, are easily fabricated by the so-called bronze process, which has led to the wide-spread commercial application of Nb_3Sn (Smathers, 1990). In the bronze process Nb rods are inserted in a bronze rod or tube which is

ArcelorMittal Ex. 2038
Page 119 of 190

then processed to obtain a multifilament wire. At the end of the wire processing, Nb_3Sn shells are formed around the Nb cores by reaction heat treatments. The final multifilament, composite superconductor consists of Nb_3Sn fibers with Nb cores which are embedded in a bronze matrix; the latter is surrounded by a coating of Nb, which serves as a diffusion barrier, and an outer Cu tube, which serves as a stabilizer and carries the current in case of transition to normal conduction. Various specific processing routes, including powder metallurgy routes, have been developed for optimized superconductor production and hybrid superconductor coils are commercially available (Hillman et al., 1980; McDonald, 1984; Gregory, 1984; Noto et al., 1986; Hecker et al., 1988; Smathers, 1990).

The superconducting properties of the composite superconductor, as well as the mechanical properties, depend on the particular microstructure which is a function of the various prior processing steps. Much work has been directed towards the details of the various processes, e.g. the effects of alloying additions (Zwicker et al., 1979), the Sn diffusion during Nb_3Sn formation (Glowacki and Evetts, 1988; Cheng and Verhoeven, 1988), the grain size dependence of the flux pinning force and the tensile strength and fracture at room temperature (Ochiai et al., 1986a, b, 1988; Watari et al., 1986), or the effects of the hardnesses of the constituent phases on the composite workability (Dew-Hughes et al., 1987). Recent new developments rely on the beneficial effects of additions of Ti, Hf, Ta, and/or Ge on the superconducting properties (Kohno et al., 1992; Kamata et al., 1992b; Tachikawa et al., 1992; Murase et al., 1992; Noto et al., 1992).

7.5 Nb_3Al

Nb_3Al with an A15 structure forms peritectically at 2060 °C and is stable below this temperature in the whole temperature range only with Al-deficient, off-stoichiometric compositions (Jorda et al., 1980; Massalski et al., 1990). The stoichiometric composition corresponds to the maximum solubility of Al in Nb_3Al, and is reached only at 1940 °C in eutectic equilibrium with the liquid Nb–Al and the σ phase Nb_2Al. The phase stability is a function of the electronic band structure which has been studied as a function of temperature (Kuzmichev et al., 1983). The formation enthalpy of Nb_3Al is significantly smaller than that of the Al-rich phase Al_3Nb, which has been discussed in Sec. 3.3 (Meschel and Kleppa, 1993). The transition to superconduction occurs at 19 K and there is no martensitic transformation (Smathers, 1990). The transition temperature of Nb_3Al is affected by deviations from stoichiometry and perfect order, as are those of the other A15 phases, but in a less sensitive way. It is noted that the A15 phase with the highest transition temperature is Nb_3Ge, which can be alloyed with Nb_3Al to form the ternary A15 phase $Nb_3(Al_{0.7}Ge_{0.3})$ with the highest critical field strength (Muller, 1986).

Nb_3Al has long been considered for electromagnet applications because of its advantageous superconducting properties (Smathers, 1990). However, the processing of Nb_3Al is very difficult because of the brittleness of Nb_3Al. Powder metallurgy methods have been used successfully for preparing Nb_3Al by reaction synthesis and producing, e.g. an Nb_3Al–Ag composite superconductor (Bowden, 1989; Tsuchida et al., 1989; Schulze et al., 1990). Nb_3Al tapes have been prepared by rapid solidification (Togano et al., 1992). A novel pro-

ArcelorMittal Ex. 2038
Page 120 of 190

cess with thin Nb–Al sandwiches as the starting material has allowed the fabrication of Nb_3Al superconducting wires with good workability (Saito et al., 1990, 1993; Ikeda et al., 1992). Furthermore, various other processes have been used successfully for producing Nb_3Al wires (Noto et al., 1992).

Presently Nb_3Al is also being considered for structural applications at high temperatures in spite of its low-temperature brittleness because of its high stability and strength at high temperatures, and various developments have been initiated (Dimiduk et al., 1991; Anton and Shah, 1991a; Yamaguchi, 1992; Bunk, 1992; Kamata et al., 1993; Suyama et al., 1993). The mechanical properties at low and high temperatures have been determined and the brittle-to-ductile transition has been observed at about 1000 °C (Barth et al., 1992; Shah and Anton, 1992a). At lower temperatures Nb_3Al is inherently brittle according to theoretical ab initio calculations (Kim et al., 1993). The dislocation configurations and slip systems have been analyzed (Aindow et al., 1991; Murayama et al., 1993a–c). The yield stress can be varied by varying the Al content and by alloying with a third element (Fujiwara et al., 1991; Kamata et al., 1992a). The solubilities of third metals in Nb_3Al differ enormously depending on the particular metal, which offers manifold possibilities of alloying (Shah and Anton, 1992a). The diffusion behavior has been studied (Slama and Vignes, 1972), and the oxidation resistance is only poor because of nonprotective scale formation (Shah and Anton 1992a; Tomizuka, 1992; Fujiwara et al., 1993).

A reduction in the Al content below the solubility limit leads to two-phase Nb_3Al–Nb alloys which offer the possibility of relieving the brittleness of Nb_3Al (Anton and Shah, 1990; Marieb et al., 1991; Kumagai et al., 1991; Davidson and Anton, 1993). The brittle-to-ductile transition temperature (BDTT) decreases with increasing volume fraction of the Nb-rich phase, and a brittle-to-ductile transition at room temperature has been obtained for an Nb–16 at.% Al alloy (Suyama and Hashimoto, 1992). The Nb phase toughens the alloy by crack bridging, plastic stretching, and interfacial bonding (Murugesh et al., 1992). However, the fracture toughness controlling, microstructural details are not yet clear (Davidson and Anton, 1993). It is noted that the Nb-rich phase, which usually crystallizes with the b.c.c. A2 structure, may be ordered with a B2 structure due to the presence of interstitial impurities (Marieb et al., 1991). The transformation and precipitation reactions have been studied in detail (Yang and Vasudevan, 1993).

Powder metallurgy methods and infiltration techniques with reaction synthesis result in such two-phase alloys with even higher Al contents because of incomplete reactions (Kumagai et al., 1991; Murayama et al., 1991). Nb–Al alloys with still higher Al contents in the range 25–33 at.% contain the σ phase Nb_2Al, which is also regarded as attractive for high-temperature applications (Bhattacharya et al., 1992). Apart from the above Nb_3Al–Nb alloys, which may be regarded as discontinuously reinforced, in situ composites, Nb_3Al has been considered for use in intermetallic matrix composites which are reinforced by continuous ceramic fibers (Anton, 1988; Shah et al., 1990). Laminated composites have been prepared in situ by high rate sputtering (Rowe and Skelly, 1992). Alloying of Nb_3Al with Ti leads to a ternary phase with a B2 structure (Shyue et al., 1993) which is related to the Ti_3Al-base, super-α_2 alloys of Sec. 3.1.2.

ArcelorMittal Ex. 2038
Page 121 of 190

Intermetallics
Gerhard Sauthoff
copyright © VCH Verlagsgesellschaft mbH, 1995

7.6 Nb_3Si

Nb_3Si is a high-temperature line compound which forms with a tetragonal crystal structure by a peritectic reaction at 1980 °C and is stable only above 1770 °C (Massalski et al., 1990). Rapid solidification of the liquid produces amorphous Nb_3Si (Bertero et al., 1991 a). The A15 structure is unstable and is obtained only by special rapid solidification techniques and by crystallization of amorphous Nb_3Si. Nb_3Si with an A15 structure is of interest because a high transition temperature for superconduction is expected, and indeed a transition temperature of 19 K was reported for near-stoichiometric Nb_3Si with an A15 structure, which was prepared by crystallization of amorphous Nb_3Si under high pressure (Wang et al., 1988). Other crystal structures are obtained for Nb_3Si doped with impurities, i.e. the $L1_2$ structure with oxygen and a hexagonal structure with carbon (Kassem and Koch, 1991). The present interest is directed at Nb–Si in situ composite alloys which contain the Nb_3Si phase and are considered for high-temperature applications (Bertero et al., 1991 a, b; Cockeram et al., 1991, 1992 a, b; Bewlay et al., 1992; Goldman, 1993).

7.7 Cr_3Si

Cr_3Si crystallizes congruently with an A15 structure from the melt and is stable down to very low temperatures with a range of homogeneity which includes the stoichiometric composition (Massalski et al., 1990). Cr_3Si does not exhibit superconduction (Smathers, 1990). However, Cr_3Si has been regarded for a long time as promising for high-temperature applications because of its high creep strength and oxidation resistance (Arbiter, 1953 a, b; Silverman, 1956; Anton and Shah, 1991 b; Dimiduk et al., 1991). The elastic moduli have been determined as well as the temperature dependence of the hardness (Fleischer et al., 1989 b, 1991; Fleischer and Zabala, 1990 c). Compressive ductility has been observed only above 1200 °C and its extent is expected to be limited because of an insufficient number of slip systems (Chang and Pope, 1991). Creep data are available (Shah and Anton, 1991). At lower temperatures Cr_3Si is brittle with a low fracture toughness (Fleischer, 1990; Fleischer et al., 1991). Sufficient oxidation resistance has been observed only below 1200 °C, i.e. below the apparent brittle-to-ductile transition temperature (McKee and Fleischer, 1991). An improved toughness may be obtained with two-phase Cr_3Si–Cr alloys, i.e. by combining the brittle Cr_3Si phase with the Cr-rich solid solution (Mazdiyasni and Miracle, 1990; Newkirk and Sago, 1990; Bewlay et al., 1992). An improved mechanical behavior is also expected for Cr_3Si-based, intermetallic matrix composites, e.g. Cr_3Si–TiC, Cr_3Si–TiB_2, or Cr_3Si–Y_2O_3, for which good bonding and chemical compatibility of matrix and reinforcements have been found (Yang et al., 1990).

8 Laves Phases

8.1 Basic Properties

The Laves phases – sometimes designated as Friauf–Laves phases – with an AB_2 composition in the binary case form a very large group of intermetallics which crystallize with the hexagonal C14 structure, the cubic C15 structure, or the dihexagonal C36 structure (Laves, 1967; Wernick, 1967; Livingston, 1992). These structures are topologically close-packed (tcp) structures (Wernick, 1967; Schulze et al., 1973; Watson and Bennet, 1984), i.e. the Laves

ArcelorMittal Ex. 2038
Page 122 of 190

phases belong to the family of the Frank–Kaspar phases, which has already been discussed in Sec. 7 in the context of the A15 phases.

The stability of the three crystal structures C14, C15, and C36 is controlled by both the atomic size ratio of the A atoms and B atoms and by the valence electron concentration of the Laves phase (Wernick, 1967; Leitner, 1971 a, b; Leitner and Schulze, 1971; Ohta and Pettifor, 1990). Deviations from stoichiometry are accommodated primarily by placing the excess atoms on sites of the other sublattice, i.e. the A and B atoms substitute for each other (Brückner, 1969; Schulze, 1972). Such composition changes affect the valence electron concentration which may induce a change in the crystal structure, as has been observed in the case of $TiCo_2$ which shows the C15 structure for the stoichiometric composition and the C36 structure for the Co-rich, off-stoichiometric composition (Aoki et al., 1966; Schulze, 1972). It is noted that the respective phase equilibria are still in discussion (Massalski et al., 1990). A similar situation has been reported for $TaCo_2$ with the additional C14 structure for the Co-poor, off-stoichiometric composition and for $NbCo_2$ (Massalski et al., 1990). Different crystal structures have also been observed at different temperatures for some Laves phases, e.g. $NbCo_2$ and the chromides MCr_2 with M = Ti, Zr, Nb, or Ta, which indicates only small energy differences between the three crystal structures (Massalski et al., 1990). Indeed the crystal structures C14, C15, and C36 differ only by the particular stacking of the same two-layered structural units which allows structure transformations between these structures and twinning by synchroshear (Allen et al., 1972; Allen and Liao, 1982; Allen, 1985; Hazzledine et al., 1993; Hazzledine and Pirouz, 1993; Liu et al., 1993; Pope and Chu, 1993). Correspondingly, stacking sequence faults may be formed easily in topologically close-packed phases, which have been studied in detail (Khantha et al., 1990). A structure transformation may be induced by a mechanical stress, a has been observed for $ZrFe_2$ with a C36/C15 transition (Liu et al., 1993).

The basic properties have only been determined for a few selected Laves phases, e.g. elastic moduli (Shannette and Smith, 1969; Schulze and Paufler, 1972; Schiltz and Smith, 1974; Balankin, 1984; Halstead and Rawlings, 1985; Fleischer et al. 1988; Fleischer and Zabala, 1990 b, c; Fleischer, 1992 b) (see also Fig. 6), thermal expansion (Giegengack et al., 1966), and diffusion properties (van der Straten et al., 1976; Wein et al., 1978; Wever, 1992; Sprengel et al., 1994). The elastic anisotropy is only small which indicates the absence of strong directional bonding (Schulze and Paufler, 1972). HfV_2 exhibits an anomalous temperature dependence of the elastic moduli which is related to a martensitic transformation at low temperatures (Livingston and Hall, 1990). The plastic deformation behavior at high and low temperatures, i.e. dislocation slip systems and mobilities, has been studied primarily for the classic Laves phases $MgZn_2$ with a C14 structure and $MgCu_2$ with a C15 structure (Moran, 1965; Paufler and Schulze, 1967; Krämer and Schulze, 1968; Paufler, 1972; Hall and Livingston, 1989; Livingston et al. 1989; Ohba and Sakuma, 1989). Recent studies have been directed at HfV_2 with a C15 structure (Hall and Livingston, 1989; Livingston and Hall, 1990; Pope and Chu, 1993), $TiCr_2$ with a C15 structure (K. C. Chen et al., 1993), $MgNi_2$ with a C36 structure (Livingston and Hall, 1991), and the ternaries $Mg(Cu,Zn)_2$ with a C36 structure (Livingston and Hall, 1991) and $Nb(Ni,Al)_2$ with a C14 structure (Saut-

ArcelorMittal Ex. 2038
Page 123 of 190

hoff, 1990b, 1991a; Machon, 1992). The Laves phases are strong and brittle with an apparent brittle-to-ductile transition temperature of about two thirds of the melting temperature (Wetzig and Wittig, 1972; Schulze and Paufler, 1972; Livingston, 1992). This brittleness is also shown by single crystals, i.e. it is not due to the presence of weak grain boundaries and an insufficient number of slip systems. It is an inherent brittleness which results from the complexity of the dislocation glide processes with high Peierls stresses and correspondingly low dislocation densities and mobilities.

The already high strengths of Laves phases can be further increased by solid-solution strengthening as a result of alloying with third elements (Sauthoff, 1989; Livingston, 1992; Fleischer, 1992b, 1993d). The alloying elements can substitute for both the A atom or the B atom in the binary AB_2 phase, as is indicated by the extension of the AB_2 field in the isothermal sections of the respective ternary phase diagrams (Anton and Shah, 1991b). Alloying with Al and Si is of particular interest in view of the beneficial effect on the oxidation resistance (Meier and Pettit, 1992). Alloying with both elements, which substitute for the B element in AB_2, may change the valence electron concentration to such an extent that a change in crystal structure is induced, i.e. each of the three alternative crystal structures C14, C15 and C36 can be stabilized by the appropriate control of the Al and Si contents (Bardos et al., 1963; Wernick, 1967; Wallace and Craig, 1967). A similar situation has been found for the ternary $Nb(Cr,Fe)_2$ which forms with the C14, C15 or C36 structure depending on temperature and Fe content (Grujicic et al., 1993).

The effect of both composition and temperature on structure stability is exemplified by the ternary phase $Nb(Co_{1-x}Al_x)_2$ which exhibits the C14 structure at high temperatures and the C15 structure at low temperatures, with a transition temperature which decreases with increasing Al content from about 1300 °C for $x=0$ to room temperature for about $x = 0.12$ (Von Keitz and Sauthoff, 1992). A similar behavior has been observed for $Nb(Co_{1-x}Si)_2$. However, $Ta(Fe_{1-x},Al_x)_2$, $Nb(Fe_{1-x},Al_x)_2$, $Nb(Fe_{1-x},Si_x)_2$, $Ti(Fe_{1-x},Al_x)_2$, and $Ti(Fe_{1-x},Si_x)_2$ only show the C14 structure (Raghavan, 1987). It has to be emphasized that some other similar ternary Laves phases, e.g. $Ta(Ni_{1-x},Al_x)_2$, $Nb(Ni_{1-x},Al_x)_2$, and $Mo(Co_{1-x},Si_x)_2$ all with C14 structures do not exist as binary phases, i.e. the cases $x = 0$ are not included and correspondingly these ternary Laves phases are frequently given as, e.g. TaNiAl, NbNiAl, and MoCoSi (Bardos et al., 1961; Benjamin et al., 1966; Skolozdra et al., 1966b; Villars and Calvert, 1991). Finally, it is noted that the already-mentioned binary $TiCr_2$ dissolves Fe to form the ternary $Ti(Fe_{1-x},Cr_x)_2$ with a C14 structure for $0 \leq x \leq 0.9$, whereas the structure of this ternary phase is either C14, C15, or C36 for $0.95 \leq x \leq 1$ depending on the composition and the temperature (Raghavan, 1987).

8.2 Applications

Various Laves phases have been regarded as promising for both functional and structural applications (Livingston, 1992), and examples are given in the following sections.

8.2.1 Superconducting Materials

A transition to superconductivity at low temperatures has been observed for a large number of Laves phases with the C14 structure or the C15 structure (B. W.

ArcelorMittal Ex. 2038
Page 124 of 190

Roberts, 1967). (Hf,Zr)V_2 with a C15 structure is of particular interest because of its advantageous superconducting properties since it combines a fairly high critical temperature with a high critical current density and magnetic field strength (Noto et al., 1986; Olzi et al., 1988). Processing is difficult because of its poor deformability. Further alloying – in particular with Nb – improves the mechanical behavior to such an extent that multifilamentary superconductors can be produced which are being considered for application in fusion reactor magnets since the superconducting properties are comparatively insensitive to neutron irradiation and mechanical strain (Noto et al., 1986). Room temperature deformation of HfV_2-base alloys occurs primarily by twinning (Hall and Livingstone, 1989; Livingston and Hall, 1990; Pope and Chu, 1993). The Hf–V–Nb phase diagram has been studied recently (Chu and Pope, 1992, 1993).

8.2.2 Magnetic Materials

Various transition-metal Laves phases, e.g. TFe_2 with T = Ti, Zr, Hf, Nb, or Mo as well as $NbCo_2$ and the closely related rare-earth Laves phases, show interesting magnetic properties as a result of their particular electronic structures (see, e.g. Brückner, 1969; Buschow, 1980; Armitage et al., 1986; Yamada and Shimizu, 1986; Smirnova and Meshkov, 1986; Asano and Ishida, 1988). The rare-earth phases $TbFe_2$ and $SmFe_2$, both with the C15 structure, exhibit huge magnetostrictions at room temperature (Clark, 1980). In addition there is a magnetoelastic interaction, i.e. unusual changes in the elastic moduli are observed under a magnetic field. The ternary C15 phase $(Tb_{1-x}Dy_x)Fe_2$ has a high potential for application as a high-power transducer, since it combines a large magnetostriction with a vanishing magnetic anisotropy (with $x \approx 0.7$) (Clark, 1980). This material is brittle like other Laves phases, whith an apparent brittle-to-ductile transition temperature of about 875 °C (Saka et al., 1991). Recently $CeAl_2$ and $TbAl_2$, both with C15 structures, have been studied with respect to the effect of microstructural defects on the magnetic behavior (Bi and Abell, 1993).

Various rare earth (R) Laves phases, in particular RFe_2, can absorb large amounts of hydrogen (see next section) which may affect their structures, i.e. they can undergo structure transformations on hydrogenation, including amorphization, which may be accompanied by decomposition reactions (Aoki and Masumoto, 1988; Pontonnier et al., 1991; Suzuki and Lin, 1993; Christodoulou and Takeshita, 1993 b; Kim and Lee, 1993 a, b; Aoki and Masumoto, 1993). Such hydrogenation and dehydrogenation reactions have been used for producing fine-grained powders for the powder metallurgical production of so-called giant magnetostrictive RFe_2 alloys (Jones et al., 1991).

8.2.3 Hydrogen Storage Materials

Various Laves phases can absorb large amounts of hydrogen and are considered for applications as hydrogen storage materials (Somenkov and Shilstein, 1979; Reilly, 1979; Ivey and Northwood, 1986 b). Such AB_2 phases contain a strong hydride former as the A element and crystallize with the C14 structure or the C15 structure. The Laves phases with the highest sorption capacities are C15 ZrV_2 with a hydrogen-to-metal ratio H/M = 1.8, C14 or C15 $ZrCr_2$ with H/M = 1.3, and C14 $ZrMn_2$ as well as C14 or C15 $TiCr_2$ with H/M = 1.2. $LaNi_2$, which was known as a C15 phase (Wernick, 1967), with

ArcelorMittal Ex. 2038
Page 125 of 190

H/M = 1.5 (Ivey and Northwood, 1986b) is a tetragonal, pseudo-Laves phase which is stabilized only by the presence of impurities according to recent findings (Gschneidner, 1993).

The formed hydrides in these binary Laves phases are too stable for easy hydrogen desorption, which is a prerequisite for hydrogen storage (Ivey and Northwood, 1986b). The hydride stability can be reduced and adjusted to practical hydrogen storage conditions by deviations from stoichiometry, substitution of the B element primarily by Fe, Co, Ni, Cu, Mn, or Cr, or substitution of the A element primarily by Ti, or any combination of these alloying possibilities.

An example of the stoichiometry effect is given by $ZrMn_2$, which exhibits an increasing hydrogen vapor pressure with increasing Mn content, and which is stable with a C14 structure up to $ZrMn_{3.8}$ (Ivey and Northwood, 1986b). Another example is C14 $TiMn_2$, which reaches its maximum H solubility at the off-stoichiometric composition corresponding to $TiMn_{1.5}$, whereas it does not absorb H at the stoichiometric composition (Sicking et al., 1981). The effects of substitution on electronic structure, alloy stability, hydride stability, and H storage capacity have been studied with respect to various systems, e.g. $(Zr_xTi_{1-x})Mn_2$ (Moriwaki et al., 1991a), $Zr(Mn_{1-x}Fe_x)_{2+y}$ (Triantafillidis et al., 1991), and $Zr(V_{1-x}Co_x)_2$ where both V and Co have been substituted for by other transition metals (Peretz et al., 1979), and $Zr(Cr_{1-x}V_x)_2$ (Ivey and Northwood, 1986a). $Zr(Cr_{1-x}V_x)_2$ exhibits polytypism, i.e. crystal structure variants of either the hexagonal C14 structure or the cubic C15 structure are formed which only differ by the stacking of the crystal structure units (Meng and Northwood, 1986; Burany and Northwood, 1991). Various rare earth (R) Laves phases undergo amorphization on hydrogenation (Aoki and Masumoto, 1988, 1993; Pontonnier et al., 1991; Suzuki and Lin, 1993; Christodoulou and Takeshita, 1993b; Kim and Lee, 1993a, b). RNi_2 with a C15 structure is easily transformed into amorphous RNi_2 which is very stable and is being considered for use as long-life electrodes in electrochemical nickel-hydrogen batteries (Miyamura et al., 1991).

The thermodynamics of hydrogenation have been studied and hydride formation enthalpies have been determined (see, e.g. Lynch et al., 1979; Sicking et al., 1981; Ivey and Nothwood, 1986b; Uchida et al., 1986; Perevesenzew et al., 1988; Drasner and Balzina, 1991; Zeng et al., 1993; Lück and Wang, 1993; Park et al., 1993). The optimization of properties has led to multinary Laves phases, e.g., Zr–Mn–Co–V alloys (Yonezu et al., 1991), Zr–Mn–Ni–V alloys (Wakao et al., 1991), Zr–Mn–Ni–V–Cr alloys (Moriwaki et al., 1991b), or Zr–Ti–Mn–Fe and Zr–Ti–V–Fe alloys (Park and Lee, 1992), which have been studied in detail in view of applications as hydrogen storage materials and electrodes in electrochemical nickel–hydrogen batteries.

8.2.4 Structural Alloys

The ternary Laves phase MoCoSi, i.e. $Mo(Co,Si)_2$ with a hexagonal C14 structure, has given rise to the development of wear resistant Co–Mo–Cr–Si alloys which contain large volume fractions of the Laves phase in a coarse distribution together with a Co-rich phase, and which are known as Tribaloys (Schmidt and Ferris, 1975; Halstead and Rawlings, 1984, 1985). Apart from their high strength and hardness they have an adequate fracture toughness of the order of 20 $MN/m^{3/2}$.

ArcelorMittal Ex. 2038
Page 126 of 190

These advantageous mechanical properties result in an excellent wear resistance which – in combination with an excellent corrosion resistance in various environments – makes the Tribaloys very appealing for applications in a broad range of temperatures and environments.

The strong binary Laves phases $TaFe_2$ and $NbFe_2$ have been considered for the development of Laves phase strengthened, ferritic Fe-base alloys for applications at elevated temperatures (Bhandarkar et al., 1976; Wert et al., 1979). Monolithic transition metal Laves phases – in particular $TiCr_2$ – have long been regarded as promising for high-temperature applications because of their high strengths at high temperatures and sufficient oxidation resistances (Arbiter, 1953a, b; Silverman, 1956; Grinthal, 1956, 1958). However, the pronounced brittleness of such Laves phases makes processing very difficult and has precluded any application of monolithic Laves phases as structural materials.

As in other alloy systems, the combination of such Laves phases with ductile phases can reduce the brittleness to a tolerable level, and indeed two-phase Ti–$TiCr_2$ alloys, as well as Ti–Nb–$(Ti,Nb)Cr_2$ alloys, have shown good prospects for obtaining high strengths with acceptable room-temperature toughness (Fleischer and Zabala, 1990b; K. C. Chen et al., 1993). The Laves phase is present in these alloys as strengthening particles which are cracked during deformation with the cracks being stopped at the phase boundaries. Similar alloy systems with Laves phases have been screened extensively with respect to strength, brittle-to-ductile transition temperature and oxidation (Anton and Shah, 1992a, 1993; Shah and Anton, 1992b). The Nb-Cr system is regarded as a candidate for high-temperature applications because the $NbCr_2$ Laves phase has a high congruent melting point of 1770 °C, high strength and creep resistance, comparatively low density, potential oxidation resistance, and a wide solubility range which offers manifold possibilities for alloying (Svedberg, 1976; Thoma and Perepezko, 1990; Anton and Shah, 1991b; Vignoul et al., 1991; Takeyama and Liu, 1991). Toughness is improved not only by embedding $NbCr_2$ as particles in a Cr matrix, but also by Cr or Nb particles in an $NbCr_2$ matrix (Anton and Shah, 1990; Takeyama and Liu, 1991). Similar toughening effects have been observed for Cr–$ZrCr_2$ and Cr–$HfCr_2$ (Mazdiyasni and Miracle, 1990). Apart from these two-phase metallic/intermetallic alloys, which may be regarded as in situ composites, such Laves phases are also considered as matrices in intermetallic matrix composites with strengthening dispersoids and fibers (Shah et al., 1990; Yang et al., 1990).

Cr-containing Laves phases may be less advantageous at very high temperatures above 1000 °C with respect to oxidation resistance because of the volatility of the Cr oxides (Hindam and Whittle, 1982). For applications at such high temperatures Al-containing phases are preferred, as already remarked upon in Sec. 2.3. Thus the ternary Al-containing Laves phases – in particular $Nb(Ni,Al)_2$ or NbNiAl, $Ta(Ni,Al)_2$ or TaNiAl, and $Ta(Fe,Al)_2$ – which have been mentioned in Sec. 8.1, have been considered for high-temperature applications because of their high melting temperature, high strength and potential oxidation resistance (Sauthoff, 1989, 1991a, 1992; Machon, 1992; Zeumer and Sauthoff, 1992; Von Keitz and Sauthoff, 1992). Again the monolithic Laves phases are too brittle for structural applications. However, these phases form stable, two-phase equilibria with the B2 aluminides NiAl and FeAl, respectively, which offers

ArcelorMittal Ex. 2038
Page 127 of 190

the possibility of preparing intermetallic two-phase alloys with reduced brittleness. NiAl-NbNiAl, NiAl-TaNiAl, NiAl-(Nb,Ta)NiAl, and FeAl-TaFeAl alloys have been prepared by ingot metallurgy methods and studied with respect to strength, ductility, toughness, brittle-to-ductile transition temperature, creep resistance, and oxidation resistance as has been discussed in Sec. 4.3.6 under the heading Structural Alloys.

9 Beryllides

The transition-metal beryllides – in particular the Be-rich phases with Ti, Zr, Hf, Nb, Ta, or Mo – have long been regarded as very attractive for applications as structural, high-temperature materials because of their low densities between 2 and 5 g/cm^3, high melting temperatures, high stiffnesses and strengths, and high oxidation resistances (Stonehouse et al., 1960; Ryba, 1967; Hove and Riley, 1967; Marder and Stonehouse, 1988; Tien et al., 1992; Kumar and Liu, 1993). Characteristic compositions of these Be-rich phases are MBe_{13} for, e.g. M = Zr, or Hf, MBe_{12} for, e.g. M = Ti, Nb, Ta, or Mo, and M_2Be_{17} for, e.g. M = Ti, Zr, Hf, Nb, or Ta. Such phases and other Be-rich phases with similar compositions are formed with most other metals. The multitude of intermetallic Be phases is similar to that of the intermetallic rare earth phases, which are addressed in the next section. No beryllides have been observed in the Al-Be and Al-Si systems (Massalski et al., 1990). These Be-rich phases have complex cubic, tetragonal, or hexagonal crystal structures, and it has to be noted that the crystallographic data in standard compilations are controversial in some cases (Massalski et al., 1990; Villars and Calvert, 1991). Beryllides with less Be have simpler structures, e.g. the Laves phases MBe_2 with M = Cr, Mo, or Fe with a C14 structure and M = Ti, Nb, or Ta with a C15 structure (see Sec. 8.1), the B2 phases NiBe and TiBe (see Sec. 4.4), or the A15 phase Mo_3Be (see Sec. 7.1). Basic data can be found in early compilations (Shaffer, 1964; Samsonov and Vinitskii, 1980).

The Be-rich phases with Nb, Zr, or similar transition metals have been prepared by powder metallurgy methods (Marder and Stonehouse, 1988; Henager et al., 1992b), though ingot metallurgy methods have also been used (Nieh et al., 1990). Processing must be done with care because of the volatility and toxicity of Be (Stonehouse and Marder, 1990). The oxidation resistance is generally excellent due to the formation of protective BeO scales (Marder and Stonehouse, 1988; Grensing, 1989), though pest-like oxidation with specimen disintegration is observed in an intermediate temperature range aroung 800 °C for Nb and Zr beryllides (Westbrook and Wood, 1964; Ryba, 1967; Aitken, 1967; Chou et al., 1992). It is noted that beryllides have been proposed for applications as protective coatings, e.g. for Ta (Lawthers and Sama, 1993).

The mechanical behavior of these Be-rich phases and its variation with temperature has been studied by means of hardness tests, bending stress-rupture tests, tension tests and compression tests (Ryba, 1967; Marder and Stonehouse, 1988; Fleischer and Zabala, 1990c; Nieh and Wadsworth, 1990; Bruemmer et al., 1993). The observed brittle-to-ductile transition temperatures are of the order of 1000 °C. The low-temperature fracture toughness K_{Ic} has been found to be between 2 and 4 MN/m$^{3/2}$ with practically no macroscopic ductility (Bruemmer et al., 1993), though there are indications of local plasticity at

ArcelorMittal Ex. 2038
Page 128 of 190

the possibility of preparing intermetallic two-phase alloys with reduced brittleness. NiAl-NbNiAl, NiAl-TaNiAl, NiAl-(Nb,Ta)NiAl, and FeAl-TaFeAl alloys have been prepared by ingot metallurgy methods and studied with respect to strength, ductility, toughness, brittle-to-ductile transition temperature, creep resistance, and oxidation resistance as has been discussed in Sec. 4.3.6 under the heading Structural Alloys.

9 Beryllides

The transition-metal beryllides – in particular the Be-rich phases with Ti, Zr, Hf, Nb, Ta, or Mo – have long been regarded as very attractive for applications as structural, high-temperature materials because of their low densities between 2 and 5 g/cm^3, high melting temperatures, high stiffnesses and strengths, and high oxidation resistances (Stonehouse et al., 1960; Ryba, 1967; Hove and Riley, 1967; Marder and Stonehouse, 1988; Tien et al., 1992; Kumar and Liu, 1993). Characteristic compositions of these Be-rich phases are MBe_{13} for, e.g. M = Zr, or Hf, MBe_{12} for, e.g. M = Ti, Nb, Ta, or Mo, and M_2Be_{17} for, e.g. M = Ti, Zr, Hf, Nb, or Ta. Such phases and other Be-rich phases with similar compositions are formed with most other metals. The multitude of intermetallic Be phases is similar to that of the intermetallic rare earth phases, which are addressed in the next section. No beryllides have been observed in the Al-Be and Al-Si systems (Massalski et al., 1990). These Be-rich phases have complex cubic, tetragonal, or hexagonal crystal structures, and it has to be noted that the crystallographic data in standard compilations are controversial in some cases (Massalski et al., 1990; Villars and Calvert, 1991). Beryllides with less Be have simpler structures, e.g. the Laves phases MBe_2 with M = Cr, Mo, or Fe with a C14 structure and M = Ti, Nb, or Ta with a C15 structure (see Sec. 8.1), the B2 phases NiBe and TiBe (see Sec. 4.4), or the A15 phase Mo_3Be (see Sec. 7.1). Basic data can be found in early compilations (Shaffer, 1964; Samsonov and Vinitskii, 1980).

The Be-rich phases with Nb, Zr, or similar transition metals have been prepared by powder metallurgy methods (Marder and Stonehouse, 1988; Henager et al., 1992b), though ingot metallurgy methods have also been used (Nieh et al., 1990). Processing must be done with care because of the volatility and toxicity of Be (Stonehouse and Marder, 1990). The oxidation resistance is generally excellent due to the formation of protective BeO scales (Marder and Stonehouse, 1988; Grensing, 1989), though pest-like oxidation with specimen disintegration is observed in an intermediate temperature range aroung 800 °C for Nb and Zr beryllides (Westbrook and Wood, 1964; Ryba, 1967; Aitken, 1967; Chou et al., 1992). It is noted that beryllides have been proposed for applications as protective coatings, e.g. for Ta (Lawthers and Sama, 1993).

The mechanical behavior of these Be-rich phases and its variation with temperature has been studied by means of hardness tests, bending stress-rupture tests, tension tests and compression tests (Ryba, 1967; Marder and Stonehouse, 1988; Fleischer and Zabala, 1990c; Nieh and Wadsworth, 1990; Bruemmer et al., 1993). The observed brittle-to-ductile transition temperatures are of the order of 1000 °C. The low-temperature fracture toughness K_{Ic} has been found to be between 2 and 4 MN/m$^{3/2}$ with practically no macroscopic ductility (Bruemmer et al., 1993), though there are indications of local plasticity at

ArcelorMittal Ex. 2038
Page 129 of 190

indentations (Ryba, 1967). The bending rupture strengths show a maximum above 1000 °C (Marder and Stonehouse, 1988; Henager et al., 1992b; Bruemmer et al., 1993) which may be due to pest-like oxidation and premature brittle fracture below 1000 °C. The elastic constants have been determined (Fleischer et al., 1989b) as well as the thermal expansion coefficients, thermal conductivities and specific heats (Marder and Stonehouse, 1988).

Recent work has been concentrated on $NbBe_{12}$ with the tetragonal $D2_b$ structure, and the deformation behavior has been studied in detail (Henager et al., 1992b). The dislocation reactions at high temperatures have been analyzed and the slip systems have been identified (Bruemmer et al., 1992b), the dislocation core structures have been studied by atomistic modeling (Shondi et al., 1992), and the twinning behavior has been analyzed (Charlot et al., 1991; Sondhi et al., 1993). The mechanical behavior of $NbBe_{12}$ may be improved by combining $NbBe_{12}$ with other metallic or intermetallic phases, e.g. Be, Nb_2Be_{17}, or $NbBe_3$ in the binary Nb–Be system (Bruemmer et al., 1990, 1992a). Likewise $NbBe_{12}$, as well as $TiBe_{12}$, $ZrBe_{13}$, Nb_2Be_{17}, or Ta_2Be_{17}, have been proposed as the reinforcing phase in intermetallic matrix composites based on the B2 phase FeAl (Tien et al., 1992). In these and other composite systems chemical compatibility may be a problem since chemical reactions between the constituent phases affect the composite stability, as has been shown by combining $NbBe_{12}$ with other materials (Brimhall and Bruemmer, 1992) or $TiBe_{12}$ with NiAl (Carbone et al., 1988).

Besides these Be-rich phases, NiBe with the B2 structure is advantageous in view of its mechanical properties and its excellent oxidation resistance up to 1100 °C (Lee and Nieh, 1989; Nieh et al., 1990; Pharr et al., 1991). In particular it does not show pest-like oxidation at intermediate temperatures (Chou et al., 1992). It has an extended range of homogeneity (Massalski et al., 1990) which offers various possibilities for alloying. The simple B2 structure nourishes the expectation that the plastic deformation of NiBe is easier than that of the Be-rich phases. The room-temperature strength of NiBe shows a minimum at the stoichiometric composition, which is due not only to the strengthening effect of constitutional point defects for the off-stoichiometric compositions, as in the case of NiAl (see Sec. 4.3.3), but also to the strengthening effect of interstitially dissolved oxygen with a minimum solubility of O in NiBe at the stoichiometric composition (Nieh and Wadsworth, 1989; Nieh et al., 1989, 1990). Encapsulated NiBe can be hot forged and extruded at 1100 °C (Nieh et al., 1990). In view of the attractive properties of NiBe and the Be-rich phases, much more work is necessary for the optimization of the mechanical behavior, i.e. for improving the low-temperature toughness and for overcoming the related processing problems.

10 Rare-Earth Compounds

There is a multitude of intermetallic rare earth phases, since the rare earth metals have much larger sizes and lower electronegativities than most other metals, which gives many possibilities for space filling (Buschow, 1980). The complex crystal structures of these phases derive from a few basic structures, e.g. the cubic $D2_1$ structure or the hexagonal $D2_d$ structure, by stacking the structural units in different ways from which the various stoichiometries result (Herget and Domazer,

ArcelorMittal Ex. 2038
Page 130 of 190

Intermetallics
Gerhard Sauthoff
copyright © VCH Verlagsgesellschaft mbH, 1995

indentations (Ryba, 1967). The bending rupture strengths show a maximum above 1000 °C (Marder and Stonehouse, 1988; Henager et al., 1992b; Bruemmer et al., 1993) which may be due to pest-like oxidation and premature brittle fracture below 1000 °C. The elastic constants have been determined (Fleischer et al., 1989b) as well as the thermal expansion coefficients, thermal conductivities and specific heats (Marder and Stonehouse, 1988).

Recent work has been concentrated on $NbBe_{12}$ with the tetragonal $D2_b$ structure, and the deformation behavior has been studied in detail (Henager et al., 1992b). The dislocation reactions at high temperatures have been analyzed and the slip systems have been identified (Bruemmer et al., 1992b), the dislocation core structures have been studied by atomistic modeling (Shondi et al., 1992), and the twinning behavior has been analyzed (Charlot et al., 1991; Sondhi et al., 1993). The mechanical behavior of $NbBe_{12}$ may be improved by combining $NbBe_{12}$ with other metallic or intermetallic phases, e.g. Be, Nb_2Be_{17}, or $NbBe_3$ in the binary Nb–Be system (Bruemmer et al., 1990, 1992a). Likewise $NbBe_{12}$, as well as $TiBe_{12}$, $ZrBe_{13}$, Nb_2Be_{17}, or Ta_2Be_{17}, have been proposed as the reinforcing phase in intermetallic matrix composites based on the B2 phase FeAl (Tien et al., 1992). In these and other composite systems chemical compatibility may be a problem since chemical reactions between the constituent phases affect the composite stability, as has been shown by combining $NbBe_{12}$ with other materials (Brimhall and Bruemmer, 1992) or $TiBe_{12}$ with NiAl (Carbone et al., 1988).

Besides these Be-rich phases, NiBe with the B2 structure is advantageous in view of its mechanical properties and its excellent oxidation resistance up to 1100 °C (Lee and Nieh, 1989; Nieh et al., 1990; Pharr et al., 1991). In particular it does not show pest-like oxidation at intermediate temperatures (Chou et al., 1992). It has an extended range of homogeneity (Massalski et al., 1990) which offers various possibilities for alloying. The simple B2 structure nourishes the expectation that the plastic deformation of NiBe is easier than that of the Be-rich phases. The room-temperature strength of NiBe shows a minimum at the stoichiometric composition, which is due not only to the strengthening effect of constitutional point defects for the off-stoichiometric compositions, as in the case of NiAl (see Sec. 4.3.3), but also to the strengthening effect of interstitially dissolved oxygen with a minimum solubility of O in NiBe at the stoichiometric composition (Nieh and Wadsworth, 1989; Nieh et al., 1989, 1990). Encapsulated NiBe can be hot forged and extruded at 1100 °C (Nieh et al., 1990). In view of the attractive properties of NiBe and the Be-rich phases, much more work is necessary for the optimization of the mechanical behavior, i.e. for improving the low-temperature toughness and for overcoming the related processing problems.

10 Rare-Earth Compounds

There is a multitude of intermetallic rare earth phases, since the rare earth metals have much larger sizes and lower electronegativities than most other metals, which gives many possibilities for space filling (Buschow, 1980). The complex crystal structures of these phases derive from a few basic structures, e.g. the cubic $D2_1$ structure or the hexagonal $D2_d$ structure, by stacking the structural units in different ways from which the various stoichiometries result (Andersen et al., 1991).

Hanwha Mital Ex. 2038
Page 131 of 190

1975; Buschow, 1980). The crystallographic data of most binary, ternary, and quaternary rare earth phases have been compiled (Gladyshevskii and Bodak, 1982). The rare earth intermetallics are mostly line compounds and have only very narrow composition ranges. Preparation of the phases is difficult because of the high affinity of the rare earths for oxygen, which leads to reactions with common crucible materials, and various processes have been developed for the preparation of the intermetallic rare earth phases (Herget and Domazer, 1975).

10.1 Magnet Materials

The rare earth intermetallics are of great practical importance because of their outstanding magnetic properties, depending on the composition and crystal structure (Buschow, 1980, 1991). $SmCo_5$ and Sm_2Co_{17} have given rise to the development of the rare earth permanent magnets (REPMs), which excel by their high energy product $[\boldsymbol{B} \cdot \boldsymbol{H}]_{max}$ ($\boldsymbol{B}$ is the magnetic induction and $\boldsymbol{H}$ the magnetic field strength) and their high coercivity (Livingston, 1990; Buschow, 1991; Stadelmaier et al., 1991). Optimized property spectra have been achieved by alloying, i.e. substituting other rare earth metals for Sm and Fe and other transition metals as well as Cu for Co, and proper processing (Strnat, 1990). The resulting multinary materials have complex multiphase structures and the effects of the various structural features on the magnetic properties are not yet completely understood (Stadelmaier et al., 1988).

Alloying with the interstitials B, C, and N has led to ternary rare earth phases with very attractive magnetic properties, and outstanding examples are $Sm_2Fe_{17}C_x$, $Sm_2Fe_{17}N_x$, $Nd_2Fe_{14}B$, and $Nd_2Fe_{14}C$ (Buschow, 1986, 1991). $Nd_2Fe_{14}B$ has become the basis for the development of the Nd–Fe–B permanent magnets which have an even higher energy product $[\boldsymbol{B} \cdot \boldsymbol{H}]_{max}$ at room temperature than the $SmCo_5$-type and Sm_2Co_{17}-type materials at lower costs, whereas their behavior at elevated temperatures is less satisfactory (Strnat, 1990; Buschow, 1991). The various REPM materials, $SmCo_5$-type, Sm_2Co_{17} type, and $Nd_2Fe_{14}B$-type, are produced primarily by powder metallurgy techniques though ingot metallurgy and rapid solidification have also been used (Herget and Domazer, 1975; Ormerod, 1988; Croker, 1990; Strnat, 1990; Buschow, 1991; Steinhorst, 1992). The materials are brittle, which makes machining difficult, and their corrosion resistance is lower, which necessitates protective coatings in corrosive environments. $SmCo_5$ suffers an environmental degradation of coercivity which is due to hydrogen absorption (Willems and Buschow, 1987). Hydrogenation of the Nd–Fe–B alloys leads to structure transformation and decomposition reactions, and is used for producing fine-grained Nd–Fe–B powders (Harris and McGuiness, 1991). Because of their most advantageous combination of properties, the rare earth magnets have found a huge market with a broad field of applications (Strnat, 1990; Buschow, 1991).

10.2 Hydrogen Storage Materials

Apart from applications as magnet materials, various rare earth phases can absorb large amounts of hydrogen and are of high interest for applications as hydrogen storage materials, as is exemplified by RCo_3 and RFe_3 (Christodoulou and Takeshita, 1993a), or the rare earth Laves phases, which have been addressed in Sec. 8.2.3. The most outstanding exam-

ArcelorMittal Ex. 2038
Page 132 of 190

ple is given by the RNi_5 phases – in particular $LaNi_5$ which may be regarded as a prototype hydrogen storage material, and which is considered for applications as rechargeable electrodes in electrochemical nickel-hydrogen batteries (Reilly, 1979; Willems and Buschow, 1987). The crystal structure of the ternary hydride $LaNi_5H_x$ and the similar RCo_5H_x is complex and various models have been proposed for the distribution of the H atoms which are still in discussion (Somenkov and Shilstein, 1979; Willems and Buschow, 1987). The stability of $LaNi_5$ is affected by absorption-desorption cycling which is due to surface degradation processes (see e.g. Uchida et al., 1991; Josephy et al., 1991). The property spectrum has been optimized by alloying with further elements as is exemplified by the development of $La_{0.8}Nd_{0.2}Ni_{2.5}Co_{2.4}Si_{0.1}$ (Willems and Buschow, 1987) or $MmNi_{3.5}Co_{0.7}Al_{0.8}$ where Mm stands for mischmetall, which is a mixture of rare earth metals (Sakai et al., 1991). The permanent-magnet phase $SmCo_5$ can also absorb large quantities of hydrogen which, however, reduces its coercive force (Buschow, 1991). It is noted that $CaNi_5$, which is isostructural with $LaNi_5$, shows an analogous behavior and is considered as a low-cost candidate phase for hydrogen storage (Yagisawa and Yoshikawa, 1979).

11 Silicides

The transition metal silicides show close similarities to the intermetallics and thus they are frequently classed with the intermetallics though silicon is no longer a metal, but a semiconductor. Silicides are generally hard and brittle with a metallic luster, high electrical and thermal conductivities, a positive temperature coefficient of resistivity, and paramagnetism (Westbrook, 1960b; Nowotny, 1963; Wehrmann, 1967; Goldschmidt, 1967b). In detail the type of bonding and the electrical conductance depend on the metal-to-silicon ratio and on the particular metal M. The highest metallicity is manifested by the metal-rich silicides M_3Si and M_2Si, in which the Si atoms are isolated. The lower the M/Si ratio, the lower the metallicity, and the more readily continuous Si chains or networks are formed in the crystal lattice (Goldschmidt, 1967b). However, it has to be emphasized that the situation is rather complex, e.g. the disilicide $CrSi_2$ with the hexagonal C40 structure is indeed a semiconductor, whereas $NbSi_2$ with the same crystal structure and $MoSi_2$ with the C40 structure at very high temperatures and the closely related tetragonal $C11_b$ structure at lower temperatures (Massalski et al., 1990) are metallic (Nowotny, 1963, 1972a; Goldschmidt, 1967b). Likewise FeSi and CoSi – both with the cubic B20 structure – form a continuous series of solid solutions with a transition from semiconduction for the Fe-rich phases to metallic conduction for the Co-rich phases (Romasheva et al., 1980), which affects the magnetic properties and the elastic behavior (Zinov'eva et al., 1984).

Silicides were considered for high-temperature applications 40 years ago because of their high strength and oxidation resistance at high temperatures (Lowrie, 1952; Fitzer, 1952; Schwarzkopf and Kieffer, 1953; Arbiter, 1953b; Wehrmann, 1956). This interest initiated extended research activities with a screening of the physical and mechanical properties, and the results have been the subject of detailed reviews and data compilations (Westbrook, 1960b; Shaffer, 1964; Hove and Riley, 1967; Wehrmann, 1967; Goldschmidt, 1967b; Samsonov and Vinitskii, 1980). The phase

ArcelorMittal Ex. 2038
Page 133 of 190

Intermetallics
Gerhard Sauthoff
copyright © VCH Verlagsgesellschaft mbH, 1995

ple is given by the RNi_5 phases – in particular $LaNi_5$ which may be regarded as a prototype hydrogen storage material, and which is considered for applications as rechargeable electrodes in electrochemical nickel-hydrogen batteries (Reilly, 1979; Willems and Buschow, 1987). The crystal structure of the ternary hydride $LaNi_5H_x$ and the similar RCo_5H_x is complex and various models have been proposed for the distribution of the H atoms which are still in discussion (Somenkov and Shilstein, 1979; Willems and Buschow, 1987). The stability of $LaNi_5$ is affected by absorption-desorption cycling which is due to surface degradation processes (see e.g. Uchida et al., 1991; Josephy et al., 1991). The property spectrum has been optimized by alloying with further elements as is exemplified by the development of $La_{0.8}Nd_{0.2}Ni_{2.5}Co_{2.4}Si_{0.1}$ (Willems and Buschow, 1987) or $MmNi_{3.5}Co_{0.7}Al_{0.8}$ where Mm stands for mischmetall, which is a mixture of rare earth metals (Sakai et al., 1991). The permanent-magnet phase $SmCo_5$ can also absorb large quantities of hydrogen which, however, reduces its coercive force (Buschow, 1991). It is noted that $CaNi_5$, which is isostructural with $LaNi_5$, shows an analogous behavior and is considered as a low-cost candidate phase for hydrogen storage (Yagisawa and Yoshikawa, 1979).

11 Silicides

The transition metal silicides show close similarities to the intermetallics and thus they are frequently classed with the intermetallics though silicon is no longer a metal, but a semiconductor. Silicides are generally hard and brittle with a metallic luster, high electrical and thermal conductivities, a positive temperature coefficient of resistivity, and paramagnetism (Westbrook, 1960b; Nowotny, 1963; Wehrmann, 1967; Goldschmidt, 1967b). In detail the type of bonding and the electrical conductance depend on the metal-to-silicon ratio and on the particular metal M. The highest metallicity is manifested by the metal-rich silicides M_3Si and M_2Si, in which the Si atoms are isolated. The lower the M/Si ratio, the lower the metallicity, and the more readily continuous Si chains or networks are formed in the crystal lattice (Goldschmidt, 1967b). However, it has to be emphasized that the situation is rather complex, e.g. the disilicide $CrSi_2$ with the hexagonal C40 structure is indeed a semiconductor, whereas $NbSi_2$ with the same crystal structure and $MoSi_2$ with the C40 structure at very high temperatures and the closely related tetragonal $C11_b$ structure at lower temperatures (Massalski et al., 1990) are metallic (Nowotny, 1963, 1972a; Goldschmidt, 1967b). Likewise FeSi and CoSi – both with the cubic B20 structure – form a continuous series of solid solutions with a transition from semiconduction for the Fe-rich phases to metallic conduction for the Co-rich phases (Romasheva et al., 1980), which affects the magnetic properties and the elastic behavior (Zinov'eva et al., 1984).

Silicides were considered for high-temperature applications 40 years ago because of their high strength and oxidation resistance at high temperatures (Lowrie, 1952; Fitzer, 1952; Schwarzkopf and Kieffer, 1953; Arbiter, 1953b; Wehrmann, 1956). This interest initiated extended research activities with a screening of the physical and mechanical properties, and the results have been the subject of detailed reviews and data compilations (Westbrook, 1960b; Shaffer, 1964; Hove and Riley, 1967; Wehrmann, 1967; Goldschmidt, 1967b; Samsonov and Vinitskii, 1980; Thalmann, 1986).

Arconic Mital Ex. 2038
Page 134 of 190

diagrams of ternary systems of interest have been analyzed (e.g. Kudielka and Nowotny, 1956; Brukl et al., 1961; Schob et al., 1962; Bardos et al., 1966; Gladyshevskii and Borusevich, 1966; Skolozdra et al., 1966a, b), as well as the crystal structures and the crystal chemistry of the various silicides (Nevitt, 1963, 1967; Nowotny, 1963, 1972a; Nowotny and Benesovsky, 1967; Jeitschko et al., 1969; Jeitschko, 1977).

Only one successful development emerged from these early efforts, and it led to the application of $MoSi_2$ as heating elements in high-temperature furnaces (Fitzer and Rubisch, 1958; Tamura, 1961; Schrewelius and Magnusson, 1966; Schlichting, 1986). Later, protective coatings on metallic alloys made use of the advantageous oxidation resistances of various silicides (e.g. Hildebrandt et al., 1978; Fitzer et al., 1978; Caillet et al., 1978; Fitzer and Schlichting, 1983; Meier, 1987; Packer, 1989). The advantageous electrical properties of various silicides have led to important applications as thin films in microelectronic devices (Nicolet and Lau, 1983; Murarka, 1983a, 1984). In view of such applications, the electrical resistivities, thermodynamical properties, thin-film formation kinetics and diffusivities of the transition-metal silicides were reviewed (Murarka, 1983b). Presently, the need for new structural materials for the highest temperatures has revived the interest in silicides for structural applications, and respective developments are under way (Kumar and Liu, 1993). In the following sections a brief overview is given on the important features of those silicides which have already been applied or are being considered for applications.

11.1 M_3Si Phases

Cr_3Si, which is a çandidate phase for high-temperature applications, and V_3Si, which is superconducting at low temperatures with a comparatively high transition temperature, both crystallize with the topologically close-packed cubic, A15 structure and have been discussed in Secs. 7.7 and 7.2, respectively.

A metal-rich silicide with a very simple crystal structure is Ni_3Si with the ordered f.c.c. $L1_2$ structure. It has a very high potential for structural applications because of its advantageous mechanical properties and its outstanding corrosion resistance. Its deformation behavior is similar to that of other $L1_2$ phases, in particular Ni_3Al, and thus Ni_3Si has been discussed in Sec. 4.2.2 together with other $L1_2$ phases.

The ordered b.c.c. $D0_3$ structure is adopted by Fe_3Si which shows close similarities to Fe_3Al (see Sec. 5.1). According to the generally accepted phase diagram (Schlatte and Pitsch, 1976; Kubaschewski, 1982), the $D0_3$ structure of Fe_3Si is stable up to about 800 °C (for the stoichiometric composition) where it transforms to the B2 structure, and at about 1000 °C Fe_3Si disorders to form the b.c.c. solid solution. The existence of the B2 structure has been questioned on the basis of neutron scattering results (Hilfrich et al., 1990) which, however, are not unambiguous (Inden, 1993). The deformation behavior of Fe_3Si has been analyzed in detail to study the effects of atomic order on the mechanical properties (Saburi et al., 1968; Lakso and Marcinkowski, 1974; Marcinkowski, 1974a; Ehlers and Mendiratta, 1984; Oertel et al., 1986). Elastic moduli and dislocation line energies have been determined (Kötter et al., 1989) as well as vacancy formation energies (Schaefer et al., 1992), and diffusion mechanisms (Sepiol

ArcelorMittal Ex. 2038
Page 135 of 190

and Vogl, 1993). The electron distribution in Fe_3Si has been studied with respect to the effects of ordering on the magnetic behavior (Himsel et al., 1980; Blau et al., 1980). The ternary $Fe_3(Si,Al)$ exhibits a high magnetic permeability and has found widespread application as a magnetic recording-head material known as Sendust alloy (Yamamoto, 1980; Brock, 1986). The magnetic properties can be optimized by proper alloying (Yamamoto and Utsushikawa, 1977; Miyazaki et al., 1992), and the processing problems due to brittleness have been overcome (Watanabe et al. 1984; Shao et al., 1991). Fe_3Si has also been applied as a structural material because of its excellent corrosion resistance (Liu et al., 1990; Lou et al., 1991; Kumar and Liu, 1993).

11.2 M_2Si Phases

M_2Si phases may be present in protective coatings (Hildebrandt et al., 1978; Meier, 1987). High-temperature structural applications are expected for the lightweight phase Mg_2Si which is regarded as highly promising for use as pistons in car engines (Schmid et al., 1990; von Oldenburg et al., 1990). Mg_2Si crystallizes with the f.c.c. *C1* structure with 12 atoms per unit cell, and its density is only 1.88 g/cm^2. The mechanisms of slip, twinning, and cleavage have been discussed (Paufler and Schulze, 1978). Mg_2Si has a comparatively high strength and a low thermal expansion coefficient. However, its brittleness with a brittle-to-ductile transition temperature of 450 °C precludes the use of single-phase Mg_2Si. The methods of induction melting have been studied in detail for various Mg_2Si alloys (G. H. Li et al., 1993). The ternary system Mg–Si–Al (Lüdecke, 1986) offers various possibilities for alloying in order to combine Mg_2Si with a second ductile phase which may relieve the brittleness. Indeed alloying with Al produces Al–Mg_2Si alloys with brittle Mg_2Si particles in a ductile Al matrix, which has given rise to a successful on-going alloy development (Schmid et al., 1990; von Oldenburg et al., 1990). The effect of the distribution of particles on the deformation behavior has been studied for model Al–Mg_2Si alloys (Liu, 1989).

Mg_2Si is a semiconductor with a high thermoelectric power and a low thermal conductivity which is advantageous for thermoelectric power generation (Noda et al., 1992a, b). The thermal conductivity can be minimized by alloying with Ge to form the ternary $Mg_2(Si,Ge)$ phase. Doping with Ag and Sb produces p-type and n-type semiconducting $Mg_2(Si,Ge)$, respectively, and the combination of both results in a thermocouple with a high efficiency for thermoelectric energy conversion. The interactions between doping, point defects and microstructure have been studied in detail (Andreyeva et al., 1988).

Metal-like M_2Si phases, as well as other transition metal silicides, are of great importance for applications as thin-film materials in electronic devices, i.e. as low-resistivity interconnects and gates, ohmic contacts, and Schottky barriers in very-large-scale-integrated circuits (VLSI) (Nicolet and Lau, 1983; Murarka, 1983a, 1984). The most eminent example is Pd_2Si which is used for shallow contacts with very small, controlled thickness and extension (Chapman et al., 1979; Kritzinger and Tu, 1981). The kinetics of thin-film formation and growth are controlled by diffusion and can be optimized by alloying with further elements (Mayer et al., 1979; Olowolafe et al., 1979; Tu et al., 1980; Eizenberg et al., 1981; Eizenberg and Tu, 1982). The film formation process affects

ArcelorMittal Ex. 2038
Page 136 of 190

the distribution of dopants in the Si substrate (Wittmer and Seidel, 1978; Kikuchi, 1983; Wittmer et al., 1983). The rate controlling mechanisms of the film formation process with nucleation and growth have been analyzed in detail (d'Heurle and Gas, 1986; d'Heurle, 1993a, b). Other M_2Si phases have also been studied with respect to thin-film formation, e.g. Ni_2Si (d'Heurle et al., 1984; Aly and Stark, 1984), Co_2Si (Hattori et al., 1988; Chen and Chang, 1993), or Mg_2Si (Lim and Stark, 1984). Diffusion in thin films has been analyzed and compared with bulk diffusion (Tu et al., 1983). Thin oxide layers may form on the silicide films by air exposure at room temperature which can be a problem for ohmic contacts or a necessity for a tunneling device (Cros, 1983).

The partial substitution of the transition element M in M_2Si by a second transition metal M′ leads to ternary silicides of approximate composition MM′Si corresponding to $(M,M')_2Si$. Such ternaries are primarily the Si-containing E phases and V phases (Jeitschko et al., 1969; Jeitschko, 1970) and the ternary Si-containing Laves phases (Bardos et al., 1961), which were discussed in Sec. 8, as well as many other phases, which all differ by composition and crystal structure (Nowotny, 1972a). This is exemplified by the Fe–Nb–Si system with the ternary silicides E, V, τ_1, τ_2, τ_3 and the Laves phase $Nb(Fe,Si)_2$ with up to 25 at.% Si (Raghavan, 1987), or the Co–Nb–Si system with the ternary silicides E, T, ν, η, ψ, and the ternary Laves phase $Nb(Co,Si)_2$ with Si contents between about 10 and 20 at.% (Argent, 1984). Finally, it is noted that other phases – in particular σ phases and A13 Mn-base phases – dissolve large amounts of Si by which these phases are stabilized (Gupta et al., 1960; Bardos et al., 1966).

11.3 M_5Si_3 Phases

The M_5Si_3 phases adopt a variety of complex crystal structures (Franceschi and Ricaldone, 1984). The transition-metal M_5Si_3 phases crystallize primarily with the tetragonal $D8_m$ structure, e.g. for M = V, Cr, Mo, or W, or the hexagonal $D8_8$ structure, e.g. for M = Mn, or Ti (Franceschi and Ricaldone, 1984; Massalski et al., 1990). Most of these phases are very stable, congruently melting line compounds with melting temperatures above 2000 °C. However, Fe_5Si_3 with a $D8_8$ structure is stable only between 825 and 1060 °C, and Cr_5Si_3 with a $D8_m$ structure undergoes a polymorphic transformation above 1500 °C (Massalski et al., 1990). Nb_5Si_3 and Ta_5Si_3 exhibit the $D8_m$ structure at low temperatures and the likewise tetragonal $D8_1$ structure at high temperatures (Parthé et al., 1955; Massalski et al., 1990). Various tetragonal M_5Si_3 phases, e.g. for M = V, Nb, Ta, Cr, Mo, or W, as well as Hf_5Si_3, crystallize with the $D8_8$ structure if they contain small amounts of interstitial impurities, in particular carbon (Parthé et al., 1955; Goldschmidt, 1967b; Franceschi and Ricaldone, 1984). Such a stabilization effect of interstitial impurities has also been observed for other intermetallics (Gschneidner, 1993).

The most attractive M_5Si_3 phase for structural high-temperature applications is Ti_5Si_3 with the hexagonal $D8_8$ structure because of its high stability with a melting temperature of 2130 °C, its high strength and hardness, and its low density (Liu et al., 1988; Beaven et al., 1989; Rosenkranz et al., 1992; Kumar and Liu, 1993). Density data between 4.0 and 4.5 g/cm^3 have been reported (Shaffer, 1964; Beaven et al., 1989; Fleischer and Zabala, 1990a; Frommeyer et al., 1990) as well as a Young's modulus of about 150 GPa (Beav-

ArcelorMittal Ex. 2038
Page 137 of 190

en et al., 1989; Frommeyer et al., 1990) and an anisotropic thermal expansion coefficient of about 6×10^{-6}/K (Frommeyer et al., 1990; Nakashima and Umakoshi, 1992). The outstanding strength of Ti_5Si_3 is correlated with a very low fracture toughness and a brittle-to-ductile transition temperature above 1000 °C (Liu et al., 1988; Frommeyer et al., 1990; Vehoff, 1992; Vehoff et al., 1993). The oxidation resistance of Ti_5Si_3 is not as high as that of NiAl, but higher than that of TiAl (Liu et al., 1988; Murata et al., 1991; Thom et al., 1993).

As with other intermetallics, it is expected that the brittleness of Ti_5Si_3 can be relieved by combining it with other less brittle phases. The crack tendency in Ti_5Si_3 can indeed be reduced by reducing the Si content and alloying with Cr and Zr to produce three-phase, Ti_5Si_3-base alloys (Liu et al., 1988). Eutectic, unidirectionally solidified Ti–Ti_5Si_3 alloys show advantageous combinations of strength, creep resistance, and fracture toughness (Crossman and Yue, 1971; Frommeyer et al., 1990). A promising materials development is based on the combination of Ti_3Al and Ti_5Si_3 (Wu et al., 1989). Such Ti_3Al–Ti_5Si_3 alloys, which are further alloyed with Nb, and similar alloys have been studied with respect to phase equilibria (J. S. Wu et al., 1991), microstructure–property relationships (Wagner et al., 1991), creep (Es-Souni et al., 1992a, d) and fracture toughness (Vehoff, 1992, 1993). Besides ingot metallurgy, powder metallurgy methods with gas-atomization (Es-Souni et al., 1992b, c) have been used as well as mechanical alloying (Calka et al., 1991), and combustion synthesis has also been considered (Bhaduri, 1992). Ti_5Si_3 has been proposed as a constituent phase in composites (Kumar, 1991; Shah and Anton, 1992b), i.e. as the matrix phase with ceramic reinforcements (Meschter and Schwartz, 1989; Bhattacharya, 1991) or as the reinforcing phase in an $MoSi_2$ matrix (Wiedemeier and Singh, 1992; Schwartz et al., 1993).

Another candidate phase for high-temperature applications is Nb_5Si_3 with a melting temperature of 2484 °C (Massalski et al., 1990), which is still more stable than Ti_5Si_3 and which shows the above-mentioned polymorphism. Again its brittleness precludes the application of single-phase Nb_5Si_3. However, the reduction in the Si content leads to two-phase Nb_5Si_3–Nb alloys with ductile Nb-rich particles in the brittle Nb_5Si_3 matrix (Lewandowski et al., 1988). These alloys show improved toughness because of crack-bridging (Rigney et al., 1991; Mendiratta et al., 1991; Mendiratta and Dimiduk, 1993). The phase relationships in these alloys and the effects of rapid solidification have been studied (Cockeram et al., 1991; Bertero et al., 1991b). Nb_5Si_3 is subject to pest-like oxidation (Westbrook and Wood, 1964), and Nb_5Si_3–Nb alloys are embrittled by oxygen and hydrogen exposure (Rigney et al., 1992).

Other M_5Si_3 phases are less attractive for applications, and thus they have been studied less. M_5Si_3 phases can be synthesized by mechanical alloying, which leads to amorphization in the case of Ta_5Si_3 (Kumar and Mannan, 1989). Y_5Si_3 and the ternary $Y_5(Si,Ge)_3$ are of interest for use as hydrogen storage materials (McColm and Ward, 1992).

11.4 MSi Phases

The transition metal silicides CrSi, MnSi, FeSi, and CoSi crystallize with the cubic B20 structure whereas NiSi and the noble metal silicides PtSi, IrSi, and PdSi crystallize with the orthorhombic B31

ArcelorMittal Ex. 2038
Page 138 of 190

structure (Massalski et al., 1990). MSi phases – in particular PtSi and also NiSi – are important thin-film materials for applications in electronic devices (see, e.g. Eizenberg et al., 1981; Cohen et al., 1982; Murarka, 1984; Tu et al., 1983; Appelbaum et al., 1984). These phases have been studied in close contact with the work on Pd_2Si, which was addressed in Sec. 11.2, and the respective cited publications are usually directed at the ensemble of thin-film silicides of interest. Besides electronic applications, NiSi is of interest as a constituent phase in oxidation resistant coatings (Meier, 1987) and as a heat storage material with high thermal conductivity (Wilson and Cavin, 1992). IrSi forms in $MoSi_2$/Ir layers which are considered for the coating of carbon–carbon composites (Chou, 1990; Chou and Nieh, 1990). MnSi and CoSi exhibit large thermoelectric powers (Samsonov and Vinitskii, 1980) and thus are promising for thermoelectric power generation (Sakata and Nishida, 1976). In particular, a CoSi–$CrSi_2$ thermogenerator has been proposed (Sakata and Tokushima, 1963).

11.5 Disilicides

The transition metal MSi_2 phases with M = Ti, Zr, Hf, V, Nb, Ta, Cr, Mo, or W crystallize with the tetragonal $C11_b$ structure, the hexagonal C40 structure or the orthorhombic C49 and C54 structures and show extended mutual solid-solubilities (Kudielka and Nowotny, 1956). These crystal structures are closely related since they only differ in the different stacking of the same structural elements (Nowotny, 1963).

$MoSi_2$ with a $C11_b$ structure has found widespread use as heating elements in high-temperature furnaces for temperatures up to 1700 °C because of its advantageous electrical properties and its excellent oxidation resistance (Fitzer and Rubisch, 1958; Tamura, 1961; Schrewelius and Magnusson, 1966; Schlichting, 1986). This high oxidation resistance, which is not shown by the other Mo-rich silicides, is due to the formation of a protective, vitreous, highly adherent SiO_2 film with prior evaporation of the volatile Mo oxide (Fitzer, 1955; Kieffer and Benesovsky, 1956; Lee et al., 1991; Meier and Pettit, 1992). However, $MoSi_2$ is subject to oxidative disintegration by pest-like oxidation at intermediate temperatures between about 300 °C and 600 °C (Fitzer, 1955; Westbrook and Wood, 1964; Chou and Nieh, 1993 a), which occurs at grain boundaries and microstructural defects and can thus be minimized by avoiding grain boundaries and microstructural defects (Chou and Nieh, 1993 b) or by alloying with small amounts of Fe and Re (Ban and Ogilvie, 1966). This high oxidation resistance makes $MoSi_2$ attractive for use as a protective coating (Fitzer, 1952; Motojima et al., 1982; Packer, 1989; Chou, 1990; Petrovic, 1993). Apart from these high-temperature applications, $MoSi_2$ is advantageous for applications in electronic devices – either as the substrate for Si films (Campisi et al., 1981) or as thin-film interconnectors in VLSI circuits (see e.g. Chow et al., 1980; Murarka, 1984; Urwank et al., 1985; and compare with Sec. 11.2). The kinetics of silicide formation in thin films have been analyzed in detail (d'Heurle, 1993 b).

Presently $MoSi_2$ is being considered for structural, high-temperature applications and various materials developments are in progress (Lugscheider et al., 1991; Kumar and Liu, 1993; Petrovic, 1993; Hardwick et al., 1993). The elastic constants are known (Nakamura et al., 1990; Nakamura, 1991; Srinivasan and Schwarz, 1992), and the plastic deformation behavior

ArcelorMittal Ex. 2038
Page 139 of 190

has been analyzed with respect to dislocation configurations and slip systems (Umakoshi et al., 1990a, b; Maloy et al., 1992; Evans et al., 1993; Rao et al., 1993), twinning (Mitchell et al., 1992), and creep (Tamura, 1961; Kimura et al., 1990; Sadananda and Feng, 1993). The brittle-to-ductile transition occurs at about 1000 °C or higher temperatures depending on the microstructure and the impurity content (Umakoshi et al., 1991; Aikin, 1992; Srinivasan et al., 1993; Petrovic, 1993). The ductility and toughness of $MoSi_2$ can be improved by special processing routes (e.g. Tiwari et al., 1991; Castro et al., 1992; Patankar and Lewandowski, 1993), microalloying with C to avoid SiO_2 layers on the grain boundaries (Maloy et al., 1991; Jayashankar and Kaufman, 1992), the application of soft, dislocation emitting surface films (Czarnik et al., 1993), or the insertion of a ductile second phase which is usually a Nb-rich phase (Lu et al., 1991; Xiao and Abbaschian, 1992; Venkkateswara Rao et al., 1992; Alman and Stoloff, 1992). Toughness can also be increased by embedding hard second phases, in particular ceramics, in an $MoSi_2$ matrix in order to hinder crack growth (see e.g. Bhattacharya and Petrovic, 1991; H. Chang et al., 1992).

In view of the beneficial effects of second phases, combinations of $MoSi_2$ with other phases are being studied with the aim of developing new $MoSi_2$-based composites (Meschter and Schwartz, 1989; Shah et al., 1990; Yang et al., 1990; Boettinger et al., 1992; Petrovic and Vasudevan, 1992; Wiedemeier and Singh, 1992; Petrovic, 1993; Sadananda and Feng, 1993). Most work has been concentrated on the $MoSi_2$–SiC system (Bhattacharya and Petrovic, 1991; Henager et al., 1992a; Jayashankar and Kaufman, 1992; Suzuki et al., 1992; Alman and Stoloff, 1993; Feng and Michel, 1993; Jeng et al., 1993; Ting, 1993). Other systems of particular interest are $MoSi_2$–TiC (Yang and Jeng, 1990; Chang and Gibala, 1993) and $MoSi_2$–Al_2O_3 (Alman et al., 1991; Y. S. Kim et al., 1991; Meschter, 1991), as well as the eutectics $MoSi_2$–Mo_5Si_3 (Mason and Van Aken, 1993) and $MoSi_2$–$Er_2Mo_3Si_4$ (Patrick and Van Aken, 1993) and the ductile-phase toughened $MoSi_2$–Nb/Ta (Carter and Martin, 1990; Lu et al., 1991; Alman and Stoloff, 1992; Venkkateswara Rao et al., 1992), and $MoSi_2$–Mo systems (Dève et al., 1992). Furthermore, $MoSi_2$ has been considered as a reinforcing phase in other composite systems, e.g. in an SiC matrix (Lim et al., 1989) or in a beryllide matrix (Bruemmer et al., 1993).

WSi_2 with a tetragonal $C11_b$ structure is another disilicide with a high oxidation resistance which relies on the formation of a vitreous, dense, adherent SiO_2 scale at high temperatures, as in the case of $MoSi_2$ (Kieffer and Benesovsky, 1956). At intermediate temperatures pest-like oxidation occurs (Westbrook and Wood, 1964). The elastic constants of WSi_2 (Nakamura, 1991) and the plastic deformation at high temperatures (Kimura et al., 1990) have been studied. Apart from possible high-temperature applications (Kumar and Liu, 1993), WSi_2 is of interest for thin-film applications in electronic devices (see, e.g. Olowolafe et al., 1979; Murarka. 1984).

$TiSi_2$ with an orthorhombic C54 structure is protected against oxidation by a vitreous, adherent TiO_2–SiO_2 scale (Kieffer and Benesovsky, 1956; Rahmel and Spencer, 1991). In view of its high oxidation resistance and its low density, $TiSi_2$ has been considered for structural applications at high temperatures (Lugscheider et al., 1991; Rosenkranz et al., 1992; Kumar and Liu, 1993). It can be synthesized by mechanical alloying (Calka et al.,

ArcelorMittal Ex. 2038
Page 140 of 190

1991; Matteazzi et al., 1992), single crystals have been prepared (Thomas et al., 1987; Peshev et al., 1989), and the microstructure has been analyzed (Jia et al., 1989). Data for thermal expansion, elastic moduli, hardness, yield strength, creep resistance, and toughness have been obtained (Lugscheider et al., 1991; Rosenkranz and Frommeyer, 1992; Vehoff, 1993). Apart from eventual high-temperature applications (Kumar and Liu, 1993), $TiSi_2$ is of interest for thin-film applications in electronic devices (see, e.g. Murarka, 1984).

$ZrSi_2$ with the orthorhombic C49 structure shows attractive physical and mechanical properties with respect to structural high-temperature applications (Rosenkranz and Frommeyer, 1992). Like other disilicides, it has a low fracture toughness with a brittle-to-ductile transition temperature of about 900 °C (Vehoff, 1993). A $ZrSi_2$ coating on Zr provides good oxidation resistance (Caillet et al., 1978) though bulk $ZrSi_2$ does not form dense, adherent scales on oxidation (Kieffer and Benesovsky, 1956).

The disilicides VSi_2, $NbSi_2$, and $TaSi_2$ crystallize with the hexagonal C40 structure (Kudielka and Nowotny, 1956). The elastic constants of VSi_2 have been determined (Fleischer et al., 1989 b; Nakamura, 1991), as well as its hardness and apparent brittle-to-ductile transition temperature (Fleischer et al., 1990). VSi_2 is of interest for applications in electronic devices and its thin-film formation reactions have been studied (Lim and Stark, 1984). $TaSi_2$ has been successfully used in producing microprocessors and other electronic devices (Murarka, 1984). The mechanisms of thin-film formation of $TaSi_2$ have been studied in detail (see, e.g. Maa et al., 1985; Natan, 1985; Nava et al., 1985).

$CrSi_2$ with a hexagonal C40 structure is being considered for high-temperature applications (Kumar and Liu, 1993) though it does not form dense, adherent, protective oxide scales at 1200 °C (Kieffer and Benesovsky, 1956; Grabke and Brumm, 1989). Single crystals have been prepared (Peshev et al., 1989), and the elastic properties (Nakamura, 1991), and the plastic deformation behavior have been studied (Umakoshi et al., 1991). $CrSi_2$ is of interest for applications as thin-film interconnectors in electronic devices (Tu et al., 1980; Appelbaum et al., 1984). It exhibits a large thermoelectric power (Samsonov and Vinitskii, 1980; Nishida and Sakata, 1978), and it has been proposed for application as thermoelectric material, e.g. in a $CrSi_2$–CoSi thermogenerator for thermoelectric power generation (Sakata and Tokushima, 1963; Ohkoshi et al., 1988).

$FeSi_2$ is another disilicide with a high thermoelectric power and has been proposed for use in a thermoelectric power generator (Hesse, 1969 b). It has an orthorhombic crystal structure and is stable only at lower temperatures, whereas at higher temperatures it decomposes to form a two-phase FeSi–Fe_2Si_5 alloy (Nishida, 1973; Kojima et al., 1990). Furthermore, it is subject to pest-like oxidation (Westbrook and Wood, 1964). Doping with Al produces p-type conducting $FeSi_2$, doping with Co produces n-type $FeSi_2$, and the combination of both materials gives a thermocouple which can be used as a thermoelectric power generator (Hesse, 1969 a).

$CoSi_2$, which crystallizes with the comparatively simple cubic C1 structure, is applied in electronic, large scale integration devices and the conditions for thin-film formation have been studied (see, e.g. Pretorius et al., 1985; Catana et al., 1992; Mantl, 1993; Kumar, 1994). In view of its simple crystal structure, $CoSi_2$ is expected to show plastic deformability and is considered for structural applications (Ya-

ArcelorMittal Ex. 2038
Page 141 of 190

maguchi et al., 1993). The Co–Si phase diagram has been analyzed (Ishida et al., 1991 b; Choi, 1992), the electron distribution has been studied by ab initio calculations (Sen Gupta and Chatterjee, 1986), the formation enthalpy of vacancies has been determined by positron annihilation (Ito et al., 1993), an excellent oxidation resistance has been found (Anton and Shah, 1989), and the plastic deformation behavior has been analyzed in detail with respect to dislocation configurations and slip systems (Takeuchi et al., 1991, 1992; Ito et al., 1992; Suzuki and Takeuchi, 1993; Yamaguchi et al., 1993; Anongba and Steinemann, 1993).

$NiSi_2$ is of primary interest for applications in electronic thin-film devices (Kumar, 1994). In view of these applications, the conditions for thin-film formation have been studied in detail for $NiSi_2$ (see, e.g. Tu et al., 1983; d'Heurle et al., 1984; Singh and Khokle, 1987) and likewise the formation of thin oxide layers on $NiSi_2$ (Cros, 1983). Apart from these applications, the termal expansion behavior of $NiSi_2$ has been studied with respect to use as a heat storage material (Wilson and Cavin, 1992). Finally, it is noted that the alloying of $NiSi_2$ with Ni and Al produces phases with distinct color – pale blue, yellow, white, and variations of these – which may be of interest for applications in jewellery (Cortie et al., 1991).

12 Prospects

As already stated in the introduction to this chapter, only a restricted selection of intermetallics could be assessed here. An enormous multitude of intermetallic phases is known (Villars and Calvert, 1991), and there are many phases which were not mentioned in the preceding sections and which are of interest, e.g. as strengthening or embrittling phases in commercial metallic alloys. This is illustrated by the topologically close-packed μ, σ, χ, and related phases (Nevitt, 1963; Bardos et al., 1966; Benjamin et al., 1966; Hall and Algie, 1966; Sinha, 1973) which pose problems in many metallic alloy systems because of their embrittling effects, but which may also be used as strengthening phases if adequately distributed (Pickering, 1976; Bhandarkar et al., 1976; Gaspard et al., 1977; Sauthoff and Speller, 1982; Schumacher and Sauthoff, 1987; Sha et al., 1993). Most of the less known phases have not been studied sufficiently to establish a database which allows estimates of their potential for applications. Thus there is a great need for the determination of the basic properties – in particular constitution, phase diagrams, densities, electrical and thermal conductivities, elastic constants, and diffusion coefficients – of the less known intermetallics.

As to the better known phases, which have been selected for materials developments or are regarded as candidate phases for new developments, the physical understanding of their properties and their behavior during processing and service is still insufficient, which impedes the progress of the present developments. Structural alloy developments usually result in complex multiphase intermetallic alloys which are optimized with respect to phase composition and phase distribution in order to obtain high strengths and corrosion resistances with sufficient formability. However, the effects of alloying elements on the basic properties of the respective phases are not yet understood sufficiently for these intermetallic alloys. One needs to know in what way a composition change in a particular phase changes, e.g., the elastic moduli. It is hoped that more experimental

ArcelorMittal Ex. 2038
Page 142 of 190

copyright © VCH Verlagsgesellschaft mbH, 1995

maguchi et al., 1993). The Co–Si phase diagram has been analyzed (Ishida et al., 1991 b; Choi, 1992), the electron distribution has been studied by ab initio calculations (Sen Gupta and Chatterjee, 1986), the formation enthalpy of vacancies has been determined by positron annihilation (Ito et al., 1993), an excellent oxidation resistance has been found (Anton and Shah, 1989), and the plastic deformation behavior has been analyzed in detail with respect to dislocation configurations and slip systems (Takeuchi et al., 1991, 1992; Ito et al., 1992; Suzuki and Takeuchi, 1993; Yamaguchi et al., 1993; Anongba and Steinemann, 1993).

$NiSi_2$ is of primary interest for applications in electronic thin-film devices (Kumar, 1994). In view of these applications, the conditions for thin-film formation have been studied in detail for $NiSi_2$ (see, e.g. Tu et al., 1983; d'Heurle et al., 1984; Singh and Khokle, 1987) and likewise the formation of thin oxide layers on $NiSi_2$ (Cros, 1983). Apart from these applications, the termal expansion behavior of $NiSi_2$ has been studied with respect to use as a heat storage material (Wilson and Cavin, 1992). Finally, it is noted that the alloying of $NiSi_2$ with Ni and Al produces phases with distinct color – pale blue, yellow, white, and variations of these – which may be of interest for applications in jewellery (Cortie et al., 1991).

12 Prospects

As already stated in the introduction to this chapter, only a restricted selection of intermetallics could be assessed here. An enormous multitude of intermetallic phases is known (Villars and Calvert, 1991), and there are many phases which were not mentioned in the preceding sections and which are of interest, e.g. as strengthening or embrittling phases in commercial metallic alloys. This is illustrated by the topologically close-packed μ, σ, χ, and related phases (Nevitt, 1963; Bardos et al., 1966; Benjamin et al., 1966; Hall and Algie, 1966; Sinha, 1973) which pose problems in many metallic alloy systems because of their embrittling effects, but which may also be used as strengthening phases if adequately distributed (Pickering, 1976; Bhandarkar et al., 1976; Gaspard et al., 1977; Sauthoff and Speller, 1982; Schumacher and Sauthoff, 1987; Sha et al., 1993). Most of the less known phases have not been studied sufficiently to establish a database which allows estimates of their potential for applications. Thus there is a great need for the determination of the basic properties – in particular constitution, phase diagrams, densities, electrical and thermal conductivities, elastic constants, and diffusion coefficients – of the less known intermetallics.

As to the better known phases, which have been selected for materials developments or are regarded as candidate phases for new developments, the physical understanding of their properties and their behavior during processing and service is still insufficient, which impedes the progress of the present developments. Structural alloy developments usually result in complex multiphase intermetallic alloys which are optimized with respect to phase composition and phase distribution in order to obtain high strengths and corrosion resistances with sufficient formability. However, the effects of alloying elements on the basic properties of the respective phases are not yet understood sufficiently for these intermetallic alloys. One needs to know in what way a composition change in a particular phase changes, e.g., the elastic moduli. It is hoped that more experimental

ArcelorMittal Ex. 2038
Page 143 of 190

work will be done with respect to the alloy systems of interest to obtain the missing data, and that more theoretical work – including quantum-mechanical, ab initio calculations – will be done to understand why the properties change with specific alloying additions in specific ways. This lacking understanding is not a characteristic of intermetallics alone. However, the problems of understanding are more pronounced for the intermetallics since the properties of the intermetallics vary with changing composition – as does the bonding character – to a larger degree than is known for the familiar metallic alloy systems.

As to applications, various functional intermetallic alloys are well established and are successfully used, e.g. magnetic FeCo alloys or superconducting A15 materials. The limited or lacking deformability poses problems for the processing of these materials, which is the subject of continuous research and development. A lot of progress has been achieved by applying advanced technologies which have been developed for other groups of materials. In particular, experiences in the processing of brittle structural intermetallics being developed now, and of the still more brittle advanced ceramics, may be useful here.

New structural intermetallic alloys for high-temperature applications are at the center of the present interest in intermetallics, which is still growing. A few developments, which are based on the classic phases Ni_3Al, Ti_3Al and TiAl, and which are known as the nickel aluminides and the titanium aluminides, are on the brink of commercialization, but even these developments are still at an early stage compared with other developments of advanced materials, e.g. the modern engineering ceramics. Much more experimental and theoretical work is necessary to solve the processing problems and to adjust the property spectra to the specific applications.

The much advanced nickel aluminides and titanium aluminides can be used only up to about 1000 °C because of their limited strength or oxidation resistance or both at higher temperatures, as has been stated before (Sauthoff, 1994). For applications significantly above 1000 °C other less-common phases with higher melting temperatures have to be used. Such phases are available, and examples are shown in Fig. 34 (Sauthoff, 1992). In comparison to the nickel aluminides and titanium alu-

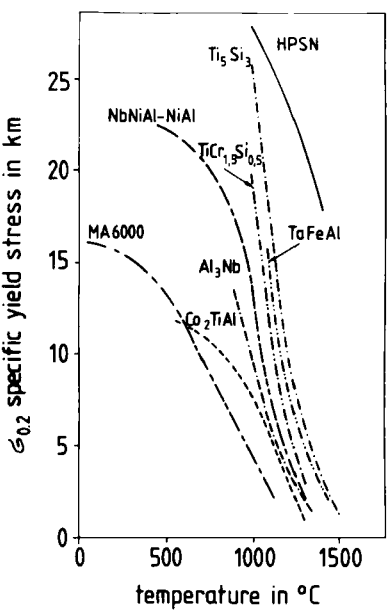


Figure 34. Specific yield strength (0.2% proof stress in compression per unit weight density at $10^{-4}\,s^{-1}$ strain rate) as a function of temperature for the $D0_{22}$ phase Al_3Nb (Reip, 1991; Reip and Sauthoff, 1993), the Heusler-type phase Co_2TiAl (Sauthoff, 1990b), the Laves phases $TiCr_{1.5}Si_{0.5}$ and TaFeAl (Sauthoff, 1990b; Machon, 1992), the two-phase alloy NbNiAl–NiAl with 15 vol.% NiAl in the Laves phase NbNiAl (Sauthoff, 1990b; Machon, 1992), and the hexagonal $D8_8$ phase Ti_5Si_3 (Frommeyer et al., 1990) compared with the superalloy MA 6000 (in tension) (Inco, 1982) and hot-pressed silicon nitride HPSN (upper limit of flexural strength) (Porz and Grathwohl, 1984).

ArcelorMittal Ex. 2038
Page 144 of 190

minides, the less-common phases are stronger and more brittle, their crystal structures are complex, their handling is difficult, and thus they are regarded as exotic. However, these exotic phases may fill the gap between metallic high-temperature alloys and ceramics, as is clear from Fig. 34. The brittleness of the less-common phases can be alleviated by combining them with softer phases to form multiphase alloys with adequate microstructures. Even strengthening hard phases may improve the toughness by impeding crack growth. The mechanical behavior can be optimized by optimizing the microstructure, which requires careful control of the processing.

However, it has to be emphasized that one cannot expect to obtain new intermetallic materials with properties similar to existing conventional metallic alloys. The "ductilizations" that have been achieved in a few cases – in particular Ni_3Al and $(Fe,Co,Ni)_3V$ – rely on rather specific mechanisms and cannot be expected for other intermetallic phases. Thus intermetallic materials have to be regarded as a materials class of their own with property spectra which differ significantly from those of other materials and which can be varied within broad limits corresponding to metals on one side and nonmetals on the other side. This offers enormous possibilities for manifold developments which are exciting with respect to both practical applications and materials science.

Finally, it is noted that much interest is concentrated on the development of intermetallic alloys for use as blades in flying gas turbines. This application is most demanding and it is not clear whether all the problems with strength, ductility, toughness, and corrosion resistance can be solved at economic costs. Less-high-technology applications may be more rewarding at present for the introduction of new intermetallic materials. An example may be the car engine, where strong, light components with sufficient corrosion resistance are needed. Here brittleness is not the problem since designers have learnt to use ceramic materials, e.g. for valves. However, new materials must be compatible with the metallic engine with respect to the physical properties, in particular thermal expansion and thermal conductivity. This requirement corresponds to the characteristics of intermetallic materials which are hard and brittle with mainly metallic atomic bonding, i.e. metallic, physical properties. Thus new intermetallic materials are expected to play an important role in the manufacture of car engines and similar applications.

Acknowledgements

The author's research on intermetallics has been supported by the Deutsche Forschungsgemeinschaft (DFG) and the Bundesminister für Forschung und Technologie (BMFT) throughout a decade, and this is gratefully acknowledged. The author is indebted to numerous colleagues whose researches are acknowledged in the references – in particular to his colleagues at the Max-Planck-Institut für Eisenforschung – for many valuable and stimulating discussions. The author thanks Mrs Erika Bartsch for a great deal of electron microscope work on various intermetallic alloys and Mr Gerhard Bialkowski for innumerable mechanical tests on rather brittle materials.

ArcelorMittal Ex. 2038
Page 145 of 190

copyright © VCH Verlagsgesellschaft mbH, 1995

References

Ahlers, M. (1986), *Prog. Mater. Sci. 30,* 135–186.

Ahlers, M., Pelegrina, J. L. (1992), *Acta Metall. Mater. 40,* 3213–3220.

Ahmed, T., Flower, H. M. (1992), *Mater. Sci. Eng. A 152,* 31–36.

Aikin, R. M., Jr. (1992), *Scr. Metall. Mater. 26,* 1025–1030.

Aindow, M., Shyue, J., Gaspar, T. A., Fraser, H. L. (1991), *Phil. Mag. A 64,* 59–65.

Aitken, E. A. (1967), in: *Intermetallic Compounds:* Westbrook, J. H. (Ed.). New York: Wiley, pp. 491–516.

Akuezue, H. C., Whittle, D. P. (1983), *Met. Sci. 17,* 27–33.

Albers, M., Sai Baba, M., Kath, D., Miller, M., Hilpert, K. (1992), *Ber. Bunsenges. Phys. Chem. 96,* 1663–1668.

Alekseyev, L. A., Dzhavadov, D. M., Tyapkin, Y. D., Levi, R. B. (1977), *Fiz. Metal. Metalloved. 43 (No. 6),* 1235–1241.

Alexander, D. J., Sikka, V. K. (1992), *Mater. Sci. Eng. A 152,* 114–119.

Alexander, H. (1986), in: *Dislocations in Solids:* Nabarro, F. R. N. (Ed.). Amsterdam: North-Holland, pp. 113–234.

Alexander, H., Haasen, P. (1968), in: *Solid State Physics,* Vol. 22: Seitz, F., Turnbull, D., Ehrenreich, H. (Eds.). New York: Academic, pp. 27–158.

Allen, C. W. (1985), in: *High-Temperature Ordered Intermetallic Alloys:* Koch, C. C., Liu, C. T., Stoloff, N. S. (Eds.). Pittsburgh, PA: MRS, pp. 141–146.

Allen, C. W., Liao, K. C. (1982), *Phys. Status Solidi (a) 74,* 673–681.

Allen, C. W., Delavignette, P., Amelinckx, S. (1972), *Phys. Status Solidi (a) 9,* 237–246.

Alman, D. E., Stoloff, N. S. (1991), in: *High Temperature Ordered Intermetallic Alloys* IV: Johnson, L. A., Pope, D. P., Stiegler, J. O. (Eds.). Pittsburgh, PA: MRS, pp. 989–1000.

Alman, D. E., Stoloff, N. S. (1992), *Mater Res. Soc. Symp. Proc. 273,* 247–252.

Alman, D. E., Stoloff, N. S. (1993), *Scr. Metall. Mater. 28,* 1525–1530.

Alman, D. E., Stoloff, N. S., Otsuki, M. (1991), in: *Proc. Int. Symp. on Intermetallic Compounds – Structure and Mechanical Properties* (JIMIS-6): Izumi, O. (Ed.). Sendai: The Japan Institute of Metals, pp. 891–899.

Aly, E.-S. M., Stark, J. P. (1984), *Acta Metall. 32,* 907–914.

Amano, M., Sasaki, Y., Watanabe, R., Shibata, M. (1983), *J. Less-Common Met. 89,* 513–518.

Amano, M., Hirata, T., Kimura, T., Sasaki, Y. (1984), *Trans. JIM 25,* 657–661.

Anderson, C. D., Hofmeister, W. H., Bayuzick, R. J. (1993), *Metall. Trans. 24 A,* 61–66.

Andreyeva, A. V., Belyanin, A. F., Bulyonkov, N. A. (1988), *Acta Metall. 36,* 2377–2385.

Andryushchenko, V. A., Gavrilyuk, V. G., Nadutov, V. M. (1985), *Phys. Met. Metall. 60 (4),* 50–55.

Anongba, P. N. B., Steinemann, S. G. (1993), *Phys. Status Solidi (a) 140,* 391–409.

Anton, D. L. (1988), in: *High Temperature/High Performance Composites:* Lemkey, F. D., Fishman, S. G., Evans, A. G., Strife, J. R. (Eds.). Pittsburgh, PA: MRS, pp. 57–64.

Anton, D. L., Shah, D. M. (1989), in: *High-Temperature Ordered Intermetallic Alloys* III: Liu, C. T., Taub, A. I., Stoloff, N. S., Koch, C. C. (Eds.). Pittsburgh, PA: Mater. Res. Soc., pp. 361–371.

Anton, D. L., Shah, D. M. (1990), in: *Intermetallic Matrix Composites:* Anton, D. L., Martin, P. L., Miracle, D. B., McMeeking, R. (Eds.). Pittsburgh, PA: MRS, pp. 45–52.

Anton, D. L., Shah, D. M. (1991a), in: *Proc. Int. Symp. on Intermetallic Compounds – Structure and Mechanical Properties* (JIMIS-6): Izumi, O. (Ed.). Sendai: The Japan Institute of Metals, pp. 379–386.

Anton, D. L., Shah, D. M. (1991b), in: *High Temperature Ordered Intermetallic Alloys* IV: Johnson, L. A., Pope, D. P., Stiegler, J. O. (Eds.). Pittsburgh, PA: MRS, pp. 63–68.

Anton, D. L., Shah, D. M. (1992a), *Mater. Sci. Eng. A 153,* 410–415.

Anton, D. L., Shah, D. M. (1992b), *Mater. Res. Soc. Symp. Proc. 273,* 157–164.

Anton, D. L., Shah, D. M. (1993), *Mater. Res. Soc. Symp. Proc. 288,* 141–150.

Aoki, K. (1990), *Mater. Trans. Jpn. Inst. Met. 31,* 443–448.

Aoki, K., Izumi, O. (1979), *J. Jpn. Inst. Met. 43,* 1190–1196.

Aoki, K., Masumoto, T. (1988), *Sci. Rep. Tohoku Univ. A 34,* 79–92.

Aoki, K., Masumoto, T. (1993), *J. Alloys Compounds 194,* 251–261.

Aoki, K., Ishikawa, K., Masumoto, T. (1993), *Scr. Metall. Mater. 29,* 651–656.

Aoki, Y., Nakamichi, T., Yamamoto, M. (1966), *J. Phys. Soc. Jpn. 21,* 565–570.

Appel, F., Beaven, P. A., Wagner, R. (1993), *Acta Metall. Mater. 41,* 1721–1732.

Appelbaum, A., Eizenberg, M., Brener, R. (1984), *J. Appl. Phys. 55,* 914–917.

Arbiter, W. (1953a), WADC Technical Report 53-190, part I, 1–85.

Arbiter, W. (1953b), WADC Technical Report 53-190, part II, 1–47.

Archambault, P., Hazotte, A. (1993), *Scr. Metall. Mater. 28,* 423–428.

Argent, B. B. (1984), in: *Niobium:* Stuart, H. (Ed.). Warrendale, PA: The Metallurgical Society of AIME, pp. 325–415.

ArcelorMittal Ex. 2038

Armitage, J. G. M., Dumelow, T., Mitchell, R. H., Riedi, P. C., Abell, J. S., Mohn, P., Schwarz, K. (1986), *J. Phys. F16,* L141–L144.

Arzt, E., Rösler, J. (1988), *Acta Metall. 36,* 1053–1060.

Arzt, E., Göhring, E., Grahle, P. (1993), *Mater. Res. Soc. Symp. Proc. 288,* 861–866.

Asano, S., Ishida, S. (1988), *J. Phys. F18,* 501–515.

Ashby, M. F., Edward, G. H. Davenport, J., Verrall, R. A. (1978), *Acta Metall. 26,* 1379–1388.

Ashby, M. F., Blunt, F. J., Bannister, M. (1989), *Acta Metall. 37,* 1847–1857.

Ashok, S., Kain, K., Tartaglia, J. M., Stoloff, N. S. (1983), *Metall. Trans. 14A,* 1997–2003.

Asta, M., van Schilfgaarde, M., De Fontaine, D. (1993), *Mater. Res. Soc. Symp. Proc. 288,* 153–158.

Aswath, P. B., Suresh, S. (1991), *Metall. Trans. 22A,* 817–828.

Au, Y. K., Wayman, C. M. (1972), *Scr. Metall. 6,* 1209–1214.

Austin, C. M., Kelly, T. J. (1993), in: *Structural Intermetallics:* Darolia, R., Lewandowski, J. J., Liu, C. T., Martin, P. L., Miracle, D. B., Nathal, M. V. (Eds.). Warrendale, PA: TMS, pp. 143–150.

Ayer, R., Ray, R. (1991), *Metall. Trans. 22A,* 1901–1910.

Baeslack, W. A., III, Cieslak, M. J., Headley, T. J. (1988), *Scr. Metall. 22,* 1155–1160.

Baker, I. (1993), *Scr. Metall. Mater. 29,* 835–836.

Baker, I., Gaydosh, D. J. (1987), *Mater. Sci. Eng. 96,* 147–158.

Baker, I., George, E. P. (1992), *Met. Mater. 8,* 318–323.

Baker, I., Munroe, P. R. (1990), in: *High-Temperature Aluminides and Intermetallics:* Whang, S. H., Liu, C. T., Pope, D. P., Stiegler, J. O. (Eds.). Warrendale, PA: TMS, pp. 425–452.

Baker, I., Nagpal, P. (1993), in: *Structural Intermetallics:* Darolia, R., Lewandowski, J. J., Liu, C. T., Martin, P. L., Miracle, D. B., Nathal, M. V. (Eds.). Warrendale, PA: TMS, pp. 463–473.

Baker, I., Liu, F., Nagpal, P., Munroe, P. R. (1991), in: *High Temperature Ordered Intermetallic Alloys* IV: Johnson, L. A., Pope, D. P., Stiegler, J. O. (Eds.). Pittsburgh, PA: MRS, pp. 533–538.

Baker, I., Yuan, J., Schulson, E. M. (1993), *Metall. Trans. 24A,* 283–292.

Bakker, H. (1984), in: *Diffusion in Crystalline Solids:* Murch, G. E., Nowick, A. S. (Eds.). Orlando, FL: Academic, pp. 189–256.

Bakker, H., Ommen, A. (1978), *Acta Metall. 26,* 1047–1053.

Bakker, H., Westerveld, J. P. A. (1988), *Phys. Status Solidi (b) 145,* 409–417.

Bakker, H., Van Winkel, A., Waegemaekers, A. A. H. J., Van Ommen, A. H., Stolwijk, N. A., Hatcher, R. D. (1985), in: *Diffusion in Solids: Recent Developments:* Dayananda, M. A., Murch, G. E. (Eds.). Warrendale, PA: TMS, pp. 39–63.

Bakker, H., Lo Cascio, D. M. R., Di, L. M. (1992), in: *Ordered Intermetallics – Physical Metallurgy and Mechanical Properties:* Liu, C. T., Cahn, R. W., Sauthoff, G. (Eds.). Dordrecht: Kluwer, 433–448.

Balankin, A. S. (1984), *Sov. Phys. Solid State 26,* 1912–1913.

Ball, A., Smallman, R. E. (1966), *Acta Metall. 14,* 1349–1355.

Ball, J., Gottstein, G. (1993), *Intermetallics 1,* 191–208.

Balsone, S. J. (1989), in: *Oxidation of High-Temperature Intermetallics:* Grobstein, T., Doychak, J. (Eds.). Warrendale, PA: TMS, pp. 219–234.

Ban, Z., Ogilvie, E. (1966), *Trans. AIME 236,* 1738–1742.

Bardos, A. M., Bardos, D. I., Beck, P. A. (1963), *Trans. AIME 227,* 991–993.

Bardos, D. I., Gupta, K. P., Beck, P. A. (1961), *Trans. AIME 221,* 1087–1088.

Bardos, D. I., Malik, R. K., Spiegel, F. X., Beck, P. A. (1966), *Trans. AIME 236,* 40–48.

Barinov, S. M., Evdokimov, V. Y. (1993), *Acta Metall. Mater. 41,* 801–804.

Barinov, S. M., Evdokimov, V. Y., Shevchenko, V. Y. (1992), *J. Mater. Sci. Lett. 11,* 1347–1348.

Bartels, A., Seeger, J., Mecking, H. (1993), *Mater. Res. Soc. Symp. Proc. 288,* 1179–1184.

Barth, E. P., Tien, J. K., Uejo, S., Kambara, S. (1992), *Mater. Sci. Eng. A153,* 398–401.

Bartholomeusz, M. F., Yang, Q., Wert, J. A. (1993), *Scr. Metall. Mater. 29,* 389–394.

Bassi, C., Peters, J. A., Blank-Bewersdorff, M. (1991), *Technische Rundschau Sulzer 1,* 5–9.

Batterman, B. W., Barrett, C. S. (1964), *Phys. Rev. Lett. 13,* 390–392.

Batterman, B. W., Barrett, C. S. (1966), *Phys. Rev. 145,* 296–301.

Bauer, G. (1939), *Z. Anorg. Allg. Chem. 242,* 1–22.

Beauchamp, P., Dirras, G. (1993), *Phil. Mag. A67,* 813–826.

Beauchamp, P., Dirras, G., Veyssière, P. (1992), *Phil. Mag. A65,* 477–496.

Beaven, P. A., Wu, J. S., Dogan, B., Hartig, C., Seeger, J., Wagner, R. (1989), GKSS-Jahresbericht, pp. 49–61.

Becker, J. D., Sanchez, J. M., Tien, J. K. (1991), in: *High Temperature Ordered Intermetallic Alloys* IV: Johnson, L. A., Pope, D. P., Stiegler, J. O. (Eds.). Pittsburgh, PA: MRS, pp. 113–118.

Becker, S., Rahmel, A., Schorr, M., Schütze, M. (1992), *Oxid. Met. 38,* 425–464.

Becker, S., Schütze, M., Rahmel, A. (1993), *Oxid. Met. 39,* 93–106.

Becquart, C. S., Clapp, P. C., Rifkin, J. A. (1993), *Mater. Res. Soc. Symp. Proc. 228,* 519–524.

Bednorz, J. G., Müller, K. A. (1988), *Angew. Chem. 100,* 757–770.

Benci, J. E., Ma, J. C., Feist, T, P. (1993), *Mater. Res. Soc. Symp. Proc. 288,* 397–402.

ArcelorMittal Ex. 2038
Page 147 of 190

Bendersky, L. A., Voorhees, P. W., Boettinger, W. J., Johnson, W. C. (1988), *Scr. Metall. 22,* 1029–1034.
Bendersky, L. A., Boettinger, W. J., Biancaniello, F. S. (1992), *Mater. Sci. Eng. A 152,* 41–47.
Benjamin, J. S., Giessen, B. C., Grant, N. J. (1966), *Trans. AIME 236,* 224–226.
Bershadsky, E., Josephy, Y., Ron, M. (1991), *J. Less-Common Met. 172–174,* 1036–1043.
Bertero, G. A., Hofmeister, W. H., Robinson, M. B., Bayuzick, R. J. (1991a), *Metall. Trans. 22A,* 2713–2721.
Bertero, G. A., Hofmeister, W. H., Robinson, M. B., Bayuzick, R. J. (1991b), *Metall. Trans. 22A,* 2723–2732.
Bertram, M., Paufler, P. (1983), *Cryst. Res. Technol. 18,* 5–11.
Bewlay, B. P., Chang, K.-M., Sutliff, J. A., Jackson, M. R. (1992), *Mater. Res. Soc. Symp. Proc. 273,* 417–424.
Bhaduri, S. B. (1992), *Scr. Metall. Mater. 27,* 1277–1281.
Bhandarkar, M. D., Bhat, M. S., Parker, E. R., Zackay, V. F. (1976), *Metall. Trans. 7A,* 753–760.
Bhattacharya, A. K. (1991), *J. Am. Ceram. Soc. 74,* 2707–2710.
Bhattacharya, A. K., Petrovic, J. J. (1991), *J. Am. Ceram. Soc. 74,* 2700–2703.
Bhattacharya, A. K., Ho, C. T., Sekhar, J. A. (1992), *J. Mater. Sci. Lett. 11,* 475–476.
Bi, Y. J., Abell, J. S. (1993), *Scr. Metall. Mater. 29,* 543–546.
Bidaux, J.-E., Ahlers, M. (1992), *Z. Metallkd. 83,* 310–313.
Bieler, T. R., Noebe, R. D., Whittenberger, J. D., Luton, M. J. (1992), *Mater. Res. Soc. Symp. Proc. 273,* 165–170.
Bieler, T. R., Whittenberger, J. D., Luton, M. J. (1993), *Mater. Res. Soc. Symp. Proc. 288,* 1149–1154.
Bittence, J. C. (1987), *Adv. Mater. Processes 12/87,* 35–39.
Blau, W., Himsel, A., Kleinstück, K. (1980), *Phys. Status Solidi (b) 100,* 541–549.
Bobeth, M., Pompe, W., Schumann, E., Rühle, M. (1992), *Acta Metall. Mater. 40,* 2669–2676.
Boettinger, W. J., Perepezko, J. H., Frankwicz, P. S. (1992), *Mater. Sci. Eng. A 155,* 33–41.
Boettner, R. C., Stoloff, N. S., Davies, R. G. (1966), *Trans. AIME 236,* 131–133.
Bohn, H. G., Schumacher, R., Vianden, R. J. (1987a), in: *High-Temperature Ordered Intermetallic Alloys* II: Stoloff, N. S., Koch, C. C., Liu, C. T., Izumi, O. (Eds.). Pittsburgh, PA: MRS, pp. 123–126.
Bohn, H. G., Williams, J. M., Barrett, J. H., Liu, C. T. (1987b), in: *High-Temperature Ordered Intermetallic Alloys* II: Stoloff, N. S., Koch, C. C., Liu, C. T., Izumi, O. (Eds.). Pittsburgh, PA: MRS, pp. 127–133.
Bond, G. M., Robertson, I. M., Birnbaum, H. K. (1989), *Acta Metall. 37,* 1407–1413.
Bondarev, B., Anoshkin, N., Molotkov, A., Notkin, A., Elagin, D. (1991), in: *Proc. Int. Symp. on Intermetallic Compounds – Structure and Mechanical Properties* (JIMIS-6): Izumi, O. (Ed.). Sendai: The Japan Institute of Metals, pp. 1009–1014.
Bose, S. K., Kudrnovsky, J., Jepsen, O., Andersen, O. K. (1991), in: *High Temperature Ordered Intermetallic Alloys* IV: Johnson, L. A., Pope, D. P., Stiegler, J. O. (Eds.). Pittsburgh, PA: MRS, pp. 25–30.
Boulghallat, M., Gerard, N. (1991), *J. Less-Common Met. 172–174,* 1052–1057.
Bowden, D. M. (1989), *Mater. Manufact. Processes 4,* 85–101.
Bowman, R. R. (1992), *Mater. Res. Soc. Symp. Proc. 273,* 145–156.
Bowman, R. R., Noebe, R. D. (1989), *Adv. Mater. Processes 8/89,* 35–40.
Bozorth, R. M. (1951), *Ferromagnetism.* Toronto: Van Nostrand, pp. 102–422.
Bradley, A. J. (1951), *JISI 168,* 233–244.
Bradley, A. J., Taylor, A. (1938), *Proc. R. Soc. A 166,* 353–375.
Brady, M. P., Hanrahan, R. J., Jr., Elder Randall, S. P., Verink, E. D., Jr. (1993), *Scr. Metall. Mater. 28,* 115–120.
Brand, R., Webb, W. W. (1969), *Solid State Commun. 7,* 19–25.
Bremer, F. J., Beyss, M., Wenzl, H. (1988), *Phys. Status Solidi (a) 110,* 77–82.
Brennan, P. C., Kao, W. H., Yang, J.-M. (1992), *Scr. Metall. Mater. 26,* 1399–1404.
Brill, U., Klöwer, J. (1991), in: *High Temperature Ordered Intermetallic Alloys* IV: Johnson, L. A., Pope, D. P., Stiegler, J. O. (Eds.). Pittsburgh, PA: MRS, pp. 963–968.
Brimhall, J. L., Bruemmer, S. M. (1992), *Scr. Metall. Mater. 27,* 1747–1752.
Brock, G. W. (1986), in: *Encyclopedia of Materials Science and Engineering:* Bever, M. B. (Ed.). Oxford: Pergamon, pp. 2679–2682.
Brooks, C. R., Cao, S. (1992), *Phil. Mag. A 65,* 327–353.
Brooks, C. R., Spruiell, J. E., Stansbury, E. E. (1984), *Int. Met. Rev. 29,* 210–248.
Brown, N. (1959), *Phil. Mag. 4,* 693–704.
Brown, S. A., Pope, D. P., Kumar, K. S. (1993), *Mater. Res. Soc. Symp. Proc. 288,* 723–729.
Brückner, W. (1969), Dr. rer. nat. Thesis, Technische Universität Dresden, pp. 1–126.
Bruemmer, S. M., Brimhall, J. L., Henager, H., Jr. (1990), in: *Intermetallic Matrix Composites:* Anton, D. L., Martin, P. L., Miracle, D. B., McMeeking, R. (Eds.). Pittsburgh, PA: MRS, pp. 257–262.
Bruemmer, S. M., Arey, B. W., Henager, C. H., Jr. (1992a), *Mater. Res. Soc. Symp. Proc. 273,* 425–432.
Bruemmer, S. M., Charlot, L. A., Brimhall, J. L., Henager, C. H., Jr. (1992b), *Phil. Mag. A 65,* 1083–1094.

ArcelorMittal Ex. 2038
Page 148 of 190

Bruemmer, S. M., Brimhall, J. L., Henager, C. H., Jr., Hirth, J. P. (1993), *Mater. Res. Soc. Symp. Proc. 288,* 799–806.

Brukl, C., Nowotny, H., Benesovsky, F. (1961), *Monatsh. Chem. 92,* 967–980.

Brumm, M. W., Grabke, H. J. (1992), *Corros. Sci. 33,* 1677–1690.

Bryant, J. D., Kampe, S. L., Sadler, P., Christodoulou, L. (1991), *Metall. Trans. 22A,* 2009–2020.

Buckley, R. A. (1975), *Met. Sci. 9,* 243–247.

Bunk, W. G. J. (1992), in: *Basic Technologies for Future Industries: The 3rd Symposium on High-Performance Materials for Severe Environments:* RIMCOF (Ed.). Tokyo: Japan Industrial Technology Association (JITA), pp. 1–15.

Burany, X. M., Northwood, D. O. (1991), *J. Less-Common Met. 170,* 27–35.

Buschow, K. H. J. (1980), in: *Ferromagnetic Materials,* Vol. 1: Wohlfarth, E. P. (Ed.). Amsterdam: North-Holland, pp. 297–414.

Buschow, K. H. J. (1986), *Mater. Sci. Rep. 1,* 1–64.

Buschow, K. H. J. (1991), *Rep. Prog. Phys. 54,* 1123–1213.

Cadoff, I. (1967), in: *Intermetallic Compounds:* Westbrook, J. H. (Ed.). New York: Wiley, pp. 517–528.

Cahn, R. W. (1989), *Met. Mater. Processes 1,* 1–19.

Cahn, R. W. (1990), in: *High-Temperature Aluminides and Intermetallics:* Whang, S. H., Liu, C. T., Pope, D. P., Stiegler, J. O. (Eds.). Warrendale, PA: TMS, pp. 245–270.

Cahn, R. W. (1991), in: *Proc. Int. Symp. on Intermetallic Compounds – Structure and Mechanical Properties* (JIMIS-6): Izumi, O. (Ed.). Sendai: The Japan Institute of Metals, pp. 771–778.

Cahn, R. W. (1992), in: *Ordered Intermetallics – Physical Metallurgy and Mechanical Properties:* Liu, C. T., Cahn, R. W., Sauthoff, G. (Eds.). Dordrecht: Kluwer, pp. 511–524.

Cahn, R. W. (1993), in: *Diffusion in Ordered Alloys and Intermetallic Compounds:* Fultz, B., Cahn, R. W., Gupta, D. (Eds.). Warrendale, PA: TMS, pp. 125–136.

Cahn, R. W., Siemers, P. A., Geiger, J. E., Bardhan, P. (1987), *Acta Metall. 35,* 2737–2751.

Caillet, M., Ayedi, H. F., Galerie, A., Besson, J. (1978), in: *Materials and Coatings to Resist High Temperature Corrosion:* Holmes, D. R., Rahmel, A. (Eds.). London: Applied Science, pp. 387–398.

Calka, A., Radlinski, A. P., Shanks, R. A., Pogany, A. P. (1991), *J. Mater. Sci. Lett. 10,* 734–737.

Campisi, G. J., Bevolo, A. J., Shanks, H. R., Schmidt, F. A. (1981), *J. Appl. Phys. 52,* 5043–5047.

Cao, H. C., Dalgleish, B. J., Dève, H. E., Elliott, C., Evans, A. G., Mehrabian, R., Odette, G. R. (1989), *Acta Metall. 37,* 2969–2977.

Carbone, A. J., Kopp, M. W., Tien, J. K., Lin, S. S., Marcus, H. L., Draper, S. L. (1988), *Scr. Metall. 22,* 1903–1906.

Carlsson, A. E. (1991), in: *High Temperature Ordered Intermetallic Alloys* IV: Johnson, L. A., Pope, D. P., Stiegler, J. O. (Eds.). Pittsburgh, PA: MRS, pp. 19–23.

Carter, D. H., Martin, P. L. (1990), in: *Intermetallic Matrix Composites:* Anton, D. L., Martin, P. L., Miracle, D. B., McMeeking, R. (Eds.). Pittsburgh, PA: MRS, pp. 131–138.

Castagna, A., Stoloff, N. S. (1992), *Scr. Metall. Mater. 26,* 673–678.

Castagna, A., Maziasz, P. J., Stoloff, N. S. (1993), *Mater. Res. Soc. Symp. Proc. 288,* 1043–1048.

Castro, R. G., Smith, R. W., Rollett, A. D., Stanek, P. W. (1992), *Scr. Metall. Mater. 26,* 207–212.

Catana, A., Schmid, P. E., Lu, P., Smith, D. J. (1992), *Phil. Mag. A66,* 933–956.

Cathcart, J. V. (1985), in: *High-Temperature Ordered Intermetallic Alloys:* Koch, C. C., Liu, C. T., Stoloff, N. S. (Eds.). Pittsburgh, PA: MRS, pp. 445–459.

Chakravorty, S., Wayman, C. M. (1976a), *Metall. Trans. 7A,* 555–568.

Chakravorty, S., Wayman, C. M. (1967b), *Metall. Trans. 7A,* 569–582.

Chakravorty, S., West, D. R. F. (1985), *Mater. Sci. Technol. 1,* 978–985.

Chakravorty, S., West, D. R. F. (1986), *Mater. Sci. Technol. 2,* 989–996.

Chakravorty, S., Hashim, H., West, D. R. F. (1985), *J. Mater. Sci. 20,* 2313–2322.

Chan, K. S. (1990), *Scr. Metall. Mater. 24,* 1725–1730.

Chan, K. S. (1992), *Metall. Trans. 23A,* 497–507.

Chan, K. S. (1993a), *Metall. Trans. 24A,* 569–583.

Chan, K. S. (1993b), *Metall. Trans. 24A,* 1095–1105.

Chan, K. S., Kim, Y.-W. (1993), *Metall. Trans. 24A,* 113–125.

Chang, C. S., Pope, D. P. (1991), in: *High Temperature Ordered Intermetallic Alloys* IV: Johnson, L. A., Pope, D. P., Stiegler, J. O. (Eds.). Pittsburgh, PA: MRS, pp. 745–750.

Chang, H., Gibala, R. (1993), *Mater. Res. Soc. Symp. Proc. 288,* 1143–1148.

Chang, H., Kung, H., Gibala, R. (1992), *Mater. Res. Soc. Symp. Proc. 273,* 253–258.

Chang, K.-M. (1992), *Mater. Res. Soc. Symp. Proc. 273,* 191–196.

Chang, K.-M., Darolia, R., Lipsitt, H. A. (1991), in: *High Temperature Ordered Intermetallic Alloys* IV: Johnson, L. A., Pope, D. P., Stiegler, J. O. (Eds.). Pittsburg, PA: MRS, pp. 597–602.

Chang, K.-M., Darolia, R., Lipsitt, H. A. (1992), *Acta Metall. Mater. 40,* 2727–2737.

Chang, Y. A., Neumann, J. P., Chen, S.-L. (1991), in: *Alloy Phase Stability and Design:* Stocks, G. M., Pope, D. P., Giamei, A. F. (Eds.). Pittsburgh, PA: MRS, pp. 131–140.

Chang, Y. A., Pike, L. M., Liu, C. T., Bilbrey, A. R., Stone, D. S. (1993), *Intermetallics 1,* 107–115.

Chapman, G. E., Lau, S. S., Matteson, S., Mayer, J. W. (1979), *J. Appl. Phys. 50,* 6321–6327.

ArcelorMittal Ex. 2038
Page 149 of 190

Charlot, L. A., Brimhall, J. L., Thomas, L. E., Bruemmer, S. M., Hirth, J. P. (1991), *Scr. Metall. Mater. 25,* 99–104.

Chen, C., Chen, G. H. (1988), *Scr. Metall. 22,* 1857–1861.

Chen, C.-P., Chang, Y. A. (1993), in: *Diffusion in Ordered Alloys and Intermetallic Compounds:* Fultz, B., Cahn, R. W., Gupta, D. (Eds.). Warrendale, PA: TMS, pp. 169–184.

Chen, C. W. (1961), *J. Appl. Phys. 32 Suppl.,* 348S–355S.

Chen, G., Sun, Z., Xie, X. (1991), in: *Advanced Structural Materials (Proc. C-MRS International '90,* Beijing, Vol. 2): Kong, M., Huang, L. (Eds.). Amsterdam: Elsevier, pp. 830–835.

Chen, G., Sun, Z., Zhou, X. (1992), *Mater. Sci. Eng. A 153,* 597–601.

Chen, G., Zhang, W., Wang, Y., Wang, J., Sun, Z., Wu, Y., Zhou, L. (1993), in: *Structural Intermetallics:* Darolia, R., Lewandowski, J. J., Liu, C. T., Martin, P. L., Miracle, D. B., Nathal, M. V. (Eds.). Warrendale, PA: TMS, pp. 319–324.

Chen, K. C., Allen, S. M., Livingston, J. D. (1993), *Mater. Res. Soc. Symp. Proc. 288,* 373–378.

Chen, X. F., Reviere, R. D., Oliver, B. F., Brooks, C. R. (1992), *Scr. Metall. Mater. 27,* 45–49.

Chen, Z. Y., Dodd, R. A. (1986), *Scr. Metall. 20,* 1709–1711.

Cheng, C. C., Verhoeven, J. D. (1988), *J. Less-Common Met. 139,* 15–28.

Cheng, G. H., Dayananda, M. A. (1979), *Metall. Trans. 10 A,* 1415–1419.

Cheng, S. C., Wolfenstine, J., Sherby, O. D. (1992), *Metall. Trans. 23 A,* 1509–1513.

Cheng, T. (1992), *Scr. Metall. Mater. 27,* 771–776.

Cheng, T., Cantor, B. (1992), *Mater. Sci. Eng. A 153,* 696–699.

Chesnutt, J. C. (1990), *Met. Mater. 6,* 509–511.

Chiba, A., Shindo, D., Hanada, S. (1991), *Acta Metall. Mater. 39,* 13–18.

Chiba, A., Hanada, S., Watanabe, S. (1992), *Mater. Sci. Eng. A 152,* 108–113.

Chin, B. A., Pound, G. M., Nix, W. D. (1977), *Metall. Trans. 8 A,* 1517–1522.

Chin, G. Y., Wernick, J. H. (1986), in: *Encyclopedia of Materials Science and Engineering,* Vol. 4: Bever, M. B. (Ed.). Oxford: Pergamon, pp. 2654–2655.

Choi, S.-D. (1992), *CALPHAD: Comput. Coupling Phase Diagrams Thermochem. 16,* 151–159.

Chou, T. C. (1990), *Scr. Metall. Mater. 24,* 1131–1136.

Chou, T. C., Nieh, T. G. (1990), *Scr. Metall. Mater. 24,* 1935–1940.

Chou, T. C., Nieh, T. G. (1991), *Scr. Metall. Mater. 25,* 2059–2064.

Chou, T. C., Nieh, T. G. (1993a), *J. Met. 45 (12),* 14–21.

Chou, T. C., Nieh, T. G. (1993b), *Mater. Res. Soc. Symp. Proc. 288,* 965–970.

Chou, T. C., Nieh, T. G., Wadsworth, J. (1992), *Scr. Metall. Mater. 27,* 897–902.

Chou, Y. C., Chou, Y. T. (1985), in: *High-Temperature Ordered Intermetallic Alloys:* Koch, C. C., Liu, C. T., Stoloff, N. S. (Eds.). Pittsburgh, PA: MRS, pp. 461–474.

Choudhury, N. S., Graham, H. C., Hinze, J. W. (1976), in: *Properties of High Temperature Alloys:* Foroulis, Z. A., Pettit, F. S. (Eds.). Princeton: The Electrochemical Society, pp. 668–680.

Chow, T. P., Brown, D. M., Steckl, A. J., Garfinkel, M. (1980), *J. Appl. Phys. 51,* 5981–5985.

Christodoulou, C. N., Takeshita, T. (1993a), *J. Alloys Compounds 191,* 279–285.

Christodoulou, C. N., Takeshita, T. (1993b), *J. Alloys Compounds 194,* 31–40.

Christodoulou, L., Parrish, P. A., Crowe, C. R. (1988), in: *High Temperature/High Performance Composites:* Lemkey, F. D., Fishman, S. G., Evans, A. G., Strife, J. R. (Eds.). Pittsburgh, PA: MRS, pp. 29–34.

Chu, F., Pope, D. P. (1992), *Scr. Metall. Mater. 26,* 399–404.

Chu, F., Pope, D. P. (1993), *Scr. Metall. Mater. 28,* 331–336.

Chu, W.-Y., Thompson, A. W. (1991), *Metall. Trans. 22 A,* 71–81.

Chu, W.-Y., Thompson, A. W. (1992), *Metall. Trans. 23 A,* 1299–1312.

Chu, W.-Y., Thompson, A. W., Williams, J. C. (1992), *Acta Metall. Mater. 40,* 455–462.

Chuang, T. H., Pan, Y. C. (1992), *Metall. Trans. 23 A,* 1187–1193.

Cieslak, M. J., Headley, T. J., Baeslack III, W. A. (1990), *Metall. Trans. 21 A,* 1273–1286.

Clark, A. E. (1980), in: *Ferromagnetic Materials,* Vol. 1: Wohlfarth, E. P. (Ed.). Amsterdam: North-Holland, pp. 531–589.

Clark, J.B., Wright, R. N. (1983), *Metall. Trans. 14 A,* 2295–2301.

Clark, J. B., Hopple, G. B., Wright, R. N. (1983), *Metal. Trans. 14 A,* 889–895.

Clemens, H., Bildstein, H. (1992), *Z. Metallkd. 83,* 429–435.

Clemens, H., Rumberg, I., Schretter, P., Grahle, P., Lang, O., Wanner, A., Arzt, E. (1993a), *Mater. Res. Soc. Symp. Proc. 288,* 1087–1092.

Clemens, H., Schretter, P., Wurzwallner, K., Bartels, A., Koeppe, C. (1993b), in: *Structural Intermetallics:* Darolia, R., Lewandowski, J. J., Liu, C. T., Martin, P. L., Miracle, D. B., Nathal, M. V. (Eds.). Warrendale, PA: TMS, pp. 205–214.

Cline, H. E., Walter, J. L., Lifshin, E., Russel, R. R. (1971), *Metall. Trans. 2,* 189–194.

Cockeram, B., Lipsitt, H. A., Srinivasan, R., Weiss, I. (1991), *Scr. Metall. Mater. 25,* 2109–2114.

Cockeram, B., Saqib, M., Srinivasan, R., Weiss, I. (1992a), *Scr. Metall. Mater. 26,* 749–754.

Cockeram, B., Srinivasan, R., Weiss, I. (1992b), *Scr. Metall. Mater. 26,* 755–760.

ArcelorMittal Ex. 2038
Page 150 of 190

Cohen, S. S., Piacente, P. A., Gildenblat, G., Brown, D. M. (1982), *J. Appl. Phys. 53,* 8856–8860.
Colgan, E. G. (1990), *Mater. Sci. Rep. 5,* 1–44.
Cortie, M. B., Wai, S., Jones, L. J., Cornish, L. A. (1991), in: *Proc. Int. Symp. on Intermetallic Compounds – Structure and Mechanical Properties* (JIMIS-6): Izumi, O. (Ed.). Sendai: The Japan Institute of Metals, pp. 865–869.
Cotton, J. D., Noebe, R. D., Kaufman, M. J. (1993a), *Intermetallics 1,* 3–20.
Cotton, J. D., Noebe, R. D., Kaufman, M. J. (1993b), in: *Structural Intermetallics:* Darolia, R., Lewandowski, J. J., Liu, C. T., Martin, P. L., Miracle, D. B., Nathal, M. V. (Eds.). Warrendale, PA: TMS, pp. 513–522.
Cotton, J. D., Noebe, R., Kaufman, M. J. (1993c), *Intermetallics 1,* 117–126.
Crimp, M. A., Vedula, K. (1986), *Mater. Sci. Eng. 78,* 193–200.
Crimp, M. A., Vedula, K. (1991), *Phil. Mag. A 63,* 559–570.
Crimp, M. A., Vedula, K. M., Gaydosh, D. J. (1987), in: *High Temperature Ordered Intermetallic Alloys* II: Izumi, O., Koch, C. C., Liu, C. T., Stoloff, N. S. (Eds.). Pittsburgh, PA: MRS, pp. 499–504.
Croker, M. (1990), *Met. Mater. 6,* 623–629.
Cros, A. (1983), in: *Passivity of Metals and Semiconductors:* Froment, M. (Ed.). Amsterdam: Elsevier, pp. 473–476.
Crossman, F. W., Yue, A. S. (1971), *Metall. Trans. 2,* 1545–1551.
Cullers, C. L., Antolovich, S. D., Noebe, R. D. (1993), *Mater. Res. Soc. Symp. Proc. 288,* 531–536.
Czarnik, C. M., Gibala, R., Nastasi, M. A., Schwarz, R. B., Srinivasan, S. R., Petrovic, J. J. (1993), *Mater. Res. Soc. Symp. Proc. 288,* 597–602.
Dadras, M. M., Morris, D. G. (1993), *Scr. Metall. Mater. 28,* 1245–1250.
Dahl, O. (1936), *Z. Metallkd. 28,* 133–138.
Dahms, M., Seeger, J., Smarsly, W., Wildhagen, B. (1991), *ISIJ Int. 31,* 1093–1099.
Dahms, M., Leitner, G., Poeßnecker, W., Schultrich, S., Schmelzer, F. (1993), *Z. Metallkd. 84,* 351–357.
Dannöhl, W. (1942), *Arch. Eisenhüttenwes. 15,* 321–330.
Darolia, R. (1991), *J. Met. 43 (3),* 44–49.
Darolia, R. (1993), in: *Structural Intermetallics:* Darolia, R., Lewandowski, J. J., Liu, C. T., Martin, P. L., Miracle, D. B., Nathal, M. V. (Eds.). Warrendale, PA: TMS, pp. 495–504.
Darolia, R., Lahrman, D., Field, R. (1992a), *Scr. Metall. Mater. 26,* 1007–1012.
Darolia, R., Lahrman, D. F., Field, R. D., Dobbs, J. R., Chang, K. M., Goldman, E. H., Konitzer, D. G. (1992b), in: *Ordered Intermetallics – Physical Metallurgy and Mechanical Behaviour:* Cahn, R. W., Liu, C. T., Sauthoff, G. (Eds.). Dordrecht: Kluwer, pp. 679–698.
Darolia, R., Chang, K.-M., Hack, J. E. (1993), *Intermetallics 1,* 65–78.
Das, S., Jewett, T. J., Perepezko, J. H. (1993a), in: *Structural Intermetallics:* Darolia, R., Lewandowski, J. J., Liu, C. T., Martin, P. L., Miracle, D. B., Nathal, M. V. (Eds.): Warrendale, PA: TMS, pp. 35–43.
Das, S., Mishurda, J. C., Allen, W. P., Perepezko, J. H., Chumbley, L. S. (1993b), *Scr. Metall. Mater. 28,* 489–494.
DasGupta, A., Horton, J. A., Liu, C. T. (1984), in: *High-Temperature Alloys: Theory and Design:* Stiegler, J. O. (Ed.). Warrendale, PA: TMS/AIME, pp. 115–124.
Dauphin, J., Dunn, B. D., Judd, M. D., Levadou, F. (1991), *Met. Mater. 7,* 422–430.
Davidson, D. L., Anton, D. L. (1993), *Mater. Res. Soc. Symp. Proc. 288,* 807–813.
Davies, R. G. (1963a), *Trans. AIME 227,* 22–25.
Davies, R. G. (1963b), *Trans. AIME 227,* 277–278.
Davies, R. G., Stoloff, N. S. (1965), *Trans. AIME 233,* 714–719.
Dayananda, M. A. (1992), in: *Ordered Intermetallics – Physical Metallurgy and Mechanical Properties:* Liu, C. T., Cahn, R. W., Sauthoff, G. (Eds.). Dordrecht: Kluwer, pp. 465–484.
de Boer, F. R., Boom, R., Mattens, W. C. M., Miedema, A. R., Niessen, A. K. (1988), in: *Cohesion in Metals – Transition Metal Alloys:* de Boer, F. R., Pettifor, D. G. (Eds.). Amsterdam: North-Holland, pp. 1–758.
De Fontaine, D. (1979), in: *Solid State Physics,* Vol. 34: Ehrenreich, H., Seitz, F., Turnbull, D. (Eds.). New York: Academic, pp. 73–274.
De Fontaine, D., Asta, M., Wolverton, C., Dreyssé, H. (1991), in: *Proc. Int. Symp. Intermetallic Compounds – Structure and Mechanical Properties* (JIMIS-6): Izumi, O. (Ed.). Sendai: The Japan Institute of Metals, pp. 199–207.
De Vos, K. J. (1969), in: *Magnetism and Metallurgy,* Vol. II: Berkowitz, A. E., Kneller, E. (Eds.). New York: Academic, pp. 473–511.
Decamps, P., Gibson, M. A., Morton, A. J., Wolfenden, A. (1991), in: *High Temperature Ordered Intermetallic Alloys* IV: Johnson, L. A., Pope, D. P., Stiegler, J. O. (Eds.). Pittsburgh, PA: MRS, pp. 685–690.
Delaey, L., Krishnan, R. V., Tas, H., Warlimont, H. (1974), *J. Mater. Sci. 9,* 1521–1535.
Delobelle, P., Oytana, C. (1983), *Phys. Status Solidi (a) 75,* 625–634.
Denbigh, K. (1971), *The Principles of Chemical Equilibrium.* Cambridge: Cambridge, University Press, pp. 1–494.
Denquin, A., Naka, S. (1993), *Phil. Mag. Lett. 68,* 13–20.
Destefani, J. D. (1989), *Adv. Mater. Processes 2/89,* 37–41.
DeVan, J. H. (1989), in: *Oxidation of High-Temperature Intermetallics:* Grobstein, T., Doychak, J. (Eds.). Warrendale, PA: TMS, pp. 107–116.

ArcelorMittal Ex. 2038
Page 151 of 190

DeVan, J. H., Hippsley, C. A. (1989), in: *Oxidation of High-Temperature Intermetallics:* Grobstein, T., Doychak, J. (Eds.). Warrendale, PA: TMS, pp. 31–40.

Dew-Hughes, D. (1986), in: *Encyclopedia of Materials Science and Engineering:* Bever, M. B. (Ed.). Oxford: Pergamon, pp. 4771–4778.

Dew-Hughes, D. (1988), *Met. Mater. 4,* 741–745.

Dew-Hughes, D., Quincey, P. G., Upadhyay, P. L. (1987), *Mater. Sci. Technol. 3,* 936–943.

Dève, H. E., Weber, C. H., Maloney, M. (1992), *Mater. Sci. Eng. A 153,* 668–675.

d'Heurle, F. M. (1993a), in: *Diffusion in Ordered Alloys and Intermetallic Compounds:* Fultz, B., Cahn, R. W., Gupta, D. (Eds.), Warrendale, PA: TMS, pp. 185–201.

d'Heurle, F. M. (1993b), *J. Mater. Res. 3,* 167–195.

d'Heurle, F. M., Gas, P. (1986), *J. Mater. Res. 1,* 205–221.

d'Heurle, F. M., Petersson, C. S., Baglin, J. E. E., La Placa, S. J., Wong, C. Y. (1984), *J. Appl. Phys. 55,* 4208–4212.

Dickson, R. W., Wachtmann, J. B., Jr., Copley, S. M. (1969), *J. Appl. Phys. 40,* 2276–2279.

Dietrich, D. W. (1990), in: *Metals Handbook,* Vol. 2, *Properties and Selection: Nonferrous Alloys and Special-Purpose Materials.* Materials Park, OH: ASM, pp. 761–777.

Dimiduk, D. .M, Mendiratta, M. G., Banerjee, D., Lipsitt, H. A. (1988), *Acta Metall. 36,* 2947–2958.

Dimiduk, D. M., Miracle, D. B., Kim, Y.-W., Mendiratta, M. G. (1991), *ISIJ Int. 31,* 1223–1234.

Dimiduk, D. M., Miracle, D. B., Ward, C. H. (1992), *Mater. Sci. Technol. 8,* 367–375.

Dimiduk, D. M., Thompson, A. W., Williams, J. C. (1993), *Phil. Mag. A 67,* 675–698.

Dirras, G., Beauchamp, P., Veyssière, P. (1992), *Phil. Mag. A 65,* 815–828.

Dogan, B., Wagner, R., Beaven, P. A. (1991), *Scr. Metall. 25,* 773–778.

Dollar, M., Dymek, S., Hwang, S. J., Nash, P. (1992), *Scr. Metall. Mater. 26,* 29–34.

Dominguez-Rodriguez, A., Castaing, J. (1993), *Scr. Metall. Mater. 28,* 1207–1211.

Douin, J., Naka, S., Thomas, M. (1993), *Mater. Res. Soc. Symp. Proc. 288,* 317–322.

Dowling, J., Donlon, W. T., Allison, J. E. (1991), in: *High Temperature Ordered Intermetallic Alloys* IV: Johnson, L. A., Pope, D. P., Stiegler, J. O. (Eds.). Pittsburgh, PA: MRS, pp. 561–567.

Doychak, J., Smialek, J. L., Barrett, C. A. (1989), in: *Oxidation of High-Temperature Intermetallics:* Grobstein, T., Doychak, J. (Eds.). Warrendale, PA: TMS, pp. 41–56.

Drasner, A., Blazina, Z. (1991), *J. Less-Common Met. 168,* 289–294.

Dunmead, S. D., Munir, Z. A., Holt, J. B., Kingman, D. D. (1991), *J. Mater. Sci. 26,* 2410–2416.

Durlu, N., Inal, O. T. (1992a), *J. Mater. Sci. 27,* 1175–1178.

Durlu, N., Inal, O. T. (1992b), *J. Mater. Sci. 27,* 3225–3230.

Durlu, N., Inal, O. T., Yost, F. G. (1991), *Scr. Metall. Mater. 25,* 2475–2479.

Dwight, A. E. (1967), in: *Intermetallic Compounds:* Westbrook, J. H. (Ed.). New York: Wiley, pp. 166–179.

Dymek, S., Dollar, M., Hwang, S. J., Nash, P. (1992), *Mater. Sci. Eng. A 152,* 160–165.

Dymek, S., Dollar, M., Hwang, S. J., Nash, P. (1993), *Mater. Res. Soc. Symp. Proc. 228,* 1117–1122.

Eckerlin, P., Kandler, H., Stegherr, A. (1971), in: *Landolt-Börnstein – Zahlenwerte und Funktionen aus Naturwissenschaften und Technik, Neue Serie, Gruppe III, Band 6: Strukturdaten der Elemente und intermetallischen Phasen:* Hellwege, K.-H., Hellwege, A. M. (Eds.). Berlin: Springer, p. 279.

Edwards, K. M., Gibala, R. (1993), *Mater. Res. Soc. Symp. Proc. 288,* 665–670.

Ehlers, S. K., Mendiratta, M. G. (1984), *J. Mater. Sci. 19,* 2203–2210.

Eisenstatt, R. L., Wright, R. N. (1980), *Metall. Trans. 11 A,* 1131–1138.

Eizenberg, M., Tu, K. N. (1982), *J. Appl. Phys. 53,* 1577–1585.

Eizenberg, M., Foell, H., Tu, K. N. (1981), *J. Appl. Phys. 52,* 861–864.

Eliezer, D., Froes, F. H., Suryanarayana, C. (1991), *J. Met. 43 (3),* 59–62.

Ellner, M., Kek, S., Predel, B. (1989), *J. Less-Common Met. 154,* 207–215.

Ellner, M., Kek, S., Predel, B. (1992), *J. Alloys Compd. 189,* 245–248.

Enami, K., Martynov, V. V., Tomie, T., Khandros, L. G., Nenno, S. (1981), *Trans. JIM 22 (5),* 357–366.

Engell, H.-J., Von Keitz, A., Sauthoff, G. (1991), in: *Advanced Structural and Functional Materials:* Bunk, W. (Ed.). Berlin: Springer, pp. 91–132.

Enomoto, M., Harada, H. (1989), *Metall. Trans. 20 A,* 649–664.

Enomoto, M., Harada, H., Yamazaki, M. (1991), *CALPHAD: Comput. Coupling Phase Diagrams Thermochem. 15,* 143–158.

Erschbaumer, R., Podloucky, R., Rogl, P., Temnitschka, G. (1993), *Intermetallics 1,* 99–106.

Esslinger, P., Smarsly, W. (1991), *MTU Focus 1,* 36–41.

Es-Souni, M., Chen, D., Dogan, B., Wagner, R., Beaven, P. A., Bartels, A. (1991), in: *Proc. Int. Symp. on Intermetallic Compounds – Structure and Mechanical Properties* (JIMIS-6): Izumi, O. (Ed.). Sendai: The Japan Institute of Metals, pp. 525–529.

Es-Souni, M., Wagner, R., Beaven, P. A., Bartels, A. (1992a), *Mater. Sci. Eng. A 153,* 444–450.

Es-Souni, M., Wagner, R., Beaven, P. A., Schimansky, F.-P., Gerling, R. (1992b), *Scr. Metall. Mater. 26,* 727–732.

Es-Souni, M., Wagner, R., Beaven, P. A., Schimansky, F.-P., Gerling, R. (1992c), *Scr. Metall. Mater. 26,* 1845–1850.

ArcelorMittal Ex. 2038
Page 152 of 190

Es-Souni, M., Wagner, R., Chen, D., Beaven, P. A., Bartels, A., Seeger, J. (1992d), in: *Advanced Structural Materials*, Vol. 2: Clyne, T. W., Withers, P. J. (Eds.). London: The Institute of Materials, pp. 349–354.

Eucken, S., Kobus, E., Hornbogen, E. (1991), *Z. Metallkd. 82*, 640–645.

Evans, A. G., Cannon, R. M. (1986), *Acta Metall. 34*, 761–800.

Evans, D. J., Court, S. A., Hazzledine, P. M., Fraser, H. L. (1993), *Mater. Res. Soc. Symp. Proc. 288*, 567–572.

Fang, J., Schulson, E. M. (1992), *Mater. Sci. Eng. A 152*, 138–145.

Faress, A., Vanderschaeve, G. (1987), *Acta Metall. 35*, 691–699.

Farkas, D., Pasianot, R., Savino, E. J., Miracle, D. B. (1991), in: *High Temperature Ordered Intermetallic Alloys* IV: Johnson, L. A., Pope, D. P., Stiegler, J. O. (Eds.). Pittsburgh, PA: MRS, pp. 223–228.

Feng, C. R., Michel, D. J. (1991), *Scr. Metall. Mater. 25*, 1793–1798.

Feng, C. R., Michel, D. J. (1993), *Mater. Res. Soc. Symp. Proc. 288*, 1051–1056.

Feng, C. R., Sadananda, K. (1990), *Scr. Metall. Mater. 24*, 2107–2112.

Feng, C. R., Michel, D. J., Crowe, C. R. (1990a), *Scr. Metall. Mater. 24*, 1895–1900.

Feng, C. R., Smith, H. H., Michel, D. J., Crowe, C. R. (1990b), in: *Intermetallic Matrix Composites:* Anton, D. L., Martin, P. L., Miracle, D. B., McMeeking, R. (Eds.). Pittsburgh, PA: MRS, pp. 219–224.

Field, R. D., Lahrman, D. F., Darolia, R. (1991a), *Acta Metall. Mater. 39*, 2951–2959.

Field, R. D., Lahrman, D. F., Darolia, R. (1991b), *Acta Metall. Mater. 39*, 2961–2969.

Field, R. D., Lahrman, D. F., Darolia, R. (1993), *Mater. Res. Soc. Symp. Proc. 288*, 423–428.

Fiepke, J. W. (1990), in: *Metals Handbook*, Vol. 2, *Properties and Selection: Nonferrous Alloys and Special-Purpose Materials*. Materials Park, OH: ASM, pp. 782–803.

Fitzer, E. (1952), in: *Pulvermetallurgie* (1. Plansee-Seminar): Benesovsky, F. (Ed.). Reutte, Tirol: Metallwerk Plansee, pp. 244–258.

Fitzer, E. (1955), in: *4. Plansee-Seminar:* Benesovsky, F. (Ed.). Reutte, Tirol: Metallwerk Plansee, pp. 56–79.

Fitzer, E., Gerasimoff, P. (1959), *Z. Metallkd. 50*, 187–196.

Fitzer, E., Rubisch, O. (1958), *Interceram. (7)*, 39–40.

Fitzer, E., Schlichting, J. (1983), in: *High Temperature Corrosion:* Rapp, R. A. (Ed.). Houston: National Association of Corrosion Engineers, pp. 604–614.

Fitzer, E., Nowak, W., Mäurer, H. J. (1978), in: *Materials and Coatings to Resist High Temperature Corrosion:* Holmes, D. R., Rahmel, A. (Eds.). London: Applied Science, pp. 313–331.

Fleischer, R. L. (1985), *J. Met. 37 (12)*, 16–20.

Fleischer, R. L. (1988), *Scr. Metall. 22*, 743–744.

Fleischer, R. L. (1989), in: *High-Temperature Ordered Intermetallic Alloys* III. Liu, C. T., Taub, A. I., Stoloff, N. S., Koch, C. C. (Eds.). Pittsburgh, PA: Mater. Res. Soc., pp. 305–310.

Fleischer, R. L. (1990), in: *Intermetallic Matrix Composites:* Anton, D. L., Martin, P. L., Miracle, D. B., McMeeking, R. (Eds.). Pittsburgh, PA: MRS, pp. 249–256.

Fleischer, R. L. (1992a), *Platinum Met. Rev. 36*, 138–145.

Fleischer, R. L. (1992b), *Scr. Metall. Mater. 27*, 799–804.

Fleischer, R. L. (1993a), *Acta Metall. Mater. 41*, 863–869.

Fleischer, R. L. (1993b), *Acta Metall. Mater. 41*, 1197–1205.

Fleischer, R. L. (1993c), *J. Mater. Res. 8*, 49–58.

Fleischer, R. L. (1993d), *Mater. Res. Soc. Symp. Proc. 288*, 165–170.

Fleischer, R. L. (1993e), *J. Mater. Res. 8*, 59–67.

Fleischer, R. L. (1993f), *Metall. Trans. 24A*, 227–230.

Fleischer, R. L., McKee, D. W. (1993), *Metall. Trans. 24A*, 759–763.

Fleischer, R. L., Zabala, R. J. (1990a), *Metall. Trans. 21A*, 1951–1957.

Fleischer, R. L., Zabala, R. J. (1990b), *Metall. Trans. 21A*, 2149–2154.

Fleischer, R. L., Zabala, R. J. (1990c), *Metall. Trans. 21A*, 2709–2716.

Fleischer, R. L., Gilmore, R. S., Zabala, R. J. (1988), *J. Appl. Phys. 64*, 2964–2967.

Fleischer, R. L., Dimiduk, D. M., Lipsitt, H. A. (1989a), *Annu. Rev. Mater. Sci. 19*, 231–263.

Fleischer, R. L., Gilmore, R. S., Zabala, R. J. (1989b), *Acta Metall. 37*, 2801–2803.

Fleischer, R. L., Field, R. D., Denike, K. K., Zabala, R. J. (1990), *Metall. Trans. 21A*, 3063–3074.

Fleischer, R. L., Briant, C. L., Field, R. D. (1991), in: *High Temperature Ordered Intermetallic Alloys* IV: Johnson, L. A., Pope, D. P., Stiegler, J. O. (Eds.). Pittsburgh, PA: MRS, pp. 463–474.

Flinn, B. D., Rühle, M., Evans, A. G. (1989), *Acta Metall. 37*, 3001–3006.

Flinn, R. A. (1986), in: *Encyclopedia of Materials Science and Engineering*, Vol. 1: Bever, M. B. (Ed.). Oxford: Pergamon, pp. 859–863.

Foiles, S. M., Daw, M. S. (1987), *J. Mater. Res. 2*, 5–14.

Forbes, K. R., Nix, W. D. (1993), *Mater. Res. Soc. Symp. Proc. 288*, 749–755.

Forbes, K. R., Glatzel, U., Darolia, R., Nix, W. D. (1993), *Mater. Res. Soc. Symp. Proc. 288*, 45–57.

Fortnum, R. T., Mikkola, D. E. (1987), *Mater Sci. Eng. 91*, 223–231.

Fox, A. G., Tabbernor, M. A. (1991), *Acta Metall. Mater. 39*, 669–678.

ArcelorMittal Ex. 2038
Page 153 of 190

Franceschi, E. A., Ricaldone, F. (1984), *Rev. Chim. Miner. 21,* 202–230.

Freeman, A. J., Hong, T., Lin, W., Xu, J.-H. (1991), in: *High Temperature Ordered Intermetallic Alloys* IV: Johnson, L. A., Pope, D. P., Stiegler, J. O. (Eds.). Pittsburgh, PA: MRS, pp. 3–18.

Freeman, A. J., Xu, J.-H., Hong, T., Win, W. (1992), in: *Ordered Intermetallics – Physical Metallurgy and Mechanical Behaviour:* Liu, C. T., Cahn, R. W., Sauthoff, G. (Eds.). Dordrecht: Kluwer, pp. 1–14.

Fridberg, J., Törndahl, L.-E., Hillert, M. (1969), *Jernkontorets Ann. 153,* 263–276.

Froes, F. H., Suryanarayana, C., Eliezer, D. (1991), *ISIJ Int. 31,* 1235–1248.

Froes, F. H., Suryanarayana, C., Eliezer, D. (1992), *J. Mater. Sci. 27,* 5113–5140.

Frommeyer, G., Rosenkranz, R., Lüdecke, C. (1990), *Z. Metallkd. 81,* 307–313.

Frommeyer, G., Wunderlich, W., Kremser, T., Liu, Z. G. (1992), *Mater. Sci. Eng. A 152,* 166–172.

Frost, H. J., Ashby, M. F. (1982), *Deformation Mechanism Maps.* Oxford: Pergamon, pp. 1–166.

Fu, C. L. (1991), in: *Proc. Int. Symp. on Intermetallic Compounds – Structure and Mechanical Properties* (JIMIS-6): Izumi, O. (Ed.). Sendai: The Japan Institute of Metals, pp. 387–396.

Fu, C. L., Yoo, M. H. (1990), *Phil. Mag. Lett. 62,* 159–165.

Fu, C. L., Yoo, M. H. (1991), in: *High Temperature Ordered Intermetallic Alloys* IV: Johnson, L. A., Pope, D. P., Stiegler, J. O. (Eds.). Pittsburgh, PA: MRS, pp. 667–672.

Fu, C. L., Yoo, M. H. (1992a), in: *Ordered Intermetallics – Physical Metallurgy and Mechanical Behaviour:* Liu, C. T., Cahn, R. W., Sauthoff, G. (Eds.). Dordrecht: Kluwer, pp. 155–164.

Fu, C. L., Yoo, M. H. (1992b), *Acta Metall. Mater. 40,* 703–711.

Fu, C. L., Yoo, M. H. (1993), *Intermetallics 1,* 59–63.

Fu, C. L., Ye, Y.-Y., Yoo, M. H. (1993a), *Mater. Res. Soc. Symp. Proc. 288,* 21–32.

Fu, C. L., Ye, Y.-Y., Yoo, M. H. (1993b), *Phil. Mag. Lett. 67,* 179–185.

Fuchs, G. E. (1989), in: *High-Temperature Ordered Intermetallic Alloys* III: Liu, C. T., Taub, A. I., Stoloff, N. S., Koch, C. C. (Eds.). Pittsburgh, PA: MRS, pp. 615–620.

Fuchs, G. E. (1993), *Mater. Res. Soc. Symp. Proc. 288,* 847–852.

Fuchs, G. E., Stoloff, N. S. (1988), *Acta Metall. 36,* 1381–1387.

Fuentes-Samaniego, R., Nix, W. D. (1981), *Scr. Metall. 15,* 15–20.

Fujitsuna, N., Ohyama, H., Miyamoto, Y., Ashida, Y. (1991), *ISIJ Int. 31,* 1147–1153.

Fujiwara, T., Yasuda, K., Kodama, H. (1991), in: *Proc. Int. Symp. on Intermetallic Compounds – Structure and Mechanical Properties* (JIMIS-6): Izumi, O. (Ed.). Sendai: The Japan Institute of Metals, pp. 633–637.

Fujiwara, T., Yasuda, K., Kodama, H. (1993), *Mater. Res. Soc. Symp. Proc. 288,* 959–964.

Furukawa, S., Inoue, A., Masumoto, T. (1988), *Mater. Sci. Eng. 98,* 515–518.

Furuto, Y. (1984), in: *Niobium:* Stuart, H. (Ed.), Warrendale, PA: The Metallurgical Society of AIME, pp. 445–494.

Furuya, Y., Sasaki, A., Taya, M. (1993), *Mater. Trans. Jpn. Inst. Met. 34,* 224–227.

Gao, M., Boodey, J. B., Wei, R. P. (1990), *Scr. Metall. Mater. 24,* 2135–2138.

Gao, Z. Q., Fultz, B. (1993), *Phil. Mag. B67,* 787–800.

Gaspard, C., Diderrich, E., Leroy, V., Huet, J. J., Habraken, L. (1977), *J. Nucl. Mater. 68,* 104–110.

Geballe, T. H., Hulm, J. K. (1975), *IEEE Trans. Magn. Mag. 11,* 119–124.

Geballe, T. H., Hulm, J. K. (1986), in: *Encyclopedia of Materials Science and Engineering:* Bever, M. B. (Ed.). Oxford: Pergamon, pp. 4737–4741.

George, E. P., Liu, C. T., Liao, J. J. (1991a), in: *Alloy Phase Stability and Design:* Stocks, G. M., Pope, D. P., Giamei, A. F. (Eds.). Pittsburgh, PA: MRS, pp. 375–380.

George, E. P., Pope, D. P., Fu, C. L., Schneibel, J. H. (1991b), *ISIJ Int. 31,* 1063–1075.

George, E. P., Liu, C. T., Pope, D. P. (1992), *Scr. Metall. Mater. 27,* 365–370.

George, E. P., Liu, C. T., Pope, D. P. (1993a), in: *Structural Intermetallics:* Darolia, R., Lewandowski, J. J., Liu, C. T., Martin, P. L., Miracle, D. B., Nathal, M. V. (Eds.). Warrendale, PA: TMS, pp. 431–436.

George, E. P., Liu, C. T., Pope, D. P. (1993b). *Mater. Res. Soc. Symp. Proc. 288,* 941–945.

George, E. P., Liu, C. T., Pope, D. P. (1993c), *Scr. Metall. Mater. 28,* 857–862.

Georgopoulos, P., Cohen, J. B. (1981), *Acta Metall. 29,* 1535–1551.

Gibala, R., Chang, H., Czarnik, C. M., Edwards, K. M., Misra, A. (1993), in: *Structural Intermetallics:* Darolia, R., Lewandowski, J. J., Liu, C. T., Martin, P. L., Miracle, D. B., Nathal, M. V. (Eds.). Warrendale, PA: TMS, pp. 561–567.

Giegengack, H., Schott, H., Schulze, G. E. R., Ulrich, H.-J. (1966), *Phys. Status Solidi 14,* K189–K193.

Gieseke, B. G., Sikka, V. K. (1992), *Mater. Sci. Eng. A 153,* 520–524.

Gieseke, B. G., Alexander, D. J., Sikka, V. K., Baldwin, R. H. (1993), *Scr. Metall. Mater. 29,* 129–134.

Girgis, K. (1983), in: *Physical Metallurgy:* Cahn, R. W., Haasen, P. (Eds.). Amsterdam: North-Holland, pp. 219–269.

Girifalco, L. A. (1964), *J. Phys. Chem. Solids 25,* 323–328.

Gladyshevskii, E. I., Bodak, O. I. (1982), *Kristallokhimiya Intermetallicheskikh Soedineniy Redkozemelnykh Metallov.* L'vov, Ukraina: Vishcha Shkola, pp. 1–251.

ArcelorMittal Ex. 2038
Page 154 of 190

Gladyshevskii, E. I., Bodak, O. I. (1994), in: *Intermetallic Compounds: Principles and Practice,* Vol. 1: Westbrook, J. H., Fleischer, R. L. (Eds.). Chichester, UK: Wiley.

Gladyshevskii, E. I., Borusevich, L. K. (1966), *Izv. Akad. Nauk SSSR, Metal. (5),* 159–164.

Glatzel, U., Feller-Kniepmeier, M. (1991), *Scr. Metall. Mater. 25,* 1845–1850.

Glatzel, U., Forbes, K. R., Nix, W. D. (1993a), *Phil. Mag. A67,* 307–323.

Glatzel, U., Forbes, K. R., Nix, W. D. (1993b), *Mater. Res. Soc. Symp. Proc. 288,* 385–390.

Glazova, V. V. (1965), *Dokl. Akad. Nauk SSSR 164,* 569–570.

Glowacki, B. A., Evetts, J. E. (1988), *J. Mater. Sci. 23,* 1961–1966.

Gmelin-Institut (1955), in: *Gmelins Handbuch der Anorganischen Chemie,* Vol. 60A, *1: Kupfer:* Gmelin-Institut (Eds.). Weinheim: Verlag Chemie, pp. 5–6.

Gödecke, T., Köster, W. (1985), *Z. Metallkd. 76,* 676–683.

Gödecke, T., Köster, W. (1986), *Z. Metallkd. 77,* 408–411.

Golberg, D., Shevakin, A. (1991), in: *Proc. Int. Symp. on Intermetallic Compounds – Structure and Mechanical Properties* (JIMIS-6): Izumi, O. (Ed.). Sendai: The Japan Institute of Metals, pp. 251–255.

Goldman, E. H. (1993), *Mater. Res. Soc. Symp. Proc. 288,* 83–94.

Goldschmidt, H. J. (1967a), *Interstitial Alloys.* London: Butterworths, pp. 187–195.

Goldschmidt, H. J. (1967b), *Interstitial Alloys.* London: Butterworths, pp. 296–348.

Goldschmidt, H. J. (1969), *J. Inst. Met. 97,* 173–179.

Gonis, A., Sluiter, M., Turchi, P. E. A., Stocks, G. M., Nicholson, D. M. (1991), *J. Less-Common Met. 168,* 127–144.

Goo, E., Duerig, T., Melton, K., Sinclair, R. (1985), *Acta Metall. 33,* 1725–1733.

Gordon, D. E., Unni, C. K. (1991), *J. Mater. Sci. 26,* 6183–6189.

Gottstein, G., Nagpal, P., Kim, W. (1989), *Mater. Sci. Eng. A 108,* 195–201.

Gottstein, G., Chang, L., Yung, H. F. (1991), *Mater. Sci. Technol. 7,* 158–166.

Grabke, H. J., Brumm, M. (1989), in: *Oxidation of High-Temperature Intermetallics:* Grobstein, T., Doychak, J. (Eds.). Warrendale, PA: TMS, pp. 245–256.

Grabke, H. J., Steinhorst, M., Brumm, M., Wiemer, D. (1990), *Werkstoffe Korros. 41,* 689–691.

Grabke, H. J., Brumm, M., Steinhorst, M. (1991a), *Fresenius Z. Anal. Chem. 341,* 378–382.

Grabke, H. J., Steinhorst, M., Brumm, M., Wiemer, D. (1991b), *Oxid. Met. 35,* 199–222.

Grabke, H. J., Brumm, M., Steinhorst, M. (1992), *Mater. Sci. Technol. 8,* 339–344.

Grala, E. M. (1960), in: *Mechanical Properties of Intermetallic Compounds:* Westbrook, J. H. (Ed.). New York: Wiley, pp. 358–404.

Greenberg, B. A., Indenbaum, V. N., Smirnov, L. V. (1991), *Acta Metall. Mater. 39,* 243–254.

Gregory, E. (1984), in: *Niobium:* Stuart, H. (Ed.). Warrendale, PA: The Metallurgical Society of AIME, pp. 503–531.

Grensing, F. (1989), in: *Oxidation of High-Temperature Intermetallics:* Grobstein, T., Doychak, J. (Eds.). Warrendale, PA: TMS, pp. 279–294.

Grinthal, R. D. (1956), WADC Technical Report 53-190, 1–57.

Grinthal, R. D. (1958), WADC Technical Report 53-190, 1–80.

Grujicic, M., Tangrila, S., Cavin, O. B., Porter, W. D., Hubbard, C. R. (1993), *Mater. Sci. Eng. A 160,* 37–48.

Grünling, H. W., Leistikow, S., Rahmel, A., Schubert, F. (1983), in: *Aufbau von Oxidschichten auf Hochtemperaturwerkstoffen und ihre technische Bedeutung:* Rahmel, A. (Ed.). Oberursel: DGM, pp. 7–32.

Gschneidner, K. A., Jr. (1993), *J. Alloys Compd. 193,* 1–6.

Guan, J., Dieckhues, G. W., Sahm, P. R. (1994), *Intermetallics 2,* 89–94.

Guard, R. W., Westbrook, J. H. (1959), *Trans. AIME 215,* 807–814.

Gudmundsson, B., Jacobson, B. E. (1988), *Mater. Sci. Eng. 100,* 207–217.

Guertler, W., Guertler, M., Anastasiadias, E. (1969), *A Compendium of Constitutional Ternary Diagrams of Metallic Systems* (WADC Technical Report 58-615). Jerusalem: Israel Program for Scientific Translations, pp. 527–548.

Guha, S., Munroe, P. R., Baker, I. (1989), in: *High-Temperature Ordered Intermetallic Alloys* III: Liu, C. T., Taub, A. I., Stoloff, N. S., Koch, C. C. (Eds.). Pittsburgh, PA: Mater. Res. Soc., pp. 633–638.

Guha, S., Baker, I., Munroe, P. R., Michael, J. R. (1992), *Mater. Sci. Eng. A 152,* 258–263.

Guilemany, J. M., Peregrin, F. (1992), *J. Mater. Sci. 27,* 863–868.

Guillet, L., Le Roux, R. (1967), in: *Intermetallic Compounds:* Westbrook, J. H. (Ed.). New York: Wiley, pp. 453–463.

Guo, J. T., Jin, O., Yin, W. M., Wang, T. M. (1993), *Scr. Metall. Mater. 29,* 783–785.

Guo, X.-Q., Podloucky, R., Freeman, A. J. (1991), *J. Mater. Res. 6,* 324–329.

Gupta, D., Vieregge, K., Rodbell, K. P., Tu, K. N. (1993), in: *Diffusion in Ordered Alloys and Intermetallic Compounds:* Fultz, B., Cahn, R. W., Gupta, D. (Eds.). Warrendale, PA: TMS, pp. 247–259.

Gupta, K. P., Rajan, N. S., Beck, P. A. (1960), *Trans. AIME 218,* 617–624.

Györffy, B. L., Barbieri, A., Johnson, D. D., Nicholson, D. M., Pinski, F. J., Shelton, W. A., Stocks, G. M. (1991), in: *Alloy Phase Stability and Design:* Stocks, G. M., Pope, D. P., Giamei, A. F. (Eds.). Pittsburgh, PA: MRS, pp. 3–20.

ArcelorMittal Ex. 2038
Page 155 of 190

Haasen, P. (1983), in: *Physical Metallurgy:* Cahn, R. W., Haasen, P. (Eds.). Amsterdam: North-Holland/Elsevier, pp. 1341–1409.

Hack, J. E., Brzeski, J. M., Darolia, R. (1992), *Scr. Metall. Mater. 27,* 1259–1263.

Hack, J. E., Brzeski, J. M., Darolia, R., Field, R. D. (1993), *Mater. Res. Soc. Symp. Proc. 288,* 1197–1202.

Hackenbracht, D., Kübler, J. (1980), *J. Phys. F 10,* 427–440.

Haff, G. R., Schulson, E. M. (1982), *Metall. Trans. A 13,* 1563–1569.

Hafner, J. (1987), *From Hamiltonians to Phase Diagrams.* Heidelberg: Springer, pp. 207–240.

Hafner, J. (1989), in: *The Structure of Binary Compounds:* de Boer, F. R., Pettifor, D. G. (Eds.). Amsterdam: North-Holland, pp. 147–286.

Hagel, W. C. (1967), in: *Intermetallic Compounds:* Westbrook, J. H. (Ed.). New York: Wiley, pp. 377–404.

Hahn, K. H., Vedula, K. (1989), *Scr. Metall. 23,* 7–12.

Hall, E. L., Livingston, J. D. (1989), in: *Proc. of the 47th Annual Meeting of the Electron Microscopy Society of America:* Bailey, G. W. (Ed.). San Francisco: San Francisco Press, pp. 318–319.

Hall, E. O., Algie, S. H. (1966), *Metall. Rev. 11,* 61–88.

Halstead, A., Rawlings, R. D. (1984), *Met. Sci. 18,* 491–500.

Halstead, A., Rawlings, R. D. (1985), *J. Mater. Sci. 20,* 1248–1256.

Hanada, S., Watanabe, S., Sato, T., Izumi, O. (1981a), *Trans. JIM 22,* 873–881.

Hanada, S., Watanabe, S., Sato, T., Izumi, O. (1981b), *Scr. Metall. 15,* 1345–1348.

Hancock, G. F., McDonnell, B. R. (1971), *Phys. Status Solidi (a) 4,* 143–150.

Hao, S. M., Takayama, T., Ishida, K., Nishizawa, T. (1984), *Metall. Trans. 15A,* 1819–1828.

Hao, S. M., Ishida, K., Nishizawa, T. (1985), *Metall. Trans. 16A,* 179–185.

Hardwick, D. A., Martin, P. L., Patankar, S. N., Lewandowski, J. J. (1993), in: *Structural Intermetallics:* Darolia, R., Lewandowski, J. J., Liu, C. T., Martin, P. L., Miracle, D. B., Nathal, M. V. (Eds.). Warrendale, PA: TMS, pp. 665–674.

Harmouche, M. R., Wolfenden, A. (1985), *J. Test. Eval. 13,* 424–428.

Harmouche, M. R., Wolfenden, A. (1986), *Mater. Sci. Eng. 84,* 35–42.

Harmouche, M. R., Wolfenden, A. (1987), *J. Test. Eval. 15,* 101–104.

Harris, I. R., McGuiness, P. J. (1991), *J. Less-Common Met. 172–174,* 1273–1284.

Hasaka, M., Morimura, T., Hisatsune, K., Uchiyama, Y., Kondo, S., Nakashima, H., Furuse, T. (1993a), *Scr. Metall. Mater. 29,* 963–966.

Hasaka, M., Morimura, T., Kondo, S., Uchiyama, Y., Hisatsune, K. (1993b), *Scr. Metall. Mater. 29,* 967–970.

Hasegawa, S., Wada, S., Takasugi, T., Izumi, O. (1993a), *Mater. Sci. Technol. 9,* 61–66.

Hasegawa, S., Wada, S., Takasugi, T., Izumi, O. (1993b), *Mater. Res. Soc. Symp. Proc. 288,* 659–663.

Hashimoto, K., Kimura, M. (1993), in: *Structural Intermetallics:* Darolia, R., Lewandowski, J. J., Liu, C. T., Martin, P. L., Miracle, D. B., Nathal, M. V. (Eds.). Warrendale, PA: TMS, pp. 309–318.

Hashimoto, K., Doi, H., Tsujimoto, T. (1986a), *Trans. JIM 27,* 94–101.

Hashimoto, K., Doi, H., Tsujimoto, T. (1986b), *Trans. JIM 27,* 141–149.

Hashimoto, K., Nobuki, M., Tsujimoto, T., Suzuki, T. (1991), *ISIJ Int. 31,* 1154–1160.

Hattori, T., Iwadate, Y., Tatsumoto, H., Mochizuki, T. (1988), *J. Mater. Sci. Lett. 7,* 481–483.

Haubold, T., Bohn, R., Birringer, R., Gleiter, H. (1992), *Mater. Sci. Eng. A 153,* 679–683.

Hayashi, N., Morii, K., Nakayama, Y. (1991), *Mater. Trans. Jpn. Inst. Met. 32,* 285–291.

Hayashi, T., Shinoda, T., Mishima, Y., Suzuki, T. (1991a), in: *High Temperature Ordered Intermetallic Alloys* IV: Johnson, L. A., Pope, D. P., Stiegler, J. O. (Eds.). Pittsburgh, PA: MRS, pp. 617–622.

Hayashi, T., Takekawa, M., Miura, S., Mishima, Y., Suzuki, T. (1991b), in: *Proc. Int. Symp. on Intermetallic Compounds – Structure and Mechanical Properties* (JIMIS-6): Izumi, O. (Ed.). Sendai: The Japan Institute of Metals, pp. 421–425.

Hayes, R. W. (1991), *Acta Metall. Mater. 39,* 569–578.

Hayes, R. W., London, B. (1992), *Acta Metall. Mater. 40,* 2167–2175.

Hazzledine, P. M., Pirouz, P. (1993), *Scr. Metall. Mater. 28,* 1277–1282.

Hazzledine, P. M., Schneibel, J. H. (1989), *Scr. Metall. 23,* 1887–1892.

Hazzledine, P. M., Kumar, K. S., Miracle, D. B., Jackson, A. G. (1993), *Mater. Res. Soc. Symp. Proc. 288,* 591–596.

Hebsur, M. G., Stephens, J. R., Smialek, J. L., Barrett, C. A., Fox, D. S. (1989), in: *Oxidation of High-Temperature Intermetallics:* Grobstein, T., Doychak, J. (Eds.). Warrendale, PA: TMS, pp. 171–184.

Hebsur, M. G., Whittenberger, J. D., Dickerson, R. M., Aikin, B. J. M. (1993), *Mater. Res. Soc. Symp. Proc. 288,* 1111–1116.

Hecker, A., Gregory, E., Wong, J. (1988), *J. Less-Common Met. 139,* 53–60.

Hellwig, A. (1990), Dr. Ing. Thesis, Universität Dortmund, pp. 1–179.

Hellwig, A., Inden, G., Palm, M. (1992), *Scr. Metall. Mater. 27,* 143–148.

Hemker, K. J., Nix, W. D. (1993), *Metall. Trans. 24A,* 335–341.

Hemker, K. J., Mills, M. J., Nix, W. D. (1991), *Acta Metall. Mater. 39,* 1901–1913.

ArcelorMittal Ex. 2038
Page 156 of 190

Henager, C. H., Jr., Brimhall, J. L., Vetrano, J. S., Hirth, J. P. (1992a), *Mater. Res. Soc. Symp. Proc. 273,* 281–288.

Henager, C. H., Jr., Jacobson, R. E., Bruemmer, S. M. (1992b), *Mater. Sci. Eng. A 153,* 416–421.

Heredia, F. E., Valencia, J. J. (1992), *Mater. Res. Soc. Symp. Proc. 273,* 197–205.

Heredia, F. E., He, M. Y., Lucas, G. E., Evans, A. G., Dève, H. E., Konitzer, D. (1993), *Acta Metall. Mater. 41,* 505–511.

Herget, C., Domazer, H.-G. (1975), *Goldschmidt informiert 35,* 3–33.

Herring, C. (1950), *J. Appl. Phys. 21,* 437–445.

Hesse, J. (1969a), *Z. Angew. Phys. 28,* 133–137.

Hesse, J. (1969b), *Z. Metallkd. 60,* 652–659.

Heusler, O. (1989), *Z. Metallkd. 80,* 908.

Hildebrandt, U. W., Wahl, G., Nicoll, A. R. (1978), in: *Materials and Coatings to Resist High Temperature Corrosion:* Holmes, D. R., Rahmel, A. (Eds.). London: Applied Science, pp. 213–231.

Hilfrich, K., Kölker, W., Petry, W., Schärpf, O., Nembach, E. (1990), *Scr. Metall. Mater. 24,* 39–44.

Hilfrich, K., Ebel, T., Petry, W., Schärpf, O., Nembach, E. (1991), *Scr. Metall. Mater. 25,* 1857–1862.

Hillman, H., Pfister, H., Springer, E., Wilhelm, M., Wohleben, K. (1980), in: *Filamentary A15 Superconductors:* Suenaga, M., Clark, A. F. (Eds.). New York: Plenum, pp. 17–23.

Hilpert, K., Kobertz, D., Venugopal, V., Miller, M., Gerads, H., Bremer, F. J. Nickel, H. (1987), *Z. Naturforsch. 42a,* 1327–1332.

Himsel, A., Blau, W., Merz, G., Niederlag, G., Querin, U., Weisbach, J., Kleinstück, K. (1980), *Phys. Status Solidi (b) 100,* 179–185.

Hindam, H., Whittle, D. P. (1982), *Oxid. Met. 18,* 245–284.

Hippsley, C. A., Strangwood, M. (1992), *Mater. Sci. Technol. 8,* 350–358.

Hippsley, C. A., Strangwood, M., DeVan, J. H. (1990), *Acta Metall. Mater. 38,* 2393–2410.

Hirano, T., Mawari, T. (1993), *Acta Metall. Mater. 41,* 1783–1789.

Hirsch, P. B. (1985), *Mater. Sci. Technol. 1,* 666–677.

Hirsch, P. B. (1993), *Mater. Res. Soc. Symp. Proc. 288,* 33–43.

Ho, C. T., Sekhar, J. A. (1991), in: *High Temperature Ordered Intermetallic Alloys* IV: Johnson, L. A., Pope, D. P., Stiegler, J. O. (Eds.). Pittsburgh, PA: MRS, pp. 1057–1062.

Ho, K., Dodd, R. A. (1978), *Scr. Metall. 12,* 1055–1058.

Hoch, M., Lin, R. Y. (1993), in: *Ternary Alloys,* Vol. 8: Petzow, G., Effenberg, G. (Eds.), Weinheim: VCH, pp. 79–88.

Hocking, L. A., Strutt, P. R., Dodd, R. A. (1971), *J. Inst. Met. 99,* 98–101.

Hodgson, D. E. (1990), in: *Metals Handbook,* Vol. 2, *Properties and Selection: Nonferrous Alloys and Special-Purpose Materials.* Materials Park, OH: ASM, pp. 897–902.

Hondros, E. D. (1978), in: *Precipitation Processes in Solids:* Russell, K. C., Aaronson, H. I. (Eds.). Warrendale, PA: TMS, pp. 1–30.

Honeycombe, R. W. K. (1968), *The Plastic Deformation of Metals.* New York: St. Martin's Press, pp. 1–467.

Hong, S. H., Weertman, J. (1986), *Acta Metall. 34,* 743–751.

Hong, T., Freeman, A. J. (1989), in: *High-Temperature Ordered Intermetallic Alloys* III: Liu, C. T., Taub, A. I., Stoloff, N. S., Koch, C. C. (Eds.). Pittsburgh, PA: MRS, pp. 75–80.

Hong, Y. M., Nakajima, H., Mishima, Y., Suzuki, T. (1989), *ISIJ Int. 29,* 78–84.

Hono, K., Chiba, A., Sakurai, T., Hanada, S. (1992), *Acta Metall. Mater. 40,* 419–425.

Hopfe, W. D., Son, Y.-H., Morral, J. E., Romig, A. D, Jr. (1993), in: *Diffusion in Ordered Alloys and Intermetallic Compounds:* Fultz, B., Cahn, R. W., Gupta, D. (Eds.). Warrendale, PA: pp. 69–76.

Hornbogen, E. (1991), in: *Advanced Structural and Functional Materials:* Bunk, W. G. J. (Ed.). Berlin: Springer, pp. 133–163.

Hornbogen, E., Kobus, E. (1992), *Z. Metallkd. 83,* 105.

Horton, J. A., Liu, C. T. (1990), *Scr. Metall. Mater. 24,* 1251–1256.

Horton, J. A., Liu, C. T., Koch, C. C. (1984), in: *High-Temperature Alloys: Theory and Design:* Stiegler, J. O. (Ed.). Warrendale, PA: TMS/AIME, pp. 309–321.

Hoshino, K., Rothmann, S. J., Averback, R. S. (1988), *Acta Metall. 36,* 1271–1279.

Hosoda, H., Mishima, Y., Suzuki, T. (1991), in: *Proc. Int. Symp. on Intermetallic Compounds – Structure and Mechanical Properties* (JIMIS-6): Izumi, O. (Ed.). Sendai: The Japan Institute of Metals, pp. 81–85.

Hosoda, H., Takahashi, M., Suzuki, T., Mishima, Y. (1993), *Mater. Res. Soc. Symp. Proc. 288,* 793–798.

Hove, J. E., Riley, W. C. (1967), in: *Modern Ceramics: Some Principles and Concepts:* Hove, J. E., Riley, W. C. (Eds.). New York: Wiley, pp. 327–399.

Hsiung, L. M., Wadley, H. N. G. (1992), *Scr. Metall. Mater. 27,* 605–610.

Huang, J. S., Kim, Y.-W. (1991), *Scr. Metall. Mater. 25,* 1901–1906.

Huang, P., Ceder, G., Menon, E. S. K., De Fontaine, D. (1991), *Scr. Metall. Mater. 25,* 1495–1500.

Huang, S.-C. (1993), in: *Structural Intermetallics:* Darolia, R., Lewandowski, J. J., Liu, C. T., Martin, P. L., Miracle, D. B., Nathal, M. V. (Eds.). Warrendale, PA: TMS, pp. 299–307.

Huang, S. C., Hall, E. L. (1991a), *Scr. Metall. Mater. 25,* 1805–1809.

Huang, S. C., Hall, E. L. (1991b), *Metall. Trans. 22A,* 427–439.

Huang, S. C., Siemers, P. A. (1989), *Metall. Trans. 20A,* 1899–1906.

ArcelorMittal Ex. 2038
Page 157 of 190

Huang, S. C., Hall, E. L., Shih, D. S. (1991a), *ISIJ Int. 31,* 1100–1106.

Huang, S. C., McKee, D. W., Shih, D. S., Chesnutt, J. C. (1991b), in: *Proc. Int. Symp. on Intermetallic Compounds – Structure and Mechanical Properties* (JIMIS-6): Izumi, O. (Ed.). Sendai: The Japan Institute of Metals, pp. 363–370.

Huetter, L. J., Stadelmaier, H. H. (1958), *Acta Metall. 6,* 367–370.

Hultgren, R. (1963), *Selected Values of Thermodynamic Properties of Metals and Alloys.* New York: Wiley, pp. 1–963.

Hwang, C. M., Wayman, C. M. (1983), *Scr. Metall. 17,* 1345–1350.

Hwang, C. M., Meichle, M., Salamon, M. B., Wayman, C. M. (1983), *Phil. Mag. A47,* 31–62.

Ichinose, S., Funatsu, Y., Otani, N., Ichikawa, T., Miyazaki, S., Otsuka, K. (1991), in: *Proc. Int. Symp. on Intermetallic Compounds – Structure and Mechanical Properties* (JIMIS-6): Izumi, O. (Ed.). Sendai: The Japan Institute of Metals, pp. 263–267.

Igarashi, M., Senba, H. (1993), in: *Structural Intermetallics:* Darolia, R., Lewandowski, J. J., Liu, C. T., Martin, P. L., Miracle, D. B., Nathal, M. V. (Eds.). Warrendale, PA: TMS, pp. 533–542.

Ikeda, K., Saito, S., Hanada, S. (1992), *Sci. Rep. Tohoku Univ. 37 (1),* 26–34.

Imai, Y., Kumazawa, M. (1959), *Sci. Rep. Tohoku Univ. 11,* 312–316.

Imayev, R., Imayev, V., Salishchev, G. (1993a), *Scr. Metall. Mater. 29,* 713–718.

Imayev, R., Imayev, V., Salishchev, G. (1993b), *Scr. Metall. Mater. 29,* 719–724.

Inco (1982), Inconel Alloy MA 6000, Inco Pamphlet.

Inden, G. (1993), unpublished report, Max-Planck-Institut für Eisenforschung, Düsseldorf, FRG.

Inden, G., Pepperhoff, W. (1990), *Z. Metallkd. 81,* 770–773.

Inoue, H., Inakazu, N. (1991), in: *Proc. Int. Symp. on Intermetallic Compounds – Structure and Mechanical Properties* (JIMIS-6): Izumi, O. (Ed.). Sendai: The Japan Institute of Metals, pp. 785–789.

Inoue, H. R. P., Hsiung, L.-M., Kato, M., Pope, D. P. (1991a), *Phys. Status Solidi (a) 123,* 399–414.

Inoue, H. R. P., Kitamura, M., Wayman, C. M., Chen, H. (1991b), *Phil. Mag. A63,* 345–353.

Inui, H., Oh, M. H., Nakamura, A., Yamaguchi, M. (1992), *Acta Metall. Mater. 40,* 3095–3104.

Inui, H., Toda, Y., Yamaguchi, M. (1993), *Phil. Mag. A67,* 1315–1332.

Ishida, K., Kainuma, R., Ueno, N., Nishizawa, T. (1991a), *Metall. Trans. 22A,* 441–446.

Ishida, K., Nishizawa, T., Schlesinger, M. E. (1991b), *J. Phase Equilibria 12,* 578–586.

Ishida, K., Kainuma, R., Nishizawa, T. (1993), *Bull. Jpn. Inst. Met. 32,* 143–150.

Ito, K., Inui, H., Hirano, T., Yamaguchi, M. (1992), *Mater. Sci. Eng. A152,* 153–159.

Ito, Y., Shirai, Y., Yamada, Y., Yamaguchi, M. (1993), *Mater. Res. Soc. Symp. Proc. 288,* 275–280.

Ivey, D. G., Northwood, D. O. (1986a), *J. Less-Common Met. 115,* 295–306.

Ivey, D. G., Northwood, D. O. (1986b), *Z. Phys. Chem. N. F. 147,* 191–209.

Izumi, O. (1989), *Mater. Trans. Jpn. Inst. Met. 30,* 627–638.

Jackson, A. G. (1993), *Scr. Metall. Mater. 28,* 673–675.

Jackson, A. G., Lee, D. S. (1992), *Scr. Metall. Mater. 26,* 1575–1579.

Jacobi, H., Engell, H.-J. (1971a), *Z. Phys. Chem. N. F. 74,* 190–205.

Jacobi, H., Engell, H.-J. (1971b), *Acta Metall. 19,* 701–711.

Jayaram, R., Miller, M. K. (1993), *Mater. Res. Soc. Symp. Proc. 288,* 355–360.

Jayashankar, S., Kaufman, M. J. (1992), *Scr. Metall. Mater. 26,* 1245–1250.

Jeitschko, W. (1970), *Metall. Trans. 1,* 2963–2965.

Jeitschko, W. (1977), *Acta Crystallogr. B33,* 2414–2417.

Jeitschko, W., Jordan, A. G., Beck, P. A. (1969), *Trans. AIME 245,* 335–339.

Jellinghaus, W. (1936), *Z. Techn. Phys. 17,* 33–36.

Jellinghaus, W. (1943), *Arch. Eisenhüttenwes. 16,* 247–252.

Jellinghaus, W. (1961), *Arch. Eisenhüttenwes. 32,* 187–197.

Jellinghaus, W. (1967), *Arch. Eisenhüttenwes. 38,* 393–400.

Jena, A. K., Sahay, S. S., Mathur, R. P. (1993), in: *Structural Intermetallics:* Darolia, R., Lewandowski, J. J., Liu, C. T., Martin, P. L., Miracle, D. B., Nathal, M. V. (Eds.). Warrendale, PA: TMS, pp. 425–430.

Jeng, Y.-L., Lavernia, E. J., Wolfenstine, J., Bailey, D. E., Sickinger, A. (1993), *Scr. Metall. Mater. 29,* 107–111.

Jha, S. C., Forster, J. A., Pandey, A. K., Delagi, R. G. (1991a), *ISIJ Int. 31,* 1267–1271.

Jha, S. C., Forster, J. A., Pandey, A. K., Delagi, R. G. (1991b), *Adv. Mater. Processes 4/91,* 87–90.

Jia, C. L., Jiang, J., Zong, X. F. (1989), *Phil. Mag. A59,* 999–1012.

Jin, Z., Bieler, T. R. (1993), *Mater. Res. Soc. Symp. Proc. 288,* 775–780.

Johnson, D. R., Joslin, S. M., Oliver, B. F., Noebe, R. D., Whittenberger, J. D. (1992), *Mater. Res. Soc. Symp. Proc 273,* 87–92.

Johnson, D. R., Joslin, S. M., Reviere, R. D., Oliver, B. F., Noebe, R. D. (1993), in: *Processing and Fabrication of Advanced Materials for High Temperature Applications* – II: Ravi, V. A., Srivatsan, T. S. (Eds.). Warrendale, PA: TMS, pp. 77–90.

Johnson, T. P., Young, J. M., Ward, R. M., Jacobs, M. H. (1993), in: *Structural Intermetallics:* Darolia, R., Lewandowski, J. J., Liu, C. T., Martin, P. L.,

ArcelorMittal Ex. 2038
Page 158 of 190

Miracle, D. B., Nathal, M. V. (Eds.). Warrendale, PA: TMS, pp. 159–165.
Jones, D. G. R., Abell, J. S., Harris, I. R. (1991), *J. Less-Common Met. 172–174,* 1285–1296.
Jones, S. A., Kaufman, M. J. (1993), *Acta Metall. Mater. 41,* 387–398.
Jorda, J. L., Flükiger, R., Muller, J. (1980), *J. Less. Common Met. 75,* 227–230.
Jordan, K. R., Stoloff, N. S. (1969), *Trans. AIME 245,* 2027–2034.
Josephy, Y., Bershadsky, E., Ron, M. (1991), *J. Less-Common Met. 172–174,* 997–1008.
Jung, I. (1986), Dr. rer. nat. Thesis, RWTH Aachen, pp. 1–120.
Jung, I., Sauthoff, G. (1987), in: *Creep and Fracture of Engineering Materials and Structures:* Wilshire, B., Evans, R. W. (Eds.). London: Institute of Metals, pp. 257–270.
Jung, I., Sauthoff, G. (1989a), *Z. Metallkd. 80,* 484–489.
Jung, I., Sauthoff, G. (1989b), *Z. Metallkd. 80,* 490–496.
Jung, I., Rudy, M., Sauthoff, G. (1987), in: *High-Temperature Ordered Intermetallic Alloys* II: Stoloff, N. S., Koch, C. C., Liu, C. T., Izumi, O. (Eds.). Pittsburgh, PA: Materials Research Society, pp. 263–274.
Kahveci, A. I., Welsch, G. E. (1986), *Scr. Metall. 20,* 1287–1290.
Kainuma, R., Ishida, K., Nishizawa, T. (1992a), private communication (unpublished report).
Kainuma, R., Ishida, K., Nishizawa, T. (1992b), *Metall. Trans. 23A,* 1147–1153.
Kainuma, R., Nakano, H., Oikawa, K., Ishida, K., Nishizawa, T. (1992c), in: *Shape-Memory Materials and Phenomena – Fundamental Aspects and Applications:* Liu, C. T., Wuttig, M. Otsuka, K., Kunsmann, H. (Eds.). Pittsburgh, PA: MRS, pp. 403–408.
Kainuma, R., Palm, M., Inden, G. (1994), *Intermetallics,* in press.
Kamata, K., Degawa, T., Nagashima, Y. (1992a), in: *Basic Technologies for Future Industries: The 3rd Symposium on High-Performance Materials for Severe Environments:* RIMCOF (Ed.). Tokyo: Japan Industrial Technology Association (JITA), pp. 151–158.
Kamata, K., Suzuki, Y., Moriai, H., Inoue, K., Itoh, K., Takeuchi, T., Tachikawa, K., Watanabe, K., Muto, Y., Katagiri, K., Noto, K., Okada, T. (1992b), *Sci. Rep. Tohoku Univ. 37,* 1, 99–107.
Kamata, K., Degawa, T., Nagashima, Y. (1993), in: *Structural Intermetallics:* Darolia, R., Lewandowski, J. J., Liu, C. T., Martin, P. L., Miracle, D. B., Nathal, M. V. (Eds.). Warrendale, PA: TMS, pp. 675–680.
Kampe, S. L., Bryant, J.D., Christodoulou, L. (1991), *Metall. Trans. 22A,* 447–454.
Kao, C. R., Chang, Y. A. (1993), *Intermetallics 1,* 237–250.
Kao, H. P., Brooks, C. R., Sanganeria, M. (1989), in: *High-Temperature Ordered Intermetallic Alloys* III: Liu, C. T., Taub, A. I., Stoloff, N. S., Koch, C. C. (Eds.). Pittsburgh, PA: Mater. Res. Soc., pp. 749–754.
Karsten, K. (1839), *Pogg. Annalen 46,* 160–166.
Kasahara, K., Hashimoto, K., Doi, H., Tsujimoto, T. (1987), *J. Jpn. Inst. Met. 51,* 278–284.
Kassem, M. A., Koch, C. C. (1991), in: *High Temperature Ordered Intermetallic Alloys* IV: Johnson, L. A., Pope, D. P., Stiegler, J. O. (Eds.). Pittsburgh, PA: MRS, pp. 801–806.
Kasul, D. B., Heldt, L. A. (1991), *Scr. Metall. Mater. 25,* 1047–1052.
Kattner, U. R., Boettinger, W. J. (1992), *Mater. Sci. Eng. A152,* 9–17.
Kattner, U. R., Lin, J.-C., Chang, Y. A. (1992), *Metall. Trans. 23A,* 2081–2090.
Kawabata, T., Takasugi, T. (1991), in: *Proc. Int. Symp. on Intermetallic Compounds – Structure and Mechanical Properties* (JIMIS-6): Izumi, O. (Ed.). Senai: The Japan Institute of Metals, pp. 679–683.
Kawabata, T., Kanai, T., Izumi, O. (1985), *Acta Metall. 33,* 1355–1366.
Kawabata, T., Kanai, T., Izumi, O. (1991a), *Phil. Mag. A63,* 1291–1298.
Kawabata, T., Tadano, M., Izumi, O. (1991b), *ISIJ Int. 31,* 1161–1167.
Kawabata, T., Abumiya, T., Izumi, O. (1992), *Acta Metall. Mater. 40,* 2557–2567.
Kawabata, T., Tamura, T., Izumi, O. (1993), *Metall. Trans. 24A,* 141–150.
Kawahara, K. (1983a), *J. Mater. Sci. 18,* 1709–1718.
Kawahara, K. (1983b), *J. Mater. Sci. 18,* 2047–2055.
Kawahara, K. (1983c), *J. Mater. Sci. 18,* 3437–3448.
Kawazoe, H., Takasugi, T., Izumi, O. (1989), *Acta Metal. 37,* 2895–2904.
Kayser, F. X., Stassis, C. (1969), *Phys. Status Solidi (a) 64,* 335–342.
Khachaturyan, A. G., Shapiro, S. M., Semenovskaya, S. (1992), *Mater. Trans. Jpn. Inst. Met. 33,* 278–281.
Khadikar, P. S., Vedula, K. (1987), *J. Mater. Res. 2,* 163–167.
Khadikar, P. S., Vedula, K., Shabel, B. S. (1987), in: *High Temperature Ordered Intermetallic Alloys* II: Izumi, O., Koch, C. C., Liu, C. T., Stoloff, N. S. (Eds.). Pittsburgh, PA: MRS, pp. 157–164.
Khadikar, P. S., Locci, I. E., Vedula, K., Michal, G. M. (1993), *Metall. Trans. 24A,* 83–94.
Khan, T., Naka, S., Veyssière, P., Costa, P. (1990), in: *High Temperature Materials for Power Engineering 1990,* II. Dordrecht: Kluwer, pp. 1533–1558.
Khantha, M., Vitek, V., Pope, D. P. (1989), in: *High-Temperature Ordered Intermetallic Alloys* III: Liu, C. T., Taub, A. I., Stoloff, N. S., Koch, C. C. (Eds.). Pittsburgh, PA: MRS, pp. 99–104.
Khantha, M., Pope, D. P., Vitek, V. (1990), *Phil. Mag. A62,* 329–346.

ArcelorMittal Ex. 2038
Page 159 of 190

Khantha, M., Vitek, V., Pope, D. P. (1991), in: *High Temperature Ordered Intermetallic Alloys* IV: Johnson, L. A., Pope, D. P., Stiegler, J. O. (Eds.). Pittsburgh, PA: MRS, pp. 229–234.

Khantha, M., Vitek, V., Pope, D. P. (1992), *Mater. Sci. Eng. A 152,* 89–94.

Khantha, M., Cserti, J., Vitek, V. (1993a), *Mater. Res. Soc. Symp. Proc. 288,* 417–422.

Khantha, M., Cserti, J., Vitek, V. (1993b), in: *Structural Intermetallics:* Darolia, R., Lewandowski, J. J., Liu, C. T., Martin, P. L., Miracle, D. B., Nathal, M. V. (Eds.). Warrendale, PA: TMS, pp. 399–408.

Khobaib, M., Vahldiek, F. W. (1988), in: *2nd Int. SAMPE Metal and Metals Processing Conf.*, Vol. 2: *Space Age Metals Technology:* Froes, F. H., Cull, R. A. (Eds.). Covina, CA: SAMPE, pp. 262–270.

Kieffer, R., Benesovsky, F. (1956), in: *Symp. on Powder Metallurgy 1954* (Special Report No. 58): London: The Iron and Steel Institute, pp. 292–301.

Kikuchi, A. (1983), *J. Appl. Phys. 54,* 3998–4002.

Kilner, J. A., Harris, I. R. (1981), *J. Mater. Sci. 16,* 3398–3404.

Kim, D., Clapp, P. C., Rifkin, J. A. (1991), in: *High Temperature Ordered Intermetallic Alloys* IV: Johnson, L. A., Pope, D. P., Stiegler, J. O. (Eds.). Pittsburgh, PA: MRS, pp. 249–254.

Kim, D., Clapp, P. C., Rifkin, J. A. (1993), *Mater. Res. Soc. Symp. Proc. 288,* 507–512.

Kim, J. T., Gibala, R. (1991), in: *High Temperature Ordered Intermetallic Alloys* IV: Johnson, L. A., Pope, D. P., Stiegler, J. O. (Eds.). Pittsburgh, PA: MRS, pp. 261–266.

Kim, J. T., Noebe, R. D., Gibala, R. (1991), in: *Proc. Int. Symp. on Intermetallic Compounds – Structure and Mechanical Properties* (JIMIS-6): Izumi, O. (Ed.). Sendai: The Japan Institute of Metals, pp. 591–595.

Kim, S. M. (1992), *Acta Metall. Mater. 40,* 2793–2798.

Kim, Y. D., Wayman, C. M. (1990), *Scr. Metall. Mater. 24,* 245–250.

Kim, Y. D., Wayman, C. M. (1992), *Metall. Trans. 23A,* 2981–2986.

Kim, Y.-G., Lee, J.-Y. (1993a), *Scr. Metall. Mater. 29,* 539–542.

Kim, Y.-G., Lee, J.-Y. (1993b), *J. Alloys Compd. 191,* 243–249.

Kim, Y. S., Johnson, M. R., Abbaschian, R., Kaufman, M. J. (1991), in: *High Temperature Ordered Intermetallic Alloys* IV: Johnson, L. A., Pope, D. P., Stiegler, J. O. (Eds.). Pittsburgh, PA: MRS, pp. 839–845.

Kim, Y.-W. (1989), *J. Met. 41 (7),* 24–30.

Kim, Y.-W. (1992), *Acta Metall. Mater. 40,* 1121–1134.

Kim, Y.-W., Dimiduk, D. M. (1991), *J. Met. 43 (8),* 40–47.

Kim, Y.-W., Dimiduk, D. M. (1993), *Mater. Res. Soc. Symp. Proc. 288,* 671–677.

Kim, Y.-W., Froes, F. H. (1990), in: *High-Temperature Aluminides and Intermetallics:* Whang, S. H., Liu, C. T., Pope, D. P., Stiegler, J. O. (Eds.). Warrendale, PA: TMS, pp. 465–492.

Kimura, K., Nakamura, M., Hirano, T. (1990), *J. Mater. Sci. 25,* 2487–2492.

Kimura, Y., Suzuki, T., Mishima, Y. (1993), *Mater. Res. Soc. Symp. Proc. 288,* 697–702.

Kitano, K., Pollock, T. M. (1993), in: *Structural Intermetallics.* Darolia, R., Lewandowski, J. J., Liu, C. T., Martin, P. L., Miracle, D. B., Nathal, M. V. (Eds.). Warrendale, PA: TMS, pp. 591–599.

Klein, O., Baker, I. (1992), *Scr. Metall. Mater. 27,* 1823–1828.

Klein, O., Nagpal, P., Baker, I. (1993), *Mater. Res. Soc. Symp. Proc. 288,* 935–940.

Klöwer, J. (1989), Dr. Ing. Thesis, RWTH Aachen, pp. 1–112.

Klöwer, J., Sauthoff, G. (1991), *Z. Metallkd. 82,* 510–518.

Klöwer, J., Sauthoff, G. (1992), *Z. Metallkd. 83,* 699–704.

Koch, J. M., Koenig, C. (1986), *Phil. Mag. B 54,* 177–197.

Kocks, U. F. (1958), *Acta Metall. 6,* 85–94.

Kocks, U. F. (1970), *Metall. Trans. 1,* 1121–1143.

Kocks, U. F., Canova, G. R. (1981), in: *Deformation of Polycrystals: Mechanisms and Microstructures:* Hansen, N., Horsewell, A., Leffers, T., Lilholt, H. (Eds.). Roskilde: Riso National Laboratory, pp. 35–44.

Kodentzov, A. A., Dunaev, S. F., Slusarenko, E. M. (1988), *J. Less-Common Met. 141,* 225–234.

Koeppe, C., Bartels, A., Seeger, J., Mecking, H. (1993), *Metall. Trans. A 24,* 1795–1806.

Kogachi, M., Minamigawa, S., Nakahigashi, K. (1992), *Acta Metall. Mater. 40,* 1113–1120.

Kohno, O., Saito, T., Sadakata, N., Sugimoto, M., Goto, K., Watanabe, K. (1992), *Sci. Rep. Tohoku Univ. 37 (1),* 84–91.

Koiwa, M. (1992), in: *Ordered Intermetallics – Physical Metallurgy and Mechanical Properties:* Liu, C. T., Cahn, R. W., Sauthoff, G. (Eds.). Dordrecht: Kluwer, pp. 449–464.

Kojima, T., Sakata, M., Nishida, I. (1990), *J. Less-Common Met. 162,* 39–49.

Kondratyev, V. V., Pushin, V. G. (1985), *Phys. Met. Metall. 60 (4),* 1–21.

Kong, C. H., Munroe, P. R. (1993), *Scr. Metall. Mater. 28,* 1241–1244.

Konoplev, A. M., Sarrak, V. I. (1982), *Phys. Met. Metall. 54 (3),* 142–148.

Korinko, P. S., Duquette, D. J. (1990), in: *Intermetallic Matrix Composites:* Anton, D. L., Martin, P. L., Miracle, D. B., McMeeking, R. (Eds.). Pittsburgh, PA: MRS, pp. 423–428.

Korinko, P. S., Duquette, D. J. (1994), *Scr. Metall. Mater. 30,* 287–290.

Korinko, P. S., Alman, D. E., Stoloff, N. S., Duquette, D. J. (1992), *Mater. Res. Soc. Symp. Proc. 273,* 183–190.

ArcelorMittal Ex. 2038
Page 160 of 190

Korner, A. (1991), *Phil. Mag. Lett. 63,* 117–122.
Kornilov, I. I. (1960), in: *Mechanical Properties of Intermetallic Compounds:* Westbrook, J. H. (Ed.). New York: Wiley, pp. 344–357.
Kornilov, I. I. (1967), in: *Intermetallic Compounds:* Westbrook, J. H. (Ed.). New York: Wiley, pp. 349–374.
Koss, D. A., Banerjee, D., Lukasak, D. A., Gogia, A. K. (1990), in: *High Temperature Aluminides and Intermetallics:* Whang, S. H., Liu, C. T., Pope, D. P., Stiegler, J. O. (Eds.). Warrendale, PA: TMS, pp. 175–196.
Köster, W., Gödecke, T. (1980), *Z. Metallkd. 71,* 765–769.
Kostrubanic, J. M., Koss, D. A., Locci, I. E., Nathal, M. V. (1991), in: *High Temperature Ordered Intermetallic Alloys* IV: Johnson, L. A., Pope, D. P., Stiegler, J. O. (Eds.). Pittsburgh, PA: MRS, pp. 679–684.
Kostrubanic, J. M., Breedis, J. B., Koss, D. A., Locci, I., Poole, J. M. (1993), in: *Structural Intermetallics:* Darolia, R., Lewandowski, J. J., Liu, C. T., Martin, P. L., Miracle, D. B., Nathal, M. V. (Eds.). Warrendale, PA: TMS, pp. 543–549.
Kötter, G., Nembach, K., Wallow, F., Nembach, E. (1989), *Mater. Sci. Eng. A 114,* 29–35.
Kouvel, J. S. (1967), in: *Intermetallic Compounds:* Westbrook, J. H. (Ed.). New York: Wiley, pp. 529–568.
Kowalski, W., Frommeyer, G. (1992), unpublished report, Max-Planck-Institut für Eisenforschung, Düsseldorf, FRG.
Kozubski, R. (1993), *Acta Metall. Mater. 41,* 2565–2575.
Krämer, U. (1983), *Phil. Mag. A 47,* 721–740.
Krämer, U., Schulze, G. E. R. (1968), *Krist. Tech. 3,* 417–430.
Krasovec, M., Jedlinski, J., Borchardt, G. (1992), in: *Advanced Structural Materials,* Vol. 2: Clyne, T. W., Withers, P. J. (Eds.). London: The Institute of Materials, pp. 401–404.
Kratochvil, P. (1990), *Z. Metallkd. 81,* 884–886.
Kratochvil, P., Biegel, W., Sprusil, B., Chalupa, B. (1992), *Phys. Status. Solidi (a), 131,* 321–332.
Krishnan, R. V., Delaey, L., Tas, H., Warlimont, H. (1974), *J. Mater. Sci. 9,* 1536–1544.
Kritzinger, S., Tu, K. N. (1981), *J. Appl. Phys. 52,* 305–310.
Kroll, S., Mehrer, H., Stolwijk, N., Herzig, C., Rosenkranz, R., Frommeyer, G. (1992), *Z. Metallkd. 83,* 591–595.
Kubaschewski, O. (1982), *Iron – Binary Phase Diagrams.* Berlin: Springer, pp. 1–185.
Kubin, L. P., Fourdeux, A., Guedou, J. Y., Rieu, J. (1982), *Phil. Mag. A 46,* 357–378.
Kuczera, H., Krammer, P., Sacher, P. (1991), Paper IAF-91-198 at the 42nd Cong. Int. Aeronautical Federation in Montreal.
Kudielka, H., Nowotny, H. (1956), *Monatsh. Chem. 87,* 471–482.
Kumagai, T., Hanada, S., Saito, S. (1991), in: *Proc. Int. Symp. on Intermetallic Compounds – Structure and Mechanical Properties* (JIMIS-6): Izumi, O. (Ed.). Sendai: The Japan Institute of Metals, pp. 1039–1044.
Kumar, K. S. (1990), *Int. Mater. Rev. 35,* 293–327.
Kumar, K. S. (1991), *ISIJ Int. 31,* 1249–1259.
Kumar, K. S. (1993), in: *Structural Intermetallics:* Darolia, R., Lewandowski, J. J., Liu, C. T., Martin, P. L., Miracle, D. B., Nathal, M. V. (Eds.). Warrendale, PA: TMS, pp. 87–96.
Kumar, K. S. (1994), in: *Intermetallic Compounds: Principles and Practice,* Vol. 2: Westbrook, J. H., Fleischer, R. L. (Eds.). Chichester, UK: Wiley, in press.
Kumar, K. S., Brown, S. A. (1992a), *Acta Metall. Mater. 40,* 1923–1932.
Kumar, K. S., Brown, S. A. (1992b), *Scr. Metall. Mater. 26,* 197–202.
Kumar, K. S., Brown, S. A. (1992c), *Phil. Mag. A 65,* 91–109.
Kumar, K. S., Brown, S. A. (1993), *Mater. Res. Soc. Symp. Proc. 288,* 781–786.
Kumar, K. S., Liu, C. T. (1993), *J. Met. 45 (6),* 28–34.
Kumar, K. S., Mannan, S. K. (1989), in: *High-Temperature Ordered Intermetallic Alloys* III: Liu, C. T., Taub, A. I, Stoloff, N. S., Koch, C. C. (Eds.). Pittsburgh, PA: Mater. Res. Soc., pp. 415–420.
Kumar, K. S., Whittenberger, J. D. (1991), in: *Proc. Int. Symp. on Intermetallic Compounds – Structure and Mechanical Properties* (JIMIS-6): Izumi, O. (Ed.). Sendai: The Japan Institute of Metals, pp. 927–934.
Kumar, K. S., Whittenberger, J. D. (1992), *Mater. Sci. Technol. 8,* 317–330.
Kumar, K. S., Brown, S. A., Montoya, K., Whittenberger, J. D., DiPietro, M. S. (1991a), in: *Proc. Int. Symp. on Intermetallic Compounds – Structure and Mechanical Properties* (JIMIS-6): Izumi, O. (Ed.). Sendai: The Japan Institute of Metals, pp. 667–671.
Kumar, K. S., Brown, S. A., Whittenberger, J. D. (1991b), in: *High Temperature Ordered Intermetallic Alloys* IV: Johnson, L. A., Pope, D. P., Stiegler, J. O. (Eds.). Pittsburgh, PA: MRS, pp. 481–486.
Kumar, K. S., DiPietro, M. S., Whittenberger, J. D. (1991c), in: *High Temperature Ordered Intermetallic Alloys* IV: Johnson, L. A., Pope, D. P., Stiegler, J. O. (Eds.). Pittsburgh, PA: MRS, pp. 1039–1044.
Kumar, K. S., Darolia, R., Lahrman, D. F., Mannan, S. K. (1992a), *Scr. Metall. Mater. 26,* 1001–1006.
Kumar, K. S., Mannan, S. K., Viswanadham, R. K. (1992b), *Acta Metall. Mater. 40,* 1201–1222.
Kumpfert, J., Grundhoff, K.-J., Schurmann, H., Lee, Y. T., Ward, C. H., Peters, M. (1992), in: *Advanced Structural Materials,* Vol. 2: Clyne, T. W., Withers, P. J. (Eds.). London: The Institute of Materials, pp. 321–332.
Kung, S.-C. (1990), *Oxid. Met. 34,* 217–228.

ArcelorMittal Ex. 2038
Page 161 of 190

Kurnakov, N. S. (1900), *Z. Anorg. Chem. 23,* 439–462.
Kurnakov, N. S. (1914), *Z. Anorg. Chem. 88,* 109–127.
Kurnakov, N. S., Zhemchuzhny, S. (1908), *Ber. Petersburg Polytech. Inst. 9,* 1–9.
Kusaka, K. (1991), *ISIJ Int. 31,* 1207–1211.
Kuzmichev, N. D., Levichenko, I. S., Motulevich, G. P. (1983), *Phys. Met. Metall. 56 (2),* 49–53.
Lahrman, D. F., Field, R. D., Darolia, R. (1991), in: *High Temperature Ordered Intermetallic Alloys* IV: Johnson, L. A., Pope, D. P., Stiegler, J. O. (Eds.). Pittsburgh, PA: MRS, pp. 603–607.
Lahrman, D. F., Field, R. D., Darolia, R. (1993a), *Mater. Res. Soc. Symp. Proc. 288,* 679–684.
Lahrman, D. F., Field, R. D., Darolia, R. (1993b), *Scr. Metall. Mater. 28,* 709–714.
Lakso, G. E., Marcinkowski, M. J. (1974), *Metall. Trans. 5,* 839–845.
Lall, C., Chin, S., Pope, D. P. (1979), *Metall. Trans. 10A,* 1323–1332.
Larsen, J. M., Williams, K. A., Balsone, S. J., Stucke, M. A. (1990), in: *High-Temperature Aluminides and Intermetallics:* Whang, S. H., Liu, C. T., Pope, D. P., Stiegler, J. O. (Eds.). Warrendale, PA: TMS, pp. 521–556.
Larsen, M., Misra, A., Hartfield-Wunsch, S., Noebe, R., Gibala, R. (1990), in: *Intermetallic Matrix Composite:* Anton, D. L., Martin, P. L., Miracle, D. B., McMeeking, R. (Eds.). Pittsburgh, PA: MRS, pp. 191–198.
Laves, F. (1967), in: *Intermetallic Compounds:* Westbrook, J. H. (Ed.). New York: Wiley, pp. 129–143.
Lawley, A., Coll, J. A., Cahn, R. W. (1960), *Trans. AIME 218,* 166–176.
Lawthers, D. D., Sama, L. (1993), in: *High Temperature Materials* II: Ault, G. M., Barclay, W. F., Munger, P. H. (Eds.). New York: Interscience, pp. 819–832.
Leamy, H. J., Kayser, F. X. (1969), *Phys. Status Solidis 34,* 765–780.
Lee, C., Grummon, D. S., Gottstein, G. (1990), in: *Intermetallic Matrix Composites:* Anton, D. L., Martin, P. L., Miracle, D. B., McMeeking, R. (Eds.). Pittsburgh, PA: MRS, pp. 301–306.
Lee, C. C., Shen, P. (1989), *J. Mater. Sci. 24,* 3707–3711.
Lee, D. S., Dimiduk, D. M., Krishnamurthy, S. (1993), *Mater. Res. Soc. Symp. Proc. 288,* 823–827.
Lee, E. W., Cook, J., Khan, A., Mahapatra, R., Waldman, J. (1991), *J. Met. 43 (3),* 54–57.
Lee, J. H., Choe, B. H., Kim, H. M. (1992), *Mater. Sci. Eng. A152,* 253–257.
Lee, J. K., Yoo, M. H. (1990), *Metall. Trans. 21A,* 2521–2530.
Lee, J. S., Nieh, T. G. (1989), in: *Oxidation of High-Temperature Intermetallics:* Grobstein, T., Doychak, J. (Eds.). Warrendale, PA: TMS, pp. 271–278.
Lee, J. S., Wayman, C. M. (1986), *Metallography 19,* 401–419.
Lee, K. H., White, C. L. (1993), *Scr. Metall. Mater. 29,* 547–552.
Lee, K. J., Nash, P. (1991a), *J. Phase Equilibria 12,* 94–104.
Lee, K. J., Nash, P. (1991b), *J. Phase Equilibria 12,* 551–562.
Lee, T. C., Robertson, I. M., Birnbaum, H. K. (1992), *Acta Metall. Mater. 40,* 2569–2579.
Lefort, A., Franzoni, U., Tassa, O., Lecoze, J., Cayla, O., Magnee, A. (1991), in: *Proc. Int. Symp. on Intermetallic Compounds – Structure and Mechanical Properties* (JIMIS-6): Izumi, O. (Ed.). Sendai: The Japan Institute of Metals, pp. 579–583.
Leitner, G. (1971a), *Wiss. Z. Tech. Univ. Dresden 20,* 391–394.
Leitner, G. (1971b), Dr. rer. nat. Thesis, Technische Universität Dresden, pp. 1–221.
Leitner, G., Schulze, G. E. R. (1971), *Krist. Tech. 6,* 449–463.
Leroux, C., Loiseau, A., Broddin, D., Van Tendeloo, G. (1991), *Phil. Mag. A64,* 57–82.
Levinstein, H. J., Greiner, E. S., Mason, H., Jr. (1966), *J. Appl. Phys. 37,* 164–166.
Lewandowski, J. J., Dimiduk, D. M., Kerr, W., Mendiratta, M. G. (1988), in: *High Temperature/High Performance Composites:* Lemkey, F. D., Fishman, S. G., Evans, A. G., Strife, J. R. (Eds.). Pittsburgh, PA: MRS, pp. 103–110.
Li, D., Li, P., Sun, D., Lin, D. (1993), *Mater. Res. Soc. Symp. Proc. 288,* 281–286.
Li, G. H., Gill, H. S., Varin, R. A. (1993), *Metall. Trans. A24,* 2383–2391.
Li, H., Chaki, T. K. (1993a), *Acta Metall. Mater. 41,* 1979–1987.
Li, H., Chaki, T. K. (1993b), *Mater. Res. Soc. Symp. Proc. 288,* 1167–1172.
Li, X. L., Hillel, R., Teyssandier, F., Choi, S. K., van Loo, F. J. J. (1992), *Acta Metall. Mater. 40,* 3149–3157.
Li, Z., Schulson, E. M. (1993), *Mater. Res. Soc. Symp. Proc. 288,* 1081–1086.
Li, Z. C., Whang, S. H. (1993), *Phil. Mag. A68,* 169–182.
Liang, X., Lavernia, E. J. (1991), *Scr. Metall. Mater. 25,* 1199–1204.
Lide, D. R. (1992), in: *CRC Handbook of Chemistry and Physics:* Lide, D. R. (Ed.). Cleveland: CRC Press.
Lim, B. S., Stark, J. P. (1984), *Acta Metall. 32,* 915–918.
Lim, C. B., Yano, T., Iseki, T. (1989), *J. Mater. Sci. 24,* 4144–4151.
Lin, D., Sun, J. (1993), *Mater. Res. Soc. Symp. Proc. 288,* 251–256.
Lin, D., Sun, J., Chen, D., Lu, M. (1993), *Mater. Res. Soc. Symp. Proc. 288,* 197–202.
Lin, H. C., Wu, S. K. (1992), *Scr. Metall. Mater. 26,* 59–62.
Lin, J. P., Chu, W. Y., Zhang, D. Z., Hsiao, C. M. (1992), *Scr. Metall. Mater. 27,* 1295–1299.

ArcelorMittal Ex. 2038
Page 162 of 190

Lin, W., Xu, J.-H., Freeman, A. J. (1991), in: *High Temperature Ordered Intermetallic Alloys* IV: Johnson, L. A., Pope, D. P., Stiegler, J. O. (Eds.). Pittsburgh, PA: MRS, pp. 131–136.

Lipsitt, H. A. (1985a), in: *High-Temperature Ordered Intermetallic Alloys:* Koch, C. C., Liu, C. T., Stoloff, N. S. (Eds.). Pittsburgh, PA: MRS, pp. 351–364.

Lipsitt, H. A. (1985b), in: *Advanced High-Temperature Alloys: Processing and Properties:* Allen, S. M., Pelloux, R. M., Widmer, R. (Eds.). Materials Park, OH: ASM, pp. 157–164.

Lipsitt, H. A. (1993), *Mater. Res. Soc. Symp. Proc. 288,* 119–130.

Lipsitt, H. A., Shechtman, D., Schafrick, R. E. (1975), *Metall. Trans. 6A,* 1991–1996.

Lipsitt, H. A., Shechtman, D., Schafrick, R. E. (1980), *Metall. Trans. 11A,* 1369–1375.

Litvinov, V. S., Arkhangelskaya, A. A., Poleva, V. V. (1974), *Fiz. Met. Metalloved. 38 (2),* 383–388.

Liu, C. T. (1984), *Int. Met. Rev. 29,* 168–194.

Liu, C. T. (1991a), in: *Proc. Int. Symp. on Intermetallic Compounds – Structure and Mechanical Properties* (JIMIS-6): Izumi, O. (Ed.). Sendai: The Japan Institute of Metals, pp. 703–712.

Liu, C. T. (1991b), *Scr. Metall. Mater. 25,* 1231–1236.

Liu, C. T. (1992), in: *Ordered Intermetallics – Physical Metallurgy and Mechanical Behaviour:* Liu, C. T., Cahn, R. W., Sauthoff, G. (Eds.). Dordrecht: Kluwer, pp. 321–334.

Liu, C. T. (1993a), *Mater. Res. Soc. Symp. Proc. 288,* 3–19.

Liu, C. T. (1993b), in: *Structural Intermetallics:* Darolia, R., Lewandowski, J. J., Liu, C. T., Martin, P. L., Miracle, D. B., Nathal, M. V. (Eds.). Warrendale, PA: TMS, pp. 365–377.

Liu, C. T., George, E. P. (1991), in: *High Temperature Ordered Intermetallic Alloys* IV: Johnson, L. A., Pope, D. P., Stiegler, J. O. (Eds.). Pittsburgh, PA: MRS, pp. 527–532.

Liu, C. T., Inouye, H. (1979), *Metall. Trans. 10A,* 1515–1525.

Liu, C. T., Kim, Y.-W. (1992), *Scr. Metall. Mater. 27,* 599–603.

Liu, C. T., Koch, C. C. (1983), in: *Technical Aspects of Critical Materials Use by the Steel Industry,* Vol. II B (NBSIR 83-2679-2). Washington: National Bureau of Standards, pp. P42-1–P42-19.

Liu, C. T., Kumar, K. S. (1993), *J. Met. 45 (5),* 38–44.

Liu, C. T., McKamey, C. G. (1990), in: *High-Temperature Aluminides and Intermetallics:* Whang, S. H., Liu, C. T., Pope, D. P., Stiegler, J. O. (Eds.). Warrendale, PA: TMS, pp. 133–151.

Liu, C. T., Oliver, W. C. (1991), *Scr. Metall. Mater. 25,* 1933–1937.

Liu, C. T., Stiegler, J. O. (1984), *Science 226,* 636–642.

Liu, C. T., Stoloff, N. S. (1993), in: *Diffusion in Ordered Alloys and Intermetallic Compounds:* Fultz, B., Cahn, R. W., Gupta, D. (Eds.). Warrendale, PA: TMS, pp. 223–246.

Liu, C. T., White, C. L. (1985), in: *High-Temperature Ordered Intermetallic Alloys:* Koch, C. C., Liu, C. T., Stoloff, N. S. (Eds.). Pittsburgh, PA: Materials Research Society, pp. 365–380.

Liu, C. T., White, C. L., Horton, J. A. (1985), *Acta Metall. 33,* 213–229.

Liu, C. T., Lee, E. H., Henson, T. J. (1988), *Initial Development of High-Temperature Titanium Silicide Alloys* (Report ORNL-6435). Oak Ridge: ORNL, pp. 1–31.

Liu, C. T., Stiegler, J. O., Froes, F. H. (1990), in: *Metals Handbook,* Vol. 2: *Properties and Selection: Non-Ferrous Alloys and Special Purpose Materials.* Materials Park, OH: ASM, pp. 913–942.

Liu, C. T., Fu, C. L., George, E. P., Painter, G. S. (1991), *ISIJ Int. 31,* 1192–1200.

Liu, J. (1989), *Scr. Metall. 23,* 1811–1816.

Liu, Y., Takasugi, T., Izumi, O. (1986), *Metall. Trans. 17A,* 1433–1438.

Liu, Y., Takasugi, T., Izumi, O., Suenaga, H. (1989a), *J. Mater. Sci. 24,* 4458–4466.

Liu, Y., Takasugi, T., Izumi, O., Yamada, T. (1989b), *Acta Metall. 37,* 507–517.

Liu, Y., Allen, S. M., Livingston, J. D. (1993), *Mater. Res. Soc. Symp. Proc. 288,* 203–208.

Livingston, J. D. (1990), *J. Met. 42 (2),* 30–34.

Livingston, J. D. (1992), *Phys. Status Solidi (a) 131,* 415–423.

Livingston, J. D., Hall, E. L. (1990), *J. Mater. Res. 5,* 5–8.

Livingston, J. D., Hall, E. L. (1991), in: *High Temperature Ordered Intermetallic Alloys* IV: Johnson, L. A., Pope, D. P., Stiegler, J. O. (Eds.). Pittsburgh, PA: MRS, pp. 443–448.

Livingston, J. D., Hall, E. L., Koch, E. F. (1989), in: *High-Temperature Ordered Intermetallic Alloys* III: Liu, C. T., Taub, A. I., Stoloff, N. S., Koch, C. C. (Eds.). Pittsburgh, PA: MRS, pp. 243–248.

Locci, I.E., Dickerson, R., Bowman, R. R., Whittenberger, J. D., Nathal, M. V., Darolia, R. (1993), *Mater. Res. Soc. Symp. Proc. 288,* 685–690.

Löhberg, K., Schmidt, W. (1938), *Arch. Eisenhüttenwes. 11,* 607–614.

Lombard, C. M., Nekkanti, R. M., Seetharaman, V. (1992), *Scr. Metall. Mater. 26,* 1559–1564.

London, B., Larsen, D. E., Jr., Wheeler, D. A., Aimone, P. R. (1993), in: *Structural Intermetallics:* Darolia, R., Lewandowski, J. J., Liu, C. T., Martin, P. L., Miracle, D. B., Nathal, M. V. (Eds.). Warrendale, PA: TMS, pp. 151–157.

Longworth, H. P., Mikkola, D. E. (1987), *Mater. Sci. Eng. 96,* 213–229.

Lou, L., Zhang, T., Zhu, Y. (1991), in: *High Temperature Ordered Intermetallic Alloys* IV: Johnson, L. A., Pope, D. P., Stiegler, J. O. (Eds.). Pittsburgh, PA: MRS, pp. 833–838.

Lowell, C. E., Barrett, C. A., Whittenberger, J. D. (1990), in: *Intermetallic Matrix Composites:* An-

ArcelorMittal Ex. 2038
Page 163 of 190

ton, D. L., Martin, P. L., Miracle, D. B., McMeeking, R. (Eds.). Pittsburgh, PA: MRS, pp. 355–360.
Lowrie, R. (1952), *Trans. AIME 194,* 1093–1100.
Lu, L., Kim, Y. S., Gokhale, A. B., Abbaschian, R. (1990), in: *Intermetallic Matrix Composites:* Anton, D. L., Martin, P. L., Miracle, D. B., McMeeking, R. (Eds.). Pittsburgh, PA: MRS, pp. 79–87.
Lu, T. C., Evans, A. G., Hecht, R. J., Mehrabian, R. (1991), *Acta Metall. Mater. 39,* 1853–1862.
Lu, Z. W., Wei, S. H., Zunger, A. (1992), *Acta Metall. Mater. 40,* 2155–2165.
Lück, R., Wang, H. (1993), *J. Alloys Compd. 191,* L11–L12.
Lüdecke, D. (1986), *Z. Metallkd. 77,* 278–283, 814 (Erratum).
Lugscheider, E., Westermann, U., Wonka, J., Meinhardt, H., Neisius, H., Arnold, R. (1991), in: *Proc. Int. Symp. on Intermetallic Compounds – Structure and Mechanical Properties* (JIMIS-6): Izumi, O. (Ed.). Sendai: The Japan Institute of Metals, pp. 621–625.
Lupinc, V., Onofrio, G., Bianchessi, A., Vimercati, G. (1991), in: *Proc. Int. Symp. on Intermetallic Compounds – Structure and Mechanical Properties* (JIMIS-6): Izumi, O. (Ed.). Sendai: The Japan Institute of Metals, pp. 549–553.
Lynch, F. E. (1991), *J. Less-Common Met. 172–174,* 943–958.
Lynch, J. F., Johnson, J. R., Reilly, J. J. (1979), *Z. Phys. Chem. N.F. 117,* 229–243.
Lynch, R. J., Heldt, D. T., Milligan, W. W. (1991), *Scr. Metall. Mater. 25,* 2147–2152.
Ma, Z., Dayananda, M. A. (1993), *Scr. Metall. Mater. 28,* 429–434.
Ma, Z., Dayananda, M. A., Allen, L. H. (1992), *Mater. Res. Soc. Symp. Proc. 273,* 59–66.
Maa, J. S., Smith, R. T., McGinn, J. T., Reed, L. H. (1985), *Mater. Lett. 3,* 314–318.
Mabuchi, H., Harada, K., Tsuda, H., Nakayama, Y. (1991), *ISIJ Int. 31,* 1272–1278.
Machon, L. (1992), Dr. rer. nat. Thesis, RWTH Aachen, pp. 1–127.
Machon, L., Sauthoff, G. (1994), unpublished report, Max-Planck-Institut für Eisenforschung, Düsseldorf, FRG.
MacKay, R. A., Brindley, P. K., Froes, F. H. (1991), *J. Met. 43 (3),* 23–29.
Magnee, A., Lefort, A., Renaux, P., Franzoni, U., Tassa, O., Le Coze, J. (1991), in: *Proc. Int. Symp. on Intermetallic Compounds – Structure and Mechanical Properties* (JIMIS-6): Izumi, O. (Ed.). Sendai: The Japan Institute of Metals, pp. 725–729.
Mahajan, S., Pinnel, M. R. Bennet, J. E. (1974), *Metall. Trans. 5,* 1263–1272.
Mahajan, S., Wernick, J. H., Chin, G. Y., Nakahara, S., Geballe, T. H. (1978), *Appl. Phys. Lett. 33,* 972–974.
Mailfert, R., Batterman, B. W., Hanak, J. J. (1969), *Phys. Status Solidi 32,* K67–K69.
Majewski, J. A., Vogl, P. (1989), in: *The Structures of Binary Compounds:* de Boer, F. R., Pettifor, D. G. (Eds.). Amsterdam: North-Holland, pp. 287–362.
Maloy, S. A., Heuer, A. H., Lewandowski, J. J., Petrovic, J. J. (1991), *J. Am. Ceram. Soc. 74,* 2704–2706.
Maloy, S. A., Heuer, A. H., Lewandowski, J. J., Mitchell, T. E. (1992), *Acta Metall. Mater. 40,* 3159–3165.
Mannan, S. K., Kumar, K. S., Whittenberger, J. D. (1990), *Metall. Trans. 21A,* 2179–2188.
Mantl, S. (1993), *Phys. Bl. 49,* 303–305.
Mantl, S., Rothman, S. J., Nowicki, L. J., Braski, D. (1984), *Phil. Mag. 50,* 591–602.
Marcinkowski, M. J. (1974a), in: *Treatise on Materials Science and Technology,* Vol. 5: Herman, H. (Ed.). New York: Academic, pp. 181–287.
Marcinkowski, M. J. (1974b), in: *Order–Disorder Transformations in Alloys:* Warlimont, H. (Ed.). Berlin, Springer, pp. 364–403.
Marcinkowski, M. J., Brown, N. (1961), *Acta Metall. 9,* 764–786.
Marder, J. M., Stonehouse, A. J. (1988), in: *2nd International SAMPE Metals and Metals Processing Conference,* Vol. 2: *Space Age Metals Technology:* Froes, F. H., Cull, R. A. (Eds.). Covina, CA: SAMPE, pp. 357–367.
Margevicius, R. W., Lewandowski, J. J., Locci, I. E. (1993a), in: *Structural Intermetallics:* Darolia, R., Lewandowski, J. J., Liu, C. T., Martin, P. L., Miracle, D. B., Nathal, M. V. (Eds.). Warrendale, PA: TMS, pp. 577–584.
Margevicius, R. W., Lewandowski, J. J., Locci, I. E., Michal, G. M. (1993b), *Mater. Res. Soc. Symp. Proc. 288,* 555–560.
Marieb, T. N., Kaiser, A. D., Nutt, S. R., Anton, D. L., Shah, D. M. (1991), in: *High Temperature Ordered Intermetallic Alloys* IV: Johnson, L. A., Pope, D. P., Stiegler, J. O. (Eds.). Pittsburgh, PA: MRS, pp. 329–336.
Marshall, D. B., Shaw, M. C., Morris, W. L. (1992), *Acta Metall. Mater. 40,* 443–454.
Marty, A., Bessiere, M., Bley, F., Calvayrac, Y., Lefebrvre, S. (1990), *Acta Metall. Mater. 38,* 345–350.
Martynov, V. V., Enami, K., Khandros, L. G., Nenno, S., Tkachenko, A. V. (1983), *Phys. Met. Metall. 55 (5),* 136–143.
Maruyama, K., Takahashi, T., Oikawa, H. (1992), *Mater. Sci. Eng. A153,* 433–437.
Masahashi, N., Takasugi, T., Izumi, O. (1988), *Acta Metall. 36,* 1823–1836.
Masahashi, N., Mizuhara, Y., Matsuo, M., Hanamura, T., Kimura, M., Hashimoto, K. (1991), *ISIJ Int. 31,* 728–737.
Mason, D. P., Van Aken, D. C. (1993), *Scr. Metall. Mater. 28,* 185–189.
Mason, D. P., Van Aken, D. C., Webber, J. G. (1990), in: *Intermetallic Matrix Composites:* Anton, D. L.,

ArcelorMittal Ex. 2038
Page 164 of 190

Martin, P. L., Miracle, D. B., McMeeking, R. (Eds.). Pittsburgh, PA: MRS, pp. 341–348.

Massalski, T. B., Murray, J. L., Bennett, L. H. Baker, H. (1990), in: *Binary Alloy Phase Diagrams:* Massalski, T. B., Murray, J. L., Bennett, L. H., Baker, H. (Eds.). Materials Park, OH: ASM.

Matsumoto, A., Saka, H. (1993), *Phil. Mag. A 67,* 217–229.

Matsumoto, H., Ishiguro, H. (1989), *J. Less-Common Met. 153,* 57–63.

Matsuo, M. (1991), *ISIJ Int. 31,* 1212–1222.

Matsuo, M., Hanamura, T., Kimura, M., Masahashi, N., Mizoguchi, T., Miyazawa, K. (1991), *ISIJ Int. 31,* 289–297.

Matteazzi, P., Miani, F., Le Caer, G., Bauer-Grosse, E. (1992), in: *Advanced Structural Materials,* Vol. 2: Clyne, T. W., Withers, P. J. (Eds.). London: The Institute of Materials, pp. 359–365.

Matuszyk, W., Camus, G., Duquette, D. J., Stoloff, N. S. (1990), *Metall. Trans. 21 A,* 2967–2976.

Mayer, J. W., Lau, S. S., Tu, K. N. (1979), *J. Appl. Phys. 50,* 5855–5859.

Mazdiyasni, S., Miracle, D. B. (1990), in: *Intermetallic Matrix Composites:* Anton, D. L., Martin, P. L., Miracle, D. B., McMeeking, R. (Eds.). Pittsburgh, PA: MRS, pp. 155–162.

Mazdiyasni, S., Miracle, D. B., Dimiduk, D. M., Mendiratta, M. G., Subramanian, P. R. (1989), *Scr. Metall. 23,* 327–331.

Maziasz, P. J., McKamey, C. G. (1992), *Mater. Sci. Eng. A 152,* 322–334.

Maziasz, P. J., Goodwin, G. M., Liu, C. T., David, S. A. (1992), *Scr. Metall. Mater. 27,* 1835–1840.

Maziasz, P. J., McKamey, C. G., Cavin, O. B., Hubbard, C. R., Zacharia, T. (1993), *Mater. Res. Soc. Symp. Proc. 288,* 209–215.

McAndrew, J. B., Kessler, H. D. (1956), *J. Met. 8,* 1348–1353.

McColm, I. J., Ward, J. M. (1992), *J. Alloys Compd. 178,* 91–100.

McCurrie, R. A. (1986), in: *Encyclopedia of Materials Science and Engineering,* Vol. 4: Bever, M. B. (Ed.). Oxford: Pergamon, pp. 2645–2651.

McDonald, W. K. (1984), in: *Niobium:* Stuart, H. (Ed.), Warrendale, PA: The Metallurgical Society of AIME, pp. 495–502.

McKamey, C. G., Carmichael, C. A. (1991), in: *High Temperature Ordered Intermetallic Alloys* IV: Johnson, L. A., Pope, D. P., Stiegler, J. O. (Eds.). Pittsburgh, PA: MRS, pp. 1051–1056.

McKamey, C. G., Lee, E. H. (1993), *Mater. Res. Soc. Symp. Proc. 288,* 983–988.

McKamey, C. G., Liu, C. T. (1990), *Scr. Metall. Mater. 24,* 2119–2122.

McKamey, C. G., Pierce, D. H. (1993), *Scr. Metall. Mater. 28,* 1173–1176.

McKamey, C. G., De Van, J. H., Tortorelli, P. F., Sikka, V. K. (1991), *J. Mater. Res. 6 (8),* 1779–1805.

McKee, D. W. (1993), *Mater. Res. Soc. Symp. Proc. 288,* 953–958.

McKee, D. W., Fleischer, R. L. (1991), in: *High Temperature Ordered Intermetallic Alloys* IV: Johnson, L. A., Pope, D. P., Stiegler, J. O. (Eds.). Pittsburgh, PA: MRS, pp. 969–974.

Medvedev, A. I., Dolgikh, V. Y., Ivanovskiy, A. L., Kuznetsov, Y. V., Gubanov, V. A., Kurmayev, E. Z. (1984), *Phys. Met. Metall. 57 (2),* 29–36.

Mei, J., Cooper, B. R. (1993), in: *Structural Intermetallics:* Darolia, R., Lewandowski, J. J., Liu, C. T., Martin, P. L., Miracle, D. B., Nathal, M. V. (Eds.). Warrendale, PA: TMS, pp. 611–615.

Meier, G. H. (1987), *Mater. Res. Soc. Symp. Proc. 81,* 443–458.

Meier, G. H. (1989), in: *Oxidation of High-Temperature Intermetallics:* Grobstein, T., Doychak, J. (Eds.). Warrendale, PA: TMS, pp. 1–16.

Meier, G. H., Pettit, F. S. (1992), *Mater. Sci. Eng. A 153,* 548–560.

Meier, G. H., Appalonia, D., Perkins, R. A., Chiang, K. T. (1989), in: *Oxidation of High-Temperature Intermetallics:* Grobstein, T., Doychak, J. (Eds.). Warrendale, PA: TMS, pp. 185–194.

Meier, G. H., Birks, N., Pettit, F. S., Perkins, R. A., Grabke, H. J. (1993), in: *Structural Intermetallics:* Darolia, R., Lewandowski, J. J., Liu, C. T., Martin, P. L., Miracle, D. B., Nathal, M. V. (Eds.). Warrendale, PA: TMS, pp. 861–877.

Mendelson, S. (1986), *Phys. Status Solidi (a) 98,* 133–138.

Mendiratta, M. G., Dimiduk, D. M. (1993), *Metall. Trans. 24 A,* 501–504.

Mendiratta, M. G., Law, C. C. (1987), *J. Mater. Sci. 22,* 607–611.

Mendiratta, M. G., Lipsitt, H. A. (1985), in: *High-Temperature Ordered Intermetallic Alloys:* Koch, C. C., Liu, C. T., Stoloff, N. S. (Eds.). Pittsburgh, PA: MRS, pp. 155–162.

Mendiratta, M. G., Kim, H.-M., Lipsitt, H. A. (1984), *Metall. Trans. 15 A,* 395–398.

Mendiratta, M. G., Ehlers, S. K., Chatterjee, D. K., Liptsitt, H. A. (1987a), *Metall. Trans. 18 A,* 283–291.

Mendiratta, M. G., Ehlers, S. K., Dimiduk, D. M., Kerr, W. R., Lipsitt, H. A. (1987b), in: *High-Temperature Ordered Intermetallic Alloys* II: Stoloff, N. S., Koch, C. C., Liu, C. T., Izumi, O. (Eds.). Pittsburgh, PA: Mater Res. Soc., pp. 393–404.

Mendiratta, M. G., Lewandowski, J. J., Dimiduk, D. M. (1991), *Metall. Trans. 22 A,* 1573–1583.

Meng, X. Y., Northwood, D. O. (1986), *J. Less-Common Met. 125,* 33–44.

Meschel, S. V., Kleppa, O. J. (1993), *J. Alloys Compounds 191,* 111–116.

Meschter, P. J. (1991), in: *High Temperature Ordered Intermetallic Alloys* IV: Johnson, L. A., Pope, D. P., Stiegler, J. O. (Eds.). Pittsburgh, PA: MRS, pp. 1027–1032.

ArcelorMittal Ex. 2038
Page 165 of 190

Meschter, P. J., Schwartz, D. S. (1989), *J. Met. 41 (11)*, 52–55.
Metelnick, M. P., Varin, R. A. (1991), *Z. Metallkd. 82*, 346–353.
Mikkola, D. E., Nic, J. P., Zhang, S., Milligan, W. W. (1991), *ISIJ Int. 31*, 1076–1079.
Miller, M. K., Horton, J. A. (1987), in: *High-Temperature Ordered Intermetallic Alloys* II: Stoloff, N. S., Koch, C. C., Liu, C. T., Izumi, O. (Eds.). Pittsburgh, PA: MRS, pp. 117–122.
Mills, M. J., Miracle, D. B. (1993), *Acta Metall. Mater. 41*, 85–95.
Mills, M. J., Daw, M. S., Foiles, S. M., Miracle, D. B. (1993), *Mater. Res. Soc. Symp. Proc. 288*, 257–262.
Minamino, Y., Jung, S. B., Yamane, T., Hirao, K. (1992), *Metall. Trans. 23 A*, 2783–2790.
Minonishi, Y. (1991), *Phil. Mag. A 63*, 1085–1093.
Miracle, D. B. (1991), *Acta Metall. Mater. 39*, 1457–1468.
Miracle, D. B. (1993), *Acta Metall. Mater. 41*, 649–684.
Mishima, Y., Oya, Y., Suzuki, T. (1985), *Trans. ISIJ 25*, 1171–1178.
Misra, A., Noebe, R. D., Gibala, R. (1993), *Mater. Res. Soc. Symp. Proc. 288*, 483–488.
Mitchell, T. E., Castro, R. G., Chadwick, M. M. (1992), *Phil. Mag. A 65*, 1339–1351.
Miura, S., Liu, C. T. (1992), *Scr. Metall. Mater. 26*, 1753–1758.
Miura, Y., Watanabe, N. (1993), *Scr. Metall. Mater. 29*, 139–144.
Miura, S., Mishima, Y., Hayashi, T., Suzuki, T. (1991), in: *High Temperature Ordered Intermetallic Alloys* IV: Johnson, L. A., Pope, D. P., Stiegler, J. O. (Eds.). Pittsburgh, PA: MRS, pp. 623–628.
Miyamura, H., Kuriyama, N., Sakai, T., Oguro, K., Kato, A., Ishikawa, H., Iwasaki, T. (1991), *J. Less-Common Met. 172–174*, 1205–1210.
Miyazaki, M., Terunuma, M., Terazono, K., Komatsu, T., Matusita, K. (1992), *J. Mater. Sci. Lett. 11*, 659–661.
Mohamed, F. A., Murty, K. L., Langdon, T. G. (1974), *Acta Metall. 22*, 325–332.
Molenat, G., Caillard, D., Couret, A., Paidar, V. (1993), *Mater. Res. Soc. Symp. Proc. 288*, 287–292.
Moran, J. B. (1965), *Trans. AIME 233* 1473–1482.
Moreen, H. A., Polonis, D. H., Taggart, R. (1971), *J. Appl. Phys. 42*, 2151–2152.
Morgand, P., Mouturat, P., Sainfort, G. (1968), *Acta Metall. 16*, 867–875.
Moriwaki, Y., Gamo, T., Iwaki, T. (1991a), *J. Less. Common Met. 172–174*, 1028–1035.
Moriwaki, Y., Gamo, T., Seri, H., Iwaki, T. (1991b), *J. Less-Common Met. 172–174*, 1211–1218.
Morral, F. R. (1934), *JISI 130*, 419–428.
Morral, F. R. (1980), in: *Metals Handbook* Vol. 3: *Properties and Selection: Stainless Steels, Tool Materials and Special-Purpose Metals*. Materials Park, OH: ASM, pp. 207–268.
Morris, D. G. (1992), in: *Ordered Intermetallics – Physical Metallurgy and Mechanical Behaviour:* Liu, C. T., Cahn, R. W., Sauthoff, G. (Eds.). Dordrecht: Kluwer, pp. 123–142.
Morris, D. G., Lerf, (1991), *Phil. Mag. A 63*, 1195–1206.
Morris, D. G., Dadras, M. M., Morris, M. A. (1993a), *Acta Metall. Mater. 41*, 97–111.
Morris, D. G., Gunther, S., Joye, J. C. (1993b), *Intermetallics 1*, 49–58.
Morris, D. G., Morris, M. A., Leboeuf, M. (1993c), *Acta Metall. Mater. 41*, 2077–2090.
Morris, M. A. (1991a), *Mater. Sci. Eng. A 148*, 33–43.
Morris, M. A. (1991b), *Scr. Metall. Mater. 25*, 2541–2546.
Morris, M. A. (1992), *Acta Metall. Mater. 40*, 1573–1586.
Moser, J. A., Aindow, M., Clark, W. A. T., Draper, S., Fraser, H. L. (1990), in: *Intermetallic Matrix Composites:* Anton, D. L., Martin, P. L., Miracle, D. B., McMeeking, R. (Eds.). Pittsburgh, PA: MRS, pp. 379–384.
Motojima, S., Yoshida, H., Sugiyama, K. (1982), *J. Mater. Sci. Lett. 1*, 23–24.
Mouldckhues, G. W., Sahm, P. R. (1992), in: *Advanced Structural Materials* Vol. 2: Clyne, T. W., Withers, P. J. (Eds.). London: The Institute of Materials, pp. 355–358.
Moyer, T. D., Dayananda, M. A. (1976), *Metall. Trans. 7 A*, 1035–1040.
Mrowec, S., Jedlinski, J. (1989), in: *Oxidation of High-Temperature Intermetallics:* Grobstein, T., Doychak, J. (Eds.). Warrendale, PA: TMS, pp. 57–66.
Mrowec, S., Danielewski, M., Godlewska, E, Godlewski, K. (1989), in: *Oxidation of High-Temperature Intermetallics:* Grobstein, T., Doychak, J. Eds.). Warrendale, PA: TMS, pp. 147–156.
Mukerjee, D., Jones, I. P., Loretto, M. H., Smallman, R. E. (1979), in: *Phase Transformations* (Spring Residential Conf. Series 3, No. 11, Vol. 2). London: Chameleon Press, pp. II-13–II-14.
Mukherjee, A. K., Bird, J. E., Dorn, J. E. (1969), *Trans. ASM 62*, 155–179.
Mukherjee, S. K., Khanra, G. P. (1991), *J. Mater. Sci. Lett. 10*, 1222–1224.
Mulder, J. H., Thoma, P. E., Beyer, J. (1993), *Z. Metallkd. 84*, 501–508.
Muller, J. (1986), in: *Encyclopedia of Materials Science and Engineering*, Vol. 1: Bever, M. B. (Ed.). Oxford: Pergamon, pp. 1–5.
Müller, P. (1986), *Neue Hütte 31*, 206–208.
Munroe, P. R., Baker, I. (1988), *Met. Mater. 4*, 435–438.
Munroe, P. R., Baker, I. (1990), *Scr. Metall. Mater. 24*, 2273–2278.
Munroe, P. R., Baker, I. (1991), *Acta Metall. Mater. 39*, 1011–1017.

ArcelorMittal Ex. 2038
Page 166 of 190

Munroe, P. R., Baker, I., Nagpal, P. (1991), *J. Mater. Sci. 26,* 4303–4306.
Murakami, Y., Otsuka, K., Hanada, S., Watanabe, S. (1992), *Mater. Trans. Jpn. Inst. Met. 33,* 282–288.
Muraleedharan, K., Gogia, A. K., Nandy, T. K., Banerjee, D., Lele, S. (1992a), *Metall. Trans. 23A,* 401–415.
Muraleedharan, K., Nandy, T. K., Banerjee, D., Lele, S. (1992b), *Metall. Trans. 23A,* 417–431.
Murarka, S. P. (1983a), *Silicides for VLSI Applications.* New York: Academic.
Murarka, S. P. (1983b), *Annu. Rev. Mater. Sci. 13,* 117–137.
Murarka, S. P. (1984), *J. Met. 36 (7),* 57–60.
Murase, S., Nakayama, S., Aoki, N., Kobayashi, N. (1992), *Sci. Rep. Tohoku Univ. 37 (1),* 125–134.
Murata, Y., Higuchi, T., Takeda, Y., Morinaga, M., Yukawa, N. (1991), in: *Proc. Int. Symp. on Intermetallic Compounds – Structure and Mechanical Properties* (JIMIS-6): Izumi, O. (Ed.). Sendai: The Japan Institute of Metals, pp. 627–631.
Murata, Y., Morinaga, M., Takeda Y. (1992), *Mater. Trans. Jpn. Inst. Met. 33,* 419–421.
Murata, Y., Morinaga, M., Shimamura, Y., Takeda, Y., Miyazaki, S. (1993), in: *Structural Intermetallics:* Darolia, R., Lewandowski, J. J., Liu, C. T., Martin, P. L., Miracle, D. B., Nathal, M. V. (Eds.). Warrendale, PA: TMS, pp. 247–256.
Murayama, Y., Hanada, S., Obara, K., Hiraga, K., Ishida, S. (1991), in: *Proc. Int. Symp. on Intermetallic Compounds – Structure and Mechanical Properties* (JIMIS-6): Izumi, O. (Ed.). Sendai: The Japan Institute of Metals, pp. 1033–1037.
Murayama, Y., Hanada, S., Obara, K. (1993a), *Mater. Trans. Jpn. Inst. Met. 34,* 325–333.
Murayama, Y., Hanada, S., Obara, K., Hiraga, K. (1993b), *Phil. Mag. A 67,* 251–260.
Murayama, Y., Kumagai, T., Hanada, S. (1993c), *Mater. Res. Soc. Symp. Proc. 288,* 95–106.
Murray, J. L. (1985), *Int. Met. Rev. 30,* 211–233.
Murray, J. L. (1988), *Metall. Trans. 19A,* 243–247.
Murthy, A. S., Goo, E. (1993), *Acta Metall. Mater. 41,* 2135–2142.
Murugesh, L., Venkateswara Rao, K. T., DeJonghe, L. C., Ritchie, R. O. (1992), *Mater. Res. Soc. Symp. Proc. 273,* 433–438.
Muto, S., Merk, N., Schryvers, D., Tanner, L. E. (1993a), *Phil. Mag. B67,* 673–689.
Muto, S., Schryvers, D., Merk, N., Tanner, L. E. (1993b), *Acta Metall. Mater. 41,* 2377–2383.
Nabarro, F. R. N., de Villiers-Filmer, H. L. (1993), *The Physics of Creep–Creep and Creep-Resistant Alloys.* London: Taylor and Francis.
Nachman, J. F., Buehler, W. J. (1954), *J. Appl. Phys. 25,* 307–313.
Nagai, H., Kitagaki, K., Shoji, K. (1987), *J. Less. Common Met. 134,* 275–286.
Nagasawa, A., Kawachi, K. (1971), *J. Phys. Soc. Jpn. 30,* 296.
Nagpal, P., Baker, I. (1990a), *Metall. Trans. 21A,* 2281–2282.
Nagpal, P., Baker, I. (1990b), *Scr. Metall. Mater. 24,* 2381–2384.
Nagpal, P., Baker, I. (1991), *Scr. Metall. Mater. 25,* 2577–2580.
Nakagawa, Y. G., Yokoshima, S., Mastuda, K. (1992), *Mater. Sci. Eng. A153,* 722–725.
Nakajima, H., Nakamura, Y., Koiwa, M., Takasugi, T., Izumi, O (1988), *Scr. Metall. 22,* 507–510.
Nakajima, H., Yasuda, H., Koiwa, M. (1991), in: *Proc. Int. Symp. on Intermetallic Compounds – Structure and Mechanical Properties* (JIMIS-6): Izumi, O. (Ed.). Sendai: The Japan Institute of Metals, pp. 57–61.
Nakamura, F., Takamura, J. (1982), in: *Point Defects and Defect Interactions in Metals:* Takamura, J., Doyama, M., Kiritani, M. (Eds.). Tokyo: University of Tokyo Press, pp. 627–630.
Nakamura, H., Takeyama, M., Yamabe, Y., Kikuchi, M. (1993), *Scr. Metall. Mater. 28,* 997–1002.
Nakamura, M. (1991), in: *Proc. Int Symp. on Intermetallic Compounds – Structure and Mechanical Properties* (JIMIS-6): Izumi, O. (Ed.). Sendai: The Japan Institute of Metals, pp. 655–659.
Nakamura, M., Kimura, K. (1991), *J. Mater. Sci. 26,* 2208–2214.
Nakamura, M., Sakka, Y. (1988), *J. Mater. Sci. 23,* 4041–4048.
Nakamura, M., Matsumoto, S., Hirano, T. (1990), *J. Mater. Sci. 25,* 3309–3313.
Nakano, T., Umakoshi, Y. (1993), *J. Alloys Compd. 197,* 17–20.
Nakao, Y., Shinozaki, K., Hamada, M. (1991), *ISIJ Int. 31,* 1260–1266.
Nakashima, T., Umakoshi, Y. (1992), *Phil. Mag. Lett. 66,* 317–321.
Nakayama, Y., Mabuchi, H. (1993), *Intermetallics 1,* 41–48.
Nandy, T. K., Mishra, R. S., Banerjee, D. (1993), *Scr. Metall. Mater. 28,* 569–574.
Nardone, V. C. (1992), *Metall. Trans. 23A,* 563–572.
Nardone, V. C., Strife, J. R. (1991), *Metall. Trans. 22A,* 183–189.
Nardone, V. C., Strife, J. R., Prewo, K. M. (1990), in: *Intermetallic Matrix Composites:* Anton, D. L., Martin, P. L., Miracle, D. B., McMeeking, R. (Eds.). Pittsburgh, PA: MRS, pp. 205–210.
Nash, P., Liang, W. W. (1985), *Metal. Trans. 16A,* 319–322.
Natan, M. (1985), *Mater. Lett. 3,* 319–324.
Natesan, K. (1988), *Oxid. Met. 30,* 53–83.
Nathal, M. V. (1992), in: *Ordered Intermetallics – Physical Metallurgy and Mechanical Behaviour:* Liu, C. T., Cahn, R. W., Sauthoff, G. (Eds.). Dordrecht: Kluwer, pp. 541–563.
Nathrath, N. (1986), *Thyssen Techn. Ber. 1/86,* 110–118.
Nava, F., Ottaviani, G., Riontino, G. (1985), *Mater. Lett. 3,* 311–313.

ArcelorMittal Ex. 2038
Page 167 of 190

Nembach, E., Tachikawa, K., Takano, S. (1970), *Phil. Mag. 21,* 869–872.
Nemoto, M., Tian, W. H., Harada, K., Han, C. S., Sano, T. (1992), *Mater. Sci. Eng. A 152,* 247–252.
Nesbitt, J. A., Lowell, C. E. (1993), *Mater. Res. Soc. Symp. Proc. 288,* 107–118.
Nesbitt, J. A., Vinarcik, E. J., Barrett, C. A., Doychak, J. (1992), *Mater. Sci. Eng. A 153,* 561–566.
Nevitt, M. V. (1963), in: *Electronic Structure and Alloy Chemistry of the Transition Elements:* Beck, P. A. (Ed.). New York: Interscience, pp. 101–178.
Nevitt, M. V. (1967), in: *Intermetallic Compounds:* Westbrook, J. H. (Ed.). New York: Wiley, pp. 217–229.
Newkirk, J. W., Sago, J. A. (1990), in: *Intermetallic Matrix Composites:* Anton, D. L., Martin, P. L., Miracle, D. B., McMeeking, R. (Eds.). Pittsburgh, PA: MRS, pp. 183–189.
Nghiep, D. M., Paufler, P., Krämer, U., Kleinstück, K., Quyen, N. H. (1980), *J. Mater. Sci. 15,* 1140–1146.
Nic, J. P., Zhang, S., Mikkola, D. E. (1991), in: *High Temperature Ordered Intermetallic Alloys* IV: Johnson, L. A., Pope, D. P., Stiegler, J. O. (Eds.). Pittsburgh, PA: MRS, pp. 697–702.
Nicholls, J. R., Rawlings, R. D. (1977), *J. Mater.Sci. 12,* 2456–2464.
Nicholls, J. R., Stephenson, D. J. (1991), *Met. Mater. 7,* 156–163.
Nicolet, M.-A., Lau, S. S. (1983), in: *VLSI Electronics, Microstructure Science,* Vol. 6: Einspruch, N. G, Larrabee, G. B. (Eds.). New York: Academic, pp. 330–350.
Nieh, T. G., Oliver, W. C. (1989), *Scr. Metall. 23,* 851–854.
Nieh, T. G., Wadsworth, J. (1989), *Scr. Metall. 23,* 871–874.
Nieh, T. G., Wadsworth, J. (1990), *Scr. Metall. Mater. 24,* 1489–1494.
Nieh, T. G., Wadsworth, J., Liu, C. T. (1989), in: *High-Temperature Ordered Intermetallic Alloys* III. Liu, C. T., Taub, A. I., Stoloff, N. S., Koch, C. C. (Eds.). Pittsburgh, PA: Mater. Res. Soc. pp. 743–748.
Nieh, T. G., Wadsworth, J., Liu, C. T. (1990), in: *High-Temperature Aluminides and Intermetallics:* Whang, S. H., Liu, C. T., Pope, D. P., Stiegler, J. O. (Eds.). Warrendale, PA: TMS, pp. 453–462.
Nishida, I. (1973), *Phys. Rev. B 7,* 2710–2713.
Nishida, I., Sakata, T. (1978), *J. Phys. Chem. Solids 39,* 499–505.
Nishida, M., Honma, T. (1984), *Scr. Metall. 18,* 1293–1298.
Nishimura, C., Liu, C. T. (1991), *Scr. Metall. Mater. 25,* 791–794.
Nishimura, C., Liu, C. T. (1992a), *Acta Metall. Mater. 40,* 723–731.
Nishimura, C., Liu, C. T. (1992b), *Mater Sci. Eng. A 152,* 146–152.
Nishiyama, Y., Miyashita, T., Isobe, S., Noda, T. (1990), in: *High-Temperature Aluminides and Intermetallics:* Whang, S. H., Liu, C. T., Pope, D. P., Stiegler, J. O. (Eds.). Warrendale, PA: TMS, pp. 557–584.
Nix, W. D., Ilschner, B. (1980), in: *Proc. Int. Conf. on the Strength of Metals and Alloys* (ICSMA 5), Vol. 3: Haasen, P., Gerold, V., Kostorz, G. (Eds.). Oxford: Pergamon, pp. 1503–1530.
Noda, Y., Kon, H., Furukawa, Y., Otsuka, N., Nishida, I. A., Masumoto, K. (1992a), *Mater. Trans. Jpn. Inst. Met. 33,* 845–850.
Noda, Y., Kon, H., Furukawa, Y., Nishida, I. A., Masumoto, K. (1992b), *Mater. Trans. Jpn. Inst. Met. 33,* 851–855.
Noebe, R. D., Behbehani, M. K. (1992), *Scr. Metall. Mater. 27,* 1795–1800.
Noebe, R. D., Lerch, B. A. (1992), *Scr. Metall. Mater. 27,* 1161–1166.
Noebe, R. D., Lerch, B. A. (1993), *Mater. Res. Soc. Symp. Proc. 288,* 743–748.
Noebe, R. D., Bowman, R. R., Eldridge, J. I. (1990), in: *Intermetallic Matrix Composites:* Anton, D. L., Martin, P. L., Miracle, D. B., McMeeking, R. (Eds.). Pittsburgh, PA: MRS, pp. 323–331.
Noebe, R. D., Misra, A., Gibala, R. (1991), *ISIJ Int. 31,* 1172–1185.
Nonaka, K., Tanosaki, K., Fujita, M., Chiba, A., Kawabata, T., Izumi, O. (1992), *Mater. Trans. Jpn. Inst. Met. 33,* 802–810.
Norman, J. H., Reynolds, G. H., Brewer, L. (1990), in: *Intermetallic Matrix Composites:* Anton, D. L., Martin, P. L., Miracle, D. B., McMeeking, R. (Eds.). Pittsburgh, PA: MRS, pp. 369–377.
Nosova, G. I., Polyakova, N. A., Novikova, Y. Y. (1986), *Phys. Met. Metall. 61 (3),* 151–164.
Noto, K., Watanabe, K., Muto, Y. (1986), *Sci. Rep. RITU A 33.* 393–414.
Noto, K., Matsukawa, M., Watanabe, K. (1992), *Sci. Rep. Tohoku Univ. 37, 1,* 7–17.
Nourbakhsh, S., Sahin, O., Rhee, W. H., Margolin, H. (1991), *Metall. Trans. 22 A,* 3059–3064.
Nourbakhsh, S., Sahin, O., Rhee, W. H., Margolin, H. (1993), *Metall. Trans. 24 A,* 435–443.
Nowotny, H. (1963), in: *Electron Structure and Alloy Chemistry of the Transition Elements:* Beck, P. A. (Ed.). New York: Interscience, pp. 179–220.
Nowotny, H. (1972a), in: *Solid State Chemistry:* Roberts, L. E. J. (Ed.). London: Butterworths, pp. 151–188.
Nowotny, H. (1972b), *Angew. Chem. 84,* 973–982.
Nowotny, H., Benesovsky, F. (1967), in: *Phase Stability in Metals and Alloys:* Rudman, P. S., Stringer, J., Jaffee, R. I. (Eds.). New York: McGraw-Hill, pp. 319–336.
Oblak, J. M., Paulonis, D. F., Duvall, D. S. (1974), *Metall. Trans. 5,* 143–153.
Ochiai, S., Ueno, M. (1988), *J. Jpn Inst. Met. 52,* 157–162.

ArcelorMittal Ex. 2038
Page 168 of 190

Ochiai, S., Oya, Y., Suzuki, T. (1984), *Acta Metall. 32,* 289–298.
Ochiai, S., Uehara, T., Osamura, K. (1986a), *J. Mater. Sci. 21,* 1020–1026.
Ochiai, S., Osamura, K., Uehara, T. (1986b), *J. Mater. Sci. 21,* 1027–1036.
Ochiai, S., Ueno, M., Noguchi, O. (1987), *J. Jpn. Inst. Met. 51,* 686–693.
Ochiai, S., Osamura, K., Ryoji, M. (1988), *ISIJ Int. 28,* 973–978.
Ochiai, S., Shirokura, T., Doi, Y., Kojima, Y. (1991), *ISIJ Int. 31,* 1106–1112.
Ochiai, S., Yagihashi, M., Osamura, K. (1994), *Intermetallics 2,* 1–7.
Oehring, M., Klassen, T., Bormann, R. (1993), *Mater. Res. Soc. Symp. Proc. 288,* 873–878.
Oertel, C. G., Krämer, U., Kleinstück, K. (1986), *J. Mater. Sci. 21,* 2585–2589.
Ogishi, H., Makimura, M., Ono, H., Minakata, S. (1991), *ISIJ Int. 31,* 1168–1171.
Ogurtani, T. (1972), *Metall. Trans. 3,* 421–425.
Oh, M. H., Inui, H., Misaki, M., Kobayashi, M., Yamaguchi, M. (1993a), *Mater. Res. Soc. Symp. Proc. 288,* 1001–1006.
Oh, M. H., Inui, H., Misaki, M., Yamaguchi, M. (1993b), *Acta Metall. Mater. 41,* 1939–1949.
Ohba, Y., Sakuma, N. (1989), *Acta Metall. 37,* 2377–2384.
Ohkoshi, T., Isoda, Y., Kaibe, H., Ichida, S., Masumoto, K., Nishida, I. (1988), *Trans. JIM 29,* 756–766.
Ohta, Y., Pettifor, D. G. (1990), *J. Phys.: Condens. Matter 2,* 8189–8194.
Oikawa, H. (1992), *Mater. Sci. Eng. A 153,* 427–432.
Okamoto, H., Chakrabarti, D. J., Laughlin, D. E., Massalski, T. B. (1987), *Bull. Alloy Phase Diagrams 8,* 454–474.
Olowolafe, J. O., Tu, K. N., Angilello, J. (1979), *J. Appl. Phys. 50,* 6316–6320.
Olzi, E., Matacotta, F. C., Setina, P. (1988), *J. Less-Common Met. 139,* 123–132.
Onodera, H., Nakazawa, S., Ohno, K., Yamagata, T., Yamazaki, M. (1991), *ISIJ Int. 31,* 875–881.
Onozuka, T., Ohnishi, N., Hirabayashi, M. (1988), *Metall. Trans. 19A,* 797–803.
Ormerod, J. (1988), *Met. Mater. 4,* 478–483.
Ortin, J., Manosa, L., Friend, C. M., Planes, A., Yoshikawa, M. (1992), *Phil. Mag. A65,* 461–475.
Oti, J. A., Yu, K. O. (1993), in: *Structural Intermetallics:* Darolia, R., Lewandowski, J. J., Liu, C. T., Martin, P. L., Miracle, D. B., Nathal, M. V. (Eds.). Warrendale, PA: TMS, pp. 505–512.
Otsuka, K., Shimizu, K. (1970), *Scr. Metall. 4,* 469–472.
Otsuka, K., Shimizu, K. (1986), *Int. Met. Rev. 31,* 93–114.
Otsuki, M., Stoloff, N. S. (1992), *Scr. Metall. Mater. 26,* 325–330.
Packer, C. M. (1989), in: *Oxidation of High-Temperature Intermetallics:* Grobstein, T., Doychak, J. (Eds.). Warrendale, PA: TMS, pp. 235–244.
Padmavardhani, D., Prasad, Y. V. R. K. (1991), *Metall. Trans. 22A,* 2993–3001.
Paidar, V., Pope, D. P., Yamaguchi, M. (1981), *Scr. Metall. 15,* 1029–1031.
Pajunen, M., Kivilahti, J. (1992), *Z. Metallkd. 83,* 17–20.
Pak, H.-R., Hsiung, L.-M., Kato, M. (1986), *Phil. Mag. A53,* 887–896.
Pak, H.-R., Chen, C.-W., Inal, O. T., Okazaki, K., Suzuki, T. (1988), *Mater. Sci. Eng. A104,* 53–60.
Pak, H. R., Pak, J. S. L., Rigsbee, J. M., Wayman, C. M. (1990), *Mater. Sci. Eng. A128,* 129–139.
Palm, M. (1990), Dr. rer. nat. Thesis, Universität Dortmund, pp. 1–145.
Pan, Y. C., Chuang, T. H., Yao, Y. D. (1991), *J. Mater. Sci. 26,* 6097–6103.
Parameswaran, V. R., Immarigeon, J.-P., Wallace, W. (1990), *Intermetallics – Canadian Perspective.* Ottawa: National Research Council Canada, pp. 1–43.
Parfitt, L. J., Smialek, J. L., Nic, J. P., Mikkola, D. E. (1991), *Scr. Metall. Mater. 25,* 727–731.
Paris, D., Lesbats, P., Levy, J. (1975), *Scr. Metall. 9,* 1373–1378.
Park, J.-M., Lee, J.-Y. (1992), *J. Alloys Compd. 182,* 43–54.
Park, J.-M., Kim, Y.-G., Lee, J.-Y. (1993), *J. Alloys Compd. 198,* L19–L23.
Park, J. W., Moon, I. G., Yu, J. (1991), *J. Mater. Sci. 26,* 3062–3066.
Parker, S. F. H., Grundy, P. J., Jones, G. A., Briggs, I., Clegg, A. G. (1988), *J. Mater. Sci. 23,* 217–222.
Parthasarathy, T. A., Rao, S. I., Dimiduk, D. M. (1993), *Phil. Mag. A67,* 643–662.
Parthé, E., Lux, B., Nowotny, H. (1955), *Monatsh. Chem. 86,* 859–867.
Paruchuri, M. R., Massalski, T. B. (1991), in: *High Temperature Ordered Intermetallic Alloys* IV: Johnson, L. A., Pope, D. P., Stiegler, J. O. (Eds.). Pittsburgh, PA: MRS, pp. 143–149.
Patankar, S. N., Lewandowski, J. J. (1993), *Mater. Res. Soc. Symp. Proc. 288,* 829–834.
Pathare, V., Michal, G. M., Vedula, K., Nathal, M. V. (1987), *Scr. Metall. 21,* 283–288.
Patnaik, P. C. (1989), *Mater. Manuf. Processes 4,* 133–152.
Patrick, D. K., Van Aken, D. C. (1993), *Mater. Res. Soc. Symp. Proc. 288,* 1135–1141.
Patrick, D. K., Chang, K.-M., Miracle, D. B., Lipsitt, H. A. (1991), in: *High Temperature Ordered Intermetallic Alloys* IV: Johnson, L. A., Pope, D. P., Stiegler, J. O. (Eds.). Pittsburgh, PA: MRS, pp. 267–272.
Patten, J. W. (1990), in: *High-Temperature Aluminides and Intermetallics:* Whang, S. H., Liu, C. T., Pope, D. P., Stiegler, J. O. (Eds.). Warrendale, PA: TMS, pp. 493–503.

ArcelorMittal Ex. 2038
Page 169 of 190

Paufler, P. (1972), *Phys. Status Solidi (b) 52,* K65–K67.
Paufler, P. (1976), in: *Intermetallische Phasen:* Autorenkollektiv. (Ed.). Leipzig: VEB Deutscher Verlag f. Grundstoffindustrie, pp. 165–187.
Paufler, P. (1985), *Z. Kristallogra*phie 170, 144.
Paufler, P., Schulze, G. E. R. (1967), *Phys. Status Solidi 24,* 77–87.
Paufler, P., Schulze, G. E. R. (1978), *Physikalische Grundlagen mechanischer Festkörpereigenschaften.* Braunschweig: Vieweg, pp. 1–135.
Pawelski, O., Hagedorn, K. E., Hop, R. (1994), Steel Res., in press.
Paxton, A. T., Pettifor, D. G. (1992), *Scr. Metall. Mater. 26,* 529–533.
Peacock, D. K. (1989), *Met. Mater. 5,* 474.
Pearson, W. B. (1958), *A Handbook of Lattice Spacings and Structures of Metals and Alloys.* London: Pergamon.
Pelegrina, J. L., Ahlers, M. (1992a), *Acta Metall. Mater. 40,* 3205–3211.
Pelegrina, J. L., Ahlers, M. (1992b), *Acta Metall. Mater. 40,* 3221–3227.
Perepezko, J. H. (1991a), *ISIJ Int. 31,* 1080–1087.
Perepezko, J. H. (1991b), in: *Proc. Int. Symp. on Intermetallic Compounds – Structure and Mechanical Properties* (JIMIS-6): Izumi, O. (Ed.). Sendai: The Japan Institute of Metals, pp. 239–243.
Peretz, M., Zamir, D., Shaltiel, D., Shinar, J. (1979), *Z. Phys. Chem. N. F. 117,* 221–228.
Perevesenzew, A., Lanzel, E., Eder, O. J., Tuscher, E, Weinierl, P. (1988), *J. Less-Common Met. 143,* 39–47.
Perkins, R. A., Chiang, K. T., Meier, G. H. (1988), *Scr. Metall. 22,* 419–424.
Perkins, R. A., Chiang, K. T., Meier, G. H., Miller, R. (1989), in: *Oxidation of High-Temperature Intermetallics:* Grobstein, T., Doychak, J. (Eds.). Warrendale, PA: TMS, pp. 157–170.
Peshev, P., Khristov, M., Gyurov, G. (1989), *J. Less-Common Met. 153,* 15–22.
Petrasek, W. D., McDanels, D. L., Westfall, L. J., Stephens, J. R. (1986), *Met. Prog. 130 (8),* 27–31.
Petrovic, J. J. (1993), *MRS Bull. 18 (7),* 35–40.
Petrovic, J. J., Vasudevan, A. K. (1992), *Mater. Res. Soc. Symp. Proc. 273,* 229–240.
Pettifor, D. G. (1988), *Mater. Sci. Technol. 4,* 675–691.
Pettifor, D. G., Aoki, M. (1991), *Phil. Trans. R. Soc. London A 334,* 439–449.
Pettit, F. S. (1967), *Trans. AIME 239,* 1296–1305.
Pettit, F. S., Goward, G. W. (1983), in: *Coatings for High Temperature Applications:* Lang, E. (Ed.). London: Applied Science, pp. 341–359.
Pharr, G. M., Courington, S. V., Wadsworth, J., Nieh, T. G. (1991), *J. Mater. Res. 6,* 2653–2659.
Piao, M., Miyazaki, S., Otsuka, K., Nishida, N. (1992a), *Mater. Trans. Jpn. Inst. Met. 33,* 337–345.
Piao, M., Miyazaki, S., Otsuka, K. (1992b), *Mater. Trans. Jpn. Inst. Met. 33,* 346–353.
Pickering, F. B. (1976), *Int. Met. Rev. 21,* 227–268.
Pinnel, M. R., Mahajan, S., Bennet, J. E. (1976), *Acta Metall. 24,* 1095–1106.
Pitsch, W., Sauthoff, G. (1992), in: *Steel,* Vol. 1: Verein Deutscher Eisenhüttenleute (Ed.). Berlin: Springer, pp. 1–166.
Pitt, C. D., Rawlings, R. D. (1983), *Met. Sci. 17,* 261–266.
Polvani, R. S., Tzeng, W.-S., Strutt, P. R. (1976), *Metall. Trans. 7A,* 33–40.
Pontonnier, L., Fruchart, D., Soubeyroux, J. L., Triantafillidis, G., Berthier, Y. (1991), *J. Less-Common Met. 172–174,* 191–197.
Pope, D. P. (1991), in: *Proc. Int. Symp. on Intermetallic Compounds – Structure and Mechanical Properties* (JIMIS-6): Izumi, O. (Ed.). Sendai: The Japan Institute of Metals, pp. 301–309.
Pope, D. P., Chu, F. (1993), in: *Structural Intermetallics:* Darolia, R., Lewandowski, J. J., Liu, C. T., Martin, P. L., Miracle, D. B., Nathal, M. V. (Eds.). Warrendale, PA: TMS, pp. 637–646.
Pope, D. P., Ezz, S. S. (1984), *Int. Met. Rev. 29,* 136–167.
Porz, F., Grathwohl, G. (1984), *KfK-Nachr. 16,* 94–108.
Prado, M., Sado, M., Lovey, F. (1993), *Scr. Metall. Mater. 28,* 545–548.
Prakash, A., Pool, M. J. (1981), *J. Mater. Sci. 16,* 2495–2500.
Prakash, U., Buckley, R. A., Jones, H. (1991a), in: *High Temperature Ordered Intermetallic Alloys* IV: Johnson, L. A., Pope, D. P., Stiegler, J. O. (Eds.). Pittsburgh, PA: MRS, pp. 691–696.
Prakash, U., Buckley, R. A., Jones, H., Sellars, C. M. (1991b), *ISIJ Int. 31,* 1113–1126.
Prakash, U., Buckley, R. A., Jones, H., Greenwood, G. W. (1992), *Phil. Mag. Lett. 65,* 129–132.
Prakash, U., Buckley, R. A., Jones, H. (1993), *Mater. Sci. Technol. 9,* 16–20.
Pregger, B. A., Kircher, T., Khan, A. (1992), *Mater. Sci. Eng. A 153,* 567–572.
Pretorius, R., Chen, M.-C., Ras, H. A. (1985), *Mater. Lett. 3,* 282–286.
Pu, Z., Zhu, D., Zou, D., Zhong, Z. (1992), *Scr. Metall. Mater. 26,* 213–218.
Quyen, N. H., Paufler, P., Berthel, K.-H., Betram, M., Krämer, U., Nghiep, D. M., San Martin, A., Gladun, A., Kleinstück, K. (1979), *Phys. Status Solidi (a) 56,* 231–236.
Rachinger, W. A., Cottrell, A. H. (1956), *Acta Metall. 4,* 109–113.
Raghavan, V. (1987), in: *Phase Diagrams of Ternary Iron Alloys,* Part 1: Raghavan, V. (Ed.). Materials Park, OH: ASM.
Rahmel, A., Schwenk, W. (1977), *Korrosion und Korrosionsschutz von Stählen.* Weinheim: Verlag Chemie, pp. 193–238.
Rahmel, A., Spencer, P. J. (1991), *Oxid. Met. 35,* 53–68.
Raj, S. V. (1992), *Metall. Trans. 23A,* 1691–1704.

ArcelorMittal Ex. 2038
Page 170 of 190

Raj, S. V., Farmer, S. C. (1993), *Mater. Res. Soc. Symp. Proc. 288,* 647–652.

Raj, S. V., Noebe, R. D., Locci, I. E. (1991), in: *High Temperature Ordered Intermetallic Alloys* IV: Johnson, L. A., Pope, D. P., Stiegler, J. O. (Eds.). Pittsburgh, PA: MRS, pp. 673–678.

Raj, S. V., Hebsur, M., Locci, I. E., Doychak, J. (1992a), *J. Mater. Res. 7,* 3219–3234.

Raj, S. V., Locci, I. E., Noebe, R. D. (1992b), *Metall. Trans. 23A,* 1705–1718.

Rajkovic, M., Buckley, R. A. (1981), *Met. Sci. 15,* 21–29.

Raman, A., Schubert, K. (1965), *Z. Metallkd. 56,* 99–104.

Ramesh, R., Vasudevan, R., Pathiraj, B., Kolster, B. H. (1992), *J. Mater. Sci. 27,* 270–278.

Ranganath, S., Dutta, A., Subrahmanyam, J. (1991), *Scr. Metall. Mater. 25,* 1593–1596.

Rao, K. T. V., Odette, G. R., Ritchie, R. O. (1992), *Acta Metall. Mater. 40,* 353–361.

Rao, S. I., Dimiduk, D. M., Mendiratta, M. G. (1993), *Phil. Mag. A68,* 1233–1249.

Ratchev, P., Van Humbeeck, J., Delaey, L. (1993), *Scr. Metall. Mater. 28,* 231–234.

Ray, R., Ayer, R. (1992), *J. Mater. Sci. 27,* 1642–1650.

Raynor, G. V., Rivlin, V. G. (1983), *Int. Met. Rev. 28,* 211–227.

Reilly, J. J. (1979), *Z. Phys. Chem. N. F. 117,* 155–184.

Reip, C.-P. (1991), Dr rer. nat. Thesis, RWTH Aachen, pp. 1–118.

Reip, C.-P., Sauthoff, G. (1993), *Intermetallics 1,* 159–169.

Reuss, S., Vehoff, H. (1990), *Scr. Metall. Mater. 24,* 1021–1026.

Reuss, S., Vehoff, H. (1992), in: *Advanced Structural Materials,* Vol. 2: Clyne, T. W., Withers, P. J. (Eds.). London: The Institute of Materials, pp. 313–320.

Reviere, R. D., Noebe, R. D., Oliver, B. F. (1992), *Mater. Lett. 14,* 149–155.

Ricker, R. E., Hall, D. E., Fink, J. L. (1990), *Scr. Metall. Mater. 24,* 291–296.

Riedel, H (1982), *Met. Sci. 16,* 569–574.

Rigney, J. D., Khadikar, P. S., Lewandowski, J. J., Vedula, K. (1989), in: *High-Temperature Ordered Intermetallic Alloys* III: Liu, C. T., Taub, A. I., Stoloff, N. S., Koch, C. C. (Eds.). Pittsburgh, PA: Mater. Res. Soc., pp. 603–608.

Rigney, J. D., Lewandowski, J. J., Mason, L., Mendiratta, M. G., Dimiduk, D. M. (1991), in: *High Temperature Ordered Intermetallic Alloys* IV: Johnson, L. A., Pope, D. P., Stiegler, J. O. (Eds.). Pittsburgh, PA: MRS, pp. 1001–1006.

Rigney, J. D., Singh, P. M., Lewandowski, J. J. (1992), *J. Met. 44 (8),* 36–41.

Roberts, B. W. (1967), in: *Intermetallic Compounds:* Westbrook, J. H. (Ed.). New York: Wiley, pp. 581–613.

Roberts, C. S. (1967), in: *Intermetallic Compounds:* Westbrook, J. H. (Ed.). New York: Wiley, pp. 569–580.

Robertson, I. M. (1990), *Scr. Metall. Mater. 24,* 1947–1952.

Robertson, I. M., Wayman, C. M. (1984), *Metallography 17,* 43–55.

Rodriguez, A. B., Barth, E. P., Tien, J. K. (1991), in: *High Temperature Ordered Intermetallic Alloys* IV: Johnson, L. A., Pope, D. P., Stiegler, J. O. (Eds.). Pittsburgh, PA: MRS, pp. 539–544.

Roh, D. W., Kim, J. W., Cho, T. J., Kim, Y G. (1991), *Mater. Sci. Eng. A136,* 17–23.

Romasheva, L. F., Krentsis, R. P., Gel'd, P. V. (1980), *Sov. Phys. – Solid State 22,* 365–366.

Ronald, T. M. F. (1989), *Adv. Mater. Processes 5/89,* 29–37.

Rosenkranz, R., Frommeyer, G. (1992), *Z. Metallkd. 83,* 685–689.

Rosenkranz, R., Frommeyer, G., Smarsly, W. (1992), *Mater. Sci. Eng. A152,* 288–294.

Rösler, J., Valencia, J. J., Levi, C. G., Evans, A. G., Mehrabian, R. (1990), in: *Intermetallic Matrix Composites:* Anton, D. L., Martin, P. L., Miracle, D. B., McMeeking, R. (Eds.). Pittsburgh, PA: MRS, pp. 241–248.

Rowe, R. G. (1990), in: *High Temperature Aluminides and Intermetallics:* Whang, S. H., Liu, C. T., Pope, D. P., Stiegler, J. O. (Eds.). Warrendale, PA: TMS, pp. 375–401.

Rowe, R. G., Huang, S. C. (1988), *Isr. J. Technol. 24,* 255–259.

Rowe, R. G., Skelly, D. W. (1992), *Mater. Res. Soc. Symp. Proc. 273,* 411–416.

Rowe, R. G., Konitzer, D. G., Woodfield, A. P., Chesnutt, J. A. (1991), in: *High Temperature Ordered Intermetallic Alloys* IV: Johnson, L. A., Pope, D. P., Stiegler, J. O. (Eds.). Pittsburgh, PA: MRS, pp. 703–708.

Rudy, M. (1986), Dr. Ing. Thesis, RWTH Aachen, pp. 1–122.

Rudy, M., Sauthoff, G. (1985), in: *High-Temperature Ordered Intermetallic Alloys:* Koch, C. C., Liu, C. T., Stoloff, N. S. (Eds.). Pittsburgh, PA: MRS, pp. 327–333.

Rudy, M., Sauthoff, G. (1986), *Mater. Sci. Eng. 81,* 525–530.

Rühle, M., Evans, A. G. (1989), *Prog. Mater. Sci. 33,* 85–167.

Rusovic, N., Henig, E.-T. (1980), *Phys. Status Solidi (a) 57,* 529–540.

Rusovic, N., Warlimont, H. (1975), in: *Shape Memory Effects in Alloys:* Perkins, J. (Ed.). New York: Plenum, pp. 467–476.

Rusovic, N., Warlimont, H. (1977), *Phys. Status Solidi (a) 44,* 609–619.

Rusovic, N., Warlimont, H. (1979), *Phys. Status Solidi 53,* 283–288.

Russell, S. M., Law, C. C., Blackburn, M. J. (1989), in: *High Temperature Ordered Intermetallic Alloys* III: Liu, C. T., Taub, A. I., Stoloff, N. S., Koch, C. C. (Eds.). Pittsburgh, PA: MRS, pp. 627–632.

ArcelorMittal Ex. 2038
Page 171 of 190

Ryba, E. (1967), in: *High-Temperature Materials and Technology:* Campbell, I. E., Sherwood, E. M. (Eds.). New York: Wiley, pp. 455–484.
Saada, G., Veyssière, P. (1993a), *Mater. Res. Soc. Symp. Proc. 288,* 411–416.
Saada, G., Veyssière, P. (1993b), in: *Structural Intermetallics:* Darolia, R., Lewandowski, J. J., Liu, C. T., Martin, P. L., Miracle, D. B., Nathal, M. V. (Eds.). Warrendale, PA: TMS, pp. 379–391.
Saburi, T., Nenno, S., Yamamoto, M. (1968), *Trans. JIM 9 Supplement,* 278–283.
Saburi, T., Yoshida, M., Nenno, S. (1984), *Scr. Metall. 18,* 363–366.
Sachs, G., Weerts, J. (1931), *Z. Phys. 67,* 507–515.
Sadananda, K., Feng, C. R. (1993), *J. Met. 45(5),* 45–48.
Saeedvafa, M., Rice, J. R. (1992), *Modell. Simul. Mater. Sci. Eng. 1,* 53–71.
Sagib, M., Mehrota, G. M., Weiss, I., Beck, H., Lipsitt, H. A. (1990), *Scr. Metall. Mater. 24,* 1889–1894.
Saigal, A., Kupperman, D. S. (1991), *Scr. Metall. Mater. 25,* 2547–2552.
Sainfort, G., Mouturat, P., Pepin, P., Petit, J., Cabane, G., Salesse, M. (1963), *Mem. Sci. Rev. Metall. LX,* 125–134.
Saito, S., Ikeda, K., Ikeda, S., Nagata, A., Noto, K. (1990), *Mater. Trans. Jpn. Inst. Met. 31,* 415–420.
Saito, S., Kodama, T., Hanada, S. (1993), *Mater. Trans. Jpn. Inst. Met. 34,* 261–269.
Saka, H., Zhu, Y. M., Kawase, M., Nohara, A., Imura, T. (1985), *Phil. Mag. A 51,* 365–371.
Saka, H., Hayakawa, T., Maruyama, K., Nakamura, M., Mizutani, H., Nakamura, E. (1991), in: *Proc. Int. Symp. on Intermetallic Compounds – Structure and Mechanical Properties* (JIMIS-6): Izumi, O. (Ed.). Sendai: The Japan Institute of Metals, pp. 651–654.
Sakai, T., Hazama, T., Miyamura, H., Kuriyama, N., Kato, A., Ishikawa, H. (1991), *J. Less-Common Met. 172–174,* 1175–1184.
Sakamoto, H., Sugimoto, K., Nakamura, Y., Tanaka, A., Shimizu, K. (1991), *Mater. Trans. Jpn. Inst. Met. 32,* 128–134.
Sakamoto, K., Yoshikawa, K., Kusamichi, T., Onoye, T. (1992), *ISIJ Int. 32,* 616–624.
Sakata, T., Nishida, I. (1976), *Bull. Jpn. Inst. Met. 15,* 11–21.
Sakata, T., Tokushima, T. (1963), *Trans. Natl. Res. Inst. Met. (Jpn.) 5,* 34–48.
Sampath, S., Tiwari, R., Gudmundsson, B., Herman, H. (1991), *Scr. Metall. Mater. 25,* 1425–1430.
Samsonov, G. V., Vinitskii, I. M. (1980), *Handbook of Refractory Compounds.* New York: IFI/Plenum, pp. 1–155.
San Martin, A., Nghiep, D. M., Paufler, P., Kleinstück, K., Krämer, U., Quyen, N. H. (1980), *Scr. Metall. 14,* 1041–1045.
San Martin, A., Kleinstück, K., Quyen, N. H., Paufler, P. (1983), *Phys. Status Solidi (a) 80,* K171–K173.
Saunders, P. G., Sikka, V. K., Howell, C. R., Baldwin, R. H. (1991), *Scr. Metall. Mater. 25,* 2365–2370.
Santella, M. L. (1993), *Scr. Metall. Mater. 28,* 1305–1310.
Saule, F., Ahlers, M., Kropff, F., Rivero, E. B. (1992), *Acta Metall. Mater. 40,* 3229–3238.
Sanders, N., Chandrasekaran, L. (1992), *J. Phase Equilibria 13,* 612–619.
Sauthoff, G. (1973a), *Scr. Metall. 7,* 1041–1042.
Sauthoff, G. (1973b), *Acta Metall. 21,* 273–279.
Sauthoff, G. (1986), *Z. Metallkd. 77,* 654–666.
Sauthoff, G. (1989), *Z. Metallkd. 80,* 337–344.
Sauthoff, G. (1990a), *Z. Metallkd. 81,* 855–861.
Sauthoff, G. (1990b), in: *High-Temperature Aluminides and Intermetallics:* Whang, S. H., Liu, C. T., Pope, D. P., Stiegler, J. O. (Eds.). Warrendale, PA: TMS, pp. 329–352.
Sauthoff, G. (1991a), in: *Proc. Inst. Symp. on Intermetallic Compounds – Structure and Mechanical Properties* (JIMIS-6): Izumi, O. (Ed.). Sendai: The Japan Institute of Metals, pp. 371–378.
Sauthoff, G. (1991b), in: *Microstructure and Mechanical Properties of Materials:* Tenckhoff, E., Vöhringer, O. (Eds.). Oberursel: Deutsche Gesellschaft für Materialkunde, pp. 141–149.
Sauthoff, G. (1992), in: *Ordered Intermetallics – Physical Metallurgy and Mechanical Behaviour:* Liu, C. T., Cahn, R. W., Sauthoff, G. (Eds.). Dordrecht: Kluwer, pp. 525–539.
Sauthoff, G. (1993a), in: *Structural Intermetallics:* Darolia, R. (Ed.). Warrendale, PA: TMS, pp. 845–860.
Sauthoff, G. (1993b), in: *Diffusion in Ordered Alloys and Intermetallic Compounds:* Fultz, B., Cahn, R. W., Gupta, D. (Eds.). Warrendale, PA: TMS, pp. 205–221.
Sauthoff, G. (1994), in: *Intermetallic Compounds: Principles and Practice:* Westbrook, J. H., Fleischer, R. L. (Eds.). Chichester, UK: Wiley.
Sauthoff, G., Speller, W. (1982), *Z. Metallkd. 73,* 35–42.
Schaefer, H.-E., Sob, M., Zak, T., Yu, W. Z., Eckert, W., Banhart, F. (1990), *Phys. Rev. B41,* 11869–11874.
Schaefer, H.-E., Würschum, R., Bub, J. (1992), *Mater. Sci. Forum 105–110,* 439–450.
Schaeffer, J. C. (1993), *Scr. Metall. Mater. 28,* 791–796.
Schäfer, H., Eisenmann, B., Müller, W. (1987), *Angew. Chem. 85,* 871–875.
Schafrik, R. E. (1977), *Metall. Trans. 8A,* 1003–1006.
Schiltz, R. J., Jr., Smith, J. F. (1974), *J. Appl. Phys. 45,* 4681–4685.
Schlapbach, L., Seiler, A., Stucki, F., Zürcher, P., Fischer, P., Schefer, J. (1979), *Z. Phys. Chem. N. F. 117,* 205–220.
Schlatte, G., Pitsch, W. (1976), *Z. Metallkd. 67,* 462–466.
Schlichting, J. (1986), in: *Encyclopedia of Materials Science and Engineering,* Vol. 6: Bever, M. B. (Ed.). Oxford: Pergamon, pp. 4401–4403.

ArcelorMittal Ex. 2038
Page 172 of 190

Schmid, E. E., von Oldenburg, K., Frommeyer, G. (1990), *Z. Metallkd. 81,* 809–815.
Schmidt, B., Nagpal, P., Baker, I. (1989), in: *High-Temperature Ordered Intermetallic Alloys* III: Liu, C. T., Taub, A. I., Stoloff, N. S., Koch, C. C. (Eds.). Pittsburgh, PA: MRS, pp. 755–760.
Schmidt, P. C. (1987), *Struct. Bonding 65,* 92–133.
Schmidt, R. D., Ferris, D. P. (1975), *Wear 32,* 279–289.
Schmidt-Mende, P., Block, G. (1989), in: *The Martensitic Transformation in Science and Technology:* Hornbogen, E., Jost, N. (Eds.). Oberursel: DGM, pp. 245–248.
Schneibel, J. H., Hazzledine, P. M. (1992), in: *Ordered Intermetallics – Physical Metallurgy and Mechanical Behaviour:* Liu, C. T., Cahn, R. W., Sauthoff, G. (Eds.). Dordrecht: Kluwer, pp. 565–581.
Schneibel, J. H., Jenkins, M. G. (1993), *Scr. Metall. Mater. 28,* 389–393.
Schneibel, J. H., Petersen, G. F., Liu, C. T. (1986), *J. Mater. Res. 1,* 68–72.
Schneibel, J. H., Becher, P. F., Horton, J. A. (1988), *J. Mater. Res. 3,* 1272–1276.
Schneibel, J. H., Horton, J. A., Porter, W. D. (1992a), *Mater. Sci. Eng. A 152,* 126–131.
Schneibel, J. H., Grahle, P., Rösler, J. (1992b), *Mater. Sci. Eng. A 153,* 684–690.
Schneibel, J. H., Darolia, R., Lahrman, D. F., Schmauder, S. (1993a), *Metall. Trans. 24 A,* 1363–1371.
Schneibel, J. H., Jenkins, M. G., Maziasz, P. J. (1993b), *Mater. Res. Soc. Symp. Proc. 288,* 549–554.
Schob, O., Nowotny, H., Benesovsky, F. (1962), *Planseeber. Pulvermetall. 10,* 65–71.
Schoeck, G. (1993), *Phil. Mag. Lett. 67,* 193–201.
Schrewelius, N., Magnusson, B. (1966), *Ind. Heat. 33,* 1050–1056.
Schroeder, T. A., Cornelis, I., Wayman, C. M. (1976), *Metall. Trans. 7 A,* 535–541.
Schröer, W., Mecking, H., Hartig, C. (1991), in: *Proc. Int. Symp. on Intermetallic Compounds – Structure and Mechanical Properties* (JIMIS-6): Izumi, O. (Ed.). Sendai: The Japan Institute of Metals, pp. 567–571.
Schröer, W., Hartig, C., Mecking, H. (1993), *Z. Metallkd. 84,* 294–300.
Schubert, K. (1967), in: *Intermetallic Compounds:* Westbrook, J. H. (Ed.). New York: Wiley, pp. 100–120.
Schulson, E. M. (1984), *Int. Metals Rev. 29,* 195–209.
Schulson, E. M. (1985), in: *High-Temperature Ordered Intermetallic Alloys:* Koch, C. C., Liu, C. T., Stoloff, N. S. (Eds.). Pittsburgh, PA: Materials Research Society, pp. 193–204.
Schultz, P. A., Davenport, J. W. (1992), *Scr. Metall. Mater. 27,* 629–634.
Schultz, P. A., Davenport, J. W. (1993), *J. Alloys Compd. 197,* 229–242.
Schulze, G. E. R. (1967), *Metallphysik.* Berlin: Akademie-Verlag, pp. 1–76.
Schulze, G. E. R. (1972), in: *Reinststoffe in Wissenschaft und Technik.* Berlin: Akademie-Verlag, pp. 641–653.
Schulze, G. E. R., Paufler, P. (1972), *Abh. Sächs. Akad. Wiss. Leipzig, Math.-Naturwiss. Kl. 51 (5),* 4–24.
Schulze, G. E. R., Leitner, G., Paufler, P. (1973), in: *Redkozemelnye Metally, Splavy i Soednineniya.* Moscow: Nauka, pp. 137–142.
Schulze, K., Müller, G., Petzow, G. (1990), *J. Less-Common Met. 158,* 71–79.
Schumacher, M., Sauthoff, G. (1987), *Z. Metallkd. 78,* 582–589.
Schuster, J. C., Ipser, H. (1990), *Z. Metallkd. 81,* 389–396.
Schwartz, D. S., Lederich, R. J., Deuser, D. A. (1993), *Mater. Res. Soc. Symp. Proc. 288,* 1075–1080.
Schwarz, R. B., Desch, P. B., Srinivasan, S., Nash, P. (1992), *Nanostruct. Mater. 1,* 37–42.
Schwarzkopf, P., Kieffer, R. (1953), *Refractory Hard Metals.* New York: Macmillan, pp. 1–426.
Seeger, J., Mecking, H. (1993), *Scr. Metall. Mater. 29,* 13–18.
Segui, C., Cesari, E., Van Humbeek, J. (1991), *Mater. Trans. Jpn. Inst. Met. 32,* 898–904.
Semiatin, S. L., Nekkanti, R., Alam, M. K., McQuay, P. A. (1993), *Metall. Trans. 24 A,* 1295–1306.
Sen Gupta, R., Chatterjee, S. (1986), *J. Phys. F 16,* 733–738.
Sepiol, B., Vogl, G. (1993), *Phys. Rev. Lett. 71,* 731–734.
Sha, W., Cerezo, A., Smith, G. D. W. (1993), *Metall. Trans. 24 A,* 1251–1265.
Shaffer, P. T. B. (1964), *Materials Index.* New York: Plenum, pp. 1–740.
Shah, D. M., Anton, D. L. (1991), in: *High Temperature Ordered Intermetallic Alloys* IV: Johnson, L. A., Pope, D. P., Stiegler, J. O. (Eds.). Pittsburgh, PA: MRS, pp. 733–738.
Shah, D. M., Anton, D. L. (1992a), *Mater. Sci. Eng. A 153,* 402–409.
Shah, D. M., Anton, D. L. (1992b), *Mater. Res. Soc. Symp. Proc. 273,* 385–398.
Shah, D. M., Anton, D. L. (1993), in: *Structural Intermetallics:* Darolia, R., Lewandowski, J. J., Liu, C. T., Martin, P. L., Miracle, D. B., Nathal, M. V. (Eds.). Warrendale, PA: TMS, pp. 755–764.
Shah, D. M., Anton, D. L., Musson, C. W. (1990), in: *Intermetallic Matrix Composites:* Anton, D. L., Martin, P. L., Miracle, D. B., McMeeking, R. (Eds.). Pittsburgh, PA: MRS, pp. 333–340.
Shah, M., Pettifor, D. G. (1993), *J. Alloys Compd. 197,* 145–152.
Shan, A., Lin, D. (1992), *Scr. Metall. Mater. 27,* 95–99.
Shankar, S., Seigle, L. L. (1978), *Metall. Trans. 9 A,* 1467–1476.
Shannette, G. W., Smith, J. F. (1969), *J. Appl. Phys. 40,* 79–82.
Shao, Y., Gu, S., Chen, N. (1991), in: *Proc. Int. Symp. on Intermetallic Compounds – Structure and*

ArcelorMittal Ex. 2038
Page 173 of 190

Mechanical Properties (JIMIS-6): Izumi, O. (Ed.). Sendai: The Japan Institute of Metals, pp. 585–589.

Sharp, J. H. (1991), *Met. Mater. 7,* 349–354.

Shashikala, H. D., Suryanarayana, S. V., Murthy, K. S. N. (1989), *J. Less-Common Met. 155,* 23–29.

Shea, M., Castagne, A., Stoloff, N. S. (1991), in: *High Temperature Ordered Intermetallic Alloys* IV: Johnson, L. A., Pope, D. P., Stiegler, J. O. (Eds.). Pittsburgh, PA: MRS, pp. 609–616.

Shechtman, D., Jacobson, L. A. (1975), *Metall. Trans. 6 A,* 1325–1328.

Shechtman, D., Blackburn, M. J., Lipsitt, H. A. (1974), *Metall. Trans. 5,* 1373–1381.

Sherby, O. D., Burke, P. M. (1967), *Prog. Mater. Sci. 13,* 325–390.

Sherman, M., Vedula, K. (1986), *J. Mater. Sci. 21,* 1974–1980.

Shida, Y., Anada, H. (1993), *Mater. Trans. Jpn. Inst. Met. 34,* 236–242.

Shih, D. S., Scarr, G. K., Wasielewski, G. E. (1989), *Scr. Metall. 23,* 973–978.

Shimizu, K., Tadaki, T. (1992), *Mater. Trans. Jpn. Inst. Met. 33,* 165–177.

Shimokawa, T., Hosomi, M., Inui, H., Yamaguchi, M. (1991), in: *Proc. Int. Symp. on Intermetallic Compounds – Structure and Mechanical Properties* (JIMIS-6): Izumi, O. (Ed.). Sendai: The Japan Institute of Metals, pp. 661–665.

Shindo, D., Kikuchi, M., Hirabayashi, M., Hanada, S., Izumi, O. (1988), *Trans. JIM 29,* 956–961.

Shindo, D., Yoo, M. H., Hanada, S., Hiraga, K. (1991), *Phil. Mag. A 64,* 1281–1290.

Shirai, Y., Yamaguchi, M. (1992), *Mater. Sci. Eng. A 152,* 173–181.

Shondi, S., Hoagland, R. G., Hirth, J. P. (1992), *Mater. Sci. Eng. A 152,* 103–107.

Shull, R. D., Cline, J. P. (1990), *High Temp. Sci. 26,* 95–117.

Shyue, J., Hou, D.-H., Johnson, S., Aindow, M., Fraser, H. (1993), *Mater. Res. Soc. Symp. Proc. 288,* 573–578.

Sicking, G., Jungblut, B. (1983), *Surf. Sci. 127,* 255–270.

Sicking, G., Magomedbekov, E., Hempelmann, R. (1981), *Ber. Bunsenges. Phys. Chem. 85,* 686–692.

Sigl, L. S., Mataga, P. A., Dalgleish, B. J., McMeeking, R. M., Evans, A. G. (1988), *Acta Metall. 36,* 945–953.

Sikka, V. K. (1988), in: *2nd International SAMPE Metals and Metals Processing Conference,* Vol. 2 – *Space Age Metals Technology:* Froes, F. H., Cull, R. A. (Eds.). Covina, CA: SAMPE, pp. 62–75.

Sikka, V. K. (1989), *Mater. Manufact. Processes 4,* 1–24.

Sikka, V. K. (1990), in: *High-Temperature Aluminides and Intermetallics:* Whang, S. H., Liu, C. T., Pope, D. P., Stiegler, J. O. (Eds.). Warrendale, PA: TMS, pp. 505–520.

Sikka, V. K. (1991), in: *High Temperature Ordered Intermetallic Alloys* IV: Johnson, L. A., Pope, D. P., Stiegler, J. O. (Eds.). Pittsburgh, PA: MRS, pp. 907–912.

Sikka, V. K., Baldwin, R. H., Reinshagen, J. H., Knibloe, J., Wright, R. N. (1991), in: *High Temperature Ordered Intermetallic Alloys* IV: Johnson, L. A., Pope, D. P., Stiegler, J. O. (Eds.). Pittsburgh, PA: MRS, pp. 901–906.

Sikka, V. K., Viswanathan, S., McKamey, C. G. (1993a), in: *Structural Intermetallics:* Darolia, R., Lewandowski, J. J., Liu, C. T., Martin, P. L., Miracle, D. B., Nathal, M. V. (Eds.). Warrendale, Pa: TMS, pp. 483–491.

Sikka, V. K., Viswanathan, S., Vyas, S. (1993b), *Mater. Res. Soc. Symp. Proc. 288,* 971–976.

Silverman, R. (1956), WADC Technical Report 53–190, 1–41.

Simmons, J. P., Rao, S. I., Dimiduk, D. M. (1993), *Mater. Res. Soc. Symp. Proc. 288,* 335–342.

Singh, A., Khokle, W. S. (1987), *Phys. Status Solidi (a) 100,* K25–K29.

Sinha, A. K. (1973), *Prog. Mater. Sci. 15,* 79–181.

Sizek, H. W., Gray, G. T., III (1993), *Acta Metall. Mater. 41,* 1855–1860.

Skolozdra, R. V., Gladyshevskii, E. I., Kripyakevich, P. I. (1966a), *Ukrain. Fiz. Zhur. 11 (2),* 206–208.

Skolozdra, R. V., Gladyshevskii, E. I., Yarmolyuk, Y. P. (1966b), *Izv. Akad. Nauk SSSR, Metal. (5),* 148–151.

Slama, G., Vignes, A. (1972), *J. Less-Common Met. 24,* 189–202.

Sluiter, M., De Fontaine, D., Guo, X.-Q., Podloucky, R., Freeman, A. J. (1990), *Phys. Rev. B 42,* 10460–10476.

Sluiter, M., Turchi, P. E. A., Pinski, F. J., Stocks, G. M. (1992), *Mater. Sci. Eng. A 152,* 1–8.

Smathers, D. B. (1990), in: *Metals Handbook* – Vol. 2: *Properties and Selection: Nonferrous Alloys and Special-Purpose Materials:* Davis, J. R., Allen, P., Lampman, S. R., Zorc, T. B., Henry, S. D., Daquila, J. L., Ronke, A. W., Jakel, J., O'Keefe, K. L. (Eds.). Materials Park, OH ASM, pp. 1060–1076.

Smialek, J. L., Hehemann, R. F. (1973), *Metall. Trans. 4,* 1571–1575.

Smialek, J. L., Humphrey, D. L. (1992), *Scr. Metall. Mater. 26,* 1763–1768.

Smialek, J. L., Doychak, J., Gaydosh, D. J. (1989), in: *Oxidation of High-Temperature Intermetallics:* Grobstein, T., Doychak, J. (Eds.). Warrendale, PA: TMS, pp. 83–96.

Smialek, J. L., Doychak, J., Gaydosh, D. J. (1990a), *Oxid. Met. 34,* 259–275.

Smialek, J. L., Gedwill, M. A., Brindley, P. K. (1990b), *Scr. Metall. Mater. 24,* 1291–1296.

Smirnova, S. V., Meshkov, L. L. (1986), *Phys. Met. Metall. 61 (5),* 189–192.

Smith, L. S., Aindow, M., Loretto, M. H. (1993), *Mater. Res. Soc. Symp. Proc. 288,* 477–482.

ArcelorMittal Ex. 2038
Page 174 of 190

Smith, T. R., Kallingal, C. G., Rajan, K., Stoloff, N. S. (1992), *Scr. Metall. Mater. 27,* 1389–1393.
Snead, C. L., Jr., Bussière, J. F. (1985), *Phil. Mag. A 52,* 441–450.
Soboyejo, W. O., Venkateswara Rao, K. T., Sastry, S. M. L., Ritchie, R. O. (1993), *Metall. Trans. 24 A,* 385–600.
Somenkov, V. A., Shilstein, S. S. (1979), *Z. Phys. Chem. N. F. 117,* 125–144.
Sondhi, S., Hoagland, R. G., Hirth, J. P., Brimhall, J. L., Charlot, L. A., Bruemmer, S. M. (1993), *Mater. Res. Soc. Symp. Proc. 288,* 453–458.
Soscia, G. B., Wright, R. N. (1986), *Metall. Trans. 17 A,* 519–525.
Sowers, S., Banko, A., Bennett, D., Nesbit, S., Craft, A. (1992), *Scr. Metall. Mater. 26,* 273–276.
Sprengel, W., Denkinger, M., Mehrer, H. (1994), *Intermetallics 2,* 127–135, 137–146.
Sridharan, S., Nowotny, H. (1983), *Z. Metallkd. 74,* 468–472.
Srinivasan, S. R., Schwarz, R. B. (1992), *J. Mater. Res. 7,* 1610–1613.
Srinivasan, S. R., Schwarz, R. B., Embury, J. D. (1993), *Mater. Res. Soc. Symp. Proc. 288,* 1099–1104.
Sriram, S., Vasudevan, V. K., Dimiduk, D. M. (1993), *Mater. Res. Soc. Symp. Proc. 288,* 737–742.
Stadelmaier, H. H., Henig, E.-T., Schneider, G., Petzow, B. (1988), *Z. Metallkd. 79,* 313–319.
Stadelmaier, H. H., Henig, E.-T., Petzow, G. (1991), *Z. Metallkd. 82,* 163–168.
Stalmans, R., Van Humbeeck, J., Delaey, L. (1992a), *Acta Metall. Mater. 40,* 501–511.
Stalmans, R., Van Humbeeck, J., Delaey, L. (1992b), *Acta Metall. Mater. 40,* 2921–2931.
Stalmans, R., Van Humbeeck, J., Delaey, L. (1992c), *Mater. Trans. Jpn. Inst. Met. 33,* 289–293.
Steinhorst, M. (1989), Dr.-Ing. Thesis, Universität Dortmund.
Steinhorst, M. (1992), *J. Alloys Compd. 186,* 177–185.
Steinhorst, M., Grabke, H. J. (1989), *Mater. Sci. Eng. A 120,* 55–59.
Steinhorst, M., Grabke, H. J. (1990), *Z. Metallkd. 81,* 732–738.
Stekly, J., Gregory, E. (1994), in: *Intermetallic Compounds: Principles and Practice,* Vol. 2: Westbrook, J. H., Fleischer, R. L. (Eds.). Chichester, UK: Wiley, in press.
Stepanov, A. P., Skripov, A. B. (1982), *Phys. Met. Metall. 53 (6),* 166–168.
Stephens, J. R. (1985), in: *High-Temperature Ordered Intermetallic Alloys:* Koch, C. C., Liu, C. T., Stoloff, N. S. (Eds.). Pittsburgh, PA: MRS, pp. 381–395.
Stephens, J. R. (1990), *Adv. Mater. Processes 4/90,* 35–38.
Stöckel, D. (1989), in: *The Martensitic Transformation in Science and Technology:* Hornbogen, E., Jost, N. (Eds.). Oberursel: DGM, pp. 223–230.
Stocks, G. M., Nicholson, D. M., Pinski, F. J., Butler, W. H., Sterne, P., Temmerman, T. M., Györffy, B. L., Johnson, D. D., Gonis, A., Zhang, X.-G., Turchi, P. E. A. (1987), in: *High-Temperature Ordered Intermetallic Alloys* II: Stoloff, N. S., Koch, C. C., Liu, C. T., Izumi, O. (Eds.). Pittsburgh, PA: MRS, pp. 15–26.
Stocks, G. M., Shelton, W. A., Nicholson, D. M., Pinski, F. J., Ginatempo, B., Barbieri, A., Györffy, B. L., Johnson, D. D., Staunton, J. B., Turchi, P. E. A., Sluiter, M. (1992), in: *Ordered Intermetallics – Physical Metallurgy and Mechanical Behaviour:* Liu, C. T., Cahn, R. W., Sauthoff, G. (Eds.). Dordrecht: Kluwer, pp. 15–36.
Stoeckel, D. (1990), *Adv. Mater. Processes 10/90,* 33–42.
Stoloff, N. S. (1984), *Int. Metals. Rev. 29,* 123–135.
Stoloff, N. S. (1989), *Int. Mater. Rev. 34,* 153–183.
Stoloff, N. S. (1992), in: *Ordered Intermetallics – Physical Metallurgy and Mechanical Behaviour:* Liu, C. T., Cahn, R. W., Sauthoff, G. (Eds.). Dordrecht: Kluwer, pp. 257–277.
Stoloff, N. S., Davies, R. G. (1964), *Acta Metall. 12,* 473–485.
Stoloff, N. S., Davies, R. G. (1966), *Prog. Mater. Sci. 13,* 3–84.
Stoloff, N. S., Duquette, D. J. (1993), *J. Met. 45 (12),* 30–35.
Stoloff, N. S., Choe, S. J., Rajan, K. (1992), *Scr. Metall. Mater. 26,* 331–336.
Stoloff, N. S., Smith, T. R., Castagna, A. (1993), *Mater. Res. Soc. Symp. Proc. 288,* 59–70.
Stonehouse, A. J., Marder, J. M. (1990), in: *Metals Handbook,* Vol. 2 – *Properties and Selection: Nonferrous Alloys and Special Purpose Materials:* Davis, J. R., Allen, P., Lampman, S. R., Zorc, T. B., Henry, S. D., Daquila, J. L., Ronke, A. W., Jakel, J., O'Keefe, K. L. (Eds.). Materials Park, OH: ASM, pp. 683–687.
Stonehouse, A. J., Paine, R. M., Beaver, W. W. (1960), in: *Mechanical Properties of Intermetallic Compounds:* Westbrook, J. H. (Ed.). New York: Wiley, pp. 297–319.
Stoner, S. L., Oliver, W. C. Mukherjee, A. K. (1992), *Mater. Sci. Eng. A 153,* 465–469.
Strangwood, M., Bennett, M. J., Hippsley, C. A., Tweed, J. H. (1992), in: *Advanced Structural Materials,* Vol. 2: Clyne, T. W., Withers, P. J. (Eds.). London: The Institute of Materials, pp. 340–348.
Strnat, K. J. (1990), *Proc. IEEE 78,* 923–946.
Strum, M. J., Henshall, G. A. (1993), *Mater. Res. Soc. Symp. Proc. 288,* 1093–1098.
Strutt, P. R., Dodd, R. A. (1970), in: *Ordered Alloys – Structural Applications and Physical Metallurgy:* Kear, B. H., Sims, C. T., Stoloff, N. S., Westbrook, J. H. (Eds.). Baton Rouge, LA: Claitor's Publ. Div., pp. 475–504.
Strutt, P. R., Kear, B. H. (1985), in: *High-Temperature Ordered Intermetallic Alloys:* Koch, C. C., Liu, C. T., Stoloff, N. S. (Eds.). Pittsburgh, PA: MRS, pp. 279–292.

ArcelorMittal Ex. 2038
Page 175 of 190

Strutt, P. R., Polvani, R. S. (1973), *Scr. Metall. 7,* 1221–1226.
Strutt, P. R., Polvani, R. S., Ingram, J. C. (1976), *Metall. Trans. 7A,* 23–31.
Stucke, M. A., Dimiduk, D. M., Hazzledine, P. M. (1993), *Mater. Res. Soc. Symp. Proc. 288,* 471–476.
Subrahmanyam, J., Annapurna, J. (1986), *Oxid. Met. 26,* 275–294.
Subramanian, P. R., Simmons, J. P. (1991), *Scr. Metall. Mater. 25,* 231–236.
Subramanian, P. R., Mendiratta, M. G., Miracle, D. B., Dimiduk, D. M. (1990a), in: *Intermetallic Matrix Composites:* Anton, D. L., Martin, P. L., Miracle, D. B., McMeeking, R. (Eds.). Pittsburgh, PA: MRS, pp. 147–154.
Subramanian, P. R., Miracle, D. B., Mazdiyasni, S. (1990b), *Metall. Trans. 21A,* 539–545.
Suganuma, K. (1993), *J. Alloys Compd. 197,* 29–34.
Sun, J., Lin, D. (1993), *Mater. Res. Soc. Symp. Proc. 288,* 349–354.
Sun, Z. Q., Huang, Y. D., Yang, W. Y., Chen, G. L. (1993), *Mater. Res. Soc. Symp. Proc. 288,* 885–890.
Suryanarayana, C., Froes, F. H., Rowe, R. G. (1991), *Int. Mater. Rev. 36,* 85–123.
Suyama, R., Hashimoto, K. (1992), in: *Basic Technologies for Future Industries: The 3rd Symposium on High-Performance Materials for Severe Environments:* RIMCOF (Ed.). Tokyo: Japan Industrial Technology Association (JITA), pp. 141–149.
Suyama, R., Kimura, M., Hashimoto, K. (1993), in: *Structural Intermetallics:* Darolia, R., Lewandowski, J. J., Liu, C. T., Martin, P. L., Miracle, D. B., Nathal, M. V. (Eds.). Warrendale, PA: TMS, pp. 681–689.
Suzuki, K., Lin, X. (1993), *J. Alloys Compd. 193,* 7–10.
Suzuki, K., Takeuchi, S. (1993), *Intermetallics 1,* 21–27.
Suzuki, M., Nutt, S. R., Aikin, R. M., Jr. (1992), *Mater. Res. Soc. Symp. Proc. 273,* 267–274.
Suzuki, T., Mishima, Y., Miura, S. (1989), *ISIJ Int. 29,* 1–23.
Suzuki, T., Goto, M., Yoshihara, M., Tanaka, R. (1991), *Mater. Trans. Jpn. Inst. Met. 32,* 1017–1023.
Svedberg, R. C. (1976), in: *Properties of High Temperature Alloys:* Foroulis, Z. A., Pettit, F. S. (Eds.). Princeton: The Electrochemical Society, pp. 331–362.
Szaruga, A., Rothenflue, L., Srinivasan, R., Lipsitt, H. A. (1992), *Scr. Metall. Mater. 26,* 1565–1570.
Tachikawa, K., Terada, M., Endo, M. (1992), *Sci. Rep. Tohoku Univ. 37,* 1, 108–115.
Tadaki, T., Takamori, M., Shimizu, K. (1987), *Trans. JIM 28,* 120–128.
Takahashi, S., Umakoshi, Y. (1991), in: *Proc. Int. Symp. on Intermetallic Compounds – Structure and Mechanical Properties* (JIMIS-6): Izumi, O. (Ed.). Sendai: The Japan Institute of Metals, pp. 93–97.
Takahashi, T., Oikawa, H. (1991), in: *High Temperature Ordered Intermetallic Alloys* IV: Johnson, L. A., Pope, D. P., Stiegler, J. O. (Eds.). Pittsburgh, PA: MRS, pp. 721–726.
Takasugi, T. (1991a), in: *High Temperature Ordered Intermetallic Alloys* IV: Johnson, L. A., Pope, D. P., Stiegler, J. O. (Eds.). Pittsburgh, PA: MRS, pp. 403–416.
Takasugi, T. (1991b), *Acta Metall. Mater. 39,* 2157–2167.
Takasugi, T. (1991c), in: *Proc. Int. Symp. on Intermetallic Compounds – Structure and Mechanical Properties* (JIMIS-6): Izumi, O. (Ed.). Sendai: The Japan Institute of Metals, pp. 713–718.
Takasugi, T., Izumi, O. (1985a), *Acta Metall. 33,* 33–38.
Takasugi, T., Izumi, O. (1985b), *Acta Metall. 33,* 39–48.
Takasugi, T., Izumi, O. (1985c), *Acta Metall. 33,* 49–58.
Takasugi, T., Izumi, O. (1985d), *Acta Metall. 33,* 1247–1258.
Takasugi, T., Izumi, O. (1986), *Acta Metall. 34,* 607–618.
Takasugi, T., Izumi, O. (1988), *J. Mater. Sci. 23,* 1265–1273.
Takasugi, T., Izumi, O. (1992), in: *Ordered Intermetallics – Physical Metallurgy and Mechanical Behaviour:* Liu, C. T., Cahn, R. W., Sauthoff, G. (Eds.). Dordrecht: Kluwer, pp. 391–411.
Takasugi, T., Yoshida, M. (1991a), *J. Mater. Sci. 26,* 3032–3040.
Takasugi, T., Yoshida, M. (1991b), *J. Mater. Sci. 26,* 3517–3525.
Takasugi, T., Yoshida, M. (1992), *Phil. Mag. A65,* 613–624.
Takasugi, T., Yoshida, M. (1993), *Phil. Mag. A67,* 447–462.
Takasugi, T., Hirakawa, S., Izumi, O., Ono, S., Watanabe, S. (1987), *Acta Metall. 35,* 2015–2026.
Takasugi, T., Takazawa, M., Izumi, O. (1990a), *J. Mater. Sci. 25,* 4226–4230.
Takasugi, T., Takazawa, M., Izumi, O. (1990b), *J. Mater. Sci. 25,* 4231–4238.
Takasugi, T., Tsurisaki, K., Izumi, O., Ono, S. (1990c), *Phil. Mag. A61,* 785–800.
Takasugi, T., Izumi, O., Yoshida, M. (1991a), *J. Mater. Sci. 25,* 2941–2948.
Takasugi, T., Izumi, O., Yoshida, M. (1991b), *J. Mater. Sci. 26,* 1173–1178.
Takasugi, T., Rikukawa, S., Hanada, S. (1991c), *Scr. Metall. Mater. 25,* 889–894.
Takasugi, T., Suenaga, H., Izumi, O. (1991d), *J. Mater. Sci. 26,* 1179–1186.
Takasugi, T., Yoshida, M., Hanada, S. (1991e), in: *Proc. Int. Symp. on Intermetallic Compounds – Structure and Mechanical Properties* (JIMIS-6): Izumi, O. (Ed.). Sendai: The Japan Institute of Metals, pp. 615–620.

ArcelorMittal Ex. 2038
Page 176 of 190

Takasugi, T., Rikukawa, S., Hanada, S. (1992a), *Acta Metall. Mater. 40,* 1895–1906.
Takasugi, T., Yoshida, M., Kawabata, T. (1992b), *Phil. Mag. A65,* 29–40.
Takasugi, T., Kishino, J., Hanada, S. (1993a), *Mater. Res. Soc. Symp. Proc. 288,* 459–464.
Takasugi, T., Kishino, J., Hanada, S. (1993b), *Acta Metall. Mater. 41,* 1009–1020.
Takasugi, T., Kishino, J., Hanada, S. (1993c), *Acta Metall. Mater. 41,* 1021–1031.
Takeuchi, S., Hashimoto, T., Shibuya, T. (1991), in: *Proc. Int. Symp. on Intermetallic Compounds – Structure and Mechanical Properties* (JIMIS-6): Izumi, O. (Ed.). Sendai: The Japan Institute of Metals, pp. 645–649.
Takeuchi, S., Hashimoto, T., Shibuya, T. (1992), *J. Mater. Sci. 27,* 1380–1384.
Takeyama, M., Liu, C. T. (1991), *Mater. Sci. Eng. A132,* 61–66.
Takeyama, M., Liu, C. T. (1992), *Mater. Sci. Eng. A153,* 538–547.
Takeyama, M., Liu, C. T., Sparks, C. J., Jr. (1991), in: *Proc. Int. Symp. on Intermetallic Compounds – Structure and Mechanical Properties* (JIMIS-6): Izumi, O. (Ed.). Sendai: The Japan Institute of Metals, pp. 871–875.
Takeyama, M., Kumagai, T., Nakamura, M., Kikuchi, M. (1993), in: *Structural Intermetallics:* Darolia, R., Lewandowski, J. J., Liu, C. T., Martin, P. L., Miracle, D. B., Nathal, M. V. (Eds.). Warrendale, PA: TMS, pp. 167–176.
Tammann, G. (1903), *Z. Anorg. Chem. 37,* 303–313.
Tammann, G. (1906), *Z. Anorg. Chem. 49,* 113–121.
Tammann, G. (1932), *Lehrbuch der Metallkunde.* Leipzig: Leopold Voss, pp. 1–536.
Tammann, G., Dahl, K. (1923), *Z. Anorg. Chem. 126,* 104–112.
Tamura, K. (1961), *J. Jpn. Soc. Powder Metall. 8,* 113–120.
Tan, Y., Shinoda, T., Mishima, Y., Suzuki, T. (1993), *Mater. Res. Soc. Symp. Proc. 288,* 757–762.
Taniguchi, S., Shibata, T. (1987), *Oxid. Met. 28,* 155–164.
Taniguchi, S., Shibata, T. (1989), in: *Oxidation of High-Temperature Intermetallics.* Grobstein, T., Doychak, J. (Eds.). Warrendale, PA: TMS, pp. 17–30.
Taniguchi, S., Shibata, T., Itoh, S. (1991a), *Mater. Trans. Jpn. Inst. Met. 32,* 151–156.
Taniguchi, S., Shibata, T., Takeuchi, K. (1991b), *Mater. Trans. Jpn. Inst. Met. 32,* 299–301.
Tanner, L. E., Pelton, A. R., VanTendeloo, G., Schryvers, D., Wall, M. E. (1990), *Scr. Metall. Mater. 24,* 1731–1736.
Tassa, O., Testani, C., Lecoze, J., Lefort, A. (1991), in: *Proc. Int. Symp. on Intermetallic Compounds – Structure and Mechanical Properties* (JIMIS-6): Izumi, O. (Ed.). Sendai: The Japan Institute of Metals, pp. 573–577.
Tawancy, H. M. (1991), *Metall. Trans. 22A,* 3067–3071.
Thier, M. (1989), in: *The Martensitic Transformation in Science and Technology:* Hornbogen, E., Jost, N. (Eds.). Oberursel: DGM, pp. 353–360.
Thom, A. J., Kim, Y., Akinc, M. (1993), *Mater. Res. Soc. Symp. Proc. 288,* 1037–1042.
Thoma, D. J., Perepezko, J. H. (1990), in: *Intermetallic Matrix Composites:* Anton, D. L., Martin, P. L., Miracle, D. B., McMeeking, R. (Eds.). Pittsburgh, PA: MRS, pp. 105–112.
Thomas, O., Madar, R., Senateur, J. P., Laborde, O. (1987), *J. Less-Common Met. 136,* 175–182.
Thompson, A. W. (1992), *Mater. Sci. Eng. A153,* 578–583.
Thompson, A. W. (1993), *Mater. Res. Soc. Symp. Proc. 288,* 947–952.
Thompson, A. W., Pollock, T. M. (1991), *ISIJ Int. 31,* 1139–1146.
Thornton, P. H., Davies, R. G., Johnston, T. L. (1970), *Metall. Trans. 1,* 207–218.
Threadgill, P. L., Baeslack III, W. A. (1991), in: *Proc. Int. Symp. on Intermetallic Compounds – Structure and Mechanical Properties* (JIMIS-6): Izumi, O. (Ed.). Sendai: The Japan Institute of Metals, pp. 1021–1025.
Tichelaar, F. D., Schapink, F. W. (1991), *Phil. Mag. A63,* 207–224.
Tichelaar, F. D., Schapink, F. W., Li, X. (1992), *Phil. Mag. A65,* 913–929.
Tien, J. K., Vignoul, G. E., Barth, E. P., Kopp, M. W. (1992), in: *Structural and Phase Stability of Alloys:* Morán-López, J. L. (Ed.). New York: Plenum, pp. 1–17.
Ting, J.-M. (1993), *Scr. Metall. Mater. 29,* 677–682.
Tiwari, R., Herman, H., Sampath, S. (1991), in: *High Temperature Ordered Intermetallic Alloys* IV: Johnson, L. A., Pope, D. P., Stiegler, J. O. (Eds.). Pittsburgh, PA: MRS, pp. 807–813.
Togano, K., Kumakura, H., Takeuchi, T., Tachikawa, K. (1992). *Sci. Rep. Tohoku Univ. 37,* 1, 18–25.
Tokizane, M., Fukami, T., Inaba, T. (1991), *ISIJ Int. 31,* 1088–1092.
Tolpygo, V. K., Grabke, H. J. (1993), *Scr. Metall. Mater. 28,* 747–752.
Tomizuka, I. (1992), in: *Basic Techologies for Future Industries: The 3rd Symposium on High-Performance Materials for Severe Environments:* RIMCOF (Ed.). Tokyo: Japan Industrial Technology Association (JITA), pp. 133–140.
Tortorelli, P. F., DeVan, J. H. (1992), *Mater. Sci. Eng. A153,* 573–577.
Tortorelli, P. F., DeVan, J. H., McKamey, C. G., Howell, M. (1990), in: *Intermetallic Matrix Composites:* Anton, D. L., Martin, P. L., Miracle, D. B., McMeeking, R. (Eds.). Pittsburgh, PA: MRS, pp. 361–366.
Triantafillidis, G., Pontonnier, L, Fruchart, D., Wolfers, P., Soubeyroux, J. L. (1991), *J. Less-Common Met. 172–174,* 183–190.
Trumble, K. P., Rühle, M. (1990), *Z. Metallkd. 81,* 749–755.

ArcelorMittal Ex. 2038
Page 177 of 190

Tsau, C. H., Jang, J. S. C., Yeh, J. W. (1992), *Mater. Sci. Eng. A 152,* 264–268.

Tsuchida, K., Tsudo, H., Kato, A. (1989), *J. Mater. Sci. Lett. 7,* 1269–1270.

Tsujimoto, T., Hashimoto, K. (1989), in: *High-Temperature Ordered Intermetallic Alloys* III: Liu, C. T., Taub, A. I., Stoloff, N. S., Koch, C. C. (Eds.). Pittsburgh, PA: MRS, pp. 391–396.

Tsujimoto, T., Hashimoto, K., Nobuki, M. (1992), *Mater. Trans. Jpn. Inst. Met. 33,* 989–1003.

Tu, K. N., Hammer, W. N., Olowolafe, J. O. (1980), *J. Appl. Phys. 51,* 1663–1668.

Tu, K. N., Ottaviani, G., Gösele, U., Föll, H. (1983), *J. Appl. Phys. 54,* 758–763.

Turchi, P. E. A., Finel, A. (1991), *J. Less-Common Met. 168,* 103–113.

Turchi, P. E. A., Sluiter, M., Pinski, F. J., Johnson, D. D., Stocks, G. M. (1991), in: *Proc. Int. Symp. on Intermetallic Compounds – Structure and Mechanical Properties* (JIMIS-6): Izumi, O. (Ed.). Sendai: The Japan Institute of Metals, pp. 215–219.

Uchida, H., Ohtani, Y., Ozawa, M., Kawahata, T., Suzuki, T. (1991), *J. Less-Common Met. 172–174,* 983–996.

Uchida, M., Bjurström, H., Suda, S., Matsubara, Y. (1986), *J. Less-Common Met. 119,* 63–74.

Uenishi, K., Sugimoto, A., Kobayashi, K. F. (1992), *Z. Metallkd. 83,* 241–245.

Ullrich, H.-J., Reinhold, U., Däbritz, S., Paufler, P., Kleinstück, K., Pietrass, B. (1978), *Phys. Status Solidi (a) 49,* 323–330.

Ulvensoen, J. H., Rorvik, G., Kyvik, T., Pettersen, K., L'Estrade, L. (1993), in: *Structural Intermetallics:* Darolia, R., Lewandowski, J. J., Liu, C. T., Martin, P. L., Miracle, D. B., Nathal, M. V. (Eds.). Warrendale, PA: TMS, pp. 707–713.

Umakoshi, Y., Nakano, T. (1993), *Acta Metall. Mater. 41,* 1155–1161.

Umakoshi, Y., Yamaguchi, M. (1980), *Phil. Mag. 41,* 573–588.

Umakoshi, Y., Yamaguchi, M. (1981), *Phil. Mag. A 44,* 711–715.

Umakoshi, Y., Yamaguchi, M., Yamane, T. (1985), *Phil. Mag. A 52,* 357–367.

Umakoshi, Y., Yamaguchi, M., Yamane, T. (1986), *Phil. Mag. A 53,* 221–232.

Umakoshi, Y., Yamaguchi, M., Yamane, T., Hirano, T. (1988), *Phil. Mag. A 58,* 651–666.

Umakoshi, Y., Yamaguchi, M., Sakagami, T., Yamane, T. (1989), *J. Mater. Sci. 24,* 1599–1603.

Umakoshi, Y., Hirano, T., Sakagami, T., Yamane, T. (1990a), in: *High-Temperature Aluminides and Intermetallics:* Whang, S. H., Liu, C. T., Pope, D. P., Stiegler, J. O. (Eds.). Warrendale, PA: TMS, pp. 111–129.

Umakoshi, Y., Sakagami, T., Hirano, T., Yamane, T. (1990b), *Acta Metall. Mater. 38,* 909–915.

Umakoshi, Y., Nakashima, T., Yamane, T., Senba, H. (1991), in: *Proc. Int. Symp. on Intermetallic Compounds – Structure and Mechanical Properties* (JIMIS-6): Izumi, O. (Ed.). Sendai: The Japan Institute of Metals, pp. 639–643.

Umakoshi, Y., Nakano, T., Yamane, T. (1992), *Mater. Sci. Eng. A 152,* 81–88.

Umakoshi, Y., Nakano, T., Sumimoto, K., Maeda, Y. (1993a), *Mater. Res. Soc. Symp. Proc. 288,* 441–446.

Umakoshi, Y., Nakano, T., Takenaka, T., Sumimoto, K., Yamane, T. (1993b), *Acta Metall. Mater. 41,* 1149–1154.

Urwank, P., Wieser, E., Hässner, A., Kaufmann, C., Lippmann, H., Melzer, I. (1985), *Phys. Status Solidi (a) 90,* 463–469.

Valiev, R. Z., Gayanov, R. M., Yang, H. S., Mukherjee, A. K. (1991), *Scr. Metall. Mater. 25,* 1945–1950.

van der Straten, J. M., Bastin, G. F., van Loo, F. J. J., Rieck, G. D. (1976), *Z. Metallkd. 67,* 152–157.

Van Humbeek, J., Delaey, L. (1989), in: *The Martensitic Transformation in Science and Technology:* Hornbogen, E., Jost, N. (Eds.). Oberursel: DGM, pp. 15–25.

van Loo, F. J. J., Rieck, G. D. (1973), *Acta Metall. 21,* 61–71.

Vanderschaeve, G., Sarrazin, T., Escaig, B. (1979), *Acta Metall. 27,* 1251–1260.

Vandervoort, R. R., Mukherjee, A. K., Dorn, J. E. (1966), *Trans. ASM 59,* 930–944.

Varin, R. A., Winnicka, M. B., Virk, I. S. (1993), in: *Structural Intermetallics:* Darolia, R., Lewandowski, J. J., Liu, C. T., Martin, P. L., Miracle, D. B., Nathal, M. V. (Eds.). Warrendale, PA: TMS, pp. 117–124.

Vedula, K. (1989), *Mater. Manuf. Processes 4,* 39–59.

Vedula, K. (1991), in: *Proc. Int. Symp. on Intermetallic Compounds – Structure and Mechanical Properties* (JIMIS-6): Izumi, O. (Ed.). Sendai: The Japan Institute of Metals, pp. 901–926.

Vedula, K., Stephens, J. R. (1987a), in: *High-Temperature Ordered Intermetallic Alloys* II: Stoloff, N. S., Koch, C. C., Liu, C. T., Izumi, O. (Eds.). Pittsburgh, PA: Mater. Res. Soc. pp. 381–391.

Vedula, K., Stephens, J. R. (1987b), *Met. Powder Rep. 42 (2),* 84–91.

Vedula, K., Pathare, V., Aslanidis, I., Titran, R. H. (1985), in: *High-Temperature Ordered Intermetallic Alloys:* Koch, C. C., Liu, C. T., Stoloff, N. S. (Eds.). Pittsburgh, PA: Materials Research Society, pp. 411–421.

Vehoff, H. (1992), in: *Ordered Intermetallics – Physical Metallurgy and Mechanical Behaviour:* Liu, C. T., Cahn, R. W., Sauthoff, G. (Eds.). Dordrecht: Kluwer, pp. 299–320.

Vehoff, H. (1993), *Mater. Res. Soc. Symp. Proc. 288,* 71–82.

Vehoff, H., Reuss, S., Vogt, W., Specht, P. (1993), in: *Structural Intermetallics:* Darolia, R., Lewandowski, J. J., Liu, C. T., Martin, P. L., Miracle, D. B., Nathal, M. V. (Eds.). Warrendale, PA: TMS, pp. 657–663.

ArcelorMittal Ex. 2038
Page 178 of 190

Venkkateswara, Rao, K. T., Soboyejo, W. O., Ritchie, R. O. (1992), *Metall. Trans. 23A,* 2249–2257.

Vennégues, P., Cadeville, M. C., Pierron-Bohnes, V., Afyouni, M. (1990), *Acta Metall. Mater. 38,* 2199–2213.

Verhoeven, J. D., Lee, J. H., Laabs, F. C., Jones, L. L. (1991), *J. Phase Equilibria 12,* 15–23.

Verlinden, B., Delaey, L. (1988a), *Acta Metall. 36,* 1771–1779.

Verlinden, B., Delaey, L. (1988b), *Metall. Trans. 19A,* 207–216.

Veyssière, P. (1991), *ISIJ Int. 31,* 1028–1048.

Veyssière, P. (1992), in: *Ordered Intermetallics – Physical Metallurgy and Mechanical Behaviour:* Liu, C. T, Cahn, R. W., Sauthoff, G. (Eds.). Dordrecht: Kluwer, pp. 165–175.

Veyssière, P., Noebe, R. (1992), *Phil. Mag. A65,* 1–13.

Vidoz, A. E., Lazarevic, D. P., Cahn, R. W. (1963), *Acta Metall. 11,* 17–33.

Vignoul, G. E., Sanchez, J. M., Tien, J. K. (1991), in: *High Temperature Ordered Intermetallic Alloys* IV: Johnson, L. A., Pope, D. P., Stiegler, J. O. (Eds.). Pittsburgh, PA: MRS, pp. 739–744.

Villars, P., Calvert, L. D. (1991), *Pearson's Handbook of Crystallographic Data for Intermetallic Phases.* Materials Park, OH: ASM.

Villars, P., Mathis, K., Hulliger, F. (1989), in: *The Structures of Binary Compounds:* de Boer, F. R., Pettifor, D. G. (Eds.). Amsterdam: North-Holland, pp. 1–104.

Vincent, M., Wachtel, E., Predel, B. (1988), *Z. Metallkd. 79,* 330–335, 416.

Virk, I. S., Varin, R. A. (1992), *Metall. Trans. 23A,* 617–625.

Viswanadham, R. K., Whittenberger, J. D., Mannan, S. K., Sprissler, B. (1988), in: *High Temperature/High Performance Composites:* Lemkey, F. D., Fishman, S. G., Evans, A. G., Strife, J. R. (Eds.). Pittsburgh, PA: MRS, pp. 89–94.

Viswanathan, S., Shelton, B. R., Wright, J. K., Sikka, V. K. (1993), *Scr. Metall. Mater. 29,* 589–594.

Vogl, G., Sepiol, B. (1994), *Acta Metall. Mater.,* in press.

Von Keitz, A., Sauthoff, G. (1991), poster at the 10th Int. Conf. on Solid Compounds of Transition Elements, Münster.

Von Keitz, A., Sauthoff, G. (1992), presentation at the DGM Annual Meeting, Hamburg.

von Mises, R. (1928), *Z. Angew. Math. Mech. 8,* 161–185.

von Oldenburg, K., Frommeyer, G., Schmid, E., Henning, W. (1990), in: *Advanced Aluminium and Magnesium Alloys:* Khan, T., Effenberg, G. (Eds.). Materials Park, OH: ASM Int., pp. 477–484.

Vyas, S., Viswanathan, S., Sikka, V. K. (1992), *Scr. Metall. Mater. 27,* 185–190.

Wachtel, E., Bahle, J. (1987), *Z. Metallkd. 78,* 229–232.

Wagner, R., Es-Souni, M., Chen, D., Dogan, B., Seeger, J., Beaven, P. A. (1991), in: *High Temperature Ordered Intermetallic Alloys* IV: Johnson, L. A., Pope, D. P., Stiegler, J. O. (Eds.). Pittsburgh, PA: MRS, pp. 1007–1012.

Wakao, S., Sawa, H., Furukawa, J. (1991), *J. Less-Common Met. 172–174,* 1219–1226.

Wallace, W. E., Craig, R. S. (1967), in: *Phase Stability in Metals and Alloys:* Rudman, P. S., Stringer, J., Jaffee, R. I. (Eds.). New York: McGraw-Hill, pp. 255–272.

Wallow, F., Neite, G., Schröer, W., Nembach, E. (1987), *Phys. Status Solidi (a) 99,* 483–490.

Walston, W. S., Darolia, R. (1993), *Mater. Res. Soc. Symp. Proc. 288,* 237–242.

Walston, W. S., Field, R. D., Dobbs, J. R., Lahrman, D. F., Darolia, R. (1993), in: *Structural Intermetallics:* Darolia, R., Lewandowski, J. J., Liu, C. T., Martin, P. L., Miracle, D. B., Nathal, M. V. (Eds.). Warrendale, PA: TMS, pp. 523–532.

Walter, J. L., Cline, H. E. (1970), *Metall. Trans. 1,* 1221–1229.

Wan, X. J., Zhu, J. H., Jing, K. L. (1992a), *Scr. Metall. Mater. 26,* 473–477.

Wan, X. J., Zhu, J. H., Jing, K. L. (1992b), *Scr. Metall. Mater. 26,* 479–484.

Wang, C. C., Akbar, S. A. (1993), in: *Diffusion in Ordered Alloys and Intermetallic Compounds:* Fultz, B., Cahn, R. W., Gupta, D. (Eds.). Warrendale, PA: TMS, pp. 3–20.

Wang, L., Arsenault, R. J. (1991), *Metall. Trans. 22A,* 3013–3018.

Wang, W. K., Wang, Y. J., He, S. A., Iwasaki, H. (1988), *Z. Phys. B69,* 481–484.

Warlimont, H., Delaey, L., Krishnan, R. V., Tas, H. (1974), *J. Mater. Sci. 9,* 1545–1555.

Wasilewski, R. J. (1966), *Trans. AIME 236,* 455–457.

Watanabe, K. (1991), *Mater. Trans. Jpn. Inst. Met. 32,* 292–298.

Watanabe, S., Nakamura, Z., Hanada, S., Sato, T., Izumi, O. (1984), *Trans. JIM 25,* 477–486.

Watari, T., Takasu, T., Shirouzu, K., Kato, A. (1986), *J. Mater. Sci. Lett. 5,* 179–180.

Waterstrat, R. M. (1990), *J. Met. 42(3),* 8–14.

Waterstrat, R. M., Okabe, T. (1994), in: *Intermetallic Compounds: Principles and Practice,* Vol. 2: Westbrook, J. H., Fleischer, R. L. (Eds.). Chichester, UK: Wiley, in press.

Watson, R. E., Bennet, L. H. (1984), *Acta Metall. 32,* 477–489.

Watson, R. E., Bennet, L. H. (1985), *Scr. Metall. 19,* 535–538.

Watts, D. C. (1992), in: *Materials Science and Technology,* Vol. 14: *Medical and Dental Materials:* Williams, D. F. (Ed.). Weinheim: VCH, pp. 211–258.

Weatherill, A. E., Gill, B. J. (1988), *Met. Mater. 4,* 551–555.

Weaver, M. L., Guy, S. L., Stone, R. K., Kaufman, M. J. (1991), in: *High Temperature Ordered Inter-*

ArcelorMittal Ex. 2038
Page 179 of 190

metallic Alloys IV: Johnson, L. A., Pope, D. P., Stiegler, J. O. (Eds.). Pittsburgh, PA: MRS, pp. 163–168.
Webb, G., De Bussac, A., Antolovich, S. D. (1993a), *Metall. Trans. 24A*, 397–401.
Webb, G., Juliet, P., Lefort, A. (1993b), *Scr. Metall. Mater. 28*, 769–772.
Weber, C. H., Yang, J. Y., Löfvander, J. P. A., Levi, C. G., Evans, A. G. (1993), *Acta Metall. Mater. 41*, 2681–2690.
Wehrmann, R. (1956), in: *High-Temperature Technology:* Campbell, I. E. (Ed.). New York: Wiley, pp. 151–170.
Wehrmann, R. (1967), in: *High-Temperature Materials and Technologies:* Campbell, I. E., Sherwood, E. M. (Eds.). New York: Wiley, pp. 399–430.
Wein, M., Levin, L., Nadiv, S. (1978), *Phil. Mag. A38*, 81–96.
Welsch, G., Kahveci, A. I. (1989), in: *Oxidation of High-Temperature Intermetallics:* Grobstein, T., Doychak, J. (Eds.). Warrendale, PA: TMS, pp. 207–218.
Wernick, J. H. (1967), in: *Intermetallic Compounds:* Westbrook, J. H. (Ed.). New York: Wiley, pp. 197–216.
Wert, J. A., Parker, E. R., Zackay, V. F. (1979), *Metall. Trans. 10A*, 1313–1322.
Westbrook, J. H. (1956), *J. Electrochem. Soc. 103*, 54–63.
Westbrook, J. H. (1960a), in: *Mechanical Properties of Intermetallic Compounds:* Westbrook, J. H. (Ed.). New York: Wiley, pp. 1–70.
Westbrook, J. H. (1960b), in: *High Temperature Technology*. New York: McGraw-Hill, pp. 113–128.
Westbrook, J. H. (1965), in: *High-Strength Materials:* Zackay, V. F. (Ed.). New York: Wiley, pp. 724–768.
Westbrook, J. H. (1967), in: *Intermetallic Compounds:* Westbrook, J. H. (Ed.). New York: Wiley, pp. 3–14.
Westbrook, J. H. (1970), in: *Ordered Alloys – Structural Applications and Physical Metallurgy:* Kear, B. H., Sims, C. T., Stoloff, N. S., Westbrook, J. H. (Eds.). Baton Rouge, LA: Claitor's Publ. Div., pp. 1–24.
Westbrook, J. H. (1974), in: *Order–Disorder Transformations in Alloys:* Warlimont, H. (Ed.). Berlin: Springer, pp. 494–539.
Westbrook, J. H. (1977), *Metall. Trans. 8A*, 1327–1360.
Westbrook, J. H. (1993), in: *Structural Intermetallics:* Darolia, R., Lewandowski, J. J., Liu, C. T., Martin, P. L., Miracle, D. B., Nathal, M. V. (Eds.). Warrendale, PA: TMS, pp. 1–15.
Westbrook, J. H., Wood, D. L. (1964), *J. Nucl. Mater. 12*, 208–215.
Westwood, A. R. C. (1990), *Mater. Sci. Technol. 6*, 958–961.
Wetzig, K., Wittig, H. (1972), *Phys. Status Solidi (a) 9*, K1–K3.
Wever, H. (1992), *Defect Diffus. Forum 83*, 55–72.
Wever, H., Hünecke, J., Frohberg, G. (1989), *Z. Metallkd. 80*, 389–397.
Whang, S. H., Hahn, Y. D. (1993), *Phil. Mag. A68*, 183–192.
Wheeler, R., Vasudevan, V. K., Fraser, H. L. (1990), *Phil. Mag. Lett. 62*, 143–151.
Whittenberger, J. D. (1985), *Mater. Sci. Eng. 73*, 87–96.
Whittenberger, J. D. (1986), *Mater. Sci. Eng. 77*, 103–113.
Whittenberger, J. D. (1987), *Mater. Sci. Eng. 85*, 91–99.
Whittenberger, J. D., Viswanadham, R. K., Mannan, S. K., Kumar, K. S. (1989), *J. Mater. Res. 4*, 1164–1171.
Whittenberger, J. D., Arzt, E., Luton, M. J. (1990a), in: *Intermetallic Matrix Composites:* Anton, D. L., Martin, P. L., Miracle, D. B., McMeeking, R. (Eds.). Pittsburgh, PA: MRS, pp. 211–218.
Whittenberger, J. D., Gaydosh, D. J., Kumar, K. S. (1990b), *J. Mater. Sci. 25*, 2771–2776.
Whittenberger, J. D., Reviere, R., Noebe, R. D., Oliver, B. F. (1992a), *Scr. Metall. Mater. 26*, 987–992.
Whittenberger, J. D., Arzt, E., Luton, M. J. (1992b), *Scr. Metall. Mater. 26*, 1925–1930.
Wiedeman, K. E., Sankaran, S. N., Clark, R. K., Wallace, T. A. (1989), in: *Oxidation of High-Temperature Intermetallics:* Grobstein, T., Doychak, J. (Eds.). Warrendale, PA: TMS, pp. 195–206.
Wiedemeier, H., Singh, M. (1992), *J. Mater. Sci. 27*, 2974–2978.
Wiederhorn, S. M. (1984), *Annu. Rev. Mater. Sci. 14*, 373–403.
Willems, J. J. G., Buschow, K. H. J. (1987), *J. Less-Common Met. 129*, 13–30.
Wilson, D. F., Cavin, O. B. (1992), *Scr. Metall. Mater. 26*, 85–88.
Winnicka, M. B., Varin, R. A. (1993), *Metall. Trans. 24A*, 935–946.
Withers, J. C., Shiao, H.-C., Loutfy, R. O., Wang, P. (1991), *J. Met. 43(8)*, 36–39.
Wittenauer, J., Bassi, C., Walser, B. (1989), *Scr. Metall. 23*, 1381–1386.
Wittmer, M., Seidel, T. E. (1978), *J. Appl. Phys. 49*, 5827–5830.
Wittmer, M., Ting, C.-Y., Tu, K. N. (1983), *J. Appl. Phys. 54*, 699–704.
Wolfenden, A., Griffin, R. B., Kharbat, E. T., Underhill, M. A., Goelz, F. R., Jr., Wickstrom, S. N. (1989), in: *Materials Architecture:* Bilde-Sorensen, J. B., Hansen, N., Jensen, D. J., Leffers, T., Lilholt, H., Pedersen, O. B. (Eds.). Roskilde: Riso National Laboratory, pp. 605–610.
Wolfenstine, J., Kim, H. K., Earthman, J. C. (1992), *Scr. Metall. Mater. 26*, 1823–1828.
Woodward, C., MacLaren, J. M., Dimiduk, D. M. (1993), *Mater. Res. Soc. Symp. Proc. 288*, 171–176.
Wright, J. K., Wright, R. N., Moore, G. A. (1993), *Scr. Metall. Mater. 28*, 501–506.

ArcelorMittal Ex. 2038
Page 180 of 190

Wright, R. N. (1977), *Metall. Trans. 8 A*, 2024–2025.
Wright, R. N., Bok, K. A. (1988), *Metall. Trans. 19 A*, 1125–1126.
Wright, R. N., Ho, J. C. (1986), *Metall. Trans. 17 A*, 401–405.
Wu, J. S., Beaven, P. A., Wagner, R., Hartig, C., Seeger, J. (1989), in: *High-Temperature Ordered Intermetallic Alloys* III: Liu, C. T., Taub, A. I., Stoloff, N. S., Koch, C. C. (Eds.). Pittsburgh, PA: Mater. Res. Soc., pp. 761–766.
Wu, J. S., Beaven, P. A., Wagner, R. (1991), *Scr. Metall. Mater. 25*, 207–212.
Wu, M. H., Wayman, C. M. (1991), *Scr. Metall. Mater. 25*, 1635–1640.
Wu, S.-K., Lin, R. Y. (1993), *Mater. Res. Soc. Symp. Proc. 288*, 1031–1036.
Wu, T.-C., Sass, S. L. (1993a), *Mater. Res. Soc. Symp. Proc. 288*, 217–222.
Wu, T.-C., Sass, S. L. (1993b), *Scr. Metall. Mater. 28*, 1287–1292.
Wu, Z. L., Pope, D. P. (1993), in: *Structural Intermetallics:* Darolia, R., Lewandowski, J. J., Liu, C. T., Martin, P. L., Miracle, D. B., Nathal, M. V. (Eds.). Warrendale, PA: TMS, pp. 107–116.
Wu, Z. L., Pope, D. P., Vitek, V. (1990a), *Scr. Metall. Mater. 24*, 2187–2190.
Wu, Z. L., Pope, D. P., Vitek, V. (1990b), *Scr. Metall. Mater. 24*, 2191–2196.
Wu, Z. L., Pope, D. P., Vitek, V. (1991), in: *High Temperature Ordered Intermetallic Alloys* IV: Johnson, L. A., Pope, D. P., Stiegler, J. O. (Eds.). Pittsburgh, PA: MRS, pp. 487–492.
Wu, Z. L., Pope, D. P., Vitek, V. (1993), *Mater. Res. Soc. Symp. Proc. 288*, 447–452.
Wunderlich, W., Machon, L., Sauthoff, G. (1992), *Z. Metallkd. 83*, 679–684.
Wunderlich, W., Kremser, T., Frommeyer, G. (1993), *Acta Metall. Mater. 41*, 1791–1799.
Wunnike-Sanders, W. (1993), Dr. Ing. Thesis, RWTH Aachen, pp. 1–123.
Wunnike-Sanders, W., Sauthoff, G. (1994), unpublished report, Max-Planck-Institut für Eisenforschung, Düsseldorf, FRG.
Wurzwallner, K., Clemens, H., Schretter, P., Bartels, A., Koeppe, C. (1993), *Mater. Res. Soc. Symp. Proc. 288*, 867–872.
Xiao, H., Baker, I. (1993), *Scr. Metall. Mater. 28*, 1411–1416.
Xiao, L., Abbaschian, R. (1992), *Metall. Trans. 23 A*, 2863–2872.
Xie, C. Y., Jiang, B. H., Hu, G. X. (1993), *Scr. Metall. Mater. 28*, 1101–1105.
Xu, D., Wang, D., Zhou, W., Yang, H., Lin, D. (1993), *Mater. Res. Soc. Symp. Proc. 288*, 817–822.
Yagisawa, K., Yoshikawa, A. (1979), *Z. Phys. Chem. N. F. 117*, 79–87.
Yamada, H., Shimizu, M. (1986), *J. Phys. F 16*, 1039–1050.
Yamada, Y., Taya, M., Watanabe, R. (1993), *Mater. Trans. Jpn. Inst. Met. 34*, 254–260.
Yamagata, T., Yoshida, H. (1973), *Mater. Sci. Eng. 12*, 95–100.
Yamaguchi, M. (1991), *ISIJ Int. 31*, 1127–1133.
Yamaguchi, M. (1992), *Mater. Sci. Technol. 8*, 299–307.
Yamaguchi, M., Inui, H. (1993), in: *Structural Intermetallics:* Darolia, R., Lewandowski, J. J., Liu, C. T., Martin, P. L., Miracle, D. B., Nathal, M. V. (Eds.). Warrendale, PA: TMS, pp. 127–142.
Yamaguchi, M., Umakoshi, Y. (1990), *Prog. Mater. Sci. 34*, 1–148.
Yamaguchi, M., Umakoshi, Y., Yamane, T. (1987), *Phil. Mag. A 51*, 301–315.
Yamaguchi, M., Shirai, Y., Umakoshi, Y. (1988), in: *Dispersion Strengthened Aluminium Alloys:* Kim, Y.-W., Griffith, W. M. (Eds.). Warrendale, PA: TMS, pp. 721–739.
Yamaguchi, M., Nishitani, S. R., Shirai, Y. (1990), in: *High-Temperature Aluminides and Intermetallics:* Whang, S. H., Liu, C. T., Pope, D. P., Stiegler, J. O. (Eds.). Warrendale, PA: TMS, pp. 63–90.
Yamaguchi, M., Shirai, Y., Inui, H. (1993), *Mater. Res. Soc. Symp. Proc. 288*, 131–139.
Yamamoto, T. (1980), in: *The Development of Sendust and Other Ferromagnetic Alloys:* Yamamoto, T. (Ed.). Chiba: Committee of Academic Achievements, pp. 1–6.
Yamamoto, T., Utsushikawa, Y. (1977), *J. Coll. Ind. Technol., Nihon Univ. 10*, 17–30.
Yan, M., Vitek, V., Ackland, G. J. (1992), in: *Ordered Intermetallics – Physical Metallurgy and Mechanical Behaviour:* Liu, C. T., Cahn, R. W., Sauthoff, G. (Eds.). Dordrecht: Kluwer, pp. 335–353.
Yan, P., Wallach, E. R. (1993), *Intermetallics 1*, 83–97.
Yaney, D. L., Nix, W. D. (1988), *J. Mater. Sci. 23*, 3088–3098.
Yang, H. S., Jin, P., Mukherjee, A. K. (1992). *Mater. Trans. Jpn. Inst. Met. 33*, 38–44.
Yang, H. S., Lee, W. B., Mukherjee, A. K. (1993), in: *Structural Intermetallics:* Darolia, R., Lewandowski, J. J., Liu, C. T., Martin, P. L., Miracle, D. B., Nathal, M. V. (Eds.). Warrendale, PA: TMS, pp. 69–76.
Yang, J.-M., Jeng, S. M. (1990), in: *Intermetallic Matrix Composites:* Anton, D. L., Martin, P. L., Miracle, D. B., McMeeking, R. (Eds.). Pittsburgh, PA: MRS, pp. 139–146.
Yang, J.-M., Jeng, S. M., Yang, C. J., Anton, D. L. (1990), in: *Intermetallic Matrix Composites:* Anton, D. L., Martin, P. L., Miracle, D. B., McMeeking, R. (Eds.). Pittsburgh, PA: MRS, pp. 385–392.
Yang, R., Leake, J. A., Cahn, R. W. (1992a), *Mater. Sci. Eng. A 152*, 227–236.
Yang, R., Saunders, N., Leake, J. A., Cahn, R. W. (1992b), *Acta Metall. Mater. 40*, 1553–1562.
Yang, R., Leake, J. A., Cahn, R. W. (1993), *Mater. Res. Soc. Symp. Proc. 288*, 489–494.
Yang, S. S., Vasudevan, V. K. (1993), *Mater. Res. Soc. Symp. Proc. 288*, 731–736.

ArcelorMittal Ex. 2038
Page 181 of 190

Yang, W. S., Mikkola, D. E. (1993), *Scr. Metall. Mater. 28,* 161–165.
Yasuda, H., Takasugi, T., Koiwa, M. (1991a), in: *Proc. Int Symp. on Intermetallic Compounds – Structure and Mechanical Properties* (JIMIS-6): Izumi, O. (Ed.). Sendai: The Japan Institute of Metals, pp. 33–37.
Yasuda, H., Takasugi, T., Koiwa, M. (1991b), *Mater. Trans. Jpn. Inst. Met. 32,* 48–51.
Yasuda, H., Takasugi, T., Koiwa, M. (1992), *Acta Metall. Mater. 40,* 381–387.
Yasuda, K. (1991), in: *Concise Encyclopedia of Medical and Dental Materials:* Williams, D., Cahn, R. W., Bever, M. B. (Eds.). Oxford: Pergamon, pp. 197–205.
Yavari, A. R., Baro, M. D., Fillion, G., Surinach, S., Gialanella, S., Clavaguera-Mora, M. T., Desré, P., Cahn, R. W. (1991), in: *High Temperature Ordered Intermetallic Alloys* IV: Johnson, L. A., Pope, D. P., Stiegler, J. O. (Eds.). Pittsburgh, PA: MRS, pp. 81–86.
Ye, H. Q., Li, D. X., Kuo, K. H. (1985), *Phil. Mag. A 51,* 829–837.
Yegorushkin, V. Y., Kulmentyev, A. I., Rubin, P. E., (1985), *Phys. Met. Metall. 60 (3),* 1–7.
Yonezu, I., Fujitani, S., Furukawa, A., Nasako, K., Yonesaki, T., Saito, T., Furukawa, N. (1991), *J. Less-Common Met. 168,* 201–209.
Yoo, M. H. (1991), in: *Proc. Int. Symp. on Intermetallic Compounds – Structure and Mechanical Properties* (JIMIS-6): Izumi, O. (Ed.). Sendai: The Japan Institute of Metals, pp. 11–20.
Yoo, M. H., Fu, C. L. (1991), *ISIJ Int. 31,* 1049–1062.
Yoo, M. H., Fu, C. L. (1992), *Mater. Sci. Eng. A 153,* 470–478.
Yoo, M. H., Fu, C. L. (1993), in: *Structural Intermetallics:* Darolia, R., Lewandowski, J. J., Liu, C. T., Martin, P. L., Miracle, D. B., Nathal, M. V. (Eds.). Warrendale, PA: TMS, pp. 283–292.
Yoo, M. H., Horton, J. A., Liu, C. T., (1988), *Acta Metall. 36,* 2935–2946.
Yoo, M. H., Takasugi, T., Hanada, S., Izumi, O. (1990), *Mater. Trans. Jpn. Inst. Met. 31,* 435–442.
Yoo, M. H., Fu, C. L., Lee, J. K. (1991), in: *High Temperature Ordered Intermetallic Alloys* IV: Johnson, L. A., Pope, D. P., Stiegler, J. O. (Eds.). Pittsburgh, PA: MRS, pp. 545–554.
Yoshida, M., Takasugi, T., (1991a), in: *Proc. Int. Symp. on Intermetallic Compounds – Structure and Mechanical Properties* (JIMIS-6): Izumi, O. (Ed.). Sendai: The Japan Institute of Metals, pp. 403–407.
Yoshida, M., Takasugi, T. (1991b), in: *High Temperature Ordered Intermetallic Alloys* IV: Johnson, L. A., Pope, D. P., Stiegler, J. O. (Eds.). Pittsburgh, PA: MRS, pp. 273–278.
Yoshida, M., Takasugi, T. (1992), *Phil. Mag. A 65,* 41–52.
Yoshihara, M., Suzuki, T., Tanaka, R. (1991), *ISIJ Int. 31,* 1201–1206.
Yoshimi, K., Hanada, S. (1993), in: *Structural Intermetallics:* Darolia, R., Lewandowski, J. J., Liu, C. T., Martin, P. L., Miracle, D. B., Nathal, M. V. (Eds.). Warrendale, PA: TMS, pp. 475–482.
Zakrevskiy, I. G., Kokorin, V. V., Shevchenko, A. D. (1986), *Phys. Met. Metall. 61 (2),* 199–202.
Zeng, K., Hämäläinen, M., Lilius, K. (1993), *CALPHAD 17,* 101–107.
Zeumer, B., Sauthoff, G. (1992), paper at the DGM Annual Meeting in Hamburg.
Zeumer, B., Von Keitz, A., Sauthoff, G. (1991), in: *2. Symposium Materialforschung des BMFT:* Jülich, KFA-PLR, pp. 2397–2399.
Zhang, M.-X., Hsieh, K.-C., Chang, Y. A. (1992a), *Mater. Res. Soc. Symp. Proc. 273,* 103–112.
Zhang, M.-X., Hsieh, K.-C., DeKock, J., Chang, Y. A. (1992b), *Scr. Metall. Mater. 27,* 1361–1366.
Zhang, T., Li, Y., Zheng, Z., Zhu, Y. (1991), in: *High Temperature Ordered Intermetallic Alloys* IV: Johnson, L. A., Pope, D. P., Stiegler, J. O. (Eds.). Pittsburgh, PA: MRS, pp. 137–142.
Zhang, W., Chen, G., Wang, Y., Sun, Z. (1993), *Scr. Metall. Mater. 28,* 1113–1118.
Zhang, Y., Lin, D. (1993), *Mater. Res. Soc. Symp. Proc. 288,* 611–616.
Zhang, Y., Tonn, S. C., Crimp, M. A. (1993), *Mater. Res. Soc. Symp. Proc. 288,* 379–384.
Zhang, Y. G., Xu, Q., Chen, C. Q. (1991), in: *Proc. Int. Symp. on Intermetallic Compounds – Structure and Mechanical Properties* (JIMIS-6): Izumi, O. (Ed.). Sendai: The Japan Institute of Metals, pp. 39–43.
Zhao, L., Baker, I., George, E. P. (1993), *Mater. Res. Soc. Symp. Proc. 288,* 501–506.
Zhou, B., Chou, Y. T., Liu, C. T. (1993), *Intermetallics 1,* 217–255.
Zhou, X. W., Hsu, T. Y. (1991), *Acta Metall. Mater. 39,* 1041–1044.
Zhu, J. H., Wan, X. J., Wu, Y. (1993), *Scr. Metall. Mater. 29,* 429–432.
Zinov'eva, G. P., Romasheva, L. F., Saperov, V. A., Gel'd, P. V. (1984), *Sov. Phys. – Solid State 26,* 2115–2117.
Zwicker, U., Pack, D., Blaufelder, C. (1979), *Z. Metallkd. 70,* 514–521.

General Reading

Baker, J., Darolia, R., Whittenberger, J. D., Yoo, M. H. (Eds.) (1993), *High-Temperature Ordered Intermetallic Alloys V.* Pittsburgh, PA: Materials Research Society.
Darolia, R., Lewandowski, J. J., Liu, C. T., Martin, P. L., Miracle, D. B., Nathal, M. V. (Eds.) (1993), *Structural Intermetallics.* Warrendale, PA: TMS.
Dimiduk, D. M., Miracle, D. B., Ward, C. H. (1992), *Mater. Sci. Technol. 8,* 367–375.

ArcelorMittal Ex. 2038
Page 182 of 190

Engell, H.-J., von Keitz, A., Sauthoff, G. (1991), in: *Advanced Structural and Functional Materials:* Bunk, W. (Ed.). Berlin: Springer-Verlag, pp. 91–132.

Fleischer, R. L. (1991), in: *Proc. Int. Symp. Intermetallic Compounds – Structure and Mechanical Properties (JIMIS-6):* Izumi, O. (Ed.). Sendai: The Japan Institute of Metals, pp. 157–164.

Izumi, O. (1989), *Mater. Trans., JIM 30,* 627–638.

Liu, C. T., Stiegler, J. O., Froes, F. H. (1990), in: *Metals Handbook, Vol. 2: Properties and Selection: Non-Ferrous Alloys and Special Purpose Materials.* Materials Park: ASM, pp. 913–942.

Liu, C. T., Cahn, R. W., Sauthoff, G. (Eds.) (1992), *Ordered Intermetallics – Physical Metallurgy and Mechanical Behaviour.* Dordrecht: Kluwer.

Materials Science and Technology: A Comprehensive Treatment: Cahn, R. W., Haasen, P., Kramer, E. J. (Eds.). Weinheim: VCH. The series comprises 19 Volumes. Gerold, V. (Ed.) (1992), *Vol. 1. Structure of Solids;* Haasen, P. (Ed.) (1991) *Vol. 5. Phase Transformations in Materials;* Mughrabi, H. (Ed.) (1992); *Vol. 6. Plastic Deformation and Fracture of Materials.* This book is derived from K. H. Matucha (Ed.) (1995); *Vol. 8. Structure and Properties of Nonferrous Alloys.*

Paufler, P. (1976), in: *Intermetallische Phasen.* Leipzig: VEB Deutscher Verlag für Grundstoffindustrie, pp. 165–187.

Westbrook, J. H. (1993), in: *Structural Intermetallics:* Darolia, R., Lewandowski, J. J., Liu, C. T., Martin, P. L., Miracle, D. B., Nathal, M. V. (Eds.). Warrendale, PA: TMS, pp. 1–5.

Yamaguchi, M., Umakoshi, Y. (1990), *Prog. Mater. Sci. 34,* 1–148.

ArcelorMittal Ex. 2038
Page 183 of 190

copyright © VCH Verlagsgesellschaft mbH, 1995

Index

A15 phases, basic properties 94ff
advanced aluminides, nickel aluminides 45
aerospace applications
– $L1_2$ trialuminides 38
– NiTi 79
– Ti_3Al 21
– TiAl 30
air-induction melting, Ni_3Al 46
Al-rich ternary intermetallics 36
Al-Ta-Ti phase diagrams 35
Al_3Hf 36
Al_3Mo 33, 36
Al_3Sc 36
Al_3Ta 35, 36
Al_2Ti 32
Al_3Ti 30, 36
$Al_{66}Ti_{25}M_9$ 37
Al_3V 32, 36
Al_3Zr 36
alloy developments, aluminides 45, 67f
alloying elements
– Fe_3Al 85
– FeAl 89
– FeCo 82
– Nb_3Al, A15 structure 99
– Ni_3V 36
– NiAl 54, 67f
– rare-earth compounds 108
– titanium aluminides 18, 27
Alnico, applications 3, 67
Alnico alloys 67
aluminides
– applications 21, 29, 45, 67ff, 84ff
– advanced 45
– alloy developments 67f
amalgams 3, 94
antiphase boundary energy, FeAl 88
applications 2f
– Al_3V 32
– Cu-Zn-Al alloys 92
– disilicides 114
– Fe-Ni-Al alloys 67f
– Laves phases 102
– M_5Si_3 phases 112
– Ni_3Al 45
– rare-earth compounds 108
– Ti_3Al 21f
– TiAl 29f
see also: aerospace applications
see also: high-temperature applications
see also: medical applications
see also individual phases
atomic bonding 2
automotive applications
– Fe_3Al 86
– Ni_3Al 46
– NiTi 79
– TiAl 30

B2 phases 51ff
Be-rich phases, mechanical behavior 106
beryllides 106ff
beryllium, alloying element, FeCo 82
binary B2 phases, aluminides 51
binary Fe-Al phase diagram 84
binary Fe-Co phase diagram 81
binary Laves phases, $TaFe_2/NbFe_2$ 105
binary Ni-Al phase diagram 39
binary Ni-Mo system 83
binary trialumides 30ff
bonding, basic properties 5, 8
boron, alloying element,
– FeAl 89
– rare-earth compounds 108
– ductilization, Ni_3Al 43
boron addition, hardening effect, NiAl 57
Bragg–Williams model 7
brittle fracture behavior, TiAl 24
brittle-to-ductile transition temperature
– aluminides 73
– beryllides 106
– Laves phases 102
– NiAl 56
– V_3Si 96
brittleness 12
– Alnico alloys 67
– polycrystalline NiAl 57
see also individual phases
bronze coatings, ancient Egypt 2
bronzes, Cu-base phases 90

ArcelorMittal Ex. 2038
Page 184 of 190

C14, C15, C36 structure 101
$CaNi_5$ 109
carbon, alloying element
– rare-earth compounds 108
– Fe_3Al 86
– Fe_3Al_x 86
– FeCo 82
– NiAl 58
cementation, applications 3
cerium, microalloying element 66
chromium alloying element
– Fe_3Al 85
– Ni_3Al 45
– NiAl 57, 71, 77
– titanium aluminides 19, 23
chromium-containing Laves phases 105
CoAl, B2 phases 77
Co-Mo-Cr-Si alloys, Tribaloys 104
Co_3Ti, $L1_2$ phases 49
Co-Sm magnets, applications 3
coating alloys, NiAl 68
coatings, protective, M_2Si phases 111
cobalt
– alloying element, Ni_3V 36
– – NiAl 54
– macroalloying element, NiAl 67
Coble creep, (Ni,Fe)Al 60
CoHf, B2 structure 80
composites 21, 29, 47, 76, 107, 115
composition, Laves phases 102
compound formation 2
compressive strength
– NiAl-Cr alloys 71
– NiAl-NbNiAl alloys 74
compressive yield strength, $Al_{66}Ti_{25}M_9$ 37
copper, macroalloying element in magnetic alloys 67
copper amalgams 94
corrosion behavior
– $MoSi_2$ 114
– NiAl 66
– Ni_3Al 44f
– TiAl 23f
– Ti_3Al 16f
corrosion resistance, Fe_3Al 85
corrosion resistant surface layer, NiAl 68
$CoSi_2$ 116
CoTi, B2 structure 80
covalent bonding 6
CoZr, B2 structure 80
Cr_3Si, A15 structure 100
creep 58ff
– Ni_3Al 40
– NiAl 58f
creep resistance 11
– disilicides 116
– multiphase NiAl-base alloys 64
critical current density, Laves phases 103
CrSi, transition metal silicides, B20 structure 113
$CrSi_2$ 109, 116
crystal growth technique, TiAl 26
crystal structures 5
– Laves phases 101
Cu-Al-Ni shape memory alloys 92
Cu_2AlMn, Heusler-type phases 83
Cu amalgams 94
Cu-Au phases 93f
Cu-base phases 90ff
Cu_2Sb, "Regulus of Venus" 2
Cu_2SnMn, Heusler-type phases 83
CuZn 90f
Cu-Zn-Al shape memory alloys 91f

$D0_{22}$ phases, basic properties, titanium aluminides 30
deformability, NiAl 12
deformation behavior
– multiphase Al_3Nb-NiAl allyos 35
– $NbBe_{12}$ 107
– silicon 65
– titanium trialuminide Al_3Ti 31
see also individual phases
density, NiAl 52
– titanium aluminides 14
dental restoratives, amalgam 4, 94
diffusion see individual phases
diffusion behavior, Cu-Au phases 93
diffusion bonding, Ti_3Al 21
diffusion coatings, MCrAlY 68
diffusion coefficient 11
– aluminides 61
diffusion processes, Ni_3Al 40
disilicides 114ff
dislocation creep 58ff
– Dorn equation 58
– niobium trialuminide Al_3Nb 34
dislocation mobility 13
dislocations, TiAl 24
dopants distribution, M_2Si phases 112
Dorn equation
– dislocation creep 58
– niobium trialuminide Al_3Nb 34
ductility
– applications, disilicides 115
– Hall–Petch-type dependence, FeCo 82
– TiAl 25f
– titanium trialuminide Al_3Ti 32
see also individual phases
ductilization, Ni_3Al 43
dynamic recrystallization, TiAl 25

elastic behavior
– Cu-Au phases 93
– CuZn 90
– NiAl 52
see also individual phases
elastic constants, Ni_3Al 39
elastic deformation, NiTi 79
elastic moduli
– $Al_{66}Ti_{25}M_9$ 37

ArcelorMittal Ex. 2038
Page 185 of 190

– B2 phases 81
– B2(Ni,Fe)Al 62
– basic properties 8
– disilicides 116
– Laves phases 101
electrical resistivity, Ni_3Al 39
electrochemical properties 2ff
electronegativity, rare-earth compounds 107
electroslag remelting
– Fe_3Al 86
– Ni_3Al 46
embrittlement
– environmental, FeAl 89
– TiAl 28
see also individual phases
enthalpy, basic properties 9
environmental effects
– aluminides 66
– Ni_3Al 44
– titanium aluminides 19f, 27f
equilibria, phases 2
see also individual phases

fatigue, Ni_3Al 40
fatigue behavior, TiAl 26
Fe-Al
– phase diagram 87
– B2 phases 77
– phases 84
Fe_3Al 84
Fe_3AlC_x, related phases 87
Fe_3Ga 47
Fe_3Ge 47
Fe-Nb-Si system, ternary silicides 112
Fe-Ni-Al Alloys 67
– B2 phases 77
FeCo, Permendur alloys 81
$(Fe,Co,Ni)_3V$, $L1_2$ phases 50
FeSi, transition metal silicides, B20 structure 113
$FeSi_2$ 116
Fe_3Si 110
FeTi, B2 structure 80
see also: iron
film formation process, M_2Si phases 112
flexural elongation, $L1_2$ trialuminides 38
flow stress, microstructure, polycrystalline NiAl 55
flow stress temperature dependence, nickel aluminides 41
formation enthalpy, Ni-Al system 9
fracture, Ni_3Al 41
fracture strength 12
fracture toughness
– NiAl 56
– NiAl-NbNiAl alloys 74
– titanium aluminides 14, 26
Frank–Kaspar phases 6, 101
– A15 structure 95
Friauf–Laves phases 100f
friction welding, linear, Ti_3Al 21

Gibbs energy, phase stability 8
grain boundary weakness
– NiAl 57
– Ni_3Al 43

hafnium, alloying element
– TiAl 27
– microalloying 66
Hall–Petch-type dependent ductility 82
hardening, boron addition, NiAl 57
hardness 2ff
– Alnico alloys 67
– CuZn 90
– disilicides 116
Heusler-type phases 83
– Cu_2MnAl/Cu_2MnSn 90
– $HfCr_2$ 105
– $HfFe_2$ 103
– HfV_2 103
– $(Hf, Zr)V_2$ 103
– Ni_2AlNb/Ni_2AlTa 75
– Ni_2AlTi 71
– Ni_2TiAl 63
high tin bronze, applications 3
high-temperature applications
– aluminides 13
– disilicides 114
– M_5Si_3 phases 112
see also individual phases
high-temperature materials, beryllides 106
high-temperature structural service, niobium trialuminide 33
historical remarks 2ff
hot extrusion, Nb_3Sn, A15 structure 97
hot pressing permanent magnetic alloys, nickel aluminides 46
Hume–Rothery phases 6
hydrogen environment, titanium aluminides 20
hydrogen solubility, in TiAl 29
hydrogen storage materials
– FeTi 80
– Laves phases 103
– rare-earth compounds 108
hydrogen-to-metal ratio, C15 ZrV_2 103
hydrogenation
– Nd-Fe-B alloys 108
– thermodynamics 104

impurities 13
impurity content, disilicides 115
induction melting, Fe_3Al 86
infiltration techniques, Nb_3Al-Nb alloys 99
ingot metallurgy
– Fe_3Al 86
– rare-earth compounds 108
internal crystal energy, basic properties 9
interstitial impurities, titanium aluminde TiAl 28
ionic bonding 6

ArcelorMittal Ex. 2038
Page 186 of 190

iron
– alloying element, Ni_3V 36
– – NiAl 54
iron aluminides, related phases 84ff
IrSi 114

K phase, Fe_3AlC_x 86
Kanthal Super, electric heating elements 3
Kear–Wilsdorf mechanism, Ni_3Al 42
Kirkendall effect, aluminides 66
Kurnakov phases 7

$L1_2$ phases, Ni_3X, X=Ga,Si,Ge 47
$L1_2$ structure, trialuminides 36f
$L2_1$ structure 83
$LaNi_2$ 103
$LaNi_5$ 109
lanthanum, microalloying element 66
lattice structure 8
Laves phases 6, 100ff
– basic properties 100ff
– two-phase Fe_3Al 85
– multiphase NiAl-base alloys 64
– two-phase NiAl 74
linear friction welding, Ti_3Al 21

M_2Si phases 111f
M_5Si_3 phases 112
magnet materials, rare-earth compounds 108
magnetic alloys, Fe-Ni-Al systems 67
magnetic field strength, Laves phases 103
magnetic head materials
– applications 2, 111
– Sendust 3, 85, 111
magnetic materials, transition-metal Laves phases 103
magnetic permeability, Fe_3Al 85
manganese
– alloying element, FeCo 82
– – TiAl 23, 27
martensitic transformation
– CuZn 91
– NiAl 53, 68
– V_3Si, A15 structure 95
matrix composites,
– NiAl 76
– TiAl 30
– Ti_3Al 21
mechanical behavior
– $Al_{66}Ti_{25}M_9$ 37
– Alnico-type alloys 67
– beryllides 106
– Cu-Al-Ni shape memory alloys 92
– disilicides 116
– Fe_3AlC_x 87
– FeCo 81
– NiAl 51
– NiBe 107
– Ni_3Al 40, 45
– polycrystalline NiAl 55
– silicides 109
– TiAl 23
– Ti_3Al 16
– titanium aluminides, related phases 14f
– titanium trialuminides Al_3Ti 31
see also: physical properties
see also individual phases
medical applications, NiTi 79
melting, Fe_3Al 86
melting point, NiAl 69
melting temperature
– basic properties 8
– Laves phases 102
see also individual phases
metal-to-silicon ratio, silicides 109
metallic bonding 6
Mg_2Si 111
Mg-Si-Al, ternary system 111
microalloying, oxygen active elements 66
microstructure
– $Al_{66}Ti_{25}M_9$ 37
– disilicides 115
– Ni_3Al 40
– polycrystalline NiAl 55
– Ti_3Al 16
– titanium trialuminide Al_3Ti 31
see also individual phases
mirrors, ancient egypt 2
MnSi, transition metal silicides, B20 structure 113
MoCoSi, ternary Laves phases 104
$Mo(Co, Si)_2$ 104
$MoFe_2$ 103
molybdenum, alloying element
– FeCo 82
– NiAl 71
– titanium aluminides 19, 23
monolithic Laves phases 105
$MoSi_2$ applications, disilicides 110, 115
Mosilit, electric heating elements 3, 114
MSi phases 113
multinary materials, rare-earth compounds 108
multiphase Al_3Nb-NiAl alloys 35
multiphase NiAl-base alloys, creep resistance 64

Nabarro–Herring creep, (Ni,Fe)Al 60
$NbBe_{12}$ 107
Nb_2Be_{17} 107
Nb_3Al, A15 structure 98
Nb_3Al-Ag composite superconductor 98
$NbFe_2$, binary Laves phases 105
Nb_3Si, A15 structure 100
Nb_5Si_3 113
Nb_3Sn, A15 structure 97
NiAl 51f
Ni_3Al 38f
Ni-Al-Co system 54
NiAl-Cr alloys 71
NiAl-Fe alloys 69
Ni-Al-Mn phase diagram 54
NiAl-Nb alloys 72
NiAl-Ta alloys 72

ArcelorMittal Ex. 2038
Page 187 of 190

NiAl-Ti alloys 71
Ni-base superalloys 12
NiBe 107
Ni-Fe-Al phase diagram 54
Ni_3Fe, $L1_2$ phases 48
Ni_3Ga 47
Ni_3Ge 47
Ni_3Mn 47
Ni_3Si, $L1_2$ phases 49
Ni_3V, $D0_{22}$ phases 35
nickel, alloying element, Fe_3Al 85
nickel aluminides, related phases 38ff
nickel-hydrogen batteries, rare-earth compounds applications 109
nickel-molybdenum phases 83f
niobium
– alloying element, FeCo 82
– – titanium aluminides 18, 23
– microalloying element 67
niobium trialuminide Al_3Nb 33
$NiSi_2$ 117
NiTi 79
Nitinol 3
nitrogen, alloying, rare-earth compounds 108
non-metals 4

ODS NiAl alloys 76
ordered alloys 1
Orowan stress, multiphase NiAl-base alloys 64
outstanding high-temperature properties 1f
overlay coatings, MCrAlY 68
oxidation behavior
– Ni_3Al 44
– titanium aluminides 19
oxidation resistance
– applications, disilicides 115
– beryllides 106
– multiphase Al_3Nb-NiAl allyos 35
– NiAl 69
– silicides 109
– TiAl 27f
oxide-dispersion strengthened superalloys 12
oxide-dispersion strengthened NiAl alloys/composites 76
oxidizing environments, Fe_3Al 85
oxygen, impurities 13
oxygen embrittlement, TiAl 28

pack aluminide coating, applications 3, 68
paramagnetism, silicides 109
Peierls stress, TiAl 24
Permalloy, applications 3
permanent magnetic materials, Alnico 3, 67
Permendur, applications 3, 81
Permendur alloys, FeCo 81
perovskite-type structure, Fe_3AlC_x 86
phase diagrams
– NiAl 53
– nickel aluminides, related phases 38
– Ti_3Al 14f
– TiAl 22
– titanium trialuminides, Al_3Ti 30
– trialuminides, $L1_2$ structure 36
phase equilibria 2
phase selection, structural applications 11f
phase stability 2, 5
physical properties 2ff, 8ff
– disilicides 116
– FeAl 87
– NiAl 51
– Ni_3Al 39
– nickel aluminides, related phases 38f
– niobium trialuminide Al_3Nb 33
– silicides 109
– TiAl 22f
– Ti_3Al 14f
– titanium aluminides, related phases 14ff
– titanium trialuminide Al_3Ti 30f
– trialuminides, $L1_2$ structure 36
see also: mechanical properties
plastic deformation
– disilicides 114
– microstructure, polycrystalline NiAl 55
– NiTi 79
– TiAl 24
see also individual phases
Poisson's ratio, titanium aluminides 15, 22
polycrystalline Ni_3Al, ductilization 43
polysynthetically twinned crystals, TiAl 26
Portevin–Le Chatelier effect, CuAu 94
powder metallurgy methods
– beryllides 106
– Fe_3Al 86
– Nb_3Al-Nb alloys 99
– Ti_3Al 21
processing, Cu-Zn-Al alloys 92

rapid solidification
– Nb_3Si, A15 structure 100
– rare-earth compounds 108
– titanium alloys 19
rare-earth compounds 107ff
rare-earth(R) Laves phases 103, 108
reactive processing, Ti_3Al 21
rechargeables electrodes, rare-earth compounds applications 108
recrystallization behavior
– CuZn 90
– Ni_3Al 41
– NiAl 56
"Regulus of Venus", violet Cu_2Sb 2

Schottky barriers, silicides 111
secondary creep, (Ni,Fe)Al 59
secondary creep rate, TiAl 26
Seebeck effect, Ni_3Al 39
segregation, boron, Ni_3Al 44
semi-metals 4
semiconductors 4
– Mg_2Si 111

ArcelorMittal Ex. 2038
Page 188 of 190

Sendust, applications 3, 85, 111
shape memory alloys
- Cu-Al-Ni 92
- Cu-Zn-Al 3
- NiAl 68
- NiTi 79
shear modulus 11
- B2(Ni,Fe)Al 62
- titanium aluminides 15, 22
silicides 109ff
silicon, deformation behavior 65
single-phase B2 alloys, creep resistance 58
$SmCo_5$ 108
Sm_2Co_{17} 108
$SmFe_2$ 103
sorption capacity, hydrogen, Laves phases 103
stabilities, phases 2
steam turbines, nickel aluminides applications 46
strength
- Al_3Nb 34
- Laves phases 102
  see also individual phases
stress-induced martensitic transformation, NiAl 54
structural alloys
- NiAl 69
- ternary Laves phases 104f
  see also individual phases
structural applications 4
- Fe_3Al 86
structural materials, beryllides 106
structure, titanium aluminides 14
structure stability, Laves phases 102
sulfidation resistance, NiAl 67
sulfidizing environments, Fe_3Al 85
superalloys, nickel aluminides 4
superconducting materials, Laves phases 102f
superconducting properties, V_3Ga, A15 structure 97
superconductivity 2f
superconductors
- A15 compounds, applications 3, 94ff
- A15 structure 95
superdislocations, TiAl 24
surface coating, applications 3

$TaFe_2$, binary Laves phases 105
$TaSi_2$ 116
tantalum
- alloying element, FeCo 82
- - titanium aluminides 19, 23
tantalum trialuminide Al_3Ta 35
$TbFe_2$ 103
temperature dependence, flow stress, nickel aluminide 41
temperature effects, Laves phases 102
tensile elongation
- $L1_2$ trialuminides 38
- TiAl 26
tensile strength, NiAl-Cr alloys 71
tensile strength, titanium aluminides 14
ternary B2 phases, aluminides 61
ternary Fe-Co-Al phase diagram 81
ternary $L1_2$phases 36
ternary Laves phases 104
- Ni-Al-base alloys 65
- transition-metal elements 75
ternary Ni-Fe-Al phase diagram 69
ternary phase diagrams, TiAl 23
ternary silicides, Fe-Nb-Si system 112
ternary systems
- Mg-Si-Al 111
- phase diagrams, silicides 109
thermal conductivity
- Ni_3Al 39
- NiAl 69
thermal expansion
- disilicides 116
- Ni_3Al 39
thermodynamic properties, CoAl 78
thermodynamics, hydrogenation, Laves phases 104
thermoelectric power generation, application 3
thermomechanical processing, titanium aluminides 18, 25
TiAl grains 25
TiAl 22f
Ti_3Al 14f
$TiBe_{12}$ 107
$TiCr_2$ 102, 105
$TiFe_2$ 103
Ti-Nb-(Ti,Nb)Cr_2 alloys 105
Ti-$TiCr_2$ alloys 105
$TiSi_2$ 115f
Ti_5Si_3 112
titanium, alloying element
- FeCo 82
- Nb_3Al, A15 structure 99
- microalloying, NiAl 67
titanium aluminides
- deformation studies 4
- related phases 14ff, 22ff
- Al_3Ti, $D0_{22}$ phases 30f
toughness
- disilicides 115f
- TiAl 26
  see also individual phases
transient primary creep, multiphase NiAl-base alloys 65
transition metal aluminides, basic properties 11
transition metal beryllides 106f
transition metal silicides 109
- B20 structure 113
trialuminides, $L1_2$ structure 36f
Tribaloys, Co-Mo-Cr-Si alloys 104
tungsten
- alloying element, FeCo 82
- - TiAl 23
turbocharger rotor, Ni_3Al 46
twinning, TiAl 24

ArcelorMittal Ex. 2038
Page 189 of 190

V_3Ga, A15 structure 97
V_3Si, A15 structure 95
vacancy formation
– Cu-Au phases 93
– Fe_3Al 84
– NiAl 51
vacuum-arc melting, Fe_3Al 86
vacuum-arc remelting, Ni_3Al 46
vacuum-induction melting, Ni_3Al 46
vanadium, alloying element
– FeCo 81
– TiAl 23, 27
vanadium trialuminide Al_3V 32
very-large-scale-integrated circuits, silicides 111
von Mises criterion 13
– Ti_3Al 17
VSi_2 116

wear resistance 2ff
– Co-Mo-Cr-Si alloys 104
Widmanstätten platelets, titanium aluminides 18
WSi_2 115

yellow brass
– applications 3
– CuZn 90
yield strength
– disilicides 116
– NiAl-NbNiAl alloys 74
– *titanium aluminides* 14
yield stress
– NiAl 12
– niobium trialuminide Al_3Nb 33
Young's modulus
– $Al_{66}Ti_{25}M_9$ 37
– B2(Ni,Fe)Al 62
– M_5Si_3 phases 112
– Ni-Al system 10
– polycrystalline NiAl 52
– titanium aluminides 14, 22
yttrium, microalloying element 66

Zintl phase 6
zirconium, alloying element
– FeCo 82
– TiAl 23
– microalloying, NiAl 66
Zr_3Al, $L1_2$ phases 50
$ZrBe_{13}$ 107
$ZrCr_2$ 103, 105
$ZrMn_2$ 104
$ZrSi_2$ 116
ZrV_2 103f

ArcelorMittal Ex. 2038
Page 190 of 190